Rudder Roll Stabilization

Lab. v. Scheepsbouwkunde
Technische Hogeschool
Delft

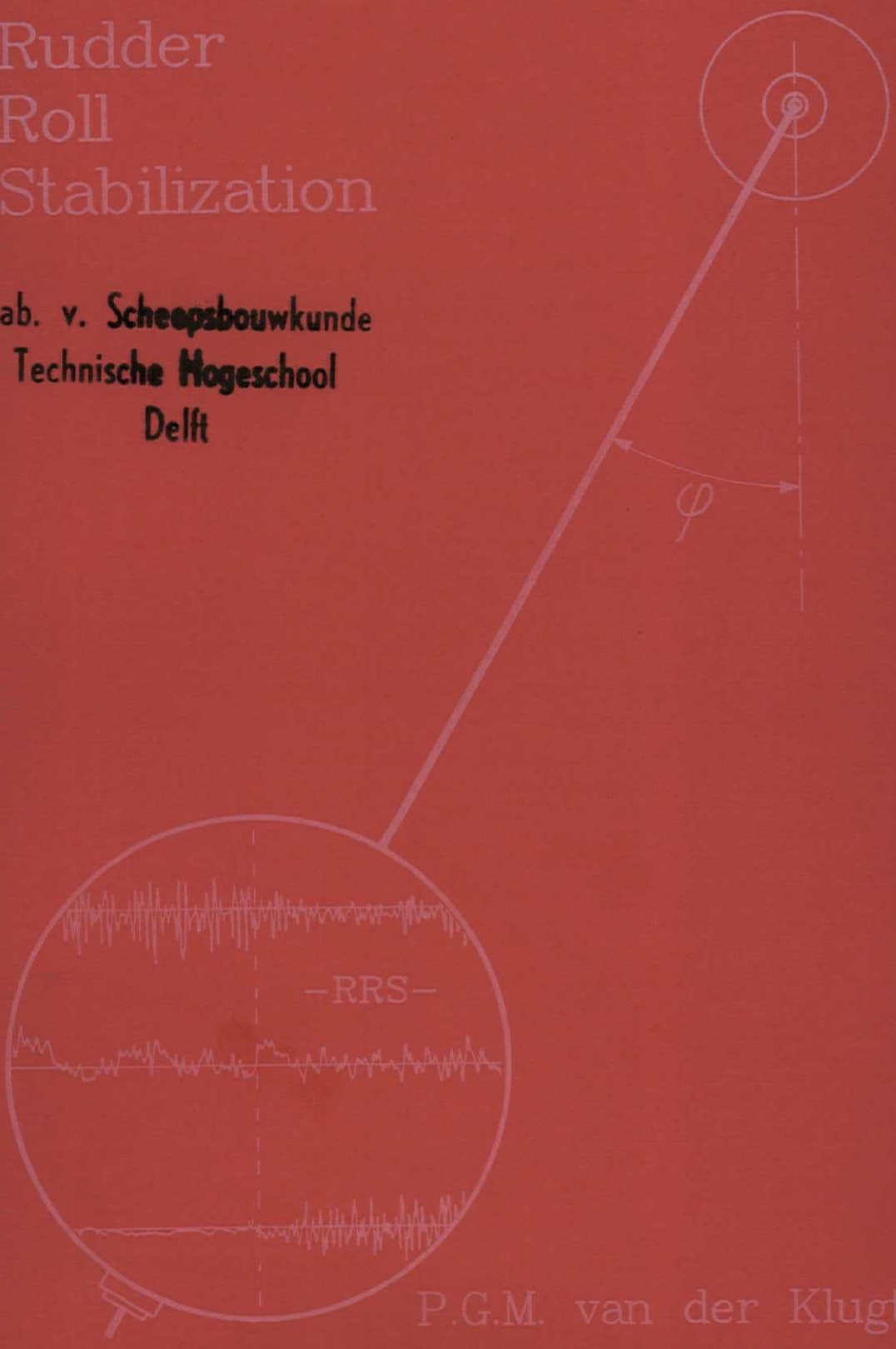

P.G.M. van der Klugt

Rudder

Roll

Stabilization

Photos: Figure 7.16 Royal Netherlands Navy
Figures 7.3, 7.14, 7.15 Delft University of Technology

Drawings: Van Rietschoten & Houwens BV, Rotterdam

Printed and bound by Alevo BV, Delft/1987

Rudder

Roll

Stabilization

PROEFSCHRIFT

ter verkrijging van de graad van doctor
aan de Technische Universiteit Delft,
op gezag van de Rector Magnificus,
prof.dr. J.M. Dirken,
in het openbaar te verdedigen
ten overstaan van een commissie
daartoe aangewezen door
het College van Dekanen
op dinsdag 13 october te 16.00 uur

door

Petrus Gerardus Maria van der Klugt

geboren te Noordwijkerhout
elektrotechnisch ingenieur

Dit proefschrift is goedgekeurd door de promotoren:

Prof.ir. H.R. van Nauta Lemke

en

Prof.dr.ir. J. van Amerongen

SAMENVATTING

Slingerstabilisatie door middel van het roer (engels: *Rudder Roll Stabilization*, **RRS**) vormt een potentieel aantrekkelijke mogelijkheid om de slingerbewegingen van schepen te verminderen. Echter, de stand van de techniek bleek tot nu toe niet ver genoeg gevorderd om de aanwezige regelproblemen op te lossen.
In 1981 begon de vakgroep regeltechniek van de afdeling der Elektrotechniek van de Technische Universiteit Delft in samenwerking met de Koninklijke Nederlandse Marine aan een haalbaarheids studie voor RRS. Interesse vanuit het bedrijfsleven leidde in 1982 tot een samenwerkingsverband tussen universiteit, marine en industrie (Van Rietschoten & Houwens, Rotterdam) met als doel de praktische realisering van een RRS automaat.
Iedere partij had zo z'n eigen specifieke inbreng, geen van de partijen zou afzonderlijk in staat zijn een dergelijke RRS automaat te realiseren:

- De universiteit stelde kennis beschikbaar over moderne regelstrategieën o.a. op het gebied van stuurautomaten voor schepen.
- De marine maakte het mogelijk om ware grootte metingen, metingen met een schaalmodel en metingen bij het *Maritime Research Institute Netherlands* (**MARIN**) in Wageningen uit te voeren.
- Van Rietschoten & Houwens gaf het project financiële ondersteuning en zou de resultaten van het onderzoek verwerken tot een commercieel produkt.

Dit proefschrift geeft de theoretische achtergrond van de uit dit samenwerkings verband voortkomende RRS automaat.

Het RRS principe biedt de regeltechnicus een uitdagend probleem: een niet-lineair proces met één ingang (het roer) en twée uitgangen (de slingerhoek en de koersafwijking) waarbij de verstoringen (golven, wind) een grotere invloed op de scheepsbewegingen kunnen hebben dan het stuursignaal.
Door een scheiding aan te brengen in het frekwentie domein kan dit process met één ingang de twee uitgangen regelen; laagfrekwente roerbewegingen worden gebruikt om het schip op koers te houden terwijl hoogfrekwente roerbewegingen worden gebruikt om het slingeren van het schip te reduceren. Hiertoe wordt een nieuw wiskundig model van een schip geintroduceerd waarmee een goede scheiding in het frekwentie domein kan worden verkregen.
De stuurmachine introduceert niet-lineariteiten in het proces die in eerste instantie lijken te verhinderen dat lineaire methoden kunnen worden toegepast voor het ontwerpen van de regelalgoritmen. Desalniettemin bleek de *Linear process Quadratic*

criterion Gaussian noise (**LQG**) regelaar ontwerp methode te kunnen worden toegepast door de introduktie van een tweetal nieuwe mechanismen:

- De *Automatische Versterkings Regeling* (**AVR**) verhindert instantaan dat de regelaar snellere signalen genereert dan de stuurmachine aan kan.
- De toegepaste LQG algoritmen werken met een kriterium waarvan de weegfactoren automatisch worden aangepast aan de omstandigheden. Te samen met de AVR kunnen hiermee tevens de niet-lineariteiten effectief worden verwijderd uit de regellus.

De LQG methode vereist het voorhanden zijn van de toestanden van een proces. Moderne filter technieken worden toegepast om de niet beschikbare toestanden te reconstrueren en om ongewenste componenten op de gemeten toestanden te verwijderen. Deze technieken vereisen op hun beurt het bekend zijn van de varianties van meet en systeem ruis. Een adaptieve methode wordt geintroduceerd waarmee dit probleem kan worden opgelost.

De resulterende regelalgoritmen werden geimplementeerd in een laboratorium versie van een RRS automaat. Zowel vanwege economische redenenen als vanwege het belang van het goed functioneren van een stuurautomaat voor de veiligheid van een schip, kon de RRS automaat niet zonder meer getest worden aan boord van een schip. Allereerst werd een aantal experimenten verricht waarbij de werkelijkheid steeds beter werd benaderd.

- Experimenten met een eenvoudig analoog model van een schip maakten het mogelijk om de regelalgoritmen te verifiëren en om de hardware van de automaat te testen.
- Vervolgens maakten experimenten met een uitgebreid wiskundig model van het zelfde schip bij het MARIN het mogelijk de invloed van niet gemodelleerde scheepsbewegingen op het regelaar gedrag te onderzoeken.
- Tenslotte werden experimenten met een op afstand bestuurbaar schaalmodel van het zelfde schip uitgevoerd om te onderzoeken of er zich in de praktijk nog onvoorziene problemen kunnen voordoen.

Na deze simulatie experimenten werden diverse ware grootte metingen verricht. De resultaten daarvan stemden overeen met de eerder uitgevoerde experimenten. Bovendien onderstreepten zij nog eens het belang van ware grootte metingen; diverse praktische toevoegingen aan de RRS automaat zijn gebaseerd op waarnemingen tijdens deze metingen.

In hoofdstuk 1 wordt het begrip "RRS" geintroduceerd. Bovendien wordt in het kort ingegaan op de voor- en nadelen van een RRS systeem ten opzichte van andere slingerstabilisatie systemen.

In hoofdstuk 2 worden eenvoudige modellen gepresenteerd van een stuurmachine en de verstoringen. Een nieuw model van een schip wordt gepresenteerd en er wordt aangegeven hoe de parameters van dit model zijn bepaald.
In de hoofdstukken 3 en 4 komt de theory aan bod op basis waarvan respectievelijk de regelalgoritmen en de filteralgoritmen zijn ontworpen. Deze theorie levert voor lineaire processen waarvan een model bekend is de optimale regelactie voor een zeker kwadratisch kriterium. Een nieuwe methode wordt voorgesteld om deze theorie toe te kunnen passen op het RRS probleem. Deze methode sluit goed aan op het in hoofdstuk 5 voorgestelde adaptatie mechanisme. Dit adaptatie mechanisme maakt het mogelijk om de theorie toe te passen op niet-lineaire processen waarbij de omstandigheden en het gewenste gedrag aan veranderingen onderhevig zijn.
Hoofdstuk 6 geeft de praktische realisatie van de regel- en filter-algoritmen in een laboratorium realisatie van een RRS automaat. Er wordt tevens aangegeven hoe de diverse aan een RRS automaat te stellen eisen worden vertaald naar eisen te stellen aan de regelaktie. Bovendien wordt aangegeven aan welke voorwaarden een schip en een stuurmachine moeten voldoen voor een goede werking van een RRS automaat.
In hoofdstuk 7 komen de resultaten van de diverse experimenten aan bod. Tenslotte worden in hoofdstuk 8 conclusies en suggesties voor verder onderzoek gegeven.

SUMMARY

Roll reduction by means of the rudder can potentially be an attractive means of reducing the roll motions of a ship. However, until now the state of the art of the technology appeared to be insufficient to solve the inherent control problems.
In 1981 the Control Laboratory of the Department of Electrical Engineering of Delft University of Technology in cooperation with the Royal Netherlands Navy started a feasibility study on *Rudder Roll Stabilization* (**RRS**). The interest shown by the industry led in 1982 to a joint project between university, navy and industry (Van Rietschoten & Houwens, Rotterdam) with the aim of realizing an RRS autopilot in practice.
Each party had its own specific contribution to make; none of the parties alone would have been able to develop an RRS autopilot:

- The university contributed knowledge concerning new control methods, in particular those in the field of modern ship autopilots.
- The navy enabled full-scale trials, trials with a scale model and measurements at the *Maritime Research Institute Netherlands* (**MARIN**) in Wageningen.
- Van Rietschoten & Houwens financially supported the project and was able to turn the results of the research into a commercial product.

This thesis provides the theoretical background for this RRS autopilot.

The RRS principle poses a challenging problem to a control engineer: a non-linear process with one controllable input (the rudder) and two outputs (the roll angle and the heading error) and with disturbances (wind and waves) which may have a larger influence on the ship's motions than the controllable input.
Separation can be obtained in the frequency domain: low-frequency rudder motions are used to maintain the heading while high-frequency rudder motions are used to reduce the roll motions. For this purpose a new mathematical model is introduced which enables the desired separation in the frequency domain.
The ship's steering machine introduces non-linearities which would normally prevent the application of linear controller-design methods. Nevertheless, it appeared to be possible to use the Linear process Quadratic criterion Gaussian noise (LQG) control method by applying two new mechanisms:

- The Automatic Gain Controller (AGC) instantaneously prevents a controller from generating signals which cannot be followed by the steering machine.
- The LQG algorithms applied use a criterion having weighting parameters which are adjusted automatically to changing conditions. In combination with the AGC

they effectively remove the non-linearities from the control loop.
The LQG method requires the states of the process to be known. Modern filter techniques are applied to estimate the states which cannot be measured and to remove undesirable components from the measurements. For their part, these techiques require the variances of the measurement noise and the process noise to be known. The adaptive approach introduced solves this problem.

The resulting control algorithms were implemented in a laboratory version of an RRS autopilot. From a safety point of view als well as for economic reasons it was not allowed to test this autopilot directly on board a ship. Therefore, initially experiments were carried out which gradually approached reality more and more.

- Experiments with a simple analog model of a ship enabled the control algorithms to be verified and the hardware of the autopilot to be tested.
- Experiments at the MARIN with an extended mathematical model of a similar ship enabled the influence of some unmodeled ship motions on the autopilot performance to be investigated.
- Finally, experiments with a remote-controlled scale model of a similar ship were carried out to investigate whether unanticipated practical problems may be encountered.

After that, several full-scale trials were carried out. In general, the results of these experiments agreed with those of the previous experiments. Moreover, they demonstrated the importance of full-scale trials; several practical additions to the RRS autopilot are based on observations made during these measurements.

In Chapter 1 the idea of reducing the roll motions by means of the rudder is introduced. In addition, it gives a short overview of the advantages and disadvantages of RRS with respect to other roll-reducing systems.
Chapter 2 describes simple models of the ship's steering machine and the disturbances. In addition, it poses a new mathematical model of a ship and it demonstrates how the parameters of this model were obtained.
Chapters 3 and 4 give the theory behind respectively the control and the filter algorithms. This theory offers the optimal (with respect to a quadratic criterion) control action under the conditions that the process be linear and that a model of the process be known. A new method is proposed which enables this theory to be applied to the RRS problem and which matches well the adaptation mechanism proposed in Chapter 5. This adaptation mechanism allows the theory to be applied to non-linear processes, even if the conditions or the desired performance are subject to change.
Chapter 6 deals with the realization of the control and filter algorithms in a

laboratory version of an RRS autopilot. In addition, it demonstrates how the requirements to be posed on an RRS autopilot can be translated into the weighting parameters of a quadratic criterion. Furthermore, it indicates which requirements should be met by a ship and its steering machine to enable a good performance of an RRS system.

Chapter 7 covers the results of the experiments which were carried out. Finally, Chapter 8 summarizes the conclusions and gives some suggestions for furthur research.

CONTENTS

1 INTRODUCTION

1.1 The RRS project

During the last two decades much research has been carried out at the Control Laboratory of the Faculty of Electrical Engineering of Delft University of Technology in the field of ship control systems. One of the results of this research has been an autopilot for ships which is easy to operate and which adjusts itself to changing weather conditions (Van Amerongen, 1982). In addition, the autopilot generates only a minimum of low-frequency rudder activity to maintain the heading of the ship.
Since 1972 several publications appeared in the literature on the subject *Rudder Roll Stabilization* (**RRS**), where the rudder is not only used to maintain the heading of the ship, but to reduce the roll motions as well. Cowley and Lambert (1972, 1975), Carley (1975) and Lloyd (1975) demonstrated through simulation studies that roll reduction by means of the rudder is possible but not very effective. These studies did not result in a successful practical application of the RRS principle. Apparently, the state of the art had not developed sufficiently to offer solutions to the inherent control problems.
After some years had passed the idea of RRS was picked up again when Baitis (1980) reported more promising results. He carried out experiments in practice in which stabilization signals were superimposed on the manual control of the heading. Källström (1981) demonstrated in a simulation study that roll stabilization by means of the rudder might be more effective than fin stabilizers. Since then, computer technology and the state of the art of the filter theory and the control theory have evolved sufficiently to enable researchers to tackle the control problems which had previously prevented the realization of an RRS autopilot.

The RRS principle requires two outputs (the roll angle and the heading error) to be controlled by one input (the rudder). The control tasks can be separated in the frequency domain; high-frequency components are used to reduce the roll motions while low-frequency components are used to maintain the heading of the ship.
Van Amerongen (1982, 1984) offered a solution to the course control problem. One of the properties of this solution is that only low-frequency rudder motions are used to maintain the heading of the ship. Therefore, it promised to be a good basis for the development of an RRS system.

In cooperation with the *Royal Netherlands Navy* modeling trials were carried out on board a naval ship. These trials resulted in a simple mathematical model which can be used as a basis for the design of an RRS-controller (Van Amerongen and Van Cappelle, 1981). Simulation experiments at the Control Laboratory indicated that a substantial roll reduction can be obtained if the maximum rudder speed is sufficiently high (Van der Klugt, 1982 and Van Amerongen and Van Nauta Lemke, 1982). These first promising results led to a joint project between industry, the Navy and the university, called *the RRS project*. The company *Van Rietschoten & Houwens* financially supported the project. The Royal Netherlands Navy contributed the facilities needed to carry out full-scale trials on board a naval ship. In addition, they arranged trials with a scale model and experiments with the simulation computer of the *Maritime Research Institute Netherlands* (**MARIN**) in Wageningen. Lastly, the Control Laboratory contributed its knowledge in the field of ship's autopilots and of advanced control methods.

The first objective of the RRS project was to find the answers to two pending problems:

1 Is it possible to realize RRS in practice?
2 Which modifications in a ship design are required to enable a successful application of an RRS system?

Within one year the answers were obtained by means of the following sequence of experiments:

- Simulation experiments at the Control Laboratory using the simulation program PSI (Van den Bosch, 1981) led to some knowledge about the demands posed on an RRS system (Van Amerongen and Van Nauta Lemke, 1982). Based on these results a simple RRS controller was added to the available laboratory realization of a ship's autopilot.
- The resulting laboratory realization of an RRS autopilot was tested by a simple analog model of a naval ship. The results agreed with the computer simulations.
- Based on a hydrodynamic approach, the MARIN in Wageningen has designed a computer model of a similar ship. Experiments were carried out, in which the RRS autopilot was connected to the MARIN simulation computer. The results of these experiments confirmed the results which were obtained at the Control Laboratory. In addition, they indicated which modifications in a ship design would improve the performance of an RRS system.
- The next series of experiments was carried out at the Haringvliet, a sea arm in the south-west of Holland, with an 8-meter long remote-controlled scale model of a naval ship. Several practical problems which were not foreseen during the

simulation experiments led to some important additions to the RRS algorithms.
- Full-scale trials were carried out in March 1983 on board a similar naval ship. The results with a carefully tuned controller agreed with the results of the simulation experiments at the Control Laboratory and at the MARIN in Wageningen (Van Amerongen, Van der Klugt and Pieffers, 1984). They demonstrated that roll stabilization by means of the rudder is indeed possible. In addition, they demonstrated that the simulation experiments are a reliable means of predicting the performance of an RRS system. Based on these results, the Royal Netherlands Navy decided to prefer RRS over fin stabilizers in their design of a new ship.

The second objective of the RRS project was to design within four years a laboratory version of an RRS system which could be the basis for an actual realization. In an early stage of the project it was recognized that the two main problems to be solved were the following:

1 The first experiments were carried out with carefully tuned RRS controllers. This is not allowed in practice. The ship's operator should have no more than one additional switch available (RRS on - RRS off) and the RRS controller should tune itself to changing conditions.
2 Due to the coupling between roll motions and yaw motions, low-frequency roll motions and high-frequency yaw motions may deteriorate the performance of an RRS system. Therefore, it is necessary to obtain a good separation in the frequency domain.

This thesis offers a solution to these problems. An adaptation mechanism is proposed which automatically adjusts the RRS controller to changing conditions. In addition, the means of obtaining the required separation in the frequency domain are introduced. The resulting control algorithms are implemented in a new laboratory realization of an RRS autopilot. They have been extensively tested during the following experiments:
- Computer simulations with the simulation package PSI, which gave some insight into the adaptation speed of the control algorithms.
- Simulations at the Control Laboratory, in which the RRS autopilot had to control a simple analog model of a naval ship.
- Simulations at the MARIN in Wageningen, in which the RRS autopilot had to control the computer models of two naval ships.

The results of these experiments demonstrate that the original objective has been met; within 4 years a laboratory version of an RRS autopilot was designed with the desired characteristics. Unfortunately, only the concluding full-scale trials could not

be carried out in that period. These initially had to be postponed because of some difficulties with the hardware. Once the trials were finally scheduled to be carried out, the weather conditions were not suitable to demonstrate roll reduction (Van Amerongen and Van der Klugt, 1987b). Nevertheless, these trials were useful to test several other properties of the RRS autopilot such as the course keeping performance and the "forced roll" option.

1.2 Roll stabilization

Even at moderate sea states the wave-induced ship motions can be large enough to endanger cargo, to make certain operations (such as landing helicopters) difficult or to make people feel uncomfortable.
This thesis mainly deals with the reduction of one of these motions, the *roll* motion.

On merchant ships large roll motions are not desirable in order to prevent cargo damage. On naval ships large roll motions can lead to a reduction in the operational time. For all ships heavy roll motions reduce the effectiveness of the crew. It is a common fact that tired people tend to make more mistakes. Therefore, from a safety point of view as well as from an operational point of view, it is desirable that the roll motions of a ship remain low.

In the past, many solutions have been realized to accomplish roll reduction. Several of them will be mentioned below, together with their main advantages or disadvantages. More detailed descriptions can be found in the literature, for example in Burger and Corbet (1966) and in Bhattacharyya (1978).

Bilge keels are the most widely used, as well as the simplest kind of roll stabilizing devices. They are inexpensive but increase the hull resistance and are effective mainly around the natural roll frequency of the ship. In addition, their effect decreases with the ship's speed.

Anti-rolling tanks provide damping of the roll motions, even if the ship's speed is low, at the expense of a lot of valuable space.
Several types are currently in use, including free-surface tanks, U-tube tanks and diversified tanks. The last are interesting for ships in which fuel, ballast or cargo can be used.

Fin stabilizers can provide a considerable damping of the roll motions of a ship if the ship's speed is not too low, but they are expensive. In addition, they introduce

drag on the ship in the forward direction even if roll stabilization is not required. Therefore, some ships are equipped with the more expensive *rectractable fin stabilizers* or fin stabilizers of the *hinged type*. *Tail flaps* may improve the effectiveness of the fin stabilizers.

Roll stabilization by means of the rudder (RRS) can be regarded as a relatively inexpensive alternative to fin stabilizers. Although the basic idea was known for many years, RRS did not manage to pass the experimental stage, partly due to some inherent control problems. This thesis offers solutions to these control problems, thus paving the way to a practical realization of an RRS system.

Although fin stabilizers are commonly accepted nowadays as a good means of reducing the roll motions of a ship, a comparison of some of the main advantages and disadvantages with those of a rudder-roll-stabilization system explains the current interest in roll stabilization by means of the rudder.

Fin stabilizers:

- have proven to be an effective means of reducing the roll motions of a ship. They can even reduce low-frequency roll motions or a stationary roll angle.

However, they

- are expensive and introduce (at least) two "extra" hydraulic systems which require space and maintainance,
- cause drag even if roll stabilization is not required (unless retractable fins are used),
- are not effective if the ship's speed is low,
- require the ship to be reinforced at those places where they are mounted; they are vulnerable and introduce additional vulnerable spots on the ship's hull,
- cause underwater noise (important for naval ships) close to the sensors, and
- are very expensive to mount on existing ships.

Rudder Roll Stabilization:

- can be as effective as fin stabilizers,
- is less expensive although it requires a fast, rigid rudder which can generate a large roll moment,
- causes no drag if roll stabilization is not required,
- can be mounted on existing ships although such a system will be more effective if it is incorporated in the ship design, and
- may cause underwater noise, but only if roll stabilization is required.

However, RRS
- is not effective if the ship's speed is low,
- is not capable of reducing low-frequency roll motions or a stationary roll angle, and
- requires some structural reinforcement in the stern.

Naturally, a multivariable approach, where both fin stabilizers and the rudder are used to reduce the roll motions and to maintain the heading of the ship, offers the optimal roll reduction. This was confirmed by Källström (1981) by means of simulation experiments. However, it is the most expensive solution.
The currently popular solution is based on having two separate controller designs, one which uses the rudder to maintain the heading of the ship and one which uses fin stabilizers to reduce the roll motions. Källström showed that RRS may offer a better solution. This was confirmed by Van Amerongen, Van der Klugt and Pieffers (1984) by means of a comparison between the results of simulation experiments and full-scale experiments.

1.3 The organization of the thesis

This thesis deals with the design of an RRS system; it is organized as follows:

Chapter two poses a simple mathematical model of a ship. It is based on the results of scale modeling experiments as well as modeling experiments with a more extended mathematical model of a similar ship. This extended model has been developed by the MARIN in Wageningen, based on a hydrodynamic approach. In addition, simple models which sufficiently describe the steering machine and the disturbances are given.
Chapter three treats the fundamental controller design, based on the LQG approach. This approach requires the process to be linear and the states of the process to be known.
The problem of estimating states which cannot be measured or which are corrupted by undesired components is treated in *Chapter four*. In addition, it gives the tools necessary to obtain the desired separation of roll motions and yaw motions in the frequency domain.
Chapter five shows how to deal with the non-linearities introduced by the steering machine. Several requirements which have to be met for the practical realization of an RRS system are discussed. These requirements set demands on the steering

machine as well as on the controller. In addition, Chapter five offers some new insights into the application of optimal-controller-design techniques resulting in a new adaptation mechanism.

In *Chapter six* the practical realization of the control algorithms is given. Furthermore, Chapter six poses several demands on the ship design and the steering machine.

Chapter seven presents the results of several experiments. Computer simulations at the Control Laboratory were followed by experiments with a first version of an RRS system. These have been carried out at the Control Laboratory (with an analog model of a naval ship) and at the MARIN in Wageningen. In addition, full-scale trials have been carried out on the North Sea.

Finally, *Chapter eight* summarizes the conclusions and offers some suggestions for a potential further improvement of the designed RRS-autopilot.

2 MATHEMATICAL MODELING

2.1 Introduction

To design a controller for a particular process first a model of the process has to be derived. This model should "sufficiently" describe the relevant dynamics of the process. In general, the more complex a model is, the more difficult the controller design will be. Therefore, the model of the process should be as simple as possible. If the information is not sufficiently available, it will be necessary to obtain the information from measurements on the process, for instance by means of modeling experiments.
In a latter stage of the design process it may be required to verify the performance of the controller design by means of simulation experiments. In general, a slightly more extensive model than that used for the controller design will be sufficient.
In many cases it is difficult to obtain the required model parameters or they may vary in time. This will lead to the design of a more complex controller.

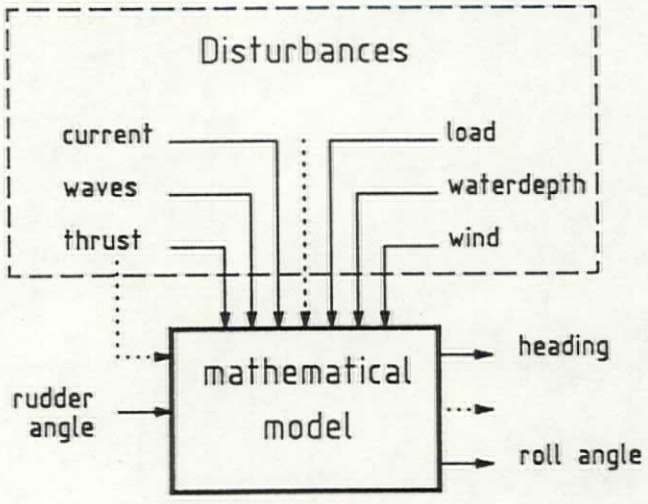

Fig. 2.1 The ship and its environment

A Rudder Roll Stabilization System maintains the ship's heading and reduces the roll angle by means of only one actuator: the rudder. Therefore, in principle such a system is a *Single-Input Multi-Output* (**SIMO**) system.
Other motions which play a role are then classified as disturbances (Fig. 2.1). These disturbances can be subdivided into two categories:

- disturbances which influence the parameters of the transfer functions (multiplicative signals) and

- disturbances which can be considered as additional input signals (additive signals).

A model based on physical laws can be a good starting point for deriving a simple mathematical model. In Section 2.2 this approach will be considered further to develop a model of a ship. Section 2.3 gives the model of a steering machine while Section 2.4 discusses the model of the disturbances. Finally, Section 2.5 presents the results of some modeling experiments.

2.2 The ship model

2.2.1 Mathematical models based on physical laws

To analyze the dynamics of a ship it is convenient to define a coordinate system as indicated in Fig. 2.2.

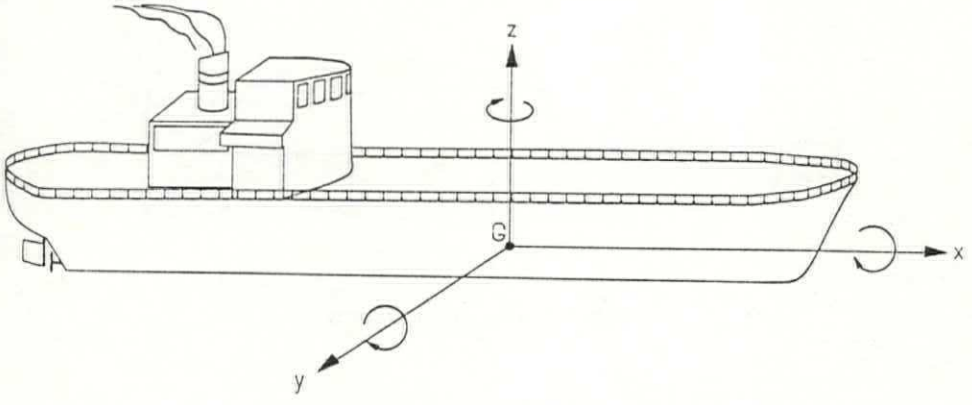

Fig. 2.2 The coordinate system.

The ship's center of gravity G is chosen as the origin of this coordinate system and the axes of symmetry are chosen as x (the intended heading in the horizontal plane), y and z.

A floating body has six degrees of freedom. To completely define the dynamics of a ship it is necessary to consider the motions in all these degrees of freedom (see Fig. 2.3).

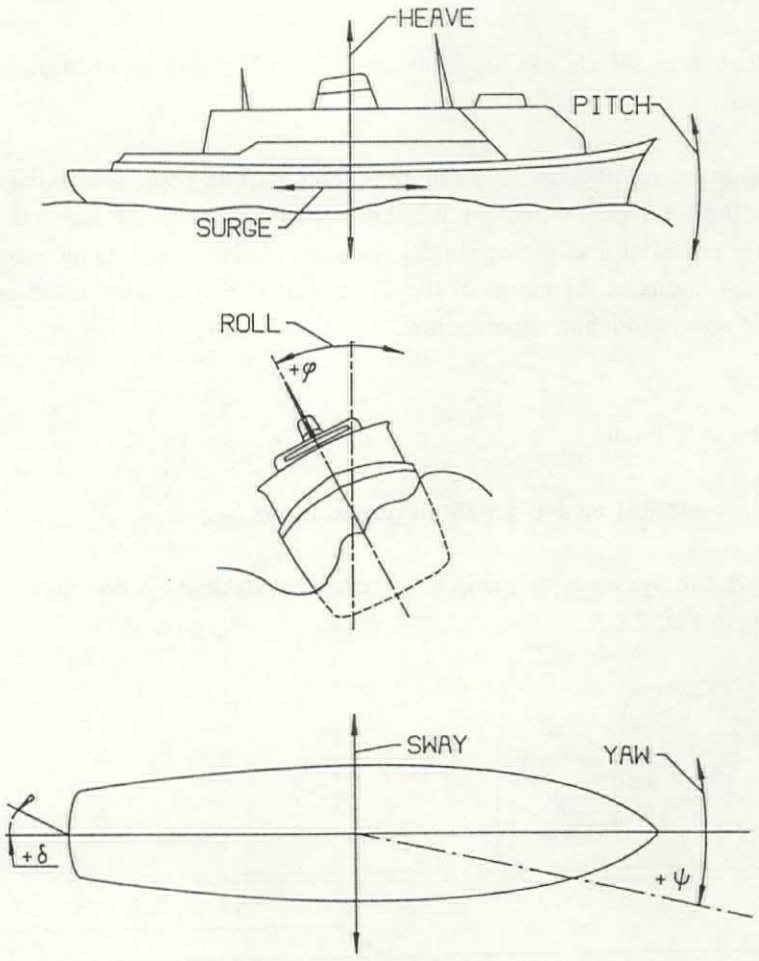

Fig. 2.3 The ship motions

It is possible to distinguish two classes of motions:

- If the motions of given points on the port side of the ship and similar points on the starboard side have no components in the y direction, they are referred to as the class of the symmetrical motions. The elements of this class are pitch, surge and heave (see Fig. 2.3).
- If these motions have components in the y direction, they are referred to as asymmetrical motions. The elements in this class are roll, yaw and sway.

Within one class the motions are coupled. Motions from different classes are to a fair approximation uncoupled. Within the context of this thesis only the asymmetrical motions are considered. The influence of the other motions is treated as a disturbance.

The basic equations for the relevant motions are obtained by writing Newton's laws in a space-fixed coordinate system:

$$m_{y0}\frac{d^2y_0}{dt^2} = Y_0 \qquad \textit{(sway)} \qquad (2.1)$$

$$I_{zz0}\frac{d^2y_0}{dt^2} = N_0 \qquad \textit{(yaw)} \qquad (2.2)$$

$$I_{xx0}\frac{d^2f_0}{dt^2} = K_0 \qquad \textit{(roll)} \qquad (2.3)$$

where

x_o, y_o, z_o = axes of a space-fixed coordinate system
m_{y0} = effective mass of the ship in the y_o direction
Y_o = force in the y_o direction
y_o = course angle or heading
f_o = roll angle
I_{zz0}, I_{xx0} = moments of inertia with respect to the z_o- and x_o-axes
N_o, K_o = moments with respect to the z_o- and x_o-axes

The index "0" in the variables indicates that they are related to the space-fixed coordinate system. Translating these equations to the coordinate system of Fig. 2.2

yields

$$m_y(\dot{v}+ur) = Y \qquad (2.4)$$

$$I_{zz}\dot{r} = N \qquad (2.5)$$

$$I_{xx}\dot{p} = K \qquad (2.6)$$

where

x, y, z = axes of the ship-fixed coordinate system
m_y = effective mass of the ship in the y direction
Y = force in the y direction
$r = \dot{\psi}$ = rate of turn
v = drift or sway speed
u = dx/dt, the speed in the forward direction
$p = \dot{\varphi}$ = roll rate
I_{ZZ}, I_{XX} = moments of inertia with respect to the z- and x-axes
N, K = moments with respect to the z- and x-axes

The force Y is the sum of all the forces which act on the hull of the ship in the y-direction. N and K are the moments caused by these forces. In general, approximations are made by writing, for example,

$$N = f(u,\dot{u},v,\dot{v},r,\dot{r},\varphi,\dot{\varphi},u^2,v^2,r^2,\varphi^2,\ldots)$$

Expansion of this equation into a Taylor series yields

$$dN = \frac{\partial f}{\partial u}u + \frac{\partial f}{\partial \dot{u}}\dot{u} + \frac{\partial f}{\partial v}v + \frac{\partial f}{\partial \dot{v}}\dot{v} + \frac{\partial f}{\partial r}r + \frac{\partial f}{\partial \dot{r}}\dot{r} + \frac{\partial f}{\partial \varphi}\varphi + \frac{\partial f}{\partial \dot{\varphi}}\dot{\varphi} + \frac{\partial f}{\partial w}w + \text{higher-order terms}$$

where u stands for Δu, and so on.

When the "hydrodynamic derivatives" are denoted as, for instance,

$$\frac{\partial f}{\partial u} = N_u$$

and the higher-order terms are omitted, Eqs. (2.4) to (2.6) can be rewritten:

$$m_y(\dot{v}+ur) = Y_v v + Y_{\dot{v}}\dot{v} + Y_r r + Y_\varphi \varphi + Y_{\dot{\varphi}}\dot{\varphi} + Y_\delta \delta + Y_w w \qquad (2.7)$$

$$I_{zz}\dot{r} = N_v v + N_r r + N_{\dot{r}}\dot{r} + N_\varphi \varphi + N_{\dot{\varphi}}\dot{\varphi} + N_\delta \delta + N_w w \qquad (2.8)$$

$$I_{xx}\dot{p} = K_v v + K_r r + K_\varphi \varphi + K_{\dot{\varphi}}\dot{\varphi} + K_\delta \delta + K_w w \qquad (2.9)$$

The force Y_w is the sum of all the forces in the y-direction which are caused by the additive disturbances w. N_w and K_w are the moments caused by these forces. Y_0, N_0 and K_0 are assumed to be zero.

For small variations linear models will suffice, but for large signals it is not allowed to leave the higher-order terms out of Eqs. (2.7) to (2.9). However, the complexity of such a non-linear model makes it unattractive for the purpose of designing a controller.

Laplace transformation of Eqs. (2.7) to (2.9) yields

$$\begin{aligned}(s(m_y(s)-Y_{\dot{v}}(s))-Y_v(s))v(s) &= (Y_r(s)-m_y(s)u(s))r(s) + \\ &+ (Y_\varphi(s)+sY_{\dot{\varphi}}(s))\varphi(s) + Y_\delta(s)\delta(s) + Y_w(s)w(s)\end{aligned} \qquad (2.10)$$

$$\begin{aligned}(s(I_{zz}(s)-N_{\dot{r}}(s))-N_r(s))r(s) &= N_v(s)v(s) + \\ &+ (N_\varphi(s)+sN_{\dot{\varphi}}(s))\varphi(s) + N_\delta(s)\delta(s) + N_w(s)w(s)\end{aligned} \qquad (2.11)$$

$$\begin{aligned}(s^2I_{xx}(s)-sK_{\dot{\varphi}}(s)-K_\varphi(s))\varphi(s) &= K_v(s)v(s) + \\ &+ K_r(s)r(s) + K_\delta(s)\delta(s) + K_w(s)w(s)\end{aligned} \qquad (2.12)$$

or

$$v(s) = H_{\delta v}(s)\delta(s)+H_{wv}(s)w(s)+H_{rv}(s)r(s)+H_{\varphi v}(s)\varphi(s) \qquad (2.13)$$

where

$$H_{\delta v}(s) = \frac{Y_{\delta}(s)}{s(m_y(s)-Y_{\dot{v}}(s))-Y_v(s)} = H'_{\delta v}(s)H_v(s) \qquad (2.13)a$$

$$H_{wv}(s) = \frac{Y_w(s)}{s(m_y(s)-Y_{\dot{v}}(s))-Y_v(s)} = H'_{wv}(s)H_v(s) \qquad (2.13)b$$

$$H_{rv}(s) = \frac{Y_r(s)-m_y(s)u(s)}{s(m_y(s)-Y_{\dot{v}}(s))-Y_v(s)} = H'_{rv}(s)H_v(s) \qquad (2.13)c$$

$$H_{\varphi v}(s) = \frac{sY_{\dot{\varphi}}(s)+Y_{\varphi}(s)}{s(m_y(s)-Y_{\dot{v}}(s))-Y_v(s)} = H'_{\varphi v}(s)H_v(s) \qquad (2.13)d$$

$$H_v(s) = \frac{1}{s(m_y(s)-Y_{\dot{v}}(s))-Y_v(s)} \qquad (2.13)e$$

and

$$r(s) = H_{\delta r}(s)\delta(s)+H_{wr}(s)w(s)+H_{vr}(s)v(s)+H_{\varphi r}(s)\varphi(s) \qquad (2.14)$$

where

$$H_{\delta r}(s) = \frac{N_{\delta}(s)}{s(I_{zz}(s)-N_{\dot{r}}(s))-N_r(s)} = H'_{\delta r}(s)H_r(s) \qquad (2.14)a$$

$$H_{wr}(s) = \frac{N_w(s)}{s(I_{zz}(s)-N_{\dot{r}}(s))-N_r(s)} = H'_{wr}(s)H_r(s) \qquad (2.14)b$$

$$H_{vr}(s) = \frac{N_v(s)}{s(I_{zz}(s)-N_r^{\cdot}(s))-N_r(s)} = H'_{vr}(s)H_r(s) \qquad (2.14)c$$

$$H_{\varphi r}(s) = \frac{sN_{\varphi}^{\cdot}(s)+N_{\varphi}(s)}{s(I_{zz}(s)-N_r^{\cdot}(s))-N_r(s)} = H'_{\varphi r}(s)H_r(s) \qquad (2.14)d$$

$$H_r(s) = \frac{1}{s(I_{zz}(s)-N_r^{\cdot}(s))-N_r(s)} \qquad (2.14)e$$

and finally

$$\varphi(s) = H_{\delta\varphi}(s)\delta(s)+H_{w\varphi}(s)w(s)+H_{r\varphi}(s)r(s)+H_{v\varphi}(s)v(s) \qquad (2.15)$$

where

$$H_{\delta\varphi}(s) = \frac{K_{\delta}(s)}{s^2I_{xx}(s)-sK_{\varphi}^{\cdot}(s)-K_{\varphi}(s)} = H'_{\delta\varphi}(s)H_{\varphi}(s) \qquad (2.15)a$$

$$H_{w\varphi}(s) = \frac{K_w(s)}{s^2I_{xx}(s)-sK_{\varphi}^{\cdot}(s)-K_{\varphi}(s)} = H'_{w\varphi}(s)H_{\varphi}(s) \qquad (2.15)b$$

$$H_{v\varphi}(s) = \frac{K_v(s)}{s^2I_{xx}(s)-sK_{\varphi}^{\cdot}(s)-K_{\varphi}(s)} = H'_{v\varphi}(s)H_{\varphi}(s) \qquad (2.15)c$$

$$H_{r\varphi}(s) = \frac{K_r(s)}{s^2I_{xx}(s)-sK_{\varphi}^{\cdot}(s)-K_{\varphi}(s)} = H'_{r\varphi}(s)H_{\varphi}(s) \qquad (2.15)d$$

$$H_{\varphi}(s) = \frac{1}{s^2 I_{xx}(s) - sK_{\dot{\varphi}}(s) - K_{\varphi}(s)} \qquad (2.15)e$$

Eqs. (2.13) to (2.15) describe three ship motions which are relevant with respect to the design of an RRS system. In the following they will be referred to as the *hydrodynamic model*. The parameters of this model may be a function of the fourth relevant motion: the ship's speed. A block diagram of the model is shown in Fig. 2.4.

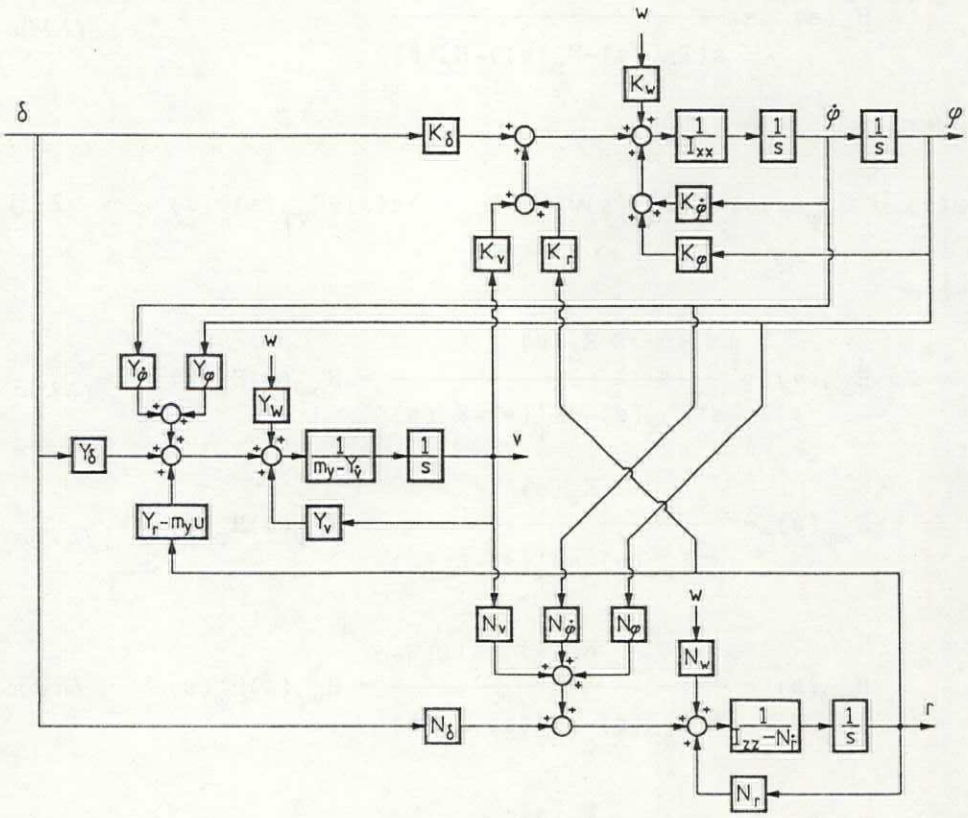

Fig. 2.4 Block diagram of the hydrodynamic model.

2.2.2 A new ship model

The hydrodynamic model, described by Eqs. (2.13) to (2.15), is not suitable for the purpose of designing a controller. However, it can be used to derive a simple model which is suitable. It will be assumed that the transfer functions $Y_w(s)$, $N_w(s)$ and $K_w(s)$, until now defined as forces and moments, are sufficiently accurately described by second-order transfer functions driven by white noise.
Eqs. (2.13) to (2.15) can be simplified by combining several terms and disregarding some hydrodynamic effects. This is confirmed by the identification experiments described in Section 2.5.
After reordering terms, these equations are rewritten into a more convenient form, resulting in the equations given below:

The sway velocity is described by

$$v(s) = H_{\delta v}(s)\delta(s) + H_{rv}(s)r(s) + H_{wv}(s)w(s) \qquad (2.16)$$

where

$$H_{\delta v}(s) = k_{\delta v}/(s\tau_v+1) = k_{\delta v}H_v(s) \qquad (2.16a)$$

$$H_{rv}(s) = k_{rv}/(s\tau_v+1) = k_{rv}H_v(s) \qquad (2.16b)$$

$$H_{wv}(s) = \frac{\omega_{wv}^2 k_{wv}(s\tau_{wv}+1)}{s^2+2z_{wv}\omega_{wv}s+\omega_{wv}^2} * \frac{1}{s\tau_v + 1} = H'_{wv}(s)H_v(s) \qquad (2.16c)$$

Comparing Eq. (2.13) and Eq. (2.16) yields:

$$k_{\delta v} = -Y_\delta(s)/Y_v(s)$$

$$\tau_v = (Y_v^{\cdot}(s)-m_y(s))/Y_v(s)$$

$$k_{rv} = (m_y(s)u(s)-Y_r(s))/Y_v(s)$$

$$H'_{wv}(s) = -Y_w(s)/Y_v(s)$$

The rate of turn is described by

$$r(s) = H_{\delta r}(s)\delta(s) + H_{vr}(s)v(s) + H_{wr}(s)w(s) \qquad (2.17)$$

where

$$H_{\delta r}(s) = k_{dr}/(s\tau_r+1) = k_{dr}H_r(s) \qquad (2.17a)$$

$$H_{rv}(s) = k_{vr}/(s\tau_r+1) = k_{vr}H_r(s) \qquad (2.17b)$$

$$H_{wr}(s) = \frac{\omega_{wr}^2 k_{wr}(s\tau_{wr}+1)}{s^2+2z_{wr}\omega_{wr}s+\omega_{wr}^2} * \frac{1}{s\tau_r + 1} = H'_{wr}(s)H_r(s) \qquad (2.17c)$$

Comparing Eq. (2.14) and Eq. (2.17) yields:

$$k_{dr} = -N_\delta(s)/N_r(s)$$

$$\tau_r = (N_r^\cdot(s)-I_{zz}(s))/N_r(s)$$

$$k_{vr} = -N_v(s)/N_r(s)$$

$$H'_{wr}(s) = -N_w(s)/N_r(s)$$

Finally, the roll angle is described by

$$\varphi(s) = H_{\delta\varphi}(s)\delta(s)+H_{r\varphi}(s)r(s)+H_{v\varphi}(s)v(s)+H_{w\varphi}(s)w(s) \qquad (2.18)$$

where

$$H_{\delta\varphi}(s) = \frac{k_{dp}\omega_n^2}{s^2 + 2z_n\omega_n s + \omega_n^2} = k_{dp}H_\varphi(s) \qquad (2.18)a$$

$$H_{r\varphi}(s) = \frac{k_{rp}\omega_n^2}{s^2 + 2z_n\omega_n s + \omega_n^2} = k_{rp}H_\varphi(s) \qquad (2.18)b$$

$$H_{v\varphi}(s) = \frac{k_{vp}\omega_n^2}{s^2 + 2z_n\omega_n s + \omega_n^2} = k_{vp}H_\varphi(s) \qquad (2.18)c$$

$$H_{w\varphi}(s) = \frac{\omega_{wp}^2 k_{wp} s}{s^2+2z_{wp}\omega_{wp}s+\omega_{wp}^2} * \frac{\omega_n^2}{s^2+2z_w\omega_w s+\omega_n^2} = H_{wp}(s)H_\varphi(s) \qquad (2.18)d$$

$$H_\varphi(s) = \frac{\omega_n^2}{s^2+2z_w\omega_w s+\omega_n^2} \qquad (2.18)e$$

Comparing Eq. (2.15) and Eq. (2.18) yields:

$$k_{dp} = K_\delta(s)/K_\varphi(s)$$

$$\omega_n^2 = K_\varphi(s)/I_{xx}(s)$$

$$2z_n\omega_n = K_\varphi^*(s)/I_{xx}(s)$$

$$k_{rp} = K_r(s)/K_\varphi(s)$$

$$k_{vp} = K_v(s)/K_\varphi(s)$$

$$H_{wp}(s) = K_w(s)/K_\varphi(s)$$

A block diagram of the resulting model is shown in Fig. 2.5. The parameters of this model depend on the speed of the ship. This is investigated in detail in Section 2.5.5. An integration can be added to describe the yaw motion.

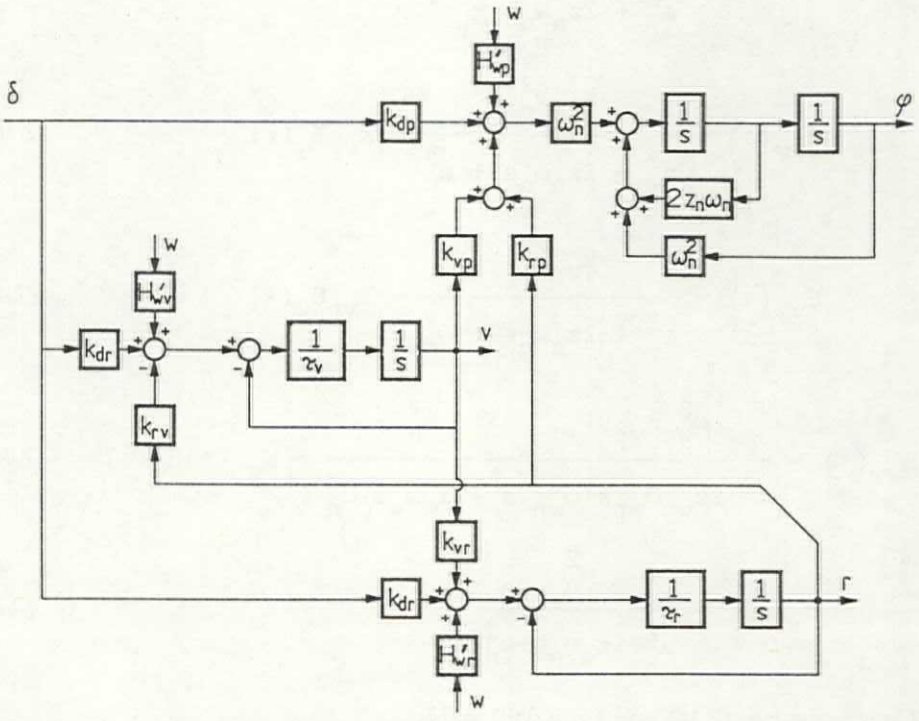

Fig. 2.5 The block diagram of the resulting model

The model is too complex to be used as a basis for a controller design. The identification experiments described in Section 2.5 indicate that it is allowed to further reduce this model to the model of Fig. 2.6. The main differences are the following:

- In Fig. 2.6 w_φ and w_ψ denote the influence of the waves on respectively the roll moment and the yaw moment. The transfer functions resulting in these signals can be derived from Fig. 2.5 (similar parameters in Figures 2.5 and 2.6 do not necessarily have the same value).
- An integration describing the yaw motion is added.
- The sway velocity v has disappeared from the model. Instead, the parameter v' denoting *the sway velocity caused by the rudder* is introduced.

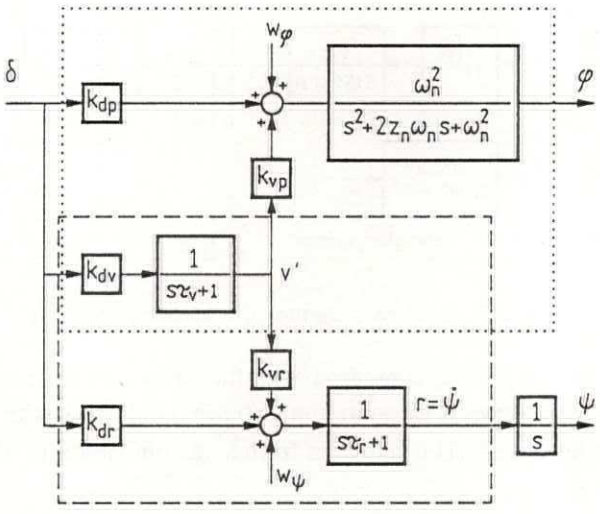

Fig. 2.6 The block diagram of the new ship model

Henceforth, the model of Fig. 2.6 will be referred to as *the fifth-order ship model.* In addition, w_φ and w_ψ will be regarded as *colored noise.*

A major advantage of this model is that it can be easily subdivided into two submodels which can be used as a basis for a controller design. The submodel within the dotted lines describes the rudder-to-roll transfer and will be referred to as *the third-order roll model.* The submodel within the dashed lines describes the rudder-to-rate-of-turn transfer and resembles a second-order Nomoto model (Nomoto et al., 1957). This model, in combination with an integration to describe the yaw motion, will be referred to as *the third-order yaw model.*

2.3 Model of the steering machine

The actuator which makes the actual rudder angle δ_w equal to the desired rudder angle δ_g set by the autopilot or the helmsman is the steering machine.
Van Amerongen (1982) describes the model of a steering machine configuration which is shown in Fig. 2.7.

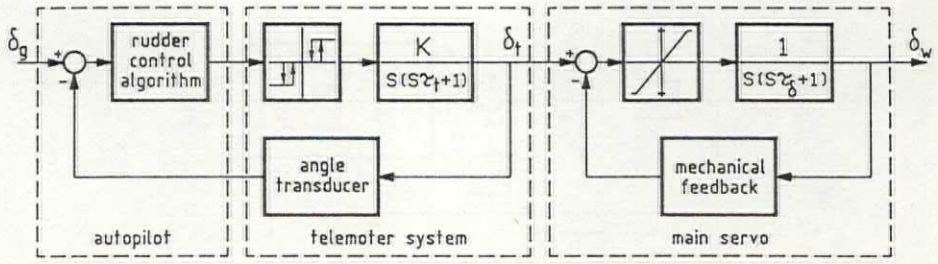

Fig. 2.7 A block diagram of a steering machine

The telemotor system is fast, compared with the main servo. In addition, the time constant of the main servo is of minor importance, compared with the influence of the limited rudder speed. This allows a further simplification of this model to the model of Fig. 2.8.

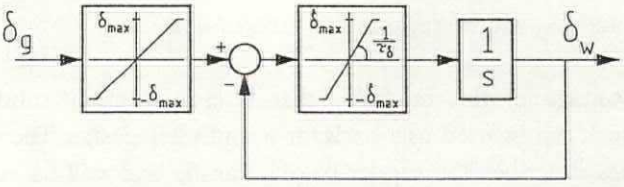

Fig. 2.8 A simplified block diagram of the steering machine

This block diagram contains two limiters, one describing the limitation of the rudder angle and the other describing the limitation of the rudder speed. The rudder limit is either determined by the rudder-angle constraints of the autopilot, or by the mechanical constraints. The maximum rudder speed is determined by the maximum valve opening and the pump capacity of the steering machine. The classification companies require the rudder to be able to move from 35 degrees port to 35 degrees starboard within 30 seconds. A maximum rudder speed of as low as 2.5 degrees per second is sufficient to meet this requirement. In Section 6.5 it is shown that an RRS system poses new demands on the steering machine.

2.4 Modeling the disturbances

2.4.1 Introduction

It is possible to distinguish three categories of disturbances which are relevant with respect to the design of an RRS-system:

- *Additive disturbances*: These can be seen as additional input signals to the process (e.g. wind, waves, current etc.). It will be assumed that it is allowed to superimpose the moments of these additive disturbances to the other moments.
- *Multiplicative disturbances*: These are the disturbances which influence the transfer function of the process (e.g. depth of water, load condition, trim, speed changes etc.).
- *Measurement disturbances*: These are the disturbances which are due to incorrect measurement or incorrect treatment of measurement signals (e.g. inaccuracy of sensors, sensor failure, round off errors etc.).

The mathematical models of a ship which are given in Section 2.2 do not describe all the ship motions; they are a submodel of a larger model describing all the ship motions. For instance, the pitch motion is not described by these models, nor is the influence of the thrust. Nevertheless, these other motions might influence the motions of the submodel.
This influence can be regarded as "disturbances" belonging to one of the above-mentioned categories. Some of these "disturbances" are controllable (by other subsystems of the ship), while others are not. An example of the latter is the heave motion. An example of a controllable "disturbance" is the revolution of the propeller(s).
The ship's thrust has such a large influence on the parameters of the submodel that it is modeled explicitly in Section 2.5.

2.4.2 Wind

The forces and moments of the wind depends on such factors as:

- the relative wind speed (the speed of the wind as it would be measured on board),
- the wind direction,
- the shape and size of the ship's superstructure.

The wind induces a roll moment which can be approximated by

$$K_{w\varphi} = c_{w\varphi} V_w^2 \sin(\gamma) \qquad (2.19)$$

as well as a yaw moment which can be approximated by

$$N_{wr} = c_{wr} V_w^2 \sin(2\gamma) \qquad (2.20)$$

where $c_{w\varphi}$ and c_{wr} depend on the shape of the ship, the relevant area of the ship's superstructure, the air density, etc. Within the context of this thesis they are considered as constants.

V_w = the relative wind speed. It consists of two components: a constant component and a component representing the stochastic variations of the speed and the relative wind angle.

γ = the relative average wind angle in degrees ($-180 < \gamma \leq 180$) defined as indicated in Fig. 2.9.

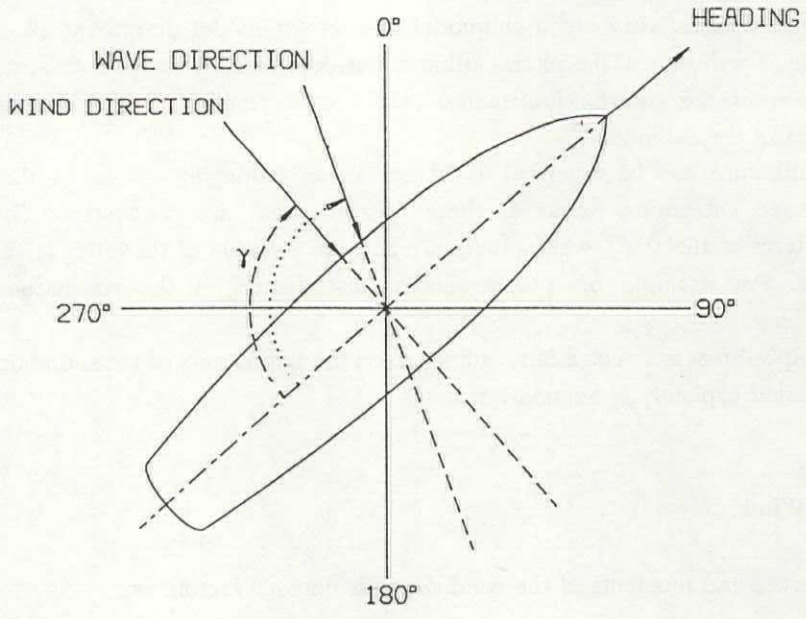

Fig. 2.9 The definition of the angle of incidence

A more detailed discussion of the wind disturbances can be found in, for example, Schelling (1977).

2.4.3 Waves

Waves may have different origins and different characteristics (see, for instance, Groen and Dorrestein, 1976). In general, the pattern of the waves is rather complex. It is a summation of waves with different amplitudes, phases and frequencies and with various directions of propagation.

With respect to the design of an RRS autopilot it is sufficient to use a simplified description of the waves by considering only unidirectional linear waves. The stochastic nature of the waves can be taken into account by describing the waves by means of a frequency spectrum. In the literature formulas are given to analytically describe a wave spectrum as a function of the wind speed or as a function of the significant wave height and the average period. In Gerritsma (1979) several descriptions of wave spectra are given of the form

$$S_\zeta(\omega) = A\omega^{-p}\exp(-B\omega^{-q}) \qquad (2.21)$$

An example is the Bretschneider spectrum, recommended by the 12th International Towing Tank Conference when statistical information is available on both the characteristic wave period and the significant wave height. In that case the following holds:

$$B = (691\bar{T}^{-4})$$

$$A = B(0.5H_{1/3})^2$$

$$p = 5$$

$$q = 4$$

$$\bar{T} = 2\pi\, m_0/m_1 = \text{the mean period}$$

$$H_{1/3} = 4\sqrt{m_0} = \text{the significant wave height}$$

$$m_0 = \int_0^\infty S(\omega)d\omega$$

$$m_1 = \int_0^\infty \omega S(\omega)d\omega$$

The influence of the waves on the motions of a ship also depends on the ship's speed and on the angle between the heading and the direction of the waves (Schelling, 1977). The relative frequency of a wave can be computed by the formula:

$$\omega(U,\gamma) = \omega_0 - \omega_0^2 U\cos(\gamma)/g \qquad (2.22)$$

where

ω_0 = the actual frequency of the wave
U = the speed of the ship
γ = the angle between the heading and the direction of the wave, defined according to Fig. 2.9
g = the acceleration of the gravity

Waves induce roll moments as well as yaw moments. The induced roll moment can be approximated by

$$K_{g\varphi}(\omega) = H_{g\varphi}(\omega)\ \sin(\gamma) \qquad (2.23)$$

while the induced yaw moment can be approximated by

$$N_{g\psi}(\omega) = H_{g\psi}(\omega)\ \sin(2\gamma) \qquad (2.24)$$

where

$H_{g\varphi}$ and $H_{g\psi}$ are functions of the wave frequency, depending on the shape of the hull, the water viscosity, appendages to the hull etc.
γ is the angle of incidence of the waves in degrees ($0 < \gamma \leq 180$).

The typical shape of the frequency spectra of the waves is generated by the system of Fig. 2.10. White noise with a zero mean is used as an input signal for a second-order low-pass filter. Koot (1983) demonstrated how the damping ratio z, the natural frequency ω and the variance of the noise can be selected to obtain the desired shape.

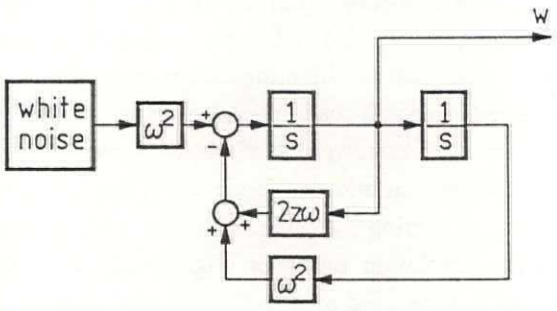

Fig. 2.10 Simulation of the wave motions

2.5 Identification of the ship-model parameters

2.5.1 Introduction

Van Amerongen and Van der Klugt (1982) describe some of the results of experiments which were carried out at the *Maritime Research Institute Netherlands* (**MARIN**) in Wageningen. Several design parameters of a ship were investigated to formulate demands to be met should the ship be equipped with an RRS system. In subsequent years, the MARIN investigated several hull forms and rudder configurations in order to find the optimal ship design. An extensive mathematical model of the resulting design has been derived based on a hydrodynamical approach. This MARIN model, being non-linear and describing most of the ship motions in the six degrees of freedom mentioned in Section 2.2, is not suitable for the purpose of designing a controller. It might be possible to reduce such a model by discarding the non-linear terms. A further model reduction can be obtained by using standard model reduction techniques. However, this approach cannot be used if the influence of the non-linear terms is too large.

The Identification and Simulation Package **PSI** (Van den Bosch, 1981) offers another approach. PSI enables model identification based on measurement data which is obtained from the actual process. A major advantage of this approach is

that the influence of non-linearities can also be investigated easily. Even if the process is non-linear it might be possible to find a reasonable linear model of the process.
Unfortunately, in this particular case the actual process, a new ship, has not yet been built. Therefore, it is not available for modeling trials.
As a second-best solution modeling trials can be carried out with the non- linear MARIN model. Assuming that the MARIN model gives a good description of the actual ship, one may expect that the identification results will be close to the results which would be obtained from full-scale modeling trials.
Zig-zag trials were carried out with the MARIN model and the data were transformed to a suitable format allowing modeling at the Control Laboratory. The initial models are given in Section 2.2.2. Fig. 2.5 shows a block diagram of the model which will be used for simulation purposes. Fig. 2.6 shows a block diagram of a simplified model which can be used as a basis for a controller design. PSI is used to identify the parameters of these models.

In this particular case, the parameters of a computer model have to be identified. Such a model not only enables the measurement of the input and the output signals, but also the signals which cannot be measured in practice (for instance the sway velocity, the rudder moment etc.). Several of these signals were "measured" to improve the reliability of the final result.

2.5.2 The identification mechanism

Van den Bosch (1981) describes how the program PSI can use measurement data to identify the parameters of a process. This approach is illustrated in Fig. 2.11.

A criterion function is defined, based on the error between an output of the process and the equivalent output of the (adjustable) model. Both are excited by the same input signal. The model may be described by continuous parts, discrete parts, non-linear or logical elements or any combination of these. The output of the process as well as the input signal are given by the measurement data.

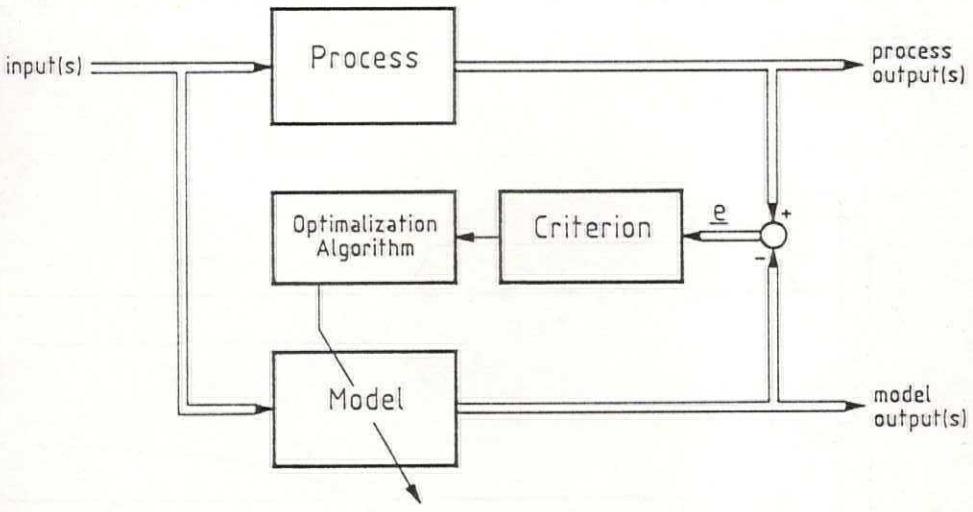

Fig. 2.11 Identification via simulation and optimization.

During the identification of the model parameters the following quadratic criterion was used:

$$J = C \int_0^T e^2 dt \qquad (2.25)$$

where

T = the total time of one simulation run
e = the difference between the output of the process and the output of the model
C = a constant

Although a similar criterion was used for all identification runs, the results of the identification of different signals under different conditions may not be compared, because the absolute value of the criterion in itself has no meaning. The criterion value depends on such things as the size of the input signal. Therefore, figures are added to give a qualitative impression of the identification results.

2.5.3 The simulation model

Zig-zag trials were carried out with the rudder as input to find the parameters of the ship model given in Fig. 2.5. The measurement data is shown in Fig. 2.12; the ship's speed is 22 knots.

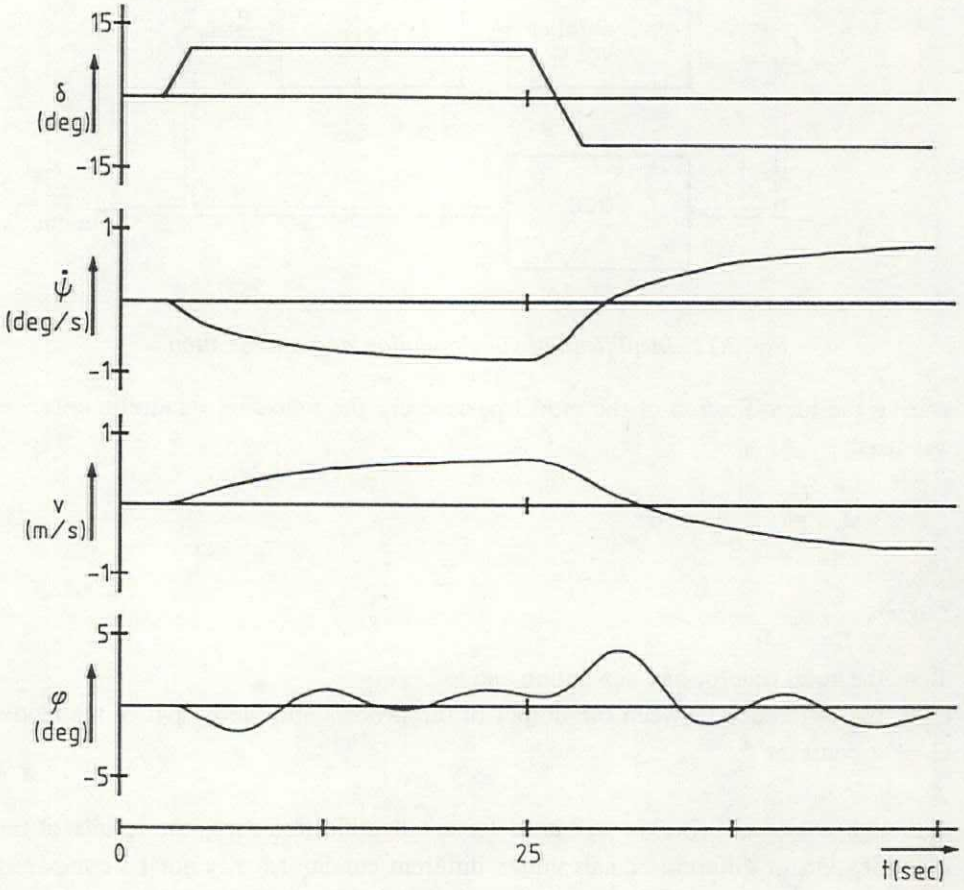

Fig. 2.12 The measurement data

The sway velocity was measured as well to allow a proper identifcation of the rudder-to-sway-velocity transfer. This transfer function is important to obtain a good description of the influence of the disturbances.

The model is given by Eqs. (2.16) to (2.18). The variable "w", describing the

disturbances, is selected to be zero. The block diagram of this model is shown in Fig. 2.5.

The identification was carried out in two steps. As a first approximation the parameters of three separate models were identified:

- the submodel which describes the roll motion and whose inputs are the rudder, the sway velocity and the rate of turn,
- the submodel which describes the rate of turn and whose inputs are the rudder and the sway velocity,
- the submodel which describes the sway velocity and whose inputs are the rudder and the rate of turn.

The second phase involves coupling these submodels to each other and further identifying this coupled model.

The identification results are given in Table 2.1.

Parameter	Value	Parameter	Value	Parameter	Value
k_{dv}	0.08	k_{dr}	-0.035	k_{dp}	-0.17
τ_v	9	τ_r	1.3	ω_n	0.64
k_{rv}	0.13	k_{vr}	-0.7	z_n	0.094
				k_{rp}	0
				k_{vp}	3.7

Table 2.1 The identification results.

The influence of the rate of turn on the roll angle is dominated by a time constant similar to the sway velocity. Therefore, it was difficult to distinguish between the influence of r and v on the rudder-to-roll transfer. Taking into account the results of the identification of the wave-height-to-roll transfer which are to be discussed next, it was decided to set k_{rp} equal to zero.

The identification results are illustrated in Fig. 2.13.

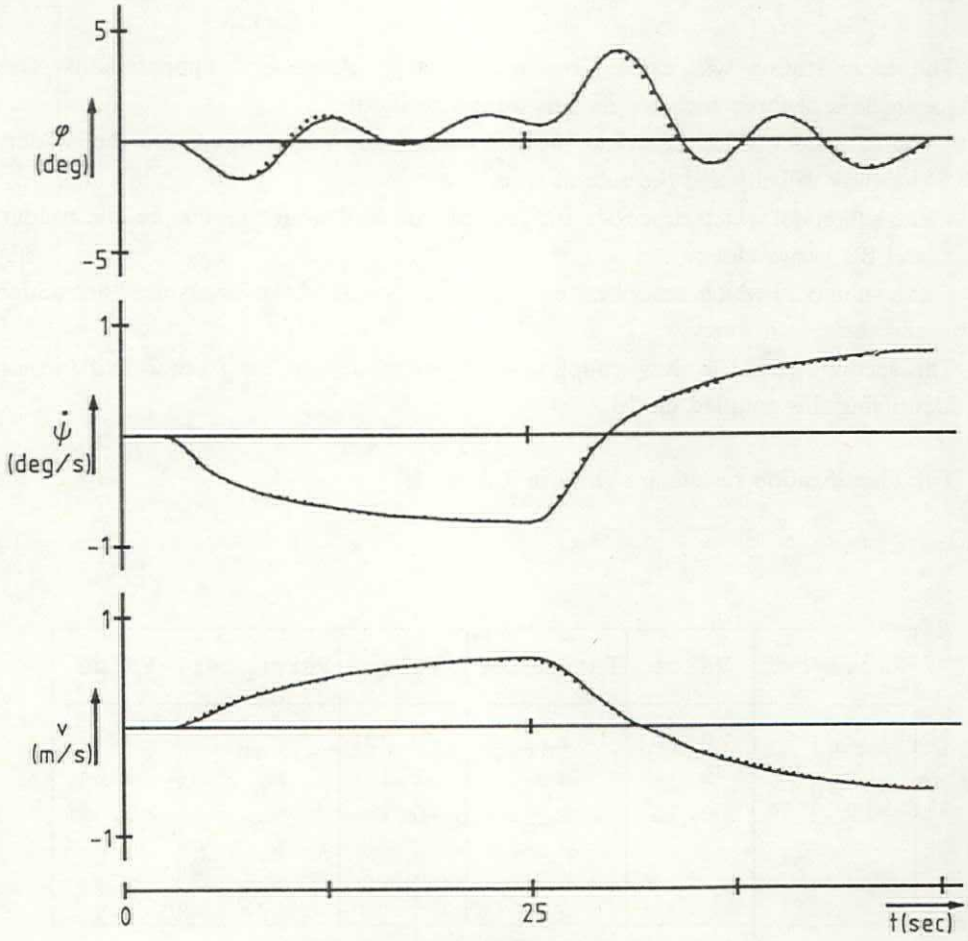

Fig. 2.13 The identification results

In Fig. 2.13 the dotted lines represent the measurement data while the solid lines represent the output of the identified model. A satisfying fit is obtained for the rudder-to-rate-of-turn transfer, the rudder-to-roll transfer and the rudder-to-sway-velocity transfer as well.

In practice, full-scale identification trials to obtain the wave-height-to-roll transfer, the wave-height-to-yaw transfer and the wave-height-to-sway-velocity transfer cannot be carried out. However, the mathematical model developed by the MARIN in Wageningen has been implemented in a computer. Therefore, it is possible to test this model with any given disturbance condition, including disturbances which will

not be met in practice like "square waves". This feature enables identification trials which are similar to the zig-zag trials with the rudder as input signal.

The initial model is again given by Eqs. (2.16) to (2.18). The parameters of this model (given by Table 2.1) were not changed during these identification experiments; the rudder angle is selected to be zero. The measurement data is shown in Fig. 2.14; the ship's speed is 22 knots.

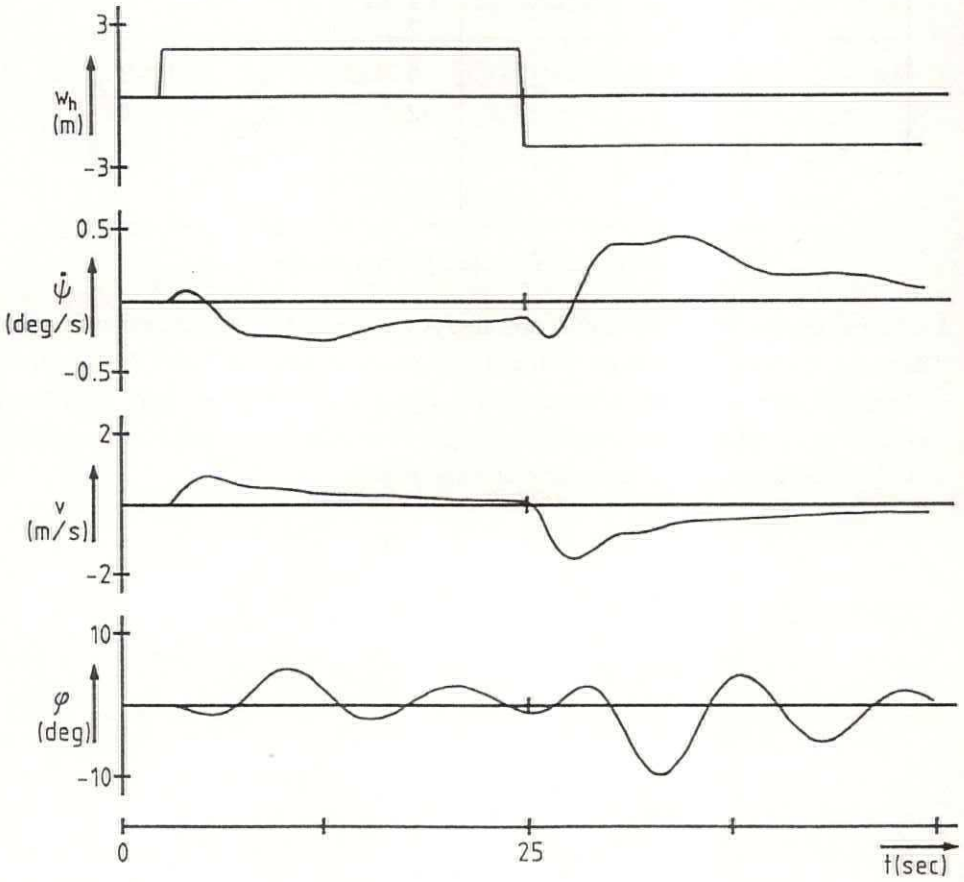

Fig. 2.14 The measurement data

The identification experiments were carried out to define the remaining three transfer functions:

- the wave height to roll angle,
- the wave height to rate of turn,
- the wave height to sway velocity.

The identification results are given in Table 2.2.

Parameter	Value	Parameter	Value	Parameter	Value
k_{wv}	0.056	k_{wr}	0.023	k_{wp}	-3.3
τ_{wv}	63	τ_{wr}	32	z_{wp}	0.47
z_{wv}	0.46	z_{wr}	0.87	ω_{wp}	0.82
ω_{wv}	1.1	ω_{wr}	0.5		

Table 2.2 The identification results

Large parameter variations could not always be noticed in the criterion function. Therefore, it was more difficult to find the parameters listed in Table 2.2 than those in Table 2.1. Probably, the influence of the higher-order terms or non-linearities is too large to be neglected. Nevertheless, Fig. 2.15 demonstrates that a reasonable fit was obtained during these identification experiments.

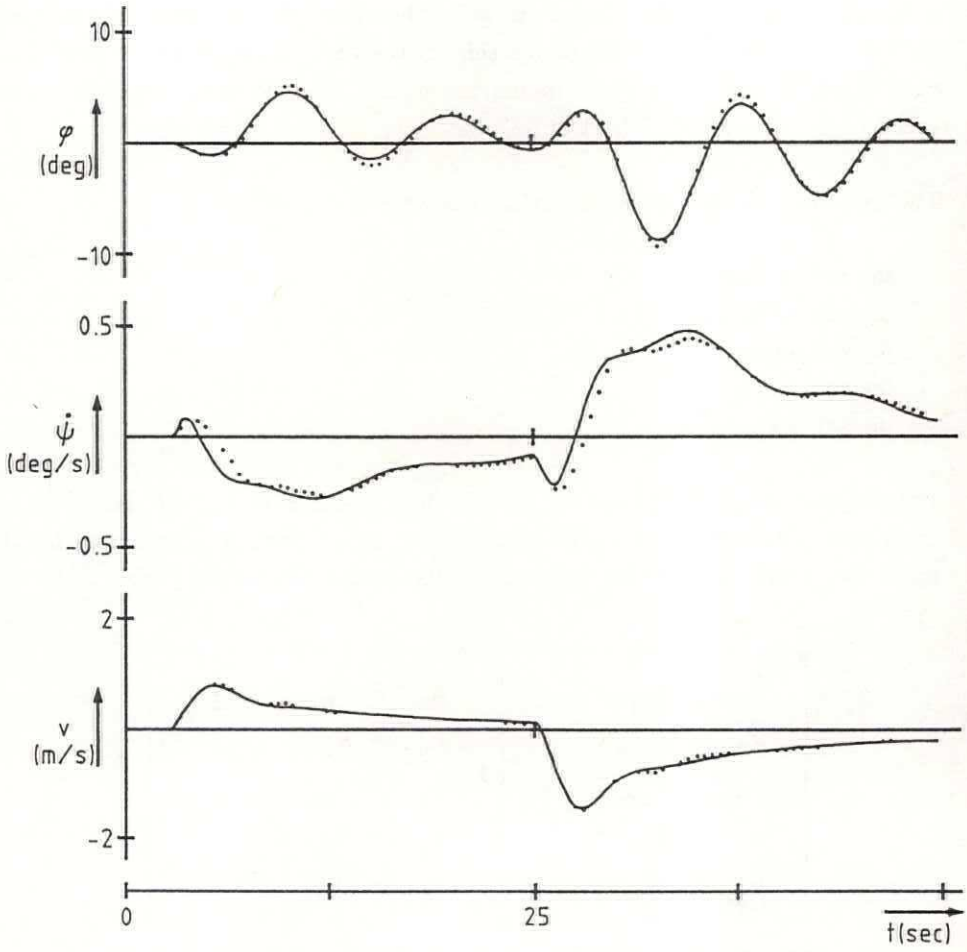

Fig. 2.15 The identification results

In Fig. 2.15 the dotted lines represent the measurement data while the solid lines represent the output of the model identified.

The resulting model is used for simulation purposes. It is valid only if the ship's speed equals 22 knots.

2.5.4 The control model

The speed of a ship has a considerable influence on the dynamics of the ship and, as a result, on the controller design as well. Therefore, the influence of the speed should be added to the model of the ship. Several identification experiments were carried out to find the desired model parameters. During these experiments the speed of the ship was 5, 7.5, 11 or 12.5 m/s.

The following relevant measurement signals were available:

the rudder angle δ_w
the rate of turn $r = \dot{\psi}$
the roll angle φ
the roll rate $p = \dot{\varphi}$
the ship's speed U

The identification is based on the model which is shown in Fig. 2.6. Based on the experience obtained during earlier identification experiments it is assumed that the ship's speed has the following influence on the model parameters (Table 2.3):

$k_{dp} = K_{dp0}U^2$	$z_n = z_{n0} + z_{n1}U$
$k_{dv} = K_{dv0}U$	$k_{vr} = K_{vr0}$
$k_{vp} = K_{vp0}U$	$\omega_n = \omega_{n0}$
$\tau_v = T_{v0}/U$	$\tau_r = T_{r0}/U$
$k_{dr} = K_{dr0}U$	$k_{rp} = 0$

Table 2.3 The model parameters as function of the ship's speed

The identification was carried out in three steps.

1 Identification of the rudder-to-roll transfer.
The identification parameters are K_{dp0}, K_{vp0}, T_{v0} and z_n, while the criterion J_φ is described by Eq. (2.25). The parameter ω_n was barely influenced by the speed. In order to reduce the calculation effort ω_n was selected to be constant.

2 Identification of the rudder-to-rate-of-turn transfer.
The identification parameters are K_{dr0}, K_{vr0} and T_{r0}, while the criterion J_r is described by Eq. (2.25). T_{v0} is found in step 1.

3 Changing T_{v0} such that the rudder-to-roll transfer as well as the rudder-to-rate-of-turn transfer give a reasonable result.

Because the sway velocity is not available, it is not possible to distinguish between the influence of k_{dv} and the influence of k_{vp} on the rudder-to-roll transfer. Likewise, it is not possible to distinguish between the influence of k_{dv} and the influence of k_{vr} on the rudder-to-rate-of-turn transfer. Therefore, the parameter K_{dv0} was set to 0.01. In addition, the parameter ω_n was selected to be 0.64.
The identification results are summarized in Fig. 2.16. In this figure the model parameters identified are denoted as solid circles. Averaging the identification results of all the experiments (indicated by the solid lines) gives a reasonable fit under all conditions (the dashed lines will be discussed later on). The resulting parameter values are summarized in Table 2.4.

Parameter	Identification results
$k_{dp} = K_{dp0} U^2$	$-0.0014\ U^2$
$k_{dv} = K_{dv0} U$	$0.01\ U$
$k_{dr} = K_{dr0} U$	$-0.0027\ U$
$k_{vp} = K_{vp0} U$	$0.21\ U$
$\tau_v = T_{vo}/U$	$78\ /\ U$
$z_n = z_{n0} + z_{n1} U$	$0.064 + 0.0038U$
$k_{vr} = K_{vr0}$	-0.46
$\omega_n = \omega_{n0}$	0.63
$\tau_r = T_{r0}/U$	$13\ /\ U$

Table 2.4 The parameters of the proposed model (U in m/s)

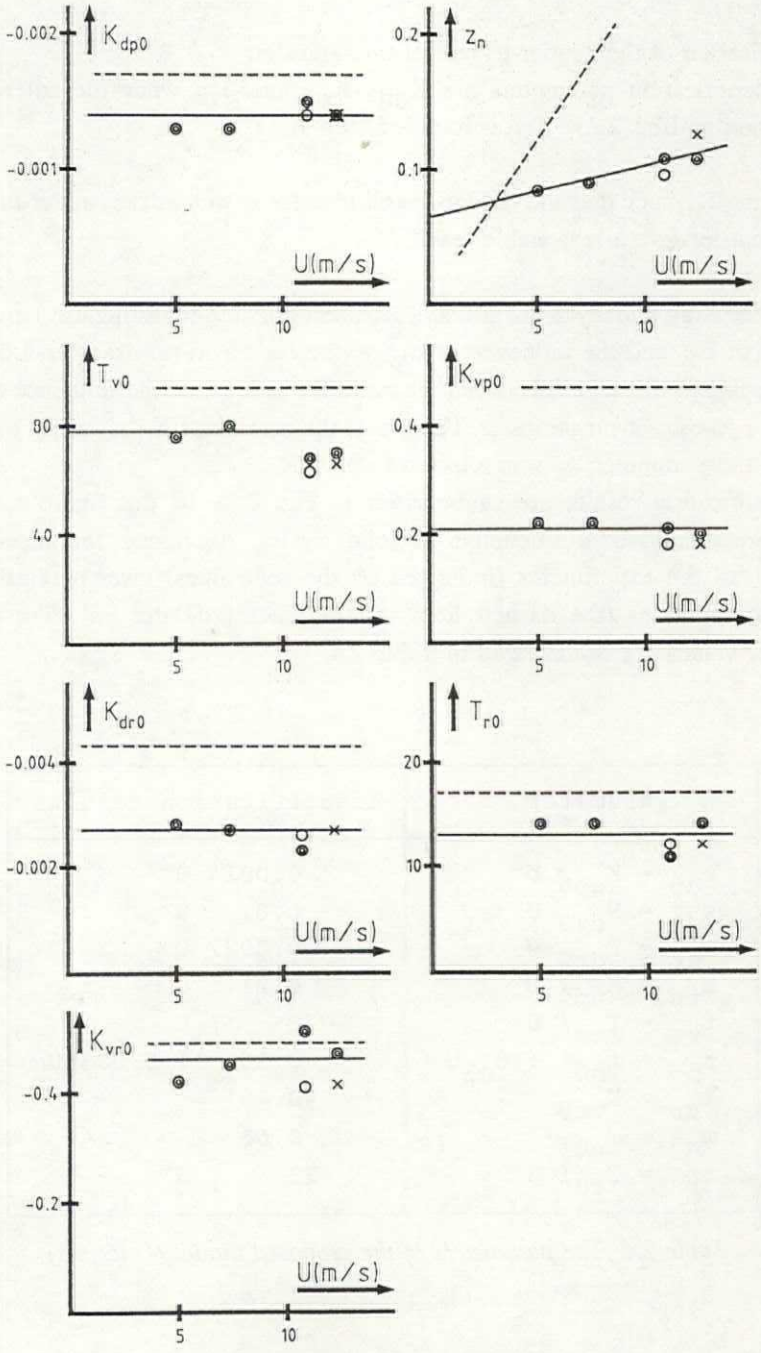

Fig. 2.16 The estimated model parameters

Fig. 2.17 and Fig. 2.18 show a qualitative comparison between the proposed model parameters (solid lines in Fig. 2.16) and the estimated model parameters (solid circles in Fig. 2.16). The speed of the ship is 12.5 m/s (the worst case situation).

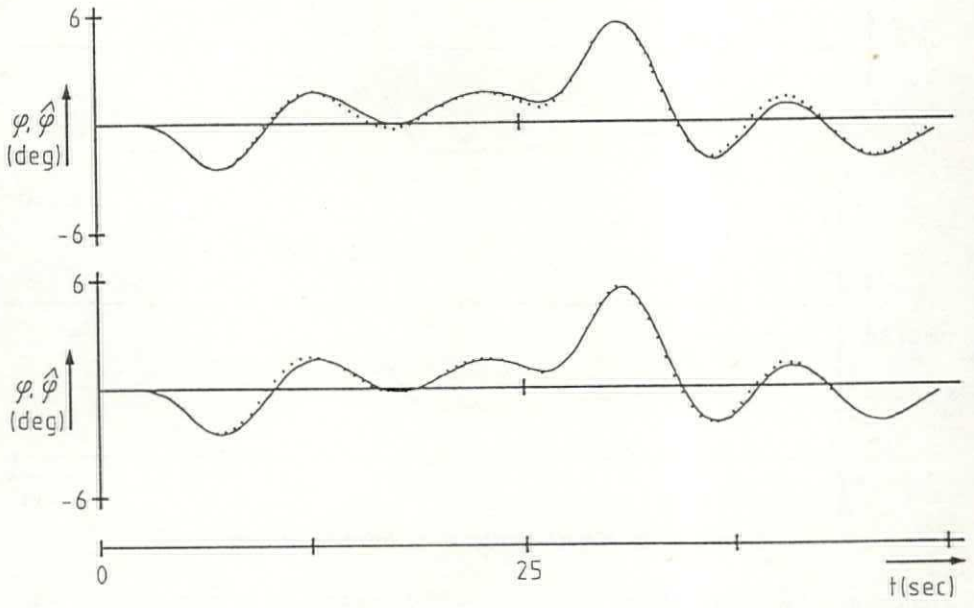

Fig. 2.17 Model comparison: the roll angle

In Fig. 2.17 the dotted lines denote the measured roll motion, while the solid lines denote the output of the proposed model (the upper part) and the output of the estimated model (the lower part). Even in this case the performance of the proposed model is good.

In Fig. 2.18 the measured rate of turn is indicated by the dotted lines. The solid lines again denote the output of the proposed model (the upper part) and the output of the optimal model (the lower part). Apparently, the differences between both results are minor.

Van Amerongen and Van Cappelle (1981) carried out full-scale modeling trials on board a naval ship. Mattaar (1986) used the resulting data to identify the parameters

of the model of Fig. 2.6, the result of which is shown in Fig. 2.16 (the dashed lines). He demonstrated that by using this model a better fit can be obtained than by using the model proposed by Van Amerongen and Van Cappelle.

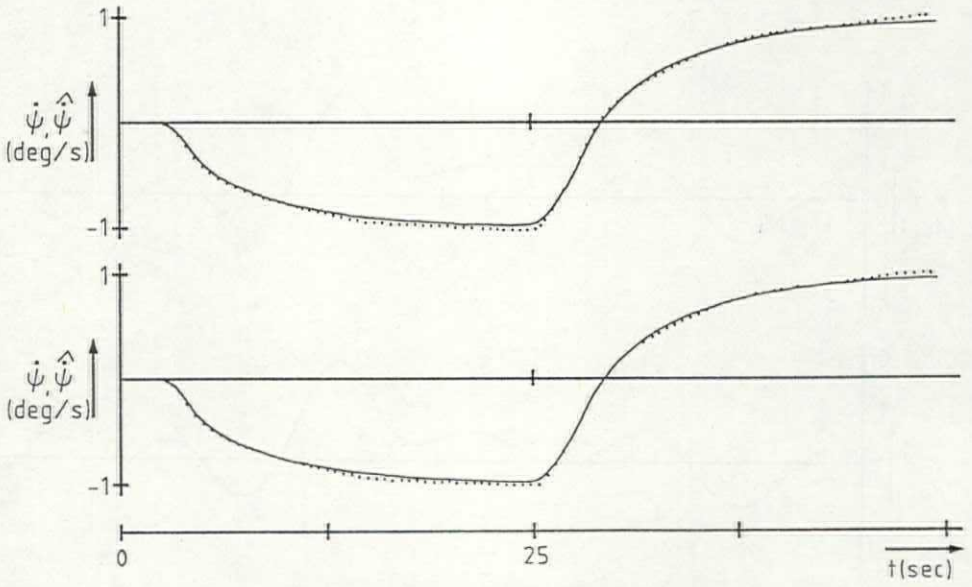

Fig. 2.18 Model comparison: the rate of turn

Henceforth, the model of the naval ship will be referred to as *ship model 1* while the model of the new ship design will be referred to as *ship model 2*. Comparing ship model 1 with ship model 2 yields the following results:

- The damping of ship model 1 is larger than the damping of ship model 2. Therefore, ship model 2 will be more sensitive to the roll motion.
- The time constants T_{v0} and T_{r0} of ship model 1 are larger than the equivalent time constants of ship model 2. Therefore, ship model 2 will have better maneuvering characteristics.
- The gains k_{dp} and k_{vp} of ship model 1 are larger than the equivalent gains of ship model 2. These gains describe the influence of the rudder on the roll motion. Therefore, it may be expected that the roll reduction potential of the rudder of ship model 1 is larger than that of ship model 2.

2.5.5 The non-linearities

In Section 2.2 the non-linearities were disregarded to derive the linear model of Fig. 2.6. One additional identification experiment was carried out to investigate whether this is allowed. The ship's speed is 11 m/s. The rudder angle has been doubled (-20 to 20 degrees). The parameter K_{dv0} is again chosen to be 0.01.

The identification results are denoted in Fig. 2.16 by an "x". They are summarized in Table 2.5.

Parameter	Value	J_r	J_φ
K_{dr0}	-0.0026	99	170
K_{vr0}	-0.42		
T_{r0}	12.3		
T_{v0}	66		
K_{dp0}	-0.0014		
K_{vp0}	0.18		
z_n	0.126		
ω_n	0.63		

Table 2.5 The identification results

Fig. 2.16 demonstrates that the parameters of Table 2.4 agree reasonably well with the other identification results. This is further confirmed by the qualitative comparison given in Fig. 2.19 and Fig. 2.20.

The upper part of Fig. 2.19 shows a comparison between the "measured" roll angle for a rudder angle of ± 20 degrees and the output of the model which is described by Fig. 2.6 and Table 2.4. A reasonable result is obtained, even though the parameters are not the optimal ones.
The lower part of Fig. 2.19 shows a comparison between this measured roll angle and the model with parameters as given by Table 2.5.

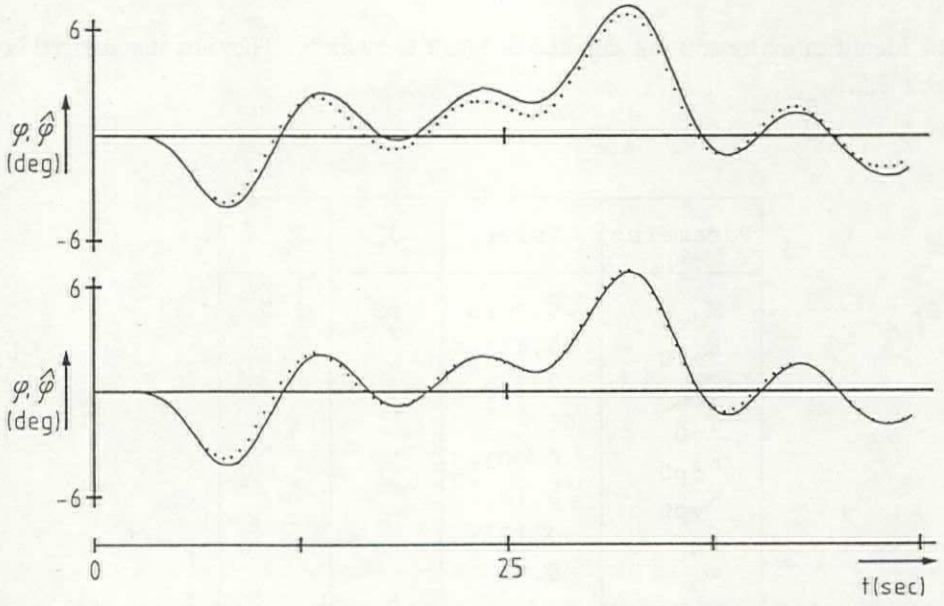

Fig. 2.19 The influence of the rudder angle on the rudder-to-roll transfer

In Fig. 2.20 similar comparisons are given for the rudder-to-rate-of-turn transfer. Again, a reasonable result is obtained with the parameters of Table 2.4. Apparently, it is not necessary to extend the linear model with non-linear elements.

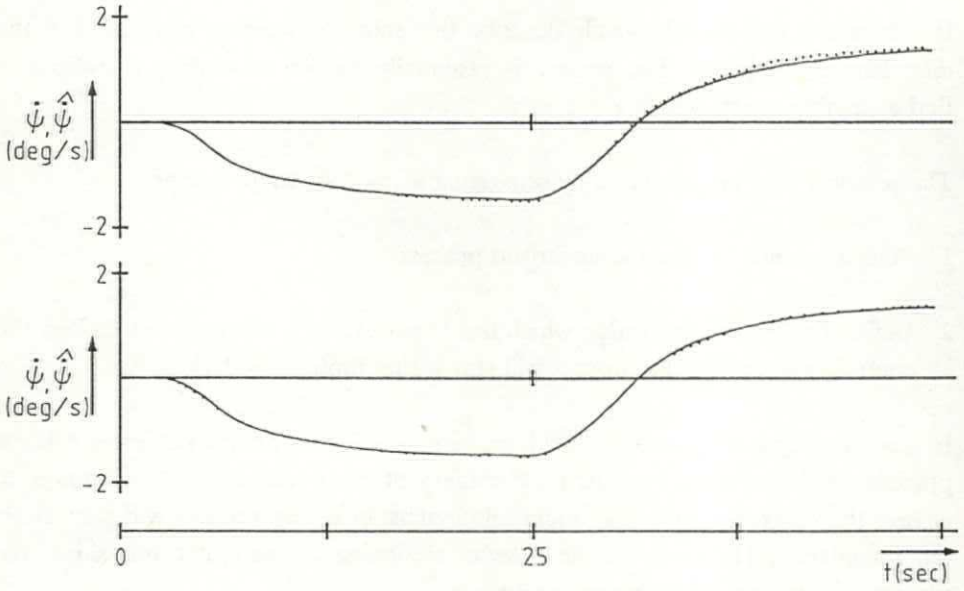

Fig. 2.20 The influence of the rudder angle on the rudder-to-rate-of-turn transfer

In principle, everything that is needed to design an RRS controller is available now. The model of Fig. 2.6 can be used as a basis for a controller design. The resulting controller can be tested by means of a simulation using the models of the steering machine and the disturbances in combination with the ship model of Fig. 2.6 or the slightly more extended model of Fig. 2.5.

3 CONTROLLER DESIGN

3.1 Introduction

In Chapter 2 the models which describe the ship, its steering machine and the disturbances are posed. The process is essentially non-linear, making it difficult to find a suitable controller.

The problem may be simplified by separating it into two subproblems:

1 Find the controller for the linearized process

2 Define the boundaries within which this linearization is allowed and change the controller such that the process will stay within those boundaries.

In general, step 2 is the most difficult problem to solve. For many processes it is not possible to define such boundaries. For many other processes it is not allowed to change the controller such that under all circumstances the process will stay within the boundaries. However, in the case of designing an autopilot for ships, the separation into two subproblems is allowed.
The process comprises two dominant non-linearities posed by the steering machine: the maximum rudder angle and the maximum rudder speed. It is assumed that the influence of other non-linearities can be disregarded. If the controller gains remain sufficiently small, it is allowed to disregard the two dominant non-linearities as well. In that case, linear control techniques are applicable. In this chapter a new method, based on the LQG method, is posed to calculate controllers for linear processes. A simple approach by block diagrams will be used to introduce the method.
The method requires the parameters of the process to be known, but it allows them to change slowly (in comparison with the dominant time constants of the process) in time.

The linearized model of the process to be controlled is comprised of models of a ship, a steering machine and the disturbances. This model is too complex to be used as a basis for a controller design. As a first step, the model may be reduced to a fifth-order model by assuming that the influence of the steering machine is negligibly small and that the disturbances are white noise with a zero mean. However, in

practice this is not always allowed. Nevertheless, this approach will be followed and it will be shown that the fifth-order model can be further reduced to two independent lower-order models describing the rudder-to-roll transfer and the rudder-to-yaw transfer. These models will be used as a basis for a controller design. Without their becoming too complex these models may even be extended with a simple model of the disturbances. This is especially important for the yaw model where the constant component in the disturbances, caused by the wind, cannot be disregarded.

In this chapter it will be shown that the controller gains depend on the weighting factors of a criterion and on the parameters of the process. The latter are a function of the ship's speed. Therefore, the controller gains are a function of the ship's speed as well. If the controller gains become too large it is not allowed to disregard the influence of the steering machine. This indicates that an "optimal" controller can make the process non-linear if the ship's speed changes. Van Amerongen and Van Nauta Lemke (1982) demonstrate that in such a case the system may even become unstable. This problem will be solved by the methods posed in Chapter 5.

To start with, in Section 3.2 a short introduction to *Optimal Linear Control Design* is given. In addition, a calculation method which gives good results is presented. It is relatively simple to use in simulations and has some suitable properties in dealing with non-linearities. The latter will be discussed in Chapter 5. In Section 3.3 this method is used to design a controller which, under certain restrictions, is capable of obtaining a substantial roll reduction while maintaining a good course keeping performance. In Section 3.4 it is shown that it is allowed to separate the fifth-order model given in Fig. 2.6 into two lower-order submodels. Finally, in Section 3.5 the influence of the ship's speed on the controller gains is considered.

3.2 Optimal Linear Control Design

3.2.1 Process disturbed by white system noise

Let a process, described by the following state-space equations, be given:

$$\dot{\underline{x}} = A\underline{x} + B\underline{u} + D\underline{w} \qquad (3.1)$$

$$\underline{y} = C\underline{x} + \underline{v} \qquad (3.2)$$

A block diagram of the process is illustrated in Fig. 3.1.

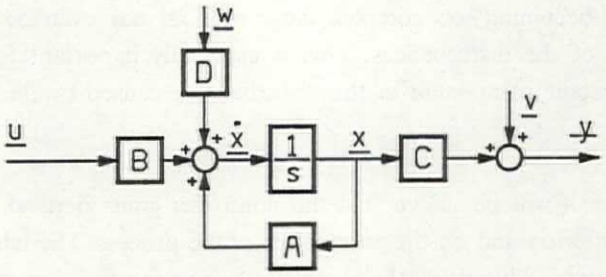

Fig. 3.1 The process

Without loss of generality for the method mentioned below it is assumed that $\underline{w}$ and $\underline{v}$ denote white noise with a zero mean.

One of the methods of designing a controller is the *Linear process Quadratic criterion Gaussian noise* (**LQG**) control method. When used, this method guarantees that the solution will be the optimal controller. However, two of the things the method requires to be known are the model and the states of the process. The model of the process is given in Chapter 2, but the states of the process are not necessarily known. In that case, the LQG approach requires an optimal filter to be designed which gives the best estimates of the states which cannot be measured or which are contaminated by measurement noise. The inputs of the optimal controller, calculated by means of the LQG method, are the states of the optimal filter. This leads to calculating the optimal controller for a process described by the following state-space equations:

$$\dot{\hat{\underline{x}}} = A\hat{\underline{x}} + B\underline{u} + D\underline{w} \tag{3.3}$$

$$\hat{\underline{y}} = C\hat{\underline{x}} \tag{3.4}$$

Note that the matrix C in Eq. (3.4) is not the same as the matrix C in Eq. (3.2). In Eq. (3.4) the matrix C is of full rank, while this is not necessarily true in Eq. (3.2).

For the moment, it will be assumed that all states are measurable. Therefore, the ^, indicating estimated values, are left out of the formulas. In Chapter 4 it will be shown how the non-measurable states can be obtained.

Define as criterion the following function:

$$J = \lim_{T\to\infty} \frac{1}{T} \int_0^T (\underline{y}^T Q \underline{y} + \underline{u}^T R \underline{u}) dt \qquad (3.5)$$

where Q is a (semi-) positive-definite weighting matrix and R is a positive-definite weighting matrix. To simplify the equations it will be assumed that Q (rank n_1) and R (rank n_2) are diagonal. In that case, and if T goes to infinity, criterion (3.5) may be reformulated:

$$J = \sum_{i=1}^{n_1} q_i E[y_i . y_i] + \sum_{j=1}^{n_2} r_j E[u_j . u_j] \qquad (3.6)$$

The "optimal" controller, with respect to criterion (3.5), is (see for instance Kwakernaak and Sivan, 1972):

$$\underline{u} = -K\underline{x} \qquad (3.7)$$

where

$$K = R^{-1} B^T P \qquad (3.8)$$

$$-\dot{P} = A^T P + PA + C^T Q C - PBK \qquad (3.9)$$

In Eq. (3.8) K approaches a constant value when T goes to infinity and the process is time-invariant. This constant value can be found by solving Eq. (3.10):

$$0 = A^T P + PA + C^T Q C - PBK \qquad (3.10)$$

and by having K satisfy Eq. (3.8).

An iterative method is posed for solving equations like Eq. (3.10). It is based on the definition of the "innovation process" described by Eqs. (3.11) and (3.12) and the calculation of the steady-state outputs of this innovation process:

$$\dot{P} = A^T P + PA + C^T Q C - PBK \qquad (3.11)$$

$$K = R^{-1}B^{T}P \qquad (3.12)$$

The steady-state outputs of this "innovation process" are the required controller gains.
Comparing Eq. (3.11) with Eq. (3.9) reveals that the minus sign on the lefthand side of Eq. (3.9) is omitted. In combination with Eq. (3.12), Eq. (3.9) resembles an unstable innovation process. Therefore, its outputs do not converge to the required stationary solution.

It is possible to reformulate Eqs. (3.11) and (3.12) such that they resemble the more commonly applied form, i.e. the process with the following state-space equations:

$$\dot{\underline{x}}_m = A_m\underline{x}_m + B_m\underline{u}_m \qquad (3.13)$$

$$\underline{y}_m = C_m\underline{x}_m \qquad (3.14)$$

where

$\underline{x}_m^T = (p_{11}, p_{12}, \ldots, p_{nn})$

$\underline{y}_m^T = (k_{11}, k_{12}, \ldots, k_{nr})$ = the elements of the matrix K

r = the number of controllable inputs of the original process

Because P is a symmetric matrix only the upper-right or the lower-left triangle has to be considered. Therefore, if P is of rank n then $\underline{x}_m$ consists of $0.5(n^2+n)$ elements.

Comparing Eq. (3.11) and Eq. (3.12) with respectively Eq. (3.13) and Eq. (3.14) yields:

$$A^{T}P + PA - PBK \leftrightarrow A_m\underline{x}_m$$

$$C^{T}QC \leftrightarrow B_m\underline{u}_m$$

$$R^{-1}B^{T}P \leftrightarrow C_m\underline{x}_m$$

A block diagram of the innovation process is shown in Fig. 3.2. Note that the block diagram is valid only if the appropriate order of the matrix multiplications is taken into account.

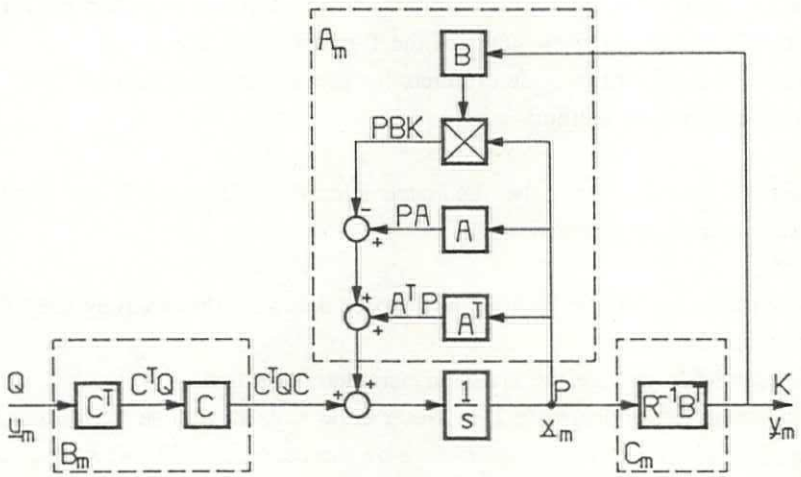

Fig. 3.2 A block diagram of the innovation process

The innovation process introduces non-linear differential equations which can be solved by numerical integration methods. The steady-state solution of this innovation process yields, by means of Eq. (3.8), the optimal gains.
In many cases, this innovation process has a slow convergence; in a real-time environment it may take quite a while before the steady state has been reached. This is especially true if the time constants of the original process and the elements of the R-matrix are large. On the other hand, in some special cases such a slow convergence is desired.
The following method is posed to circumvent these problems:

Introduce the diagonal matrix L with non-zero elements l_i on the diagonal. This changes the innovation process described by Eqs. (3.13) and (3.14) to:

$$L\dot{\underline{x}}_m = A_m\underline{x}_m + B_m\underline{u}_m \qquad (3.15)$$

$$\underline{y}_m = C_m\underline{x}_m \qquad (3.16)$$

The introduction of the L-matrix is similar to time scaling in analog computing. Within certain boundaries it creates the possibility to select freely the rate of

convergence of the innovation process.
The upper boundaries of the elements of the L-matrix are determined by the variation in time of the process parameters. In most cases the convergence speed should be fast enough to follow the fluctuations of the parameters of the process. The influence of these fluctuations on the controller parameters can be reduced by intentionally selecting the elements of the L-matrix too large.
The lower boundaries are determined by the available computer time and the numerical integration method.

The method introduced to solve the matrix-Riccati equations (3.8) and (3.10) on line has some interesting properties:

- The parameters of the process have to be known although they are allowed to change in time.
- It is allowed to change the criterion parameters on line.
- By selecting the appropriate L-matrix it is possible to reduce the influence of the fluctuations of the process parameters on the controller gains (for instance, those caused by parameter estimation) or to increase the convergence speed.
- The method can be used for *Multi Input Multi Output* (**MIMO**) processes.

The optimal linear control problem is a dual of the optimal linear filter problem (Kwakernaak and Sivan, 1972). The same holds for the method introduced to design the optimal linear controller. In Chapter 4 it will be shown that a similar method can be applied to solve the optimal linear filter problem.

3.2.2 Process disturbed by colored system noise

In Eq. (3.1) $\underline{w}$ is assumed to be white noise. This is not a limitation of the validity of the above-mentioned methodology. If $\underline{w}$ is non-white noise it is possible to define a new process including the states of the shaping filter describing the coloring of $\underline{w}$.

Let a process, described by the following state-space equations, be given:

$$\dot{\underline{x}}_p = A_p\underline{x}_p + B_p\underline{u}_p + D_p\underline{w}_p \qquad (3.17)$$

$$\underline{y}_p = C_p\underline{x}_p \qquad (3.18)$$

where $\underline{w}_p$ denotes colored noise, described by the following shaping filter:

$$\dot{\underline{x}}_f = A_f\underline{x}_f + D_f\underline{w}_f \tag{3.19}$$

$$\underline{y}_f = C_f\underline{x}_f = \underline{w}_p \tag{3.20}$$

A block diagram of this process is given in Fig. 3.3.
Combining Eqs. (3.17) to (3.20) into one model results in the process described by the following state-space equations:

$$\dot{\underline{x}} = A\underline{x} + B\underline{u} + D\underline{w} \tag{3.21}$$

$$\underline{y} = C\underline{x} \tag{3.22}$$

where

$$A = \begin{bmatrix} A_p & A_c \\ 0 & A_f \end{bmatrix} \quad B = \begin{bmatrix} B_p \\ 0 \end{bmatrix} \quad D = \begin{bmatrix} 0 \\ D_f \end{bmatrix} \quad C = \begin{bmatrix} C_p & 0 \\ 0 & C_f \end{bmatrix}$$

$$\underline{x}^T = (\underline{x}_p^T \; \underline{x}_f^T)$$

$$\underline{y}^T = (\underline{y}_p^T \; \underline{y}_f^T)$$

The matrix A_c denotes the coupling between the model of the process described by Eqs. (3.17) and (3.18) and the model of the disturbances described by Eqs. (3.19) and (3.20).

Define the following criterion:

$$J = \lim_{T\to\infty} \frac{1}{T} \int_0^T (\underline{y}^T Q \underline{y} + \underline{u}^T R \underline{u}) dt \tag{3.23}$$

where

$$Q = \begin{bmatrix} Q_p & 0 \\ 0 & 0 \end{bmatrix} \qquad R = R_p$$

Fig. 3.3 depicts a block diagram of the controlled process.

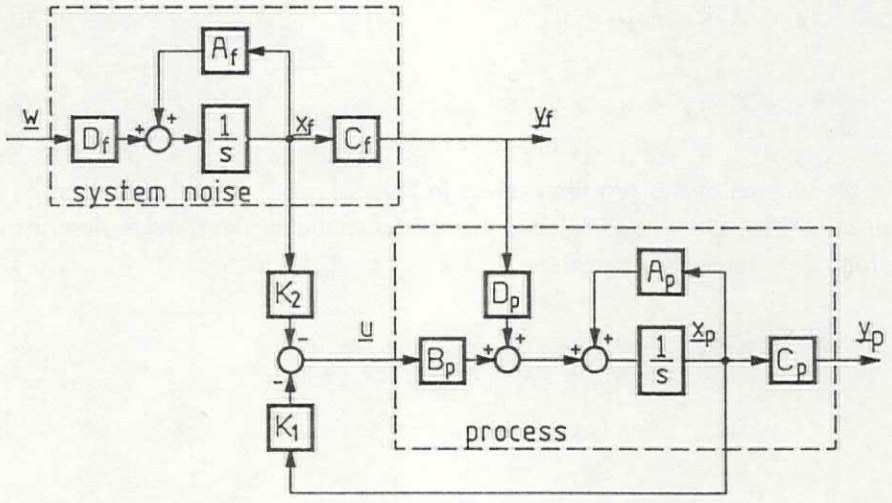

Fig. 3.3 A block diagram of the process

The optimal controller, with respect to criterion (3.23), is given by Eq. (3.7) and can be found by solving Eqs. (3.8) and (3.10) where

$$P = \begin{bmatrix} P_1 & P_2 \\ P_2^T & P_3 \end{bmatrix} \qquad K = (K_1 \; K_2)$$

Solving Eq. (3.8) yields:

$$K = R^{-1}B^TP = R_p^{-1}(B_p^T \; 0)\begin{bmatrix} P_1 & P_2 \\ P_2^T & P_3 \end{bmatrix} =$$

$$= (R_p^{-1}B_p^TP_1 \quad R_p^{-1}B_p^TP_2) = (K_1 \; K_2)$$

Therefore,

$$K_1 = R_p^{-1}B_p^TP_1 \quad \text{(feedback of the process)} \tag{3.24}$$

and

$$K_2 = R_p^{-1} B_p^T P_2 \qquad \text{(feedback of the noise)} \tag{3.25}$$

The matrices P_1 and P_2 can be found by solving Eq. (3.10):

$$0 = \begin{bmatrix} A_p & 0 \\ A_c^T & A_f^T \end{bmatrix} \begin{bmatrix} P_1 & P_2^T \\ P_2^T & P_3 \end{bmatrix} + \begin{bmatrix} P_1 & P_2 \\ P_2^T & P_3 \end{bmatrix} \begin{bmatrix} A_p & A_c \\ 0 & A_f \end{bmatrix} +$$

$$+ \begin{bmatrix} C_p^T & 0 \\ 0 & C_f^T \end{bmatrix} \begin{bmatrix} Q_p & 0 \\ 0 & 0 \end{bmatrix} \begin{bmatrix} C_p & 0 \\ 0 & C_f \end{bmatrix} - \begin{bmatrix} P_1 & P_2 \\ P_2^T & P_3 \end{bmatrix} \begin{bmatrix} B_p \\ 0 \end{bmatrix} (K_1 \; K_2) =$$

$$= \begin{bmatrix} A_p^T P_1 & A_p^T P_2 \\ A_c^T P_1 + A_f^T P_2^T & A_c^T P_2 + A_f^T P_3 \end{bmatrix} + \begin{bmatrix} P_1 A_p & P_1 A_c + P_2 A_f \\ P_2^T A_p & P_2^T A_c + P_3 A_f \end{bmatrix} +$$

$$+ \begin{bmatrix} C_p^T Q_p C_p & 0 \\ 0 & 0 \end{bmatrix} - \begin{bmatrix} P_1 B_p K_1 & P_1 B_p K_2 \\ P_2^T B_p^T K_1 & P_2^T B_p K_2 \end{bmatrix}$$

Therefore,

$$0 = A_p^T P_1 + P_1 A_p - P_1 B_p K_1 + C_p^T Q_1 C_p \tag{3.26}$$

$$0 = A_p^T P_2 + P_1 A_c + P_2 A_f - P_1 B_p K_2 \tag{3.27}$$

$$0 = A_c^T P_2 + P_2^T A_c + A_f^T P_3 + P_3 A_f - P_2^T B_p K_2 \tag{3.28}$$

The following conclusions can be drawn from Eqs. (3.24) to (3.28):

- If in the process described by Eqs. (3.17) and (3.18) $\underline{w}_p$ denotes white noise with zero mean, then Eqs. (3.24) and (3.26) are sufficient to calculate the optimal controller for that process.
- Eqs. (3.24) and (3.26) show that the resulting controller parameters K_1 do not depend on the colored character of the system noise $\underline{w}_p$.
- Eqs. (3.24), (3.25), (3.26) and (3.27) form a set of 4 equations with 4 unknown parameters. Eq. (3.28) is not required to calculate the matrix K.

Appendix A shows an example of the calculation of a controller for a second-order process disturbed by colored system noise. This colored noise is described by a second-order shaping filter.

3.3 The fifth-order model

In Chapter 2 models of a ship, a steering machine and the disturbances are derived. The steering machine makes the process basically non-linear. This suggests that it is not allowed to apply the Linear Optimal Control method given in Section 3.2. However, if the controller output does not become too large the method posed in Section 3.2 is applicable. For the moment, it will be assumed that the non-linearities of the steering machine can be disregarded. Chapter 5 gives a solution for the case in which these non-linearities cannot be disregarded. In addition, it will be assumed that the following holds:

1 The model parameters are known.
2 The disturbances are assumed to be white noise with zero mean.
3 All the states of the process are measurable.

This reduces the control problem to finding the controller for a fifth-order linear process. A block diagram of this process is given in Fig. 2.6. It is described by the following state-space equations:

$$\dot{\underline{x}} = A\underline{x} + B\underline{u} + D\underline{w} \tag{3.29}$$

$$\underline{y} = C\underline{x} \tag{3.30}$$

where

$$A = \begin{bmatrix} 0 & 1 & 0 & 0 & 0 \\ -\omega_n^2 & -2z_n\omega_n & \omega_n^2 k_{vp} & 0 & 0 \\ 0 & 0 & -1/\tau_v & 0 & 0 \\ 0 & 0 & k_{vr}/\tau_r & -1/\tau_r & 0 \\ 0 & 0 & 0 & 1 & 0 \end{bmatrix} \quad B = \begin{bmatrix} 0 \\ k_{dp}\omega_n^2 \\ k_{dv}/\tau_v \\ k_{dr}/\tau_r \\ 0 \end{bmatrix}$$

$$C = \begin{bmatrix} c_1 & 0 & 0 & 0 & 0 \\ 0 & c_2 & 0 & 0 & 0 \\ 0 & 0 & c_3 & 0 & 0 \\ 0 & 0 & 0 & c_4 & 0 \\ 0 & 0 & 0 & 0 & c_5 \end{bmatrix} \qquad D = \begin{bmatrix} 0 & 0 \\ \omega_n^2 & 0 \\ 0 & 0 \\ 0 & 1/\tau_r \\ 0 & 0 \end{bmatrix}$$

$$\underline{x}^T = (\varphi,\ \dot{\varphi}\ ,x_3\ ,\dot{\psi}\ ,\psi) \qquad \underline{u} = \delta$$

$$\underline{w}^T = (w_\varphi,\ w_\psi) = \text{white noise with zero mean}$$

The optimal controller, with respect to the following criterion

$$J = \sum_{i=1}^{5} q_i E[y_i . y_i]/r + E[\delta . \delta] \qquad (3.31)$$

can be found by solving Eqs. (3.8) and (3.10). The application of the method which is introduced in Section 3.2 yields as solution the steady-state outputs of the "innovation" process described by the following state-space equations:

$$L\dot{\underline{x}}_m = A_m \underline{x}_m + B_m \underline{u}_m \qquad (3.32)$$

$$\underline{y}_m = C_m \underline{x}_m \qquad (3.33)$$

where

$$\underline{x}_m^T = (p_1,\ p_2,\ \ldots\ldots,\ p_{15})$$

$$\underline{u}_m^T = (q_1,\ q_2,\ q_3,\ q_4,\ q_5)$$

$$\underline{y}_m^T = (y_1,\ y_2,\ y_3,\ y_4,\ y_5)$$

The matrices A_m, B_m and C_m are given in Appendix B.

By using the Interactive Simulation Package **PSI** (Van den Bosch, 1985a) it is possible to simulate the (non-linear) process described by Eqs. (3.32) and (3.33).

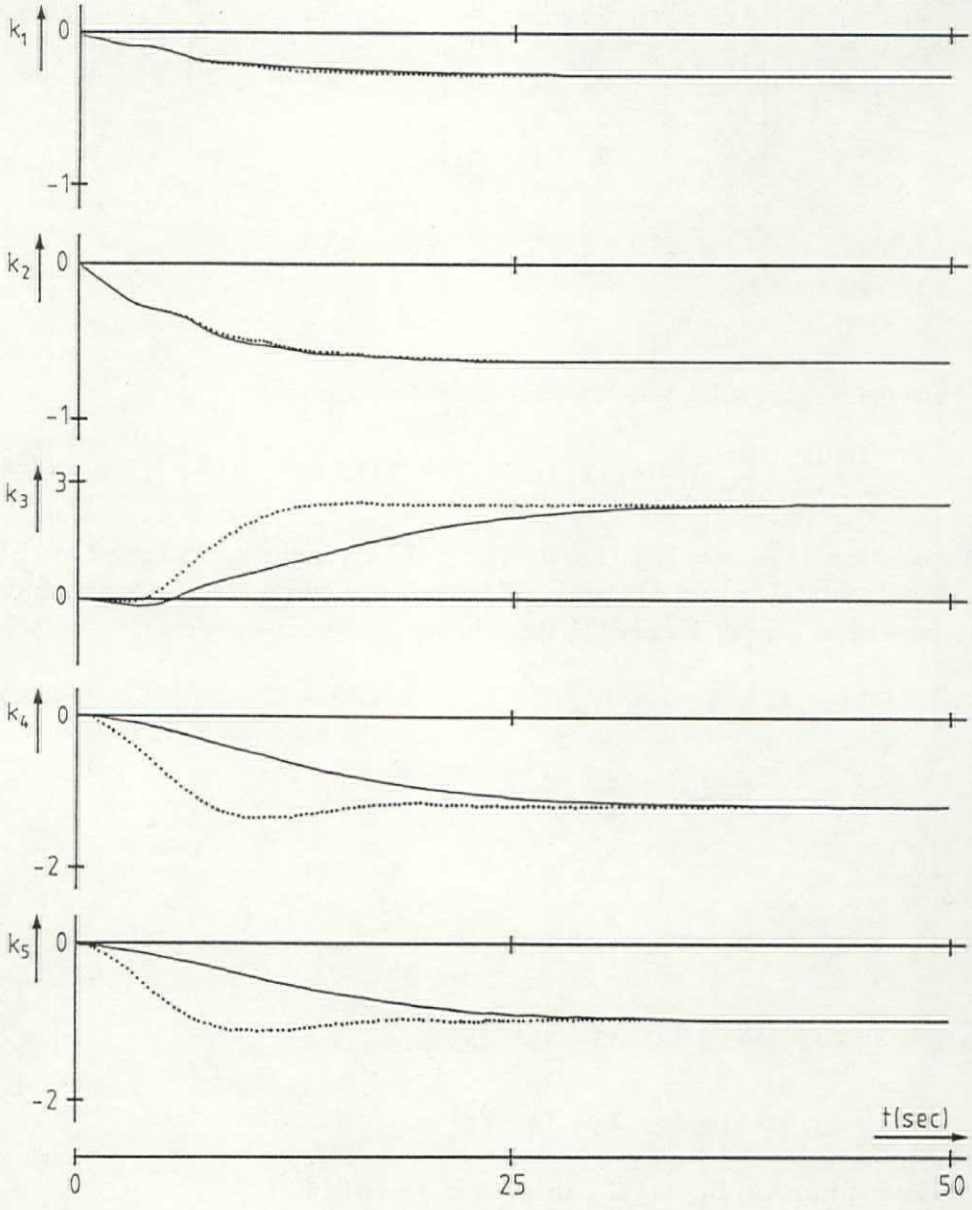

Fig. 3.4 Simulation of the innovation process

Fig. 3.4 shows the result of a simulation of the innovation process. The model parameters are given in Table 2.4; the ship's speed is 11 m/s. The criterion

parameters are given in Table 3.1.

parameter	value
q_1	1
q_2	1
q_3	0
q_4	1
q_5	1
r	1

Table 3.1 The criterion parameters

Fig. 3.4 demonstrates the effect of introducing the scaling matrix L in Eq. (3.31). The solid lines represent the outputs of the innovation process without the L-matrix. Within 40 seconds the innovation process reaches the steady state. The dotted lines represent the outputs of the innovation process while the largest time constant is scaled in time with a factor of 5 by introducing the appropriate L-matrix. In that case, the steady state is found within less than half the time.

3.4 Separation into submodels

In this section the fifth-order ship model is separated into two third-order models. The third-order roll model describes the rudder-to-roll transfer (Section 3.4.1) while the third-order yaw model describes the rudder-to-yaw transfer (Section 3.4.2). Controllers are calculated for both submodels and the results are compared with the results which are obtained with a controller for the fifth-order model. This comparison will be done in the frequency domain by means of Bode diagrams. Such a comparison can easily be made by using the Transformation and Identification Program **TRIP** (Van den Bosch, 1985b). The conditions under which such a separation is allowed are formulated as well.

3.4.1 The third-order roll model

From the block diagram of the fifth-order ship model, shown in Fig. 2.6, the third-order roll model given in Fig. 3.5 can be derived.

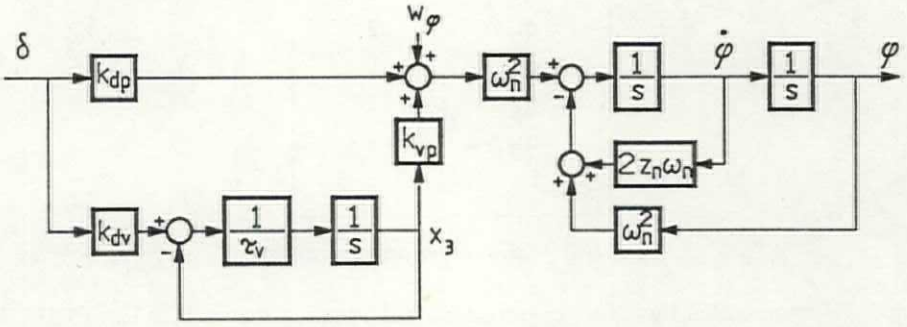

Fig. 3.5 Block diagram of the third-order roll model

This model is described by the following state-space equations:

$$\dot{\underline{x}} = A\underline{x} + B\underline{u} + D\underline{w} \qquad (3.34)$$

$$\underline{y} = C\underline{x} \qquad (3.35)$$

where

$$A = \begin{bmatrix} 0 & 1 & 0 \\ -\omega_n^2 & -2z_n\omega_n & \omega_n^2 k_{vp} \\ 0 & 0 & -1/\tau_v \end{bmatrix} \qquad B = \begin{bmatrix} 0 \\ \omega_n^2 k_{dp} \\ k_{dv}/\tau_v \end{bmatrix}$$

$$C = \begin{bmatrix} 1 & 0 & 0 \\ 0 & 1 & 0 \\ 0 & 0 & 1 \end{bmatrix} \qquad D = \begin{bmatrix} 0 \\ \omega_n^2 \\ 0 \end{bmatrix}$$

$$\underline{x}^T = (\varphi,\ \dot{\varphi},\ x_3) \qquad \underline{u} = \delta \qquad \underline{y}^T = (y_1,\ y_2,\ y_3)$$

$\underline{w} = w_\varphi$ = white noise with zero mean

The optimal controller with respect to criterion

$$J = \sum_{i=1}^{3} q_i E[y_i \cdot y_i]/r + E[\delta \cdot \delta] \qquad (3.36)$$

can be found by solving Eqs. (3.8) and (3.10). Application of the method which is introduced in Section 3.2 results in a solution which equals the steady state of the innovation process described by the following state-space equations:

$$\dot{\underline{x}}_m = A_m \underline{x}_m + B_m \underline{u}_m \qquad (3.37)$$

$$\underline{y}_m = C_m \underline{x}_m \qquad (3.38)$$

where

$$\underline{x}_m^T = (p_1, p_2, \ldots, p_6)$$

$$\underline{y}_m^T = (k_1, k_2, k_3)$$

$$\underline{u}_m = (q_1, q_2, q_3)$$

In this case, only the roll angle and the roll rate are important. Therefore, it will be henceforth assumed that q_3 equals 0. The matrices A_m, B_m and C_m are derived in Appendix C. They are subsets of the corresponding matrices of the solution of the fifth-order model given in Appendix B.
Fig. 3.6 shows some results of simulating the innovation process. The model parameters are given in Table 2.4; the ship's speed is 11 m/s.

In Fig. 3.6 the solid lines indicate the controller parameters k_i as a function of the criterion parameter q_1 while the dotted lines indicate the parameters k_i as a function of q_2. Apparently, the influence of q_2 on the controller parameters is less than the influence of q_1.

The roll angle does not have the same influence on the criterion described by Eq. (3.36) as the roll rate does. Thus, changing q_1 can have (much) more influence on the resulting controller than changing q_2. A *balanced* criterion does not have such a disadvantage. A balanced criterion is obtained if the following holds:

$$q_1 E[\varphi \cdot \varphi] = q_2 E[\dot{\varphi} \cdot \dot{\varphi}] \qquad (3.39)$$

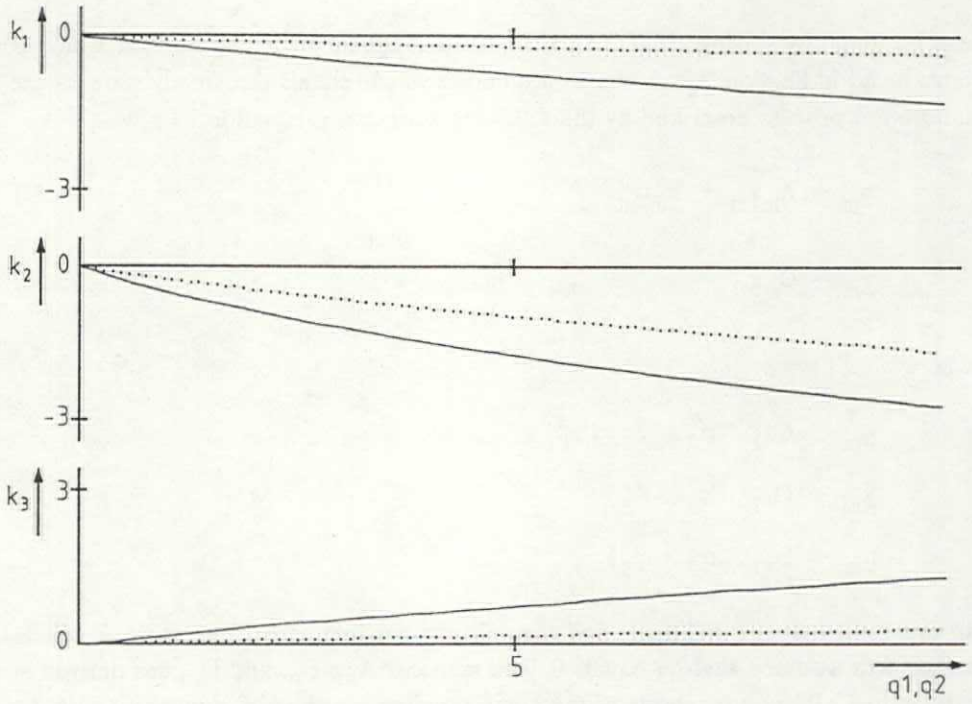

Fig. 3.6 The rudder-to-roll model: k_i as a function of q_j.

A balanced criterion can easily be found if the roll motion is a sinusoid:

Let the roll motion be a sinusoid described by

$$\varphi = u\sin(\omega t)$$

Using Eq. (3.39) yields

$$q_1 E[u\sin(\omega t).u\sin(\omega t)] = q_2 E[u\omega\cos(\omega t).u\omega\cos(\omega t)]$$

or

$$q_1 u^2 E[\sin(\omega t).\sin(\omega t)] = q_2 u^2 \omega^2 E[\cos(\omega t).\cos(\omega t)]$$

and finally:

$$q_1 = \omega^2 q_2$$

Therefore, the following criterion is a reasonable basic choice for the design of a roll controller:

$$J_\varphi = E[\delta.\delta] + q_1 E[\varphi.\varphi]/r + q_2 E[\dot{\varphi}.\dot{\varphi}]/r\omega^2 \qquad (3.40)$$

A balanced criterion is obtained by selecting q_2 to be equal to q_1. A more detailed discussion of the criterion parameters can be found in Chapter 5.

A comparison between the fifth-order rudder-to-roll model and the third-order model will indicate whether it is allowed to base the design of the roll controller on the latter. A Bode diagram can be used to make such a comparison in the frequency domain. It should be demonstrated that the relevant part (i.e. around the natural frequency) of the Bode diagram of the third-order model is similar to the corresponding part of the Bode diagram of the fifth-order model.

Fig. 3.7 gives the Bode diagram of the fifth-order rudder-to-roll transfer (dashed lines) and the third-order rudder-to-roll transfer. The criterion parameters are given in Table 3.2.

criterion parameter	fifth-order model	third-order model
q_1	10	10
q_2	30	30
q_3	0	0
q_4	500	0
q_5	1	0
r	1	1

Table 3.2 The criterion parameters

The ship's speed is 11 m/s and the parameters of the models are given in Table 2.4.

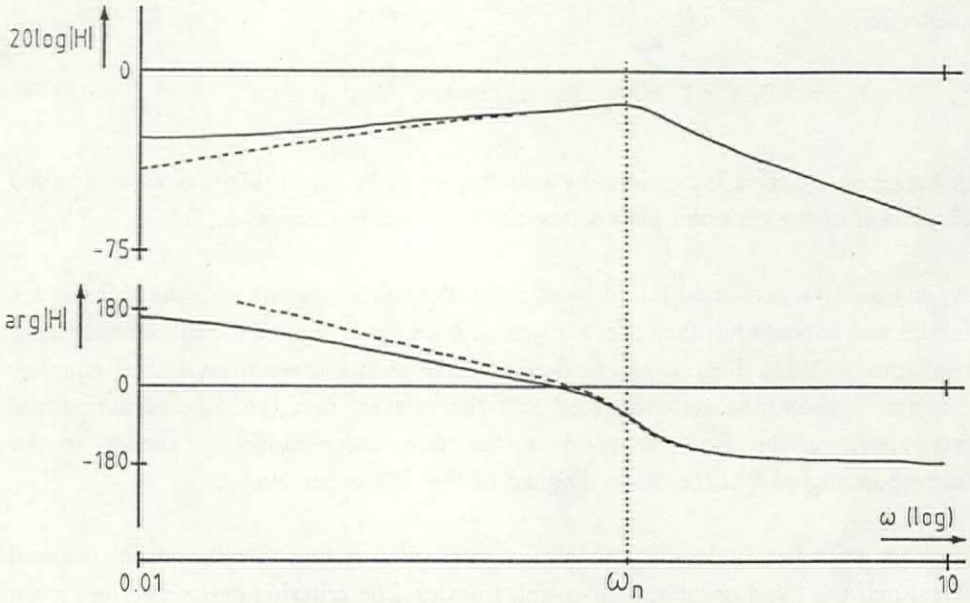

Fig. 3.7 Bode diagram of the rudder-to-roll transfer

Three parts can be recognized in Fig. 3.7:

- The high-frequency roll motions are the roll motions which are well above the natural roll frequency of the ship.
- The medium-frequency roll motions are roll motions just around the natural roll frequency (in the figure indicated as ω_n).
- The roll motions which are of a (much) lower frequency than the natural roll frequency are referred to as low-frequency roll motions.

Fig. 3.7 shows that in the high-frequency range the Bode diagrams of the fifth-order model and the third-order model are identical. Just below the natural frequency a phase shift arises which becomes larger while going to the low-frequency range. In the low-frequency range the gain differs. Therefore, it may be concluded that it is allowed to disregard the yaw influence only if the low-frequency components are removed from the roll motions. This filter problem will be examined in Chapter 4. The difference between the Bode diagram of the fifth-order model and the Bode diagam of the third-order model increases if the weighting of the yaw motions

increases. Therefore, an additional requirement is that the criterion parameters q_5 and q_4 must remain below a certain high limit. Reasonable high limits of these parameters are respectively 10 and 500.

3.4.2 The third-order yaw model

Fig. 3.8 shows a block diagram of the third-order yaw model, derived from the block diagram of the fifth-order ship model (see Fig. 2.6).

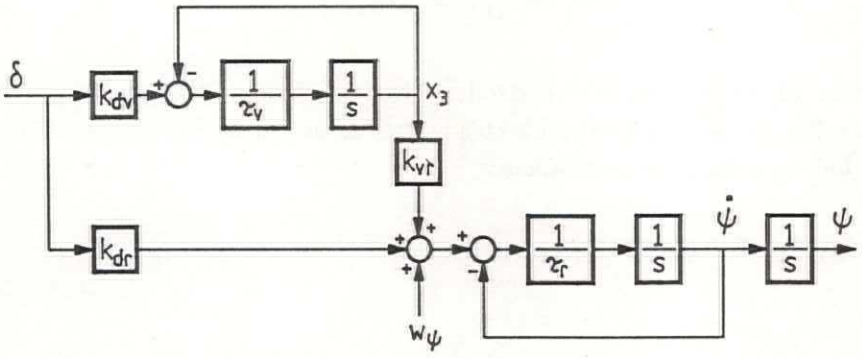

Fig. 3.8 Block diagram of the third-order yaw model

The model can be described by the following state-space equations:

$$\dot{\underline{x}} = A\underline{x} + B\underline{u} + D\underline{w} \qquad (3.41)$$

$$\underline{y} = C\underline{x} \qquad (3.42)$$

where

$$A = \begin{bmatrix} -1/\tau_v & 0 & 0 \\ k_{vr}/\tau_r & -1/\tau_r & 0 \\ 0 & 1 & 0 \end{bmatrix} \qquad B = \begin{bmatrix} k_{dv}/\tau_v \\ k_{dr}/\tau_r \\ 0 \end{bmatrix}$$

$$C = \begin{bmatrix} 1 & 0 & 0 \\ 0 & 1 & 0 \\ 0 & 0 & 1 \end{bmatrix} \qquad D = \begin{bmatrix} 0 \\ 1/\tau_r \\ 0 \end{bmatrix}$$

$$\underline{x}^T = (x_3,\ \dot{\psi},\ \psi) \qquad \underline{u} = \delta \qquad y = (y_3,\ y_4,\ y_5)$$

$$\underline{w} = w_\psi = \text{white noise with zero mean}$$

Let the criterion be described by Eq. (3.43):

$$J = \sum_{i=3}^{5} q_i E[y_i . y_i]/r + E[\delta . \delta] \qquad (3.43)$$

Similar to the optimal roll controller, given in Section 3.4.1, the optimal yaw controller can be found to be the steady state of an innovation process described by the following state-space equations:

$$\dot{\underline{x}}_m = A_m \underline{x}_m + B_m \underline{u}_m \qquad (3.44)$$

$$\underline{y}_m = C_m \underline{x}_m \qquad (3.45)$$

where

$$\underline{x}_m^T = (p_1,\ p_2,\ \ldots\ldots,p_6)$$

$$\underline{y}_m^T = (k_3,\ k_4,\ k_5)$$

$$\underline{u}_m = (q_3,\ q_4,\ q_5)$$

In this case, only the rate of turn and the heading error are important. Therefore, it will henceforth be assumed that q_3 equals 0. The matrices A_m, B_m and C_m are derived in Appendix D. They are subsets of the corresponding matrices of the solution of the fifth-order model given in Section 3.3 (see Appendix B).
Several simulations were carried out with the process described by Eqs. (3.44) and (3.45). Fig. 3.9 shows the yaw controller gains as a function of the criterion parameters q_4 (the dotted lines) and q_5 (the solid lines). The parameters of the process are given in Table 2.4; the ship's speed is 11 m/s.

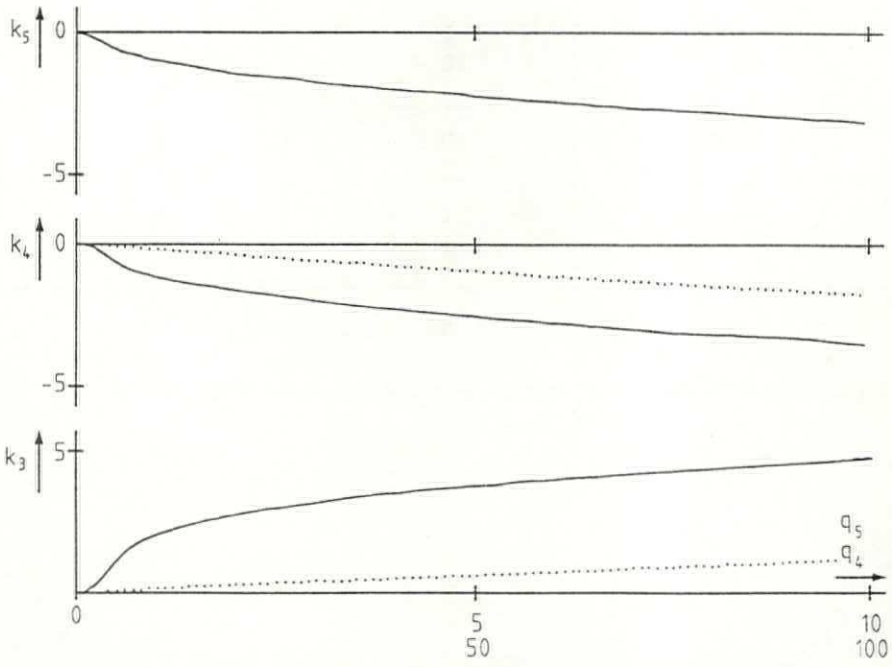

Fig. 3.9 The rudder-to-yaw model: k_i as a function of q_j.

Apparently, the influence of q_4 on the controller parameters is small in comparison to the influence of q_5. Furthermore, q_4 has no influence on parameter k_5. This can be found from Eqs. (3.44) and (3.45) (see Appendix D) as well.

A comparison in the frequency domain between the fifth-order model given in Section 3.3 and the third-order yaw model will indicate whether it is allowed to base the design of the yaw controller on the latter.

In Fig. 3.10 a comparison is given between the Bode diagram of the fifth-order model (the dashed lines) and the Bode diagram of the third-order yaw model (the solid lines). The dotted lines represent the Bode diagram of the non-controlled process. The criterion parameters are given in Table 3.3.

criterion parameter	fifth-order model	third-order model
q_1	10	0
q_2	30	0
q_3	0	0
q_4	500	500
q_5	1	1
r	1	1

Table 3.3 The criterion parameters

The parameters of the models are given in Table 2.4; the ship's speed is 11 m/s.

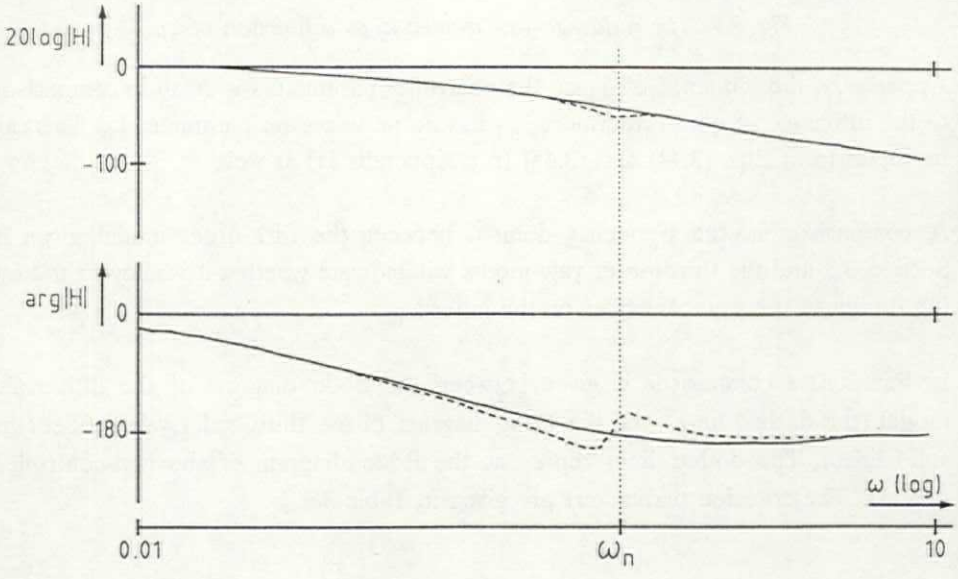

Fig. 3.10 Bode diagram of the rudder-to-yaw transfer

In Fig. 3.10 three areas can be recognized:

- the low-frequency area and the high-frequency area where the influence of the roll motions on the rudder-to-yaw transfer is low.
- the medium-frequency area where the roll motions influence the performance of the yaw controller.

This figure shows that for high-frequency motions (well above the natural roll frequency) as well as for low-frequency motions it is allowed to use the third-order yaw model instead of the fifth-order model. In the neighborhood of the natural roll frequency a considerable phase shift arises. Therefore, it is allowed to use the third-order yaw model as a basis for a control design only if these medium- frequency components are removed from the yaw motions. This corresponds to the current ideas concerning a modern autopilot design. In Van Amerongen (1982) and Duetz (1985), to name a few, it is shown that a properly designed controller should compensate only the low-frequency disturbances. In Chapter 4 a filter which is able to suppress the medium and high-frequency yaw motions is designed.

Note that the upper part of Fig. 3.10 shows a small difference between the Bode diagram of the fifth-order model and the Bode diagram of the submodel. If the disturbances are present in this area, the roll controller may improve the course keeping performance.

3.5 The influence of the ship's speed

The ship's speed greatly influences some of the parameters of the ship model and thus the parameters of the corresponding "innovation" process (see Section 3.2). The controller parameters depend on the steady state of the innovation process. It can be expected that they are influenced by the ship's speed as well. In that case, two problems may be encountered in practice:

- If the controller gains become too large the steering machine may saturate even during small roll motions or yaw motions. Thus, it is not allowed to disregard the influence of the steering machine.
- The time constants of the innovation process determine the convergence speed of the process and the required computer time. The convergence speed increases if

the time constants increase. The required computer time increases if the time constants become small.

Several simulations were carried out with the innovation processes given in Section 3.4. Some results are shown in Figs. 3.11 and 3.12, which give the controller gains as a function of the ship's speed. The model parameters are given in Table 2.4 while the criterion parameters are given in Table 3.4. The ship's speed ranges from 12 m/s. to 2 m/s.

criterion parameter	value
q_1	10
q_2	30
q_3	0
q_4	100
q_5	10
r	1

Table 3.4 The criterion parameters

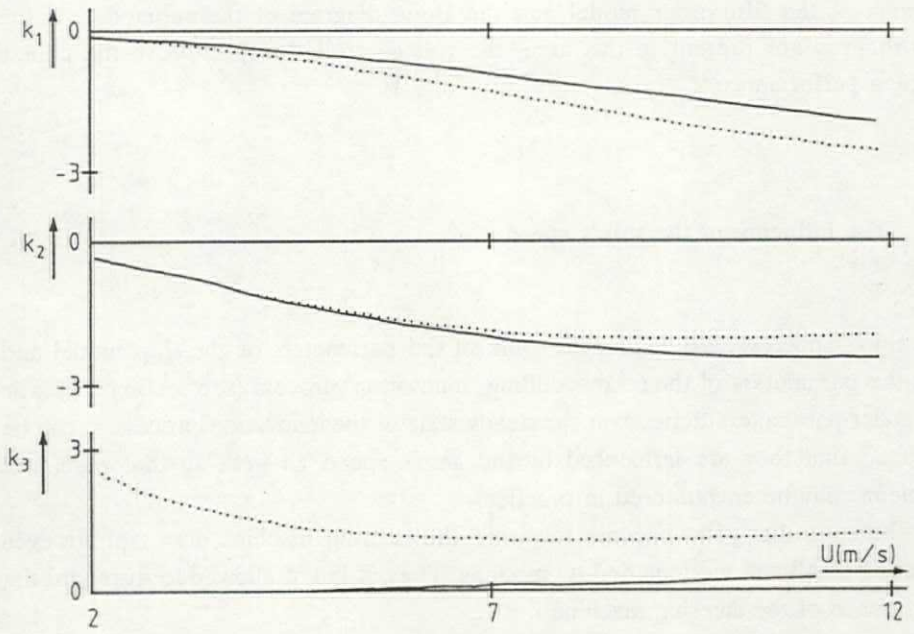

Fig. 3.11 The influence of the ship's speed on the roll controller

In this figure the dotted lines represent the gains of the roll controller based on the fifth-order model while the solid lines represent those based on the third-order roll model.

Fig. 3.11 demonstrates that the roll controller gains become large if the ship's speed increases. Therefore, even small disturbances may cause considerable rudder motions. Precautions should be taken to prevent the steering machine from saturating and thus to guarantee that the process will remain linear. This problem will be solved in Chapter 5.

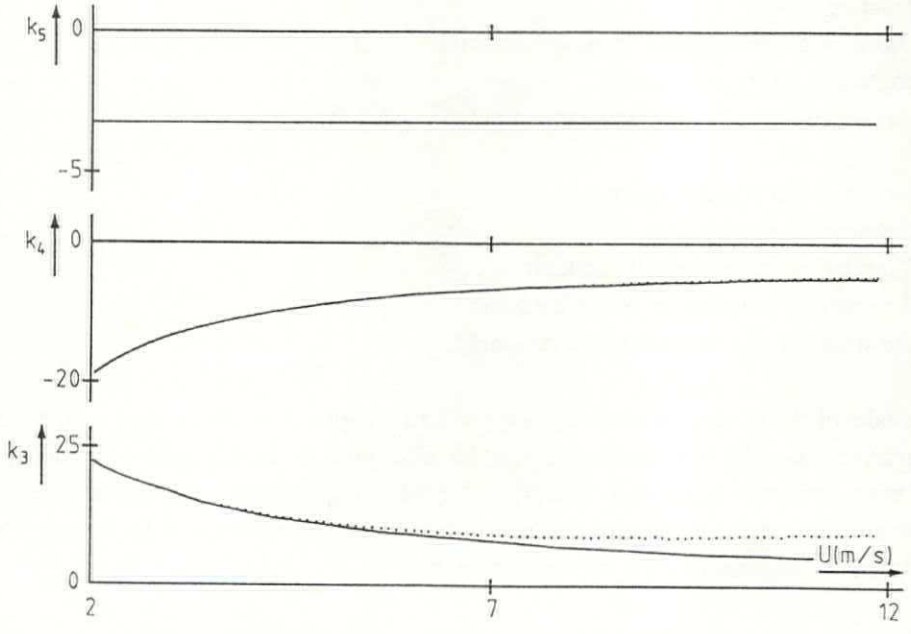

Fig. 3.12 The influence of the ship's speed on the yaw controller

The dotted lines represent the gains of the yaw controller based on the fifth-order model. The solid lines represent those based on the third-order yaw model.

Fig. 3.12 shows that the absolute values of two of the yaw controller gains (k_3 and k_4) increase rapidly if the ship's speed becomes low. Therefore, precautions should be taken to guarantee that the process will remain linear. The gain k_5 does not depend on the ship's speed.

Concluding remarks

In this chapter a method to design a controller is proposed. It is based on the LQG method and has the following properties:

The method
- guarantees that a solution will be stable and will be be optimal with respect to the selected criterion,
- allows that the parameters of the process or the weighting factors of the criterion change in time,
- calculates the solution in an iterative way which can be easily implemented in practice,
- allows a good understanding of the influence of the process parameters on the controller parameters and
- can be easily implemented in the simulation package PSI.

However, the method requires
- the process to be linear,
- a model of the process to be known,
- a quadratic criterion to be defined and
- the states of the process to be measured.

A model of the process is given in Chapter 2. In Chapter 5 methods are posed which guarantee that the non-linearities can be disregarded. In Chapter 6 a suitable quadratic criterion is derived. Finally, in the following chapter a method is given to estimate the states of the process which cannot be measured and to remove the undesired components from the measurements.

4 THE FILTER DESIGN

4.1 Introduction

In Chapter 3 a method for designing the "optimal" controller for a linear process is introduced. This method requires the states of the process to be available. If the states are not measurable or if they are contaminated by noise, a filter should be designed. This filter should yield "good" estimates of the unknown states and remove the undesired components from the measurements. The optimal controller uses the states of the filter as its input.

The problem of designing an "optimal" filter for linear processes is well known in the literature (e.g. Kwakernaak and Sivan, 1972). Designing an "optimal" filter requires that a performance criterion be defined. In addition, it is required that the properties of system noise and measurement noise be known. Based on the available knowledge of the process, the noise properties and the input signals a prediction is made concerning the output of the process. This prediction is compared with the measured output of the process and the result of this comparison is taken into account in the next prediction of the output. The optimal filter is obtained if the error between the predicted and the measured output of the process is as small as possible. The Linear Optimal Filter Theory offers a mathematical tool to update the prediction such that the covariance of this error is as small as possible.
The problem of designing an optimal filter by using the "Optimal Linear Filter Theory" is the dual of the problem of designing an optimal controller by using the LQG method. Therefore, this problem can be tackled in a way similar to the controller problem in Chapter 3.

This chapter is organized as follows:
In Section 4.2 a short introduction of the Optimal Linear Filter Theory is given. A calculation method similar to the method mentioned in Chapter 3 is proposed. In Section 4.3 processes with colored measurement noise and colored system noise are considered. In Section 4.4 the implications of the assumption that the system noise is only partly known are demonstrated. Filters are designed which are able to remove the high-frequency components from the yaw model and to remove the low-frequency components from the roll model. Finally, in Section 4.5 the filtering of the ship's speed will be taken into account.

4.2 The Optimal Linear Filter Design

This section gives a comprehensive derivation of the theory of optimal filtering.

In general, a linear process can be described by the block diagram of Fig. 3.1. A process may contain several known inputs $\underline{u}$ and it can be influenced by unknown inputs (disturbances) $\underline{w}$. These unknown inputs will be referred to from now on as state excitation noise or "system noise".
Furthermore, it is possible to measure one or more signals $\underline{y}$ of the process. The measurements are contaminated by "measurement noise" $\underline{v}$. Contrary to system noise, measurement noise does not affect the states of the process.
Such a process can be described by the following state-space equations:

$$\dot{\underline{x}}(t) = A\underline{x}(t) + B\underline{u}(t) + D\underline{w}(t) \qquad (4.1)$$

$$\underline{y}(t) = C\underline{x}(t) + \underline{v}(t) \qquad (4.2)$$

To shorten the notation $\underline{x}(t)$, $\underline{y}(t)$, $\underline{v}(t)$, $\underline{w}(t)$ and $\underline{u}(t)$ will be written respectively as $\underline{x}$, $\underline{y}$, $\underline{v}$, $\underline{w}$, and $\underline{u}$. Furthermore, it will be assumed that the parameters of the process change slowly in time such that it is allowed to consider the matrices A, B, C and D to be time invariant.

Fig. 4.1 contains the block diagram of the process along with that of a state estimator. The block diagram of the state estimator contains a structure similar to that of the process. This structure represents the knowledge of the process and is used to generate a prediction of the state variables of the process. The update vector $\underline{z}$ denotes the difference between the measured and the predicted output of the process. This vector updates the states of the filter by an update matrix "K". The update matrix K determines the properties of the filter. In the last two decades, many articles have been published describing the calculation of K depending on the available knowledge of the process and the disturbances and on the desired criterion. A summary of the basic principles can be found in Sage (1968) and Kwakernaak and Sivan (1972), to cite two examples.

In Chapter 2 a model of the process involved was derived. In this chapter it will be assumed that the process is fully known. All the modeling errors can be included in the noise vector $\underline{w}$ (denoting white noise with a zero mean) without affecting the

validity of the subsequent derivations.

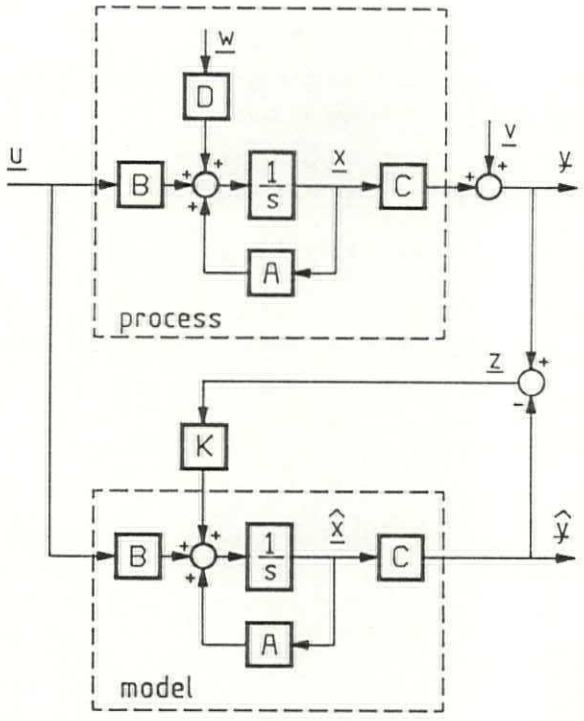

Fig. 4.1 Block diagram of process and state estimator

The assumption that the process is fully known implies that it is allowed to describe the transfer function $\underline{u}$ to $\hat{\underline{x}}$ by the following state-space equations:

$$\dot{\hat{\underline{x}}} = A\hat{\underline{x}} + B\underline{u} + K\underline{z} \tag{4.3}$$

$$\hat{\underline{y}} = C\hat{\underline{x}} \tag{4.4}$$

$$\underline{z} = \underline{y} - \hat{\underline{y}} = \underline{y} - C\hat{x} \tag{4.5}$$

In Eqs.(4.3) and (4.5) $\underline{z}$ stands for the *prediction-error vector.*

From these equations it follows that

$$\dot{\hat{\underline{x}}} = A\hat{\underline{x}} + B\underline{u} + K(\underline{y} - C\hat{\underline{x}}) \qquad (4.6)$$

The expectation E of the error vector $\underline{e} = \underline{x} - \hat{\underline{x}}$ is referred to as $E[\underline{e}] = E[\underline{x} - \hat{\underline{x}}]$. For the derivative of $E[\underline{e}]$ the following holds:

$$\dot{E}[\underline{e}] = E[\dot{\underline{x}} - \dot{\hat{\underline{x}}}] = E[A\underline{x} + B\underline{u} + D\underline{w} - A\hat{\underline{x}} - B\underline{u} - K\underline{z}] =$$

$$= E[(A - KC)(\underline{x} - \hat{\underline{x}}) + D\underline{w} - K\underline{v}]$$

Let $\underline{w}$ and $\underline{v}$ be uncorrelated white noise with zero mean. In that case this can be further reduced to

$$\dot{E}[\underline{e}] = (A - KC)E[\underline{e}] \qquad (4.7)$$

For a zero mean process where $E[\underline{x}] = 0$, the covariance P of the error vector $\underline{e}$ is given by:

$$P = E[\underline{e}.\underline{e}^T] \qquad (4.8)$$

The optimal filter is defined as the filter where P is as small as possible. If the process is time-invariant, the minimum of P is found if the rate of change of P equals 0.
The rate of change of P is given by:

$$\dot{P} = E[\dot{\underline{e}}.\underline{e}^T] + E[\underline{e}.\dot{\underline{e}}^T] \qquad (4.9)$$

From Eqs. (4.1), (4.3) and (4.5) it follows that

$$\dot{\underline{e}} = (A - KC)\underline{e} - K\underline{v} + D\underline{w} \qquad (4.10)$$

Substituting Eq. (4.10) in Eq. (4.9) yields:

$$\dot{P} = E[((A-KC)\underline{e} - K\underline{v} + D\underline{w}).\underline{e}^T] + E[\underline{e}.((A-KC)\underline{e} - K\underline{v} + D\underline{w})^T]$$

$$= (A-KC)E[\underline{e}.\underline{e}^T] + E[\underline{e}.\underline{e}^T](A-KC)^T - KE[\underline{v}.\underline{e}^T] - E[\underline{e}.\underline{v}^T]K^T + DE[\underline{w}.\underline{e}^T] + E[\underline{e}.\underline{w}^T]D^T$$

$$= (A-KC)E[\underline{e}.\underline{e}^T] + E[\underline{e}.\underline{e}^T](A-KC)^T + KE[\underline{v}.\hat{\underline{x}}^T] + E[\hat{\underline{x}}.\underline{v}^T]K^T + DE[\underline{w}.\underline{x}^T] + E[\underline{x}.\underline{w}^T]D^T$$

Taking into account that $\underline{v}$ and $\underline{w}$ are white noise with zero mean, this reduces further to:

$$\dot{P} = (A-KC)E[\underline{e}.\underline{e}^T] + E[\underline{e}.\underline{e}^T](A-KC)^T + KE[\underline{v}.\underline{v}^T]K^T + DE[\underline{w}.\underline{w}^T]D^T$$

or

$$\dot{P} = (A-KC)P + P(A-KC)^T + KRK^T + DQD^T \qquad (4.11)$$

where

$$R = E[\underline{v}.\underline{v}^T]$$

$$Q = E[\underline{w}.\underline{w}^T]$$

Finally, reordering the terms in (4.11) yields:

$$\dot{P} = AP + PA^T + DQD^T - PC^TR^{-1}CP + [K-PC^TR^{-1}]R[K-PC^TR^{-1}]^T \qquad (4.12)$$

The righthand side of Eq. (4.12) is minimized by selecting the appropriate K according to:

$$K = PC^TR^{-1} \qquad (4.13)$$

where P is to be calculated by using the following "Riccati equation":

$$\dot{P} = AP + PA^T + DQD^T - PC^TR^{-1}CP \qquad (4.14)$$

The process is assumed to be time invariant; therefore:

$$0 = AP + PA^T + DQD^T - PC^TR^{-1}CP \qquad (4.15)$$

From this result it follows that the covariance P, defined in (4.8), is minimized if K is selected according to Eq. (4.13). Eqs. (4.13) and (4.15) are the basic equations which will be used to calculate the "optimal" filter.
Many variations of Eqs. (4.13) and (4.15), in which other process knowledge is included, can be found in the literature. Several of these variations, such as processes disturbed by colored measurement noise or by colored system noise, will be discussed in Section 4.3.

In Eq. (4.7) it is assumed that $\underline{w}$ and $\underline{v}$ are uncorrelated. If $\underline{w}$ and $\underline{v}$ are correlated it is necessary to include this extra information in the filter design.

Let the correlation between $\underline{w}$ and $\underline{v}$ be described by

$$E[\underline{w}.\underline{v}^T] = S \neq 0$$

In that case, Eq. (4.13) changes to

$$K = (PC^T + DS)R^{-1} \qquad (4.16)$$

while Eq. (4.15) changes to

$$0 = AP + AP^T + DQD^T - (PC^T+DS)R^{-1}(PC^T+DS)^T \qquad (4.17)$$

Eqs. (4.16) and (4.17) demonstrate that including more knowledge about the process in the filter design results in a larger update matrix K and a lower covariance matrix P.

In general, an analytical solution of Eq. (4.15) can be found if the order of the process is one or two. If the order of the process is higher this may pose problems. In that case, the iterative method which is proposed in Chapter 3 can be applied.

Define the "innovation process" given by Eqs. (4.18) and (4.19):

$$\dot{P} = AP + PA^T + DQD^T - KCP \qquad (4.18)$$

$$K = PC^T R^{-1} \qquad (4.19)$$

Eqs. (4.18) and (4.19) can be rewritten such that they resemble the more commonly applied form, i.e. the "innovation" process with the following state-space equations:

$$L\dot{\underline{x}}_m = A_m \underline{x}_m + B_m \underline{u}_m \qquad (4.20)$$

$$\underline{y}_m = C_m \underline{x}_m \qquad (4.21)$$

where

$$\underline{x}_m^T = (p_{11}, p_{12}, p_{13}, \ldots . p_{nn})$$

$$\underline{y}_m^T = (k_{11}, k_{12}, \ldots . k_{nr}) = \text{the elements of the matrix K}$$

r = the number of measured process outputs

If P is rank n, $\underline{x}_m$ consists of $0.5n(n+1)$ elements.

Comparing (4.18) and (4.19) with (4.20) and (4.21) yields

$$AP + PA^T - KCP \leftrightarrow A_m \underline{x}_m$$

$$DQD^T \leftrightarrow B_m \underline{u}_m$$

$$PC^T R^{-1} \leftrightarrow C_m \underline{x}_m$$

The innovation process introduces non-linear differential equations which can be solved by numerical integration methods. The steady-state outputs of this process are the gains of the optimal filter.

The convergence of this "innovation process" can be influenced by the diagonal matrix L (see Chapter 3). As this matrix does not influence the steady state of the innovation process, it does not affect the resulting filter gains either.

4.3 Colored noise

4.3.1 Process disturbed by colored measurement noise

In Eq. (4.2) $\underline{v}$ is assumed to be white noise with a zero mean. This is not a limitation of the validity of the methodology introduced in Section 4.2. Kwakernaak and Sivan (1972) describe a method of calculating the optimal filter should $\underline{v}$ be colored noise. In this section a different approach is followed because of the nature of the problem which has to be solved.
Duetz (1985) demonstrates that a course controller should reduce only the low-frequency yaw motions of the ship. Van Amerongen (1982) defines the high-frequency yaw motions as "measurement noise". In that case, the measurement noise contains a white noise component and a colored noise component. Both components should be removed from the measurements. The general solution for such a problem can be found as follows:

Let a process be given by the block diagram of Fig. 4.2.

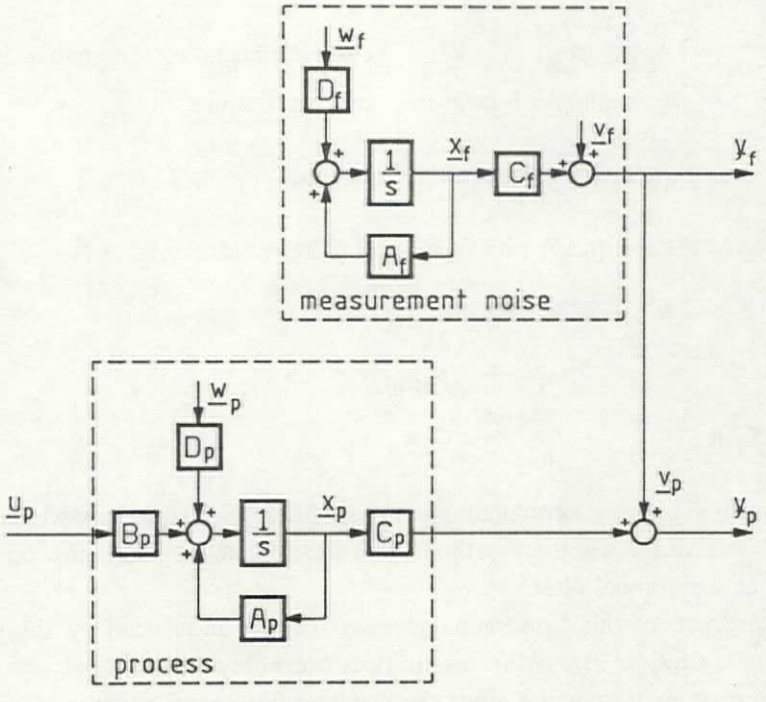

Fig. 4.2 Process with colored measurement noise

This process can be described by the following state-space equations:

$$\dot{\underline{x}}_p = A_p\underline{x}_p + B_p\underline{u}_p + D_p\underline{w}_p \tag{4.22}$$

$$\underline{y}_p = C_p\underline{x}_p + \underline{v}_p \tag{4.23}$$

where $\underline{w}_p$ denotes white noise with zero mean and covariance matrix Q_p.

Let $\underline{v}_p$ be colored noise, described by the following shaping filter:

$$\dot{\underline{x}}_f = A_f\underline{x}_f + D_f\underline{w}_f \tag{4.24}$$

$$\underline{y}_f = C_f\underline{x}_f + \underline{v}_f = \underline{v}_p \tag{4.25}$$

where $\underline{v}_f$ denotes white noise with zero mean and covariance matrix R_f.

Combining Eqs. (4.22) and (4.25) into one model yields:

$$\dot{\underline{x}} = A\underline{x} + B\underline{u} + D\underline{w} \tag{4.26}$$

$$\underline{y} = C\underline{x} + \underline{v} \tag{4.27}$$

where

$$A = \begin{bmatrix} A_p & 0 \\ 0 & A_f \end{bmatrix} \qquad B = \begin{bmatrix} B_p \\ 0 \end{bmatrix} \qquad C = (C_p \; C_f) \qquad D = \begin{bmatrix} D_p & 0 \\ 0 & D_p \end{bmatrix}$$

$$\underline{x}^T = (\underline{x}_p^T \; \underline{x}_f^T) \qquad \underline{y} = \underline{y}_p + \underline{y}_f \qquad v = \underline{v}_f$$

The optimal filter is described by:

$$\dot{\hat{\underline{x}}} = A\hat{\underline{x}} + B\underline{u} + K\underline{z} \tag{4.28}$$

$$\hat{\underline{y}} = C\hat{\underline{x}} \tag{4.29}$$

$$\underline{z} = \underline{y} - \hat{\underline{y}} = \underline{y} - C\hat{\underline{x}} \tag{4.30}$$

In Fig. 4.3 a block diagram of the resulting filter structure is given.

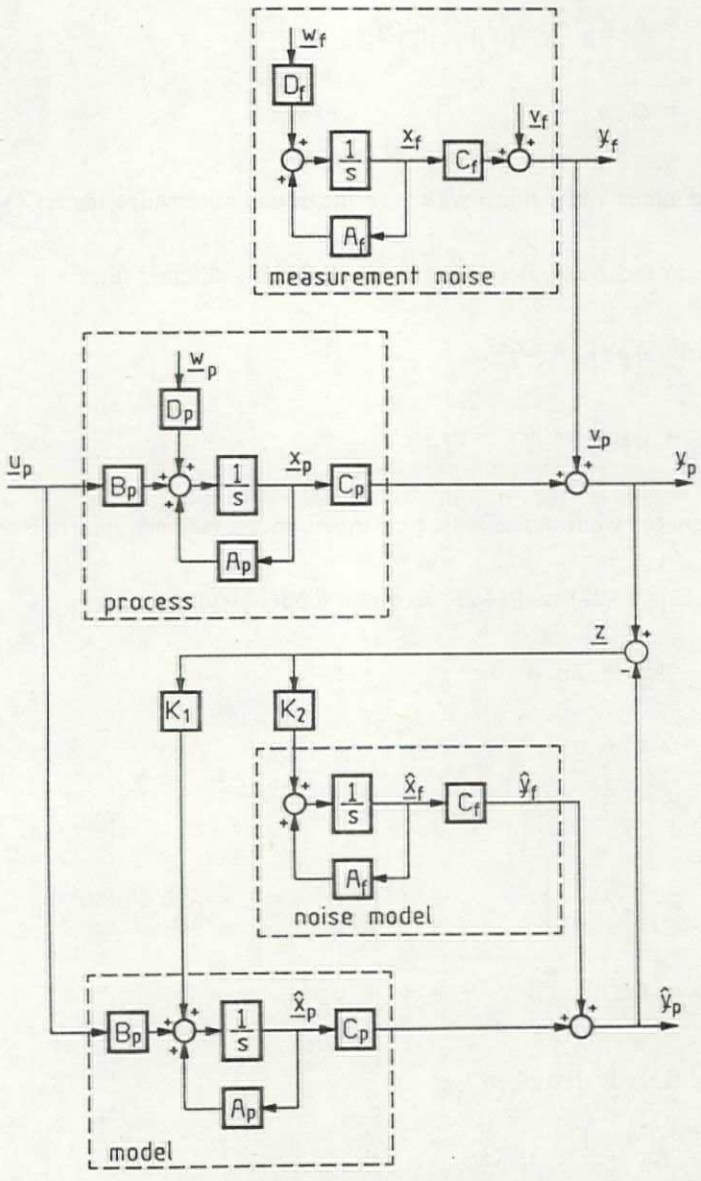

Fig. 4.3 Block diagram of the optimal filter

Clearly, the optimal filter comprises a model of the process as well as a model of the measurement noise. The models are updated by respectively the update matrices K_1 and K_2. These matrices can be found by solving the following equations:

$$\dot{P} = AP + PA^T + DQD^T - KCP \tag{4.31}$$

$$K = PC^T R^{-1} \tag{4.32}$$

where

$$P = \begin{bmatrix} P_1 & P_2 \\ P_2^T & P_3 \end{bmatrix} \quad K = \begin{bmatrix} K_1 \\ K_2 \end{bmatrix} \quad Q = \begin{bmatrix} Q_p & 0 \\ 0 & Q_f \end{bmatrix} \quad R = R_f$$

Eq. (4.32) is solved as follows:

$$K = PC^T R^{-1} = \begin{bmatrix} P_1 & P_2 \\ P_2^T & P_3 \end{bmatrix} \begin{bmatrix} C_p^T \\ C_f^T \end{bmatrix} R_f^{-1} = \begin{bmatrix} (P_1 C_p^T + P_2 C_f^T) R_f^{-1} \\ (P_2^T C_p^T + P_3 C_f^T) R_f^{-1} \end{bmatrix} = \begin{bmatrix} K_1 \\ K_2 \end{bmatrix}$$

Therefore

$$K_1 = (P_1 C_p^T + P_2 C_f^T) R_f^{-1} \tag{4.33}$$

$$K_2 = (P_2 C_p^T + P_3 C_f^T) R_f^{-1} \tag{4.34}$$

while P is to be found from

$$\dot{P} = \begin{bmatrix} \dot{P}_1 & \dot{P}_2 \\ \dot{P}_2^T & \dot{P}_3 \end{bmatrix} = \begin{bmatrix} A_p & 0 \\ 0 & A_f \end{bmatrix} \begin{bmatrix} P_1 & P_2 \\ P_2^T & P_3 \end{bmatrix} + \begin{bmatrix} P_1 & P_2 \\ P_2^T & P_3 \end{bmatrix} \begin{bmatrix} A_p^T & 0 \\ 0 & A_f^T \end{bmatrix} +$$

$$+ \begin{bmatrix} D_p & 0 \\ 0 & D_f \end{bmatrix} \begin{bmatrix} Q_p & 0 \\ 0 & Q_f \end{bmatrix} \begin{bmatrix} D_p^T & 0 \\ 0 & D_f^T \end{bmatrix} - \begin{bmatrix} K_1 \\ K_2 \end{bmatrix} (C_p \quad C_f) \begin{bmatrix} P_1 & P_2 \\ P_2^T & P_3 \end{bmatrix} =$$

$$= \begin{bmatrix} A_p P_1 & A_p P_2 \\ A_f P_2^T & A_f P_3 \end{bmatrix} + \begin{bmatrix} P_1 A_p^T & P_2 A_f^T \\ P_2^T A_p^T & P_3 A_f^T \end{bmatrix} + \begin{bmatrix} D_p Q_p D_p^T & 0 \\ 0 & D_f Q_f D_f^T \end{bmatrix} -$$

$$- \begin{bmatrix} K_1 C_p P_1 + K_1 C_f P_2^T \\ K_2 C_p P_1 + K_2 C_f P_2^T \end{bmatrix} \begin{bmatrix} K_1 C_p P_2 + K_1 C_f P_3 \\ K_2 C_p P_2 + K_2 C_f P_3 \end{bmatrix}$$

or

$$\dot{P}_1 = A_p P_1 + P_1 A_p^T - K_1 C_p P_1 - K_1 C_f P_2^T + D_p Q_p D_p^T \qquad (4.35)$$

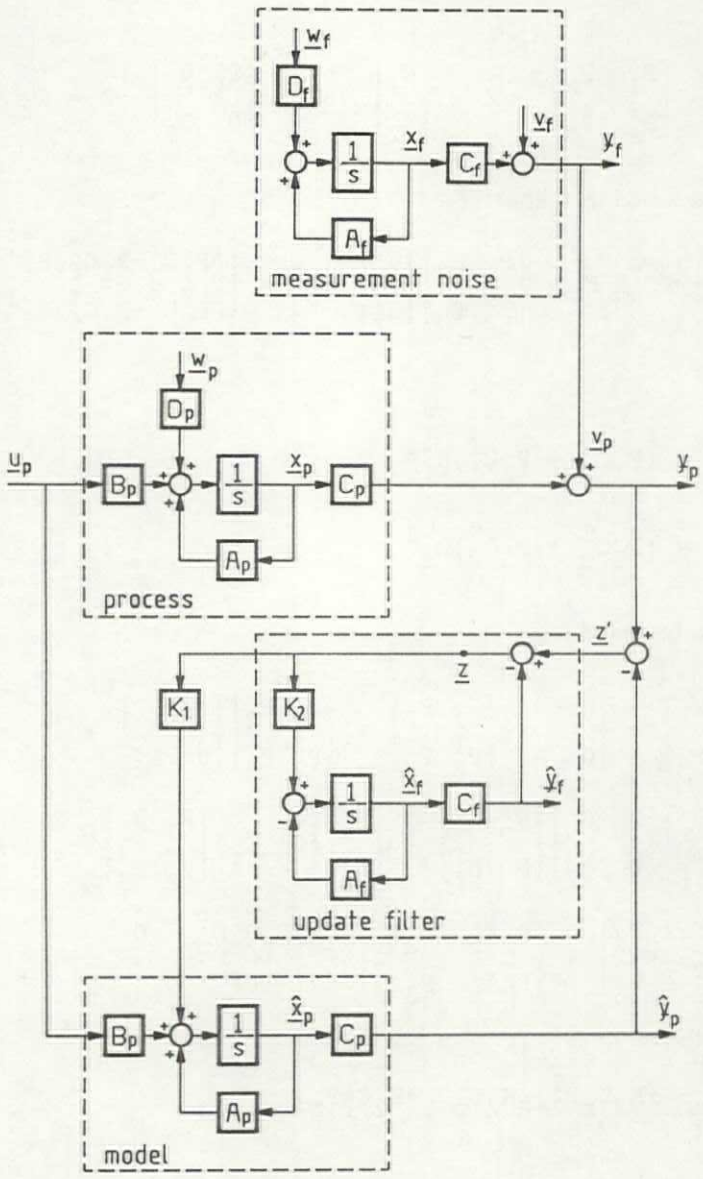

Fig. 4.4 Modified filter structure

$$\dot{P}_2 = A_p P_2 + P_2 A_f^T - K_1 C_p P_2 - K_1 C_f P_3 \qquad (4.36)$$

$$\dot{P}_3 = A_f P_3 + P_3 A_f^T - K_2 C_p P_2 - K_2 C_f P_3 + D_f Q_f D_f^T \qquad (4.37)$$

The block diagram of Fig. 4.3 can be modified to the block diagram of Fig. 4.4. Fig. 4.1 shows the optimal filter if the measurement noise is white noise. If the measurement noise is non-white noise the optimal filter structure changes (see Fig. 4.4). A comparison of Fig. 4.1 and Fig. 4.4 shows that in Fig 4.1 the update matrix K has been replaced by an update *filter*. In addition, the update vector $\underline{z}$ has been replaced by $\underline{z}'$.
The structure of the update filter is determined by the coloring of the measurement noise. The matrices K_1 and K_2 are described by Eqs. (4.33) and (4.34).

In Appendix E a calculation example is given. The optimal filter is calculated for a second-order process disturbed by colored measurement noise. This colored noise is described by a first-order shaping filter.

4.3.2 Process disturbed by colored system noise

In Eq. (4.1) it is assumed that $\underline{w}$ denotes white noise with zero mean. If $\underline{w}$ denotes colored noise, a method similar to the one given in Section 4.3.1 can be applied to find the optimal filter.

Let a process be described by the following state-space equations:

$$\dot{\underline{x}}_p = A_p \underline{x}_p + B_p \underline{u}_p + D_p \underline{w}_p \qquad (4.38)$$

$$\underline{y}_p = C_p \underline{x}_p + \underline{v}_p \qquad (4.39)$$

where $\underline{v}_p$ denotes white noise with zero mean and covariance matrix R_p.

Let $\underline{w}_p$ be colored noise, described by the following shaping filter:

$$\dot{\underline{x}}_f = A_f \underline{x}_f + D_f \underline{w}_f \qquad (4.40)$$

$$\underline{w}_p = C_f \underline{x}_f \tag{4.41}$$

where $\underline{w}_f$ denotes white noise with zero mean and covariance matrix Q_f.

Combining Eqs. (4.38) to (4.41) into one model results in the process described by the following state-space equations:

$$\dot{\underline{x}} = A\underline{x} + B\underline{u} + D\underline{w} \tag{4.42}$$

$$\underline{y} = C\underline{x} + \underline{v} \tag{4.43}$$

where

$$A = \begin{bmatrix} A_p & A_c \\ 0 & A_f \end{bmatrix} \quad B = \begin{bmatrix} B_p \\ 0 \end{bmatrix} \quad C = (C_p \; 0) \quad D = \begin{bmatrix} 0 \\ D_f \end{bmatrix}$$

$$\underline{x}^T = (\underline{x}_p^T \; \underline{x}_f^T) \quad \underline{y} = (\underline{y}_p \; \underline{y}_f) \quad v = \underline{v}_f \quad \underline{w} = \underline{w}_f \quad A_c = D_p C_f$$

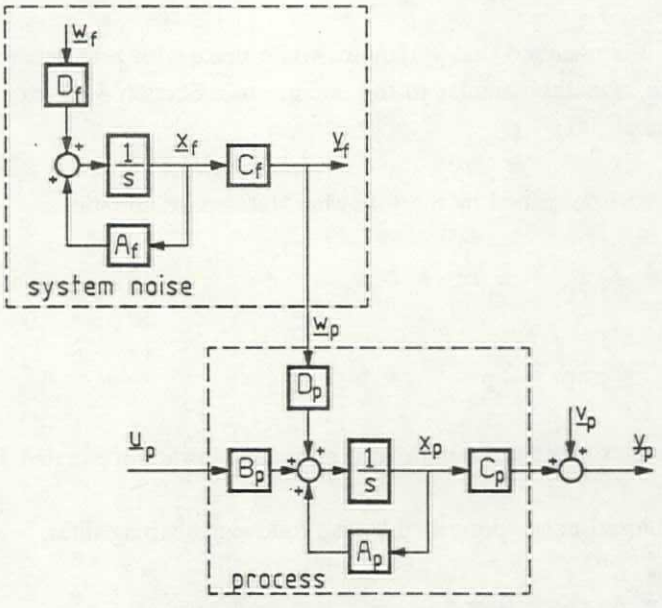

Fig. 4.5 Process with colored system noise

A block diagram of this process is given in Fig. 4.5. Fig. 4.6 shows a block diagram of the process in combination with the corresponding filter structure.

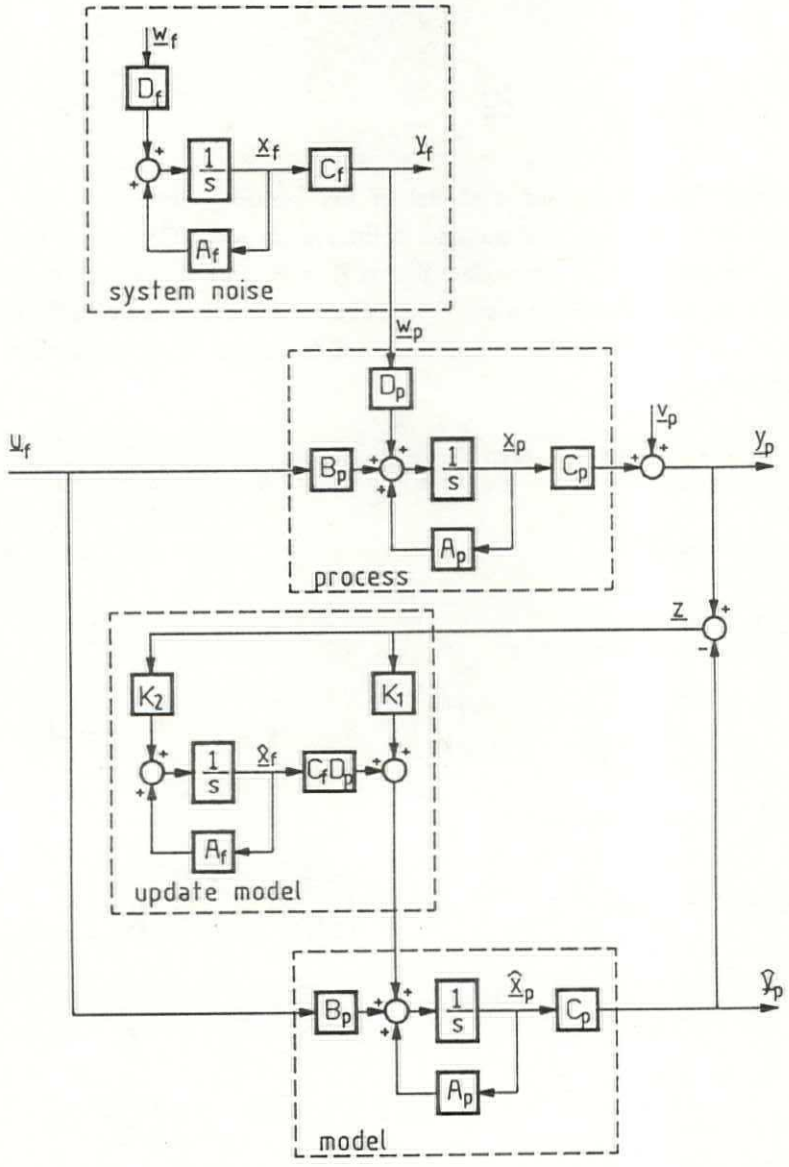

Fig. 4.6 Process and corresponding filter

The optimal filter is described by equations similar to Eqs. (4.28), (4.29) and (4.30) in Section 4.3.1:

$$\dot{\hat{\underline{x}}} = A\hat{\underline{x}} + B\underline{u} + K\underline{z} \tag{4.44}$$

$$\hat{\underline{y}} = C\hat{\underline{x}} \tag{4.45}$$

$$\underline{z} = \underline{y} - \hat{\underline{y}} = \underline{y} - C\hat{\underline{x}} \tag{4.46}$$

The optimal filter comprises a model of the process, describing the available knowledge of the process, and a model of the system noise. Comparing Fig. 4.6 with Fig. 4.1 demonstrates that the update matrix K in Fig. 4.1 is replaced by an update filter. This update filter comprises a model of the system noise and the update matrices K_1 and K_2. The latter can be found by solving equations similar to Eqs. (4.31) and (4.32):

$$\dot{P} = AP + PA^T + DQD^T - KCP \tag{4.47}$$

$$K = PC^T R^{-1} \tag{4.48}$$

where

$$P = \begin{bmatrix} P_1 & P_2 \\ P_2^T & P_3 \end{bmatrix} \qquad K = \begin{bmatrix} K_1 \\ K_2 \end{bmatrix} \qquad Q = Q_f \qquad R = R_p$$

Eq. (4.48) is solved as follows:

$$K = PC^T R^{-1} = \begin{bmatrix} P_1 & P_2 \\ P_2^T & P_3 \end{bmatrix} \begin{bmatrix} C_p^T \\ 0 \end{bmatrix} R_p^{-1} = \begin{bmatrix} P_1 C_p^T \\ P_2^T C_p^T \end{bmatrix} R_p^{-1} = \begin{bmatrix} K_1 \\ K_2 \end{bmatrix}$$

Therefore

$$K_1 = P_1 C_p^T R_p^{-1} \tag{4.49}$$

$$K_2 = P_2 C_p^T R_p^{-1} \tag{4.50}$$

P is to be found from

$$\dot{P} = \begin{bmatrix} \dot{P}_1 & \dot{P}_2 \\ \dot{P}_2^T & \dot{P}_3 \end{bmatrix} = \begin{bmatrix} A_p & A_c \\ 0 & A_f \end{bmatrix} \begin{bmatrix} P_1 & P_2 \\ P_2^T & P_3 \end{bmatrix} + \begin{bmatrix} P_1 & P_2 \\ P_2^T & P_3 \end{bmatrix} \begin{bmatrix} A_p^T & 0 \\ A_c^T & A_f^T \end{bmatrix} +$$

$$+ \begin{bmatrix} 0 \\ D_f \end{bmatrix} Q_f \, (0 \;\; D_f^T) - \begin{bmatrix} K_1 \\ K_2 \end{bmatrix} (C_p \;\; 0) \begin{bmatrix} P_1 & P_2 \\ P_2^T & P_3 \end{bmatrix} =$$

$$= \begin{bmatrix} A_pP_1+A_cP_2^T & A_pP_1+A_cP_3 \\ A_fP_2^T & A_fP_3 \end{bmatrix} + \begin{bmatrix} P_1A_p^T+P_2A_c^T & P_2A_f^T \\ P_2^TA_p^T+P_c^TA_3 & P_3A_f^T \end{bmatrix} + \begin{bmatrix} 0 & 0 \\ 0 & D_fQ_fD_f^T \end{bmatrix}$$

$$- \begin{bmatrix} K_1C_pP_1 & K_1C_pP_2 \\ K_2C_pP_1 & K_2C_pP_2 \end{bmatrix}$$

or

$$\dot{P}_1 = A_pP_1 + P_1A_p^T + A_cP_2^T + P_2A_c^T - K_1C_pP_1 \qquad (4.51)$$

$$\dot{P}_2 = A_pP_1 + P_2A_f^T + A_cP_3 - K_1C_pP_2 \qquad (4.52)$$

$$\dot{P}_3 = A_fP_3 + P_3A_f^T + D_fQ_fD_f^T - K_2C_pP_2 \qquad (4.53)$$

Appendix F gives a calculation example of a second-order process disturbed by colored system noise. This system noise can be described by a first-order shaping filter.

4.4 Filter calculation

In Sections 4.2 and 4.3 the *Optimal Linear Filter Theory* has been introduced as a solution to the problem of estimating unknown or noisy states. In this section this theory is applied to the RRS problem. Several state estimators are designed to remove undesired signals from the measurements and to reconstruct the unknown states of the process (the ship).

4.4.1 Model reduction

In Chapter 2 models of the ship, the steering machine and the disturbances are given. The Optimal Linear Filter Theory requires that these models be combined into one linear model. Therefore, the model of the steering machine should be linearized. As indicated in Section 2.2, the order of such a combined model is at least 10. It can be demonstrated that in such a case the order of the innovation process, introduced in Section 4.2, is $0.5n(n+1) = 55$ ("n" is the rank of the model of the process). In practice, this is not acceptable and not necessary either. This can be demonstrated by a simple discussion of the various subsystems of the process.

The steering machine

In Chapter 5 an adaptation mechanism will be introduced which prevents the steering machine from saturating. Application of this adaptation mechanism allows the steering machine to be regarded as a linear system.
In addition, in Chapter 6 demands will be posed with respect to the dynamics of the steering machine. In this Section it will be assumed that these demands are met. This enables the dynamics of the steering machine to be disregarded.

The disturbances

The ship motions are mainly disturbed by wind and waves. The parameters which describe the models of wind and waves depend on the ship's speed and the angle of incidence of the wind and the waves. The same holds for the models which describe the transfers of the wave height to the roll moment, the yaw moment and the sway force. Theoretically, it is possible to estimate these models by means of parameter-estimation techniques or by combining state estimation with parameter estimation in an extended Kalman filter (Hoogenraad, 1983). The number of parameters involved makes this unattractive for a practical design. An alternative is to treat these disturbances as white noise with non-zero mean and unknown variance. However, the theory given in Section 4.2 and Section 4.3 assumes the variance of the system noise to be known. In Chapter 5 it will be shown that this problem can be circumvented by estimating the noise variance.

Based on these considerations the ship model can be reduced to the model given in Fig. 4.7.

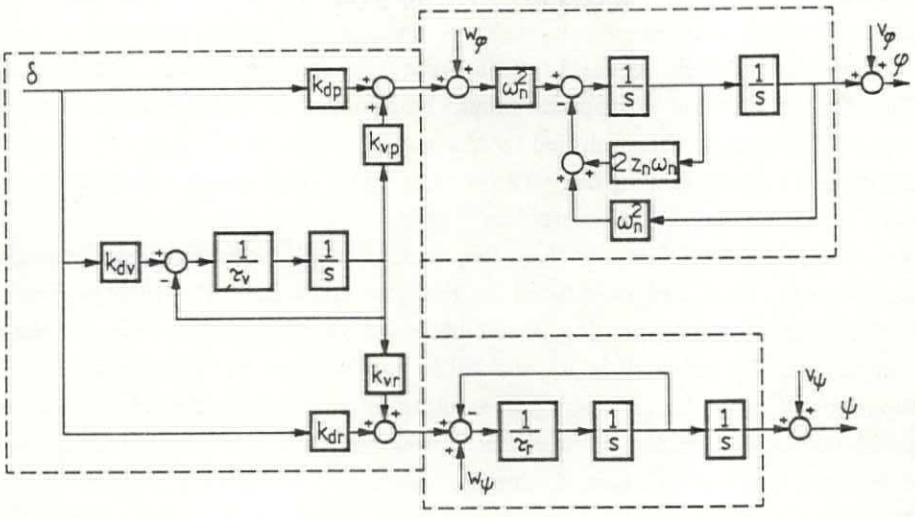

Fig. 4.7 Model of ship and disturbances

The model given in Fig. 4.7 consists of three parts. One part describes the roll-moment-to-roll-angle transfer and another part describes the yaw-moment-to-yaw transfer. The third part describes the rudder-angle-to-roll-moment transfer and the rudder-angle-to-yaw-moment transfer. This third part is not influenced by system noise.

For the derivation of the filter algorithms it will be assumed that uncorrelated disturbances act upon two different parts of the process. The system noise which acts on the roll angle does not have any influence on the yaw motions. Similarly, the system noise which acts on the yaw motions has no influence on the roll angle. The experiment results given in Chapter 7 indicate that these asumptions are allowed. In that case, the fifth-order model can be separated in two third-order models. The filter which is designed based on these sub models will be identical to the filter which is designed based on the fifth-order model. The filter problem can thus be separated into two subproblems: reconstruction of the states of the rudder-to-roll transfer (Section 4.4.2) and reconstruction of the states of the rudder-to-heading-error transfer (Section 4.4.3).

Normally, state-reconstruction filters make a distinction between system noise, which influences the states, and measurement noise, which should be suppressed. However, in the control problem studied in this thesis additional filter problems can be recognized:

- The roll controller is based on the feedback of the states of the roll model and cannot reduce a constant roll angle. A constant roll angle causes a constant rudder angle, which would in turn cause the ship to change the heading. Therefore, a constant component should be removed from the states of the roll model. This can be accomplished by treating a constant component as a non-zero mean which is present in the measurement noise. The theory posed in Section 4.3.1 offers a solution to this problem.
  An additional problem is that the rudder angle contains low-frequency components which are introduced by the yaw controller. The theory given in Section 4.3 does not provide a suitable solution to remove these undesired components. Therefore, it is not allowed to use the measured rudder angle as the input of the roll filter. By using the output of the roll controller instead this problem can be avoided. Henceforth, it will be assumed that the rudder angle does not contain any undesired components.
- The course controller is based on the feedback of the states of the yaw model. It should not generate high-frequency rudder motions which will influence the roll motions. This requires that the high-frequency components be removed from the states of the yaw model. In Section 4.4.3 these undesired high-frequency components will be treated as "colored measurement noise" although they are due to system noise (which may be caused by wind or waves).
  The rudder angle contains high-frequency components which are introduced by the roll controller. These components can be suppressed by using the output of the course controller as the input of the yaw filter.

Because only the rudder can be used, the process has a single input and two outputs. A decoupling of the control action is obtained in the frequency domain; low-frequency rudder motions are used to maintain the heading while high-frequency rudder motions are used to reduce the roll of the ship.

4.4.2 The roll motions

Fig. 4.8 is a block diagram of the model which describes the roll motions. In this figure the following holds:

- The measurement noise v_φ is assumed to be white noise with a non-zero mean. By describing this constant component as integrated white noise it can be treated as "colored measurement noise".
- The system noise w_φ is assumed to be white noise with a zero mean. Any constant

component is assumed to be part of the measurement noise.
- The input signal δ_φ is the rudder angle necessary for roll reduction. It does not contain any low-frequency components.
- The dotted blocks c denote the place where the constant components are actually introduced.

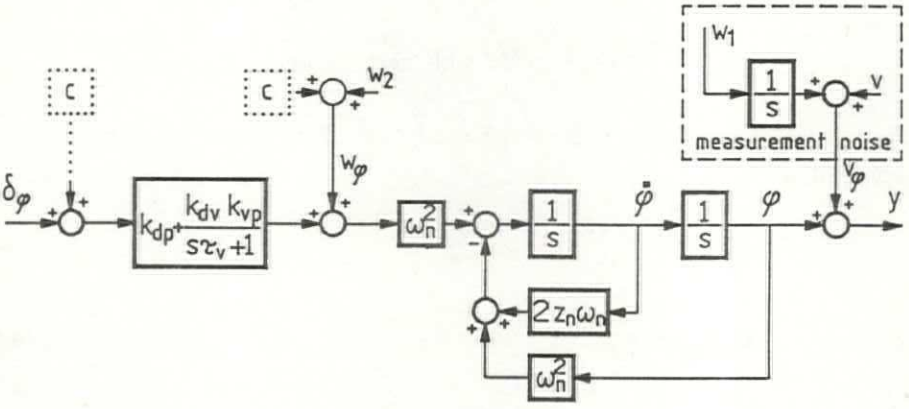

Fig. 4.8 The roll model

In practice, the measured roll angle contains not only the high-frequency components which have to be reduced but also low-frequency components. These components generate low-frequency rudder motions, which in return deteriorate the course-keeping performance. Therefore, it is essential to remove the low-frequency components from the measurements.
In this section the suppression of only the constant component of the measured roll angle will be considered. It can be shown that this will result in sufficient reduction of other low-frequency components as well. The theory, given in Section 4.3, offers a solution to remove such (colored) measurement noise from the measurements.

The roll model can be described by the following state-space equations:

$$\dot{\underline{x}}_p = A_p\underline{x}_p + B_p\underline{u}_p + D_p\underline{w}_p \qquad (4.54)$$

$$\underline{y}_p = C_p\underline{x}_p + \underline{v}_p \qquad (4.55)$$

where

$$A_p = \begin{bmatrix} 0 & 1 & 0 \\ -\omega_n^2 & -2z_n\omega_n & \omega_n^2 k_{vp} \\ 0 & 0 & 1/\tau_v \end{bmatrix} \quad B_p = \begin{bmatrix} 0 \\ \omega_n^2 \\ 0 \end{bmatrix} \quad D_p = \begin{bmatrix} 0 \\ \omega_n^2 \\ 0 \end{bmatrix}$$

$$\underline{x}_p^T = (\varphi \quad \dot{\varphi} \quad x_3) \qquad \underline{u}_p = \delta_\varphi$$

$$C_p = (1 \quad 0 \quad 0)$$

$$\underline{w}_p^T = w_1 \quad = \text{white noise with zero mean}$$

$\underline{v}_p$ is colored measurement noise which can be described by the following first-order shaping filter:

$$\dot{\underline{x}}_v = A_v\underline{x}_v + D_v\underline{w}_v \tag{4.56}$$

$$\underline{y}_v = C_v\underline{x}_v + \underline{v}_v \tag{4.57}$$

where

$$A_v = 0 \quad D_v = 1 \quad C_v = 1 \quad \underline{y}_v = \underline{v}_p = v_\varphi$$

$$\underline{v}_v = v \qquad \text{(where } v = \text{white noise with zero mean)}$$

Combining Eqs. (4.54) to (4.57) into one fourth-order model results in the process described by the following state-space equations:

$$\dot{\underline{x}} = A\underline{x} + B\underline{u} + D\underline{w} \tag{4.58}$$

$$\underline{y} = C\underline{x} + \underline{v} \tag{4.59}$$

where

$$A = \begin{bmatrix} 0 & 1 & 0 & 0 \\ -\omega_n^2 & -2z_n\omega_n & \omega_n^2 k_{vp} & 0 \\ 0 & 0 & 1/\tau_v & 0 \\ 0 & 0 & 0 & 0 \end{bmatrix} \quad B = \begin{bmatrix} 0 \\ \omega_n^2 \\ 0 \\ 0 \end{bmatrix} \quad D = \begin{bmatrix} 0 & 0 \\ \omega_n^2 & 0 \\ 0 & 0 \\ 0 & 1 \end{bmatrix}$$

$$C = (1 \quad 0 \quad 0 \quad 1)$$

$$\underline{x}^T = (\underline{x}_p^T \; \underline{x}_v^T) \qquad \underline{w}^T = (\underline{w}_p^T \; \underline{w}_v^T) = (w_1 \; w_2)$$

$$\underline{u} = \delta_\varphi \qquad \underline{y} = \underline{y}_v = v$$

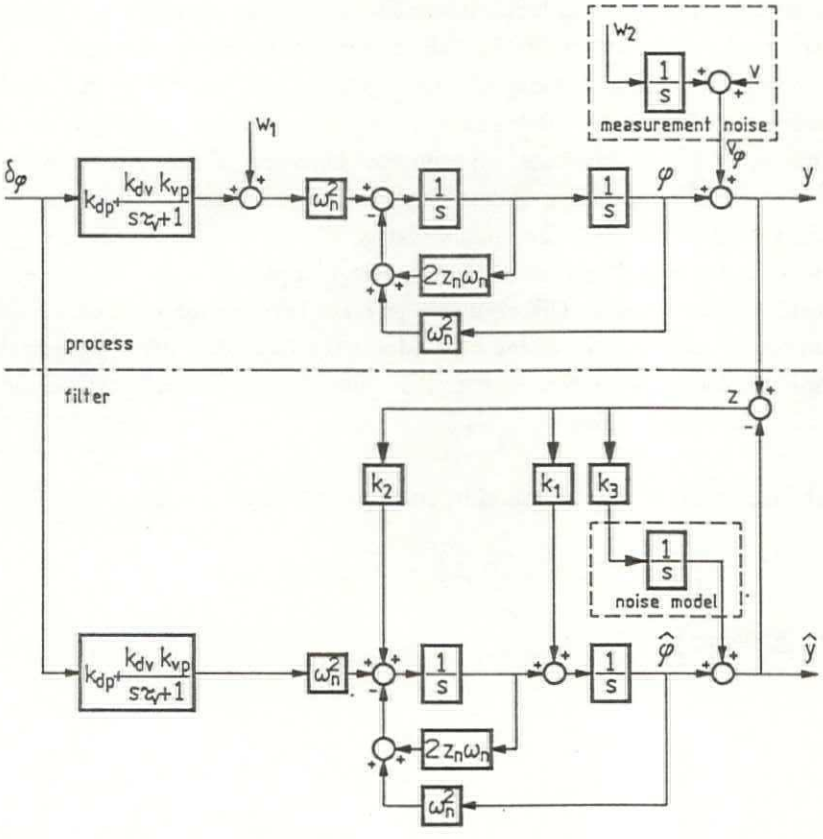

Fig. 4.9 The roll filter

The "optimal" filter for this process is described by the following state-space equations:

$$\dot{\hat{\underline{x}}} = A\hat{\underline{x}} + B\underline{u} + K\underline{z} \qquad (4.60)$$

$$\hat{\underline{y}} = C\hat{\underline{x}} \tag{4.61}$$

$$\underline{z} = \underline{y} - \hat{\underline{y}} \tag{4.62}$$

Fig. 4.9 shows a block diagram of the process in combination with the optimal filter. A part of the model is not influenced by system noise. It can be shown that any part of the model which is not influenced by noise can be disregarded with respect to the calculation of the update matrix K. This feature can be made plausible by a simple discussion of the submodel in Fig. 4.9. The input and the parameters of the submodel are assumed to be exactly known, so that the state of the submodel is known as well. This makes updating this state superfluous; therefore, if the update matrix K is calculated, the corresponding update element of K will be zero, which simplifies the equations used to calculate the update matrix.
In practice, the model parameters are never completely equal to the equivalent parameters of the process. This results in an error between the state of the submodel in the process and the state of the submodel in the filter. Any error in the estimation of the other states of the process which is caused by this inequality is assumed to be caused by the system noise w_i.

The update matrix K can be found by solving the following equations:

$$\dot{P} = A_r P + P A_r^T + D_r Q_r D_r^T - K C_r P \tag{4.63}$$

$$K = P C_r^T \tag{4.64}$$

where

$$A_r = \begin{bmatrix} 0 & 1 & 0 \\ -\omega_n^2 & -2z_n\omega_n & 0 \\ 0 & 0 & 0 \end{bmatrix} \quad D_r = \begin{bmatrix} 0 & 0 \\ \omega_n^2 & 0 \\ 0 & 1 \end{bmatrix} \quad C_r = (1\ 0\ 1)$$

$$P = \begin{bmatrix} p_2 & p_3 & p_1 \\ p_3 & p_4 & p_5 \\ p_1 & p_5 & p_6 \end{bmatrix} \quad Q = \begin{bmatrix} E[w_1.w_1]/E[v.v] & 0 \\ 0 & E[w_2.w_2]/E[v.v] \end{bmatrix} = \begin{bmatrix} q_1 & 0 \\ 0 & q_2 \end{bmatrix}$$

As is shown in Section 4.2 the solution of Eqs. (4.63) and (4.64) can be found to be the steady state of an innovation process described by the following state-space

equations:

$$\dot{\underline{x}}_m = \underline{A}_m \underline{x}_m + \underline{B}_m \underline{u}_m \qquad (4.65)$$

$$\underline{y}_m = \underline{C}_m \underline{x}_m \qquad (4.66)$$

where

$$\underline{x}_m^T = (p_1,\ p_2,\ \ldots\ldots,\ p_6)$$

$$\underline{y}_m^T = (k_1,\ k_2,\ k_3)$$

The matrices A_m, B_m and C_m are calculated in Appendix E.

4.4.3 The yaw motions

Fig. 4.10 gives a block diagram of the process. Three different parts, indicated by the dashed lines, can be recognized:

- the third-order yaw model given in Chapter 2.
- a model which describes the coloring of the measurement noise. Frequency components with a frequency higher than $1/\tau_f$ rad/sec. are considered to be "measurement noise". In addition, white measurement noise exists due to imperfect measurements.
- the system noise which is assumed to be white noise with a non-zero mean. This constant component is described by an integrated white noise component and can thus be treated as "colored system noise".

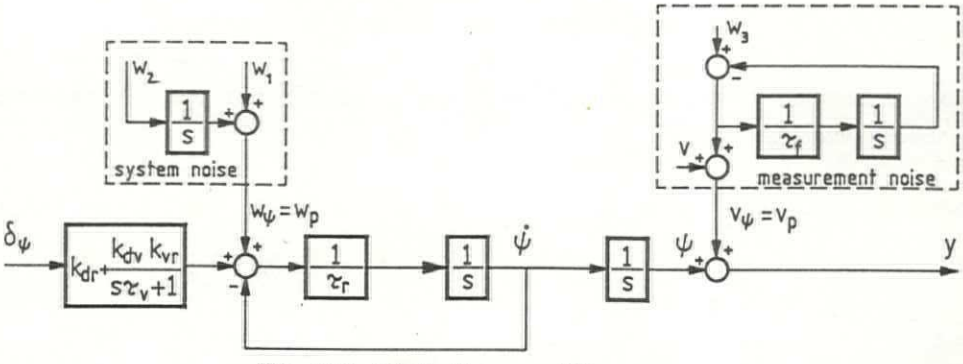

Fig. 4.10 Block diagram of the process

The yaw model can be described by the following state-space equations:

$$\dot{\underline{x}}_p = A_p\underline{x}_p + B_p\underline{u}_p + D_p\underline{w}_p \tag{4.67}$$

$$\underline{y}_p = C_p\underline{x}_p + \underline{v}_p \tag{4.68}$$

where

$$A_p = \begin{bmatrix} -1/\tau_v & 0 & 0 \\ 0 & 0 & 1 \\ k_{dv}/\tau_r & 0 & -1/\tau_r \end{bmatrix} \quad B_p = \begin{bmatrix} k_{dv}/\tau_v \\ 0 \\ k_{dr}/\tau_r \end{bmatrix} \quad D_p = \begin{bmatrix} 0 \\ 0 \\ 1/\tau_r \end{bmatrix}$$

$$C_p = (0\ 1\ 0)$$

$$\underline{x}_p^T = (x_1\ \psi\ \dot{\psi}) \qquad \underline{u}_p = \delta_\psi$$

$\underline{v}_p$ is colored noise, described by the first-order shaping filter:

$$\dot{\underline{x}}_v = A_v\underline{x}_v + D_v\underline{w}_3 \tag{4.69}$$

$$\underline{y}_v = C_v\underline{x}_v + F_v\underline{v}_v \tag{4.70}$$

where

$$A_v = -1/\tau_f \quad D_v = 1/\tau_f \quad C_v = -1 \quad F_v = (1\ \ 1) \quad \underline{y}_v = \underline{v}_p = v_\psi$$

$$\underline{w}_3 = w_3$$

$\underline{v}_v^T = (w_3\ v)$ (w_3 and v denote white noise with zero mean)

$\underline{w}_p$ is assumed to be colored noise which can be described by the following state-space equations:

$$\dot{\underline{x}}_w = A_w\underline{x}_w + D_w\underline{w}_2 \tag{4.71}$$

$$\underline{y}_w = C_w\underline{x}_w + \underline{v}_w \tag{4.72}$$

where

$$A_w = 0 \quad D_w = 1 \quad C_w = 1 \quad \underline{y}_w = \underline{w}_p = w_\psi$$

$$\underline{w}_2 = w_2 \quad (w_2 = \text{white noise with zero mean})$$

$$\underline{v}_w = w_1 \quad (w_1 = \text{white noise with zero mean})$$

Combining (4.67) to (4.72) into one fifth-order model results in the process described by the following state-space equations:

$$\dot{\underline{x}} = A\underline{x} + B\underline{u} + D\underline{w} \tag{4.73}$$

$$\underline{y} = C\underline{x} + F\underline{v} \tag{4.74}$$

where

$$A = \begin{bmatrix} -1/\tau_v & 0 & 0 & 0 & 0 \\ 0 & 0 & 1 & 0 & 0 \\ k_{vr}/\tau_r & 0 & -1/\tau_r & 1/\tau_r & 0 \\ 0 & 0 & 0 & 0 & 0 \\ 0 & 0 & 0 & 0 & -1/\tau_f \end{bmatrix} \quad B = \begin{bmatrix} k_{dv}/\tau_v \\ 0 \\ k_{dr}/\tau_r \\ 0 \\ 0 \end{bmatrix}$$

$$D = \begin{bmatrix} 0 & 0 & 0 \\ 0 & 0 & 0 \\ 1/\tau_r & 0 & 0 \\ 0 & 1 & 0 \\ 0 & 0 & 1/\tau_f \end{bmatrix} \quad C = (0\ 1\ 0\ 0\ -1) \quad F = (1\ \ 1)$$

$$\underline{x}^T = (x_1\ \psi\ \dot{\psi}\ x_v\ x_w) \quad \underline{w}^T = (w_1\ w_2\ w_3)$$

$$\underline{u} = \delta_\psi \quad \underline{v}^T = (w_3\ v)$$

The "optimal" filter for this process is described by the following state-space equations:

$$\dot{\hat{\underline{x}}} = A\hat{\underline{x}} + B\underline{u} + K\underline{z} \tag{4.75}$$

$$\hat{\underline{y}} = C\hat{\underline{x}} \tag{4.76}$$

$$\underline{z} = \underline{y} - \hat{\underline{y}} \tag{4.77}$$

Fig. 4.11 is a block diagram of the resulting filter structure.

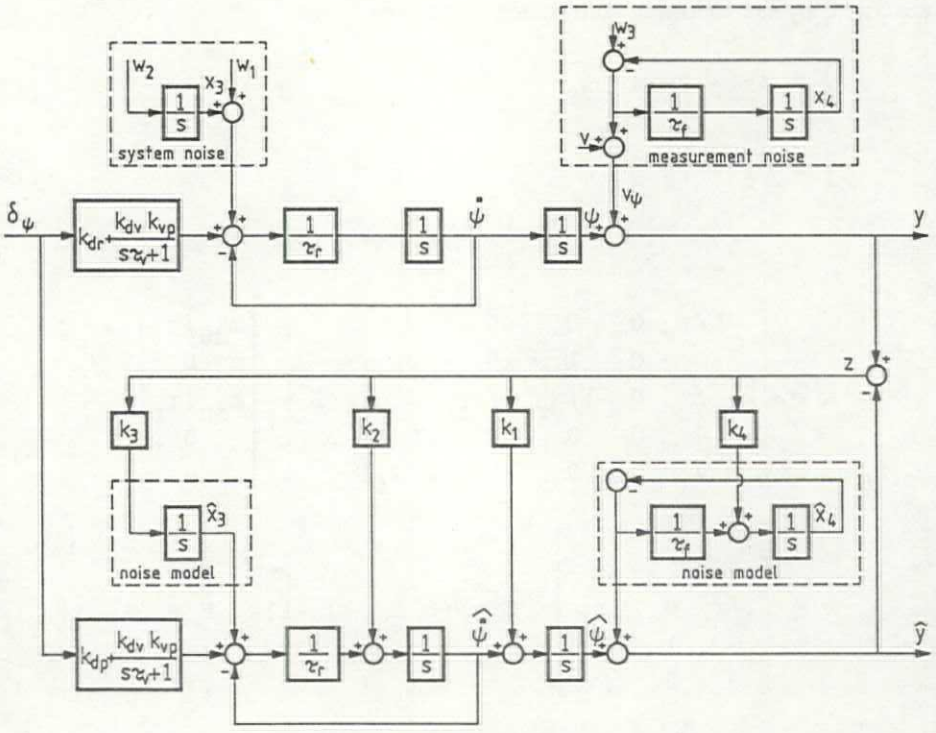

Fig. 4.11 The optimal filter

The process described by Eqs. (4.73) and (4.74) has correlated system and measurement noise; $\underline{w}$ and $\underline{v}$ both contain w_3.

In addition, a part of the process is not influenced by system noise. This part can be disregarded with respect to calculating the matrix K. Any errors which are caused by differences between the parameters of the remaining model and the equivalent parameters of the process are assumed to be caused by the system noise w_1.

This leaves K to be found by solving the following equations:

$$\dot{P} = A_r P + P A_r^T + D_r Q D_r^T - K(PC_r^T + D_r S F^T)^T \qquad (4.78)$$

$$K = (PC_r^T + D_r S F^T)(FRF^T)^{-1} \qquad (4.79)$$

where

$$P = \begin{bmatrix} p_5 & p_6 & p_1 & p_2 \\ p_6 & p_7 & p_3 & p_4 \\ p_1 & p_3 & p_8 & p_9 \\ p_2 & p_4 & p_9 & p_{10} \end{bmatrix} \qquad Q = \begin{bmatrix} E[w_1.w_1] & 0 & 0 \\ 0 & E[w_2.w_2] & 0 \\ 0 & 0 & E[w_3.w_3] \end{bmatrix}$$

$$R = E[w_3.w_3] + E[v.v] \qquad S = \begin{bmatrix} 0 & 0 \\ 0 & 0 \\ E[w_3.w_3] & 0 \end{bmatrix}$$

Similar to the solution presented in Section 4.2, the solution of Eqs. (4.78) and (4.79) can be found to be the steady state of an innovation process described by the following state-space equations:

$$L\dot{\underline{x}}_m = A_m \underline{x}_m + B_m \underline{u}_m \qquad (4.80)$$

$$\underline{y}_m = C_m \underline{x}_m + D_m \underline{u}_m \qquad (4.81)$$

where

$$\underline{x}_m^T = (p_1, p_2, \ldots\ldots, p_{15})$$

$$\underline{y}_m^T = (k_1, k_2, \ldots\ldots, k_5)$$

$$\underline{u}_m^T = (E[w_1.w_1]/r, E[w_2.w_2]/r, E[w_3.w_3]/r)$$

$$r = E[w_3.w_3] + E[v.v]$$

The matrices A_m, B_m, C_m and D_m are given in Appendix F.

4.5 Filtering the ship's speed

The speed of the ship "U" has a large influence on some of the parameters of the ship model given in Section 2, for instance the parameter k_{dp} which is a function of U^2. This indicates that it is important to remove the disturbances which are present in the measured speed.
Besides measurement noise the measured ship's speed contains components which can be subdivided into three groups:

1 The high-frequency components. These are due to mainly wind and wave disturbances and have to be suppressed.
2 The medium-frequency components. These may be due to wind and wave disturbances or to changes in the operation mode of the ship (such as acceleration, course changes etc.) and should not be suppressed.
3 The constant component. This is caused by the ship's propulsion and constant components which are present in the disturbances and should be estimated accurately.

A relatively simple method to remove the high-frequency components is to apply a first-order low-pass filter with a large time constant. During the stationary mode, the time constant of such a filter has to be large to suppress the undesired components. However, if the ship's speed rapidly increases, a smaller time constant is required in order to give a faster estimation of the ship's speed accepting less suppression of the undesired components.
The theory given in Section 4.2 and Section 4.3 offers a method to find a compromise between these contradictory requirements. It requires the ship's speed to be treated as the output of a "process". The inputs of this process are, for example, the ship's propulsion, the wind and the waves. The output of this process is the ship's speed perturbed by measurement noise. Fig. 4.12 shows a block diagram of the process.

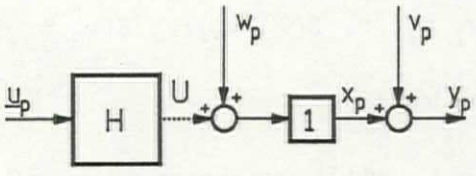

Fig. 4.12 Block diagram of the speed process

In Fig. 4.12 the following holds:

w_p = the disturbances which influence the ship's speed
$\underline{u}_p$ = the known inputs which influence the ship's speed (for instance the ship's propulsion).
U = the actual ship's speed. In the following it will be assumed that U is unknown and thus can be included in w_p.
v_p = the undesired components on the measurements
y_p = the measured ship's speed
H = the transfer function describing the influence of known inputs on the ship's speed.

The system noise w_p can be regarded as colored noise with a large non-zero mean. The measurement noise v_p can be regarded as colored noise as well. It is relatively large and has to be removed from the measurements. This section will demonstrate how to apply the theory given in Section 4.2 and Section 4.3 to this particular problem. In Chapter 5 it will be shown how the resulting filter can be improved by making it adaptive to changing conditions.

4.5.1 The first-order low-pass filter

Let the process be given by the block diagram of Fig. 4.12 and let it be disturbed by white noise with non-zero mean and $E[w_p.w_p] = 0$.
The constant component can be treated as integrated white noise. Fig. 4.13 shows a modified block diagram of the process, including the coloring of the system noise.

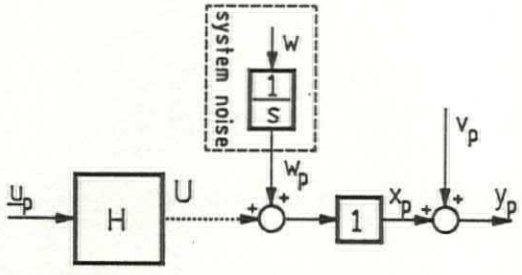

Fig. 4.13 The modified block diagram of the process

This process can be described by the following state-space equations:

$$\dot{\underline{x}} = A\underline{x} + D\underline{w} \tag{4.82}$$

$$\underline{y} = C\underline{x} + \underline{v} \tag{4.83}$$

where

$A = 0 \quad D = 1 \quad C = 1$

$\underline{v} = v_p$ = white noise with zero mean

$\underline{w} = w$ = white noise with zero mean

$\underline{x} = x_p$ = the ship's speed

The optimal filter of such a process is described by the following state-space equations:

$$\dot{\hat{\underline{x}}} = A\hat{\underline{x}} + K\underline{z} \tag{4.84}$$

$$\hat{\underline{y}} = C\hat{\underline{x}} \tag{4.85}$$

$$\underline{z} = \underline{y} - \hat{\underline{y}} \tag{4.86}$$

K can be found by solving the following equations:

$$0 = AP + PA^T + DQD^T - KCP \tag{4.87}$$

$$K = PC^T \tag{4.88}$$

where

$P = p \quad K = k \quad Q = E[w.w]/E[v.v]$

The analytical solution of Eqs. (4.87) and (4.88) is:

$$0 = 0p + p0 + Q - kp = Q - k^2 \longrightarrow k = \sqrt{Q}$$

or

$$k = \sqrt{E[w.w]/E[v.v]} \qquad (4.89)$$

The resulting filter structure is shown in Fig. 4.14. The filtered ship's speed is denoted by $\hat{x}_p$.

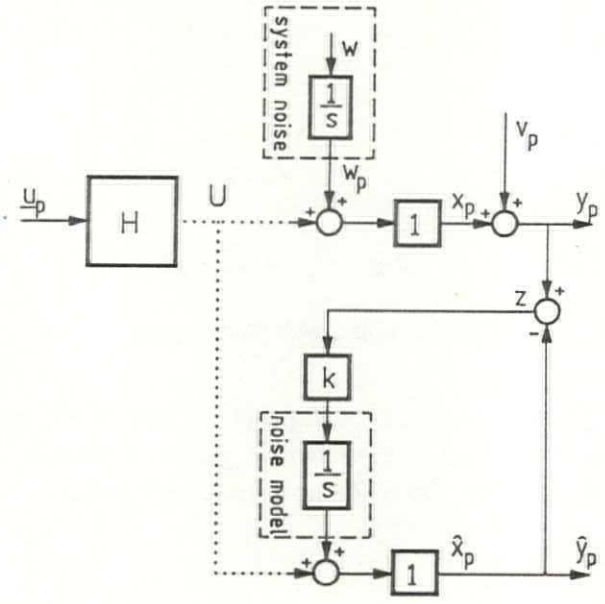

Fig. 4.14 The resulting filter structure

The y_p-to-$\hat{x}_p$ transfer resembles the following first-order low-pass filter:

$$\frac{\hat{x}_p}{y_p} = \frac{1}{s\tau + 1} \qquad \tau = 1/k = \sqrt{E[v.v]/E[w.w]} \qquad (4.90)$$

Conclusion:

If a first-order low-pass filter is used to smooth the speed signal, the time constant should be selected to be the square root of the ratio of the variances of the measurement noise and the system noise.

4.5.2 High-frequency components

In Section 4.5.1 it is assumed that the measurement noise is white noise with zero mean. In this section it will be assumed that the measurement noise contains only high-frequency components.

Let the coloring of the measurement noise be described by the following state-space equations:

$$\dot{\underline{x}}_v = A_v \underline{x}_v + D_v \underline{w}_v \tag{4.91}$$

$$y_v = C_v \underline{x}_v + \underline{v}_v \tag{4.92}$$

where

$$A_v = -1/\tau \qquad D_v = 1/\tau \qquad C_v = -1$$

$$\underline{v}_v = \underline{w}_v = v = \text{white noise with zero mean}$$

Combining the process described by Eqs. (4.82) and (4.83) and the process described by Eqs. (4.91) and (4.92) into one process results in a second-order process which is described by the following state-space equations:

$$\dot{\underline{x}} = A\underline{x} + D\underline{w} \tag{4.93}$$

$$y = C\underline{x} + \underline{v} \tag{4.94}$$

where

$$A = \begin{bmatrix} 0 & 0 \\ 0 & -1/\tau \end{bmatrix} \qquad D = \begin{bmatrix} 1 & 0 \\ 0 & 1/\tau \end{bmatrix} \qquad C = (1 \ -1)$$

$$\underline{v} = v$$

$$\underline{w}^T = (w, v) \quad \text{(white noise with zero mean)}$$

$$x_p = \text{the ship's speed}$$

As was indicated in Section 4.2 the "optimal" filter for this process is described by the following state-space equations:

$$\dot{\hat{\underline{x}}} = A\hat{\underline{x}} + B\underline{u} + K\underline{z} \qquad (4.95)$$

$$\hat{\underline{y}} = C\hat{\underline{x}} \qquad (4.96)$$

$$\underline{z} = \underline{y} - \hat{\underline{y}} \qquad (4.97)$$

K is to be found by solving the following equations:

$$0 = AP + PA^T + DQD^T - K(PC^T+DS)^T \qquad (4.98)$$

$$K = (PC^T+ DS)R^{-1} \qquad (4.99)$$

where

$$P = \begin{bmatrix} p_1 & p_2 \\ p_2 & p_3 \end{bmatrix} \qquad Q = \begin{bmatrix} E[w.w] & 0 \\ 0 & E[v.v] \end{bmatrix}$$

$$R = E[v.v] \qquad S = E[\underline{w}.\underline{v}^T] = \begin{bmatrix} 0 \\ E[v.v] \end{bmatrix}$$

Solving Eqs. (4.98) and (4.99) yields:

$$k_1 = \sqrt{E[w.w]/E[v.v]} \qquad (4.100)$$

$$k_2 = \frac{k_1\tau + 1 - \sqrt{(k_1^2\tau^2+2k_1\tau)}}{\tau} \qquad (4.101)$$

Comparing Eqs. (4.100) and Eqs. (4.89) shows that k_1 does not depend on the coloring of the measurement noise. This solution of k_1 is identical to the solution of k in Section 4.5.1, where v is considered to be white noise with zero mean.
The resulting filter is shown in Fig. 4.15. It differs from Fig. 4.14 only in that the influence of the coloring of the measurement noise has been introduced in the filter.

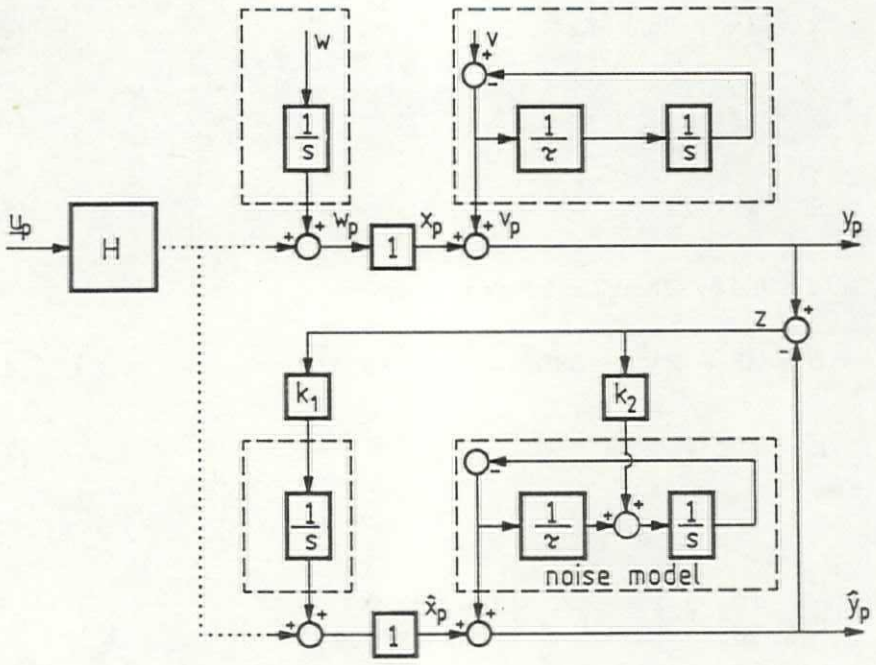

Fig. 4.15 The filter structure

Fig. 4.16 shows a modified block diagram of the filter structure. Comparing Fig. 4.16 and Fig. 4.14 demonstrates that the gain k in Fig. 4.14 is replaced by the equivalent gain k_1 in Fig. 4.16 and the additional first-order filter which is indicated by the dotted lines. This filter can be described by the following transfer function:

$$\frac{z}{z'} = \frac{s\tau + 1}{s\tau + 1 - k_2\tau} = K\,\frac{s\tau_a + 1}{s\tau_b + 1} \qquad (4.102)$$

This transfer function approaches one if only the high-frequency components of the error signal z' are considered or if the product $k_2\tau$ becomes small. The latter is the case if the product $k_1\tau$ becomes large, which implies a high system-noise-to-measurement-noise ratio or a large time constant τ.

The transfer function enlarges the low-frequency components of the error signal z'. This corresponds to an enlargement of the gain k_1. Therefore, the second-order speed filter causes less reduction of the low-frequency components than the first-order speed filter does.

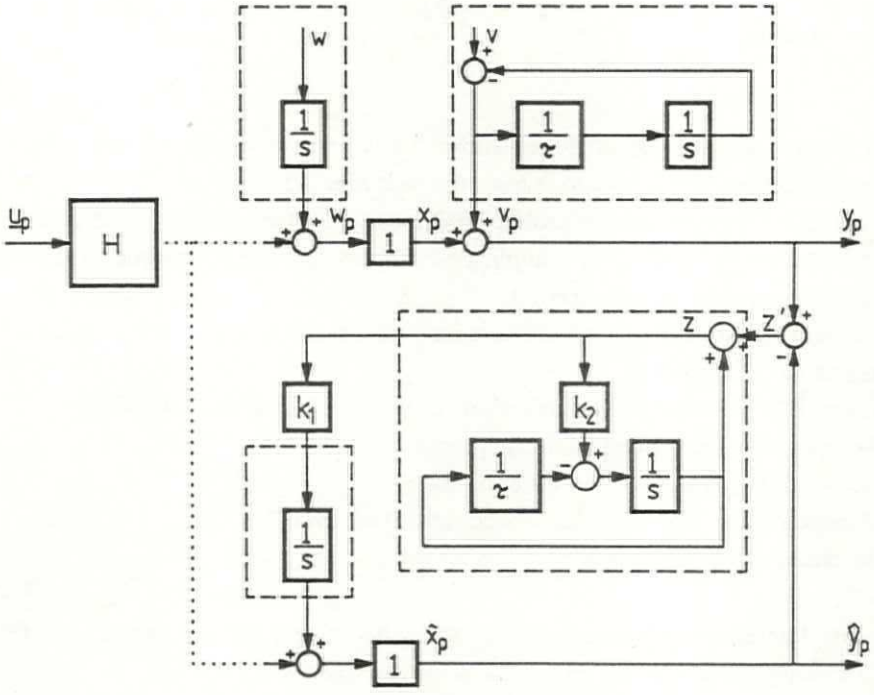

Fig. 4.16 The modified filter structure

5 APPLYING THE THEORY TO RRS

5.1 Introduction

LQG control methods form a well-known basis for the design of controllers for various processes. These methods have the following advantages:

- A solution to the controller problem for linear processes can be found. Numerical methods can be applied for complicated processes, while for simple processes an analytical solution can be derived.
- The method guarantees that the solution will be stable and will be optimal with respect to the criterion.

However, LQG methods have limitations as well, including the following:

- They can only be applied to linear processes.
- The weighting factors of the criterion have to be selected.
- A mathematical model of the process has to be available.
- The states of the process have to be known.

The first limitation may be circumvented by linearizing the process. The criterion may be determined by, for example, economic reasons. However, in most cases "suitable" weighting factors have to be selected by a trial and error method. In the control problem considered here, these limitations cannot be avoided so easily:

- The steering machine introduces, for example, non-linear elements in the process which cannot be disregarded or linearized without taking special precautions. Section 5.2 demonstrates the deteriorating influence of the steering machine.
- The desired autopilot performance depends on operational requirements which are subject to change. In confined waters other controller characteristics are desired than in the open sea. Likewise, in heavy weather other controller characteristics are desired than in light weather. Therefore, it is not possible to select a criterion having weighting factors which are suitable under all circumstances.
- In Chapter 2 a suitable mathematical model of the process is introduced. However, not all of the state variables of the process can be measured while those which can be measured are contaminated by noise.

In this chapter solutions to these problems are proposed. In Section 5.3 a mechanism to prevent the worst consequences of the deteriorating influence of the steering

machine is introduced. In addition, the mechanism allows the steering machine to be regarded as linear.
In Section 5.4 a new method is proposed to select an appropriate criterion. It is based on translating the operational requirements into the weighting factors of a quadratic criterion. These operational requirements may depend on measurements as well as on pre-knowledge of the process. This approach simultaneously solves the problem of certain non-linear elements.
Straightforward application of the optimal control techniques given in Chapter 3 subsequently yields the optimal values of the controller gains.

The remaining limitation of the LQG methods can be circumvented by applying optimal filter methods to estimate the states of the process which cannot be measured and to remove the undesired components from the measurements.
Optimal filter methods form a good basis for the design of filters for various processes. However, there are some limitations on the field of application, including:

- That part of the process which is influenced by system noise must be linear.
- The statistics of both the measurement noise and the system noise must be known.

In the filter problems considered here, the noise statistics are not known.
They depend on such factors as the wind force, the sea state and the angle of incidence of waves and wind. In Section 5.5 a method is proposed to deal with this problem. It appears to be possible to obtain a quantitative impression of the noise statistics. Analogous to the adaptive solution of the controller problem, a method is introduced to translate this knowledge into the parameters of the covariance matrices of the measurement noise and the system noise. Straightforward application of the optimal filter techniques given in Chapter 4 subsequently yields the required filter performance. In Section 5.5.3 and in Section 5.5.4 it will be demonstrated that the method introduced here can be used to solve several filter problems.

5.2 Controller requirements

5.2.1 Limitation of the rudder angle

Fig. 5.1 shows a simplified block diagram of the system which will be considered. It is comprised of a ship and its disturbances together with a controller and a rudder limit. It is assumed that the time constant(s) of the steering machine is (are) negligibly small and that the rudder is sufficiently fast so that the influence of the

limited rudder speed may be neglected as well.

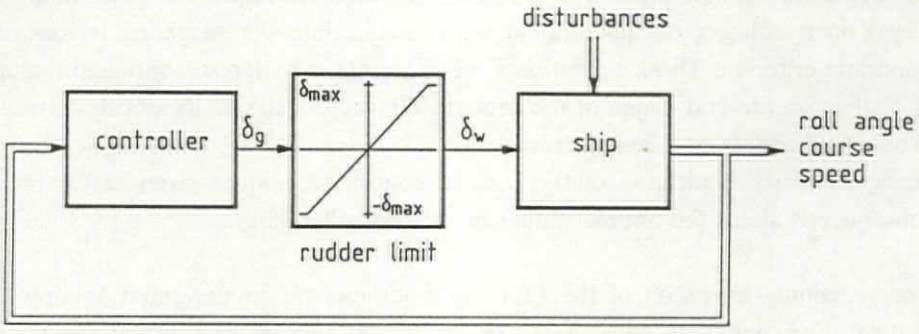

Fig. 5.1 System with rudder limit

In this figure the following holds:

- δ_w = the actual rudder angle
- δ_g = the set point rudder

The influence of the rudder limit on the system's performance can be illustrated by considering the desired-rudder-to-actual-rudder transfer $\delta_g \rightarrow \delta_w$ where:

$$\frac{\delta_w}{\delta_g} = 1 \quad (\text{if } |\delta_g| \leq \delta_{max})$$

$$= \delta_{max} \quad (\text{if } |\delta_g| > \delta_{max})$$

Let the controller output be given by:

$$\delta_g = u_\delta \sin(\omega t) \tag{5.1}$$

Fig. 5.2 shows the resulting rudder angle for two conditions: $u_\delta = \delta_{max}$ and $u_\delta = 2\delta_{max}$.
This figure demonstrates that the influence of the rudder limit can be regarded as a reduction in the amplitude of the required rudder signal (dotted line). A rudder limit does not result in any phase shift in the $\delta_g \rightarrow \delta_w$ transfer. Furthermore, the rudder limit has no influence if u_δ is smaller than δ_{max}.

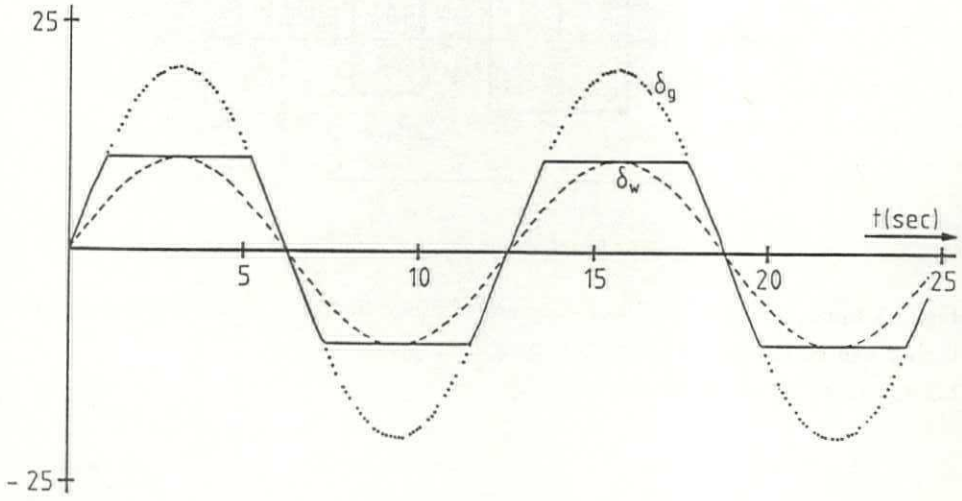

Fig. 5.2 Influence of the rudder limit

Although the system depicted in Fig. 5.1 is essentially non-linear, it is allowable to use the linear controller design techniques described in Chapter 3. The resulting controller will be optimal with respect to the defined criterion until the rudder reaches its limitation. Several simulation experiments have been carried out which indicate that no problems will be encountered if the rudder does reach its limitation unless this happens too frequently, resulting in a bang-bang character of δ_w.

5.2.2 Limitation of the rudder speed

Already in an early stage of the RRS project the limited rudder speed was found to be a severe problem. Van der Klugt (1982) and Van Amerongen and Van Nauta Lemke (1982) describe the consequences for the system's performance if the ship's steering machine cannot follow the desired control signal. This was confirmed by the results of experiments which were carried out at the MARIN in Wageningen (Van Amerongen and Van der Klugt, 1982) and by experiments with a wireless-controlled 8-meter-long scale model at the Haringvliet (Van Amerongen and Van der Klugt, 1983). The roll performance may become worse than without roll stabilization. In addition, the course keeping performance may deteriorate as well. This can be explained with reference to Fig. 5.3 and Fig. 5.4.

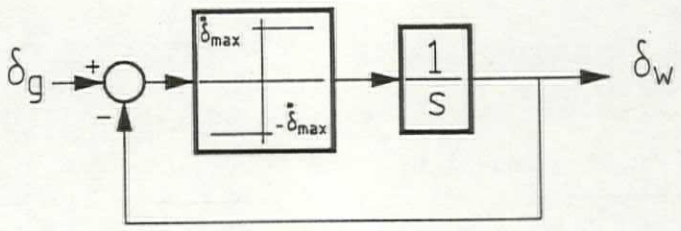

Fig. 5.3 Block diagram of a rate limiter

Fig. 5.3 shows a simplified block diagram of a rate limiter. The influence of this rate limiter can be described by the following example.
Let the input signal δ_g be described by:

$$\delta_g = \text{asin}(bt) \tag{5.2}$$

where

$ab = 3\dot{\delta}_{max}$ ($\dot{\delta}_{max}$ denotes the maximum angular rudder speed)

Fig. 5.4 shows a comparison between the input signal δ_g (dotted line) and the resulting output signal δ_w (solid line). The rate limiter causes a considerable phase lag. In addition, a low-frequency component is generated. In the case of a purely sinusoidal input this component will asymptotically converge to zero.

In Chapter 4 it is explained that low-frequency control signals are used for course keeping while high-frequency control signals are used for roll stabilization. However, it follows from Fig. 5.4 that the rate limiter may cause low-frequency signals as soon as it cannot follow the high-frequency signals generated by the roll controller. This implies that both controllers are no longer decoupled and that the course-keeping performance will deteriorate.
In addition, the rate limiter causes a temporary phase lag which can make the system unstable. This may cause large roll motions which can be increased further by the large yaw motions.
In practice, this will happen in situations where the disturbances are of a relatively high frequency and in extreme weather conditions causing large roll motions. Therefore, solving this problem is crucial.

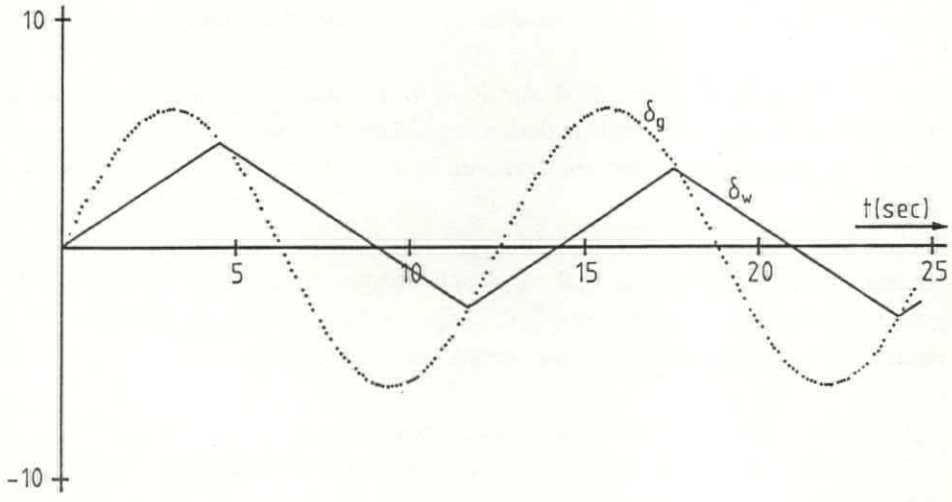

Fig. 5.4 Influence of the rate limiter

It is not possible to design a linear controller with constant gains which is able to obtain a reasonable roll reduction for moderate disturbances and which has an acceptable performance for large disturbances as well. This problem can only partly be solved by selecting a "suitable" steering machine. Several of the design aspects of a steering machine will be discussed in Chapter 6.
Van Amerongen and Van der Klugt (1982) demonstrate that different disturbance conditions require different controllers. This indicates the need for designing an adaptation mechanism which adjusts the controller to changing weather conditions. In addition, such an adaptation mechanism should prevent control signals which cannot be followed by the steering machine from being generated.

5.2.3 The criterion

In general, a controller for a specific process will be designed to obtain a desired performance of the system. Therefore, the first design step will be to formulate the operational requirements. When the LQG method is applied, these operational requirements have to be translated into one (quadratic) criterion function. Once such a criterion function is defined, finding the optimal controller is rather straightforward.

If ships are considered several requirements are posed on the course keeping performance and the roll motions of the ship. These demands can be subdivided into three categories: *ship-design*, *technical* and *operational* requirements.

Ship-design requirements are the demands which are posed on the ship, the steering machine and the autopilot in their design stage. They determine the limitations of the operational requirements and are discussed in Section 6.5.

Technical requirements are the restrictions posed on the autopilot to prevent the control algorithms from causing the system to surpass its technical limitations and to guarantee that the linear controller design techniques remain valid under all circumstances. Some of these requirements are the following:

- The rudder activity should be as small as possible.
  The amount of rudder activity should remain low to reduce the wear and tear on the rudder.
- The required rudder speed should remain lower than the limitations posed by the steering machine.
  In Section 5.2.2 it is pointed out that the system's performance will deteriorate rapidly if this demand is not met.
- The controller parameters should remain below a certain limit.
  The controller design, given in Section 3, will result in a stable system. However, with too high controller gains stability problems may occur due to non-linear and unmodeled dynamics.
- The adjustment of the controller parameters should be slow enough to follow only weather changes. It should not respond to single large peaks in the roll motions. Stability problems may occur if this demand is not met.
- The controller output should be a smooth signal to prevent unnecessary wear and tear on the steering machine and the rudder.
- The rudder angle should remain below a certain limit. This limit depends on the forces which act on the rudder. They become large when the ship's speed increases. Precautions have to be taken to prevent these forces from becoming too large.

Operational requirements are the demands posed by the ship's operator. They are restricted by the ship-design and the technical requirements. The ship's operator can, for example, pose the following demands:

- The roll angle should not exceed a certain value.

The allowed roll motions are determined by such things as the safety of the cargo or the comfort of passengers and crew. Under some circumstances, e.g. a helicopter landing on a naval ship, the roll motions should be as low as possible.

- The heading error should not exceed a certain value.
  The allowed heading deviations depend on the fairway conditions. In confined waters other heading deviations are allowed than in the open sea.
- The drag introduced by the rudder should be as low as possible.
  Under some circumstances the ship's speed may increase if the rudder motions are reduced.
- The underwater noise introduced by the rudder should be as low as possible.
- The controller output should be a smooth signal.
  Abrupt rudder changes will make the ship motions less comfortable.

If the disturbance conditions are known (whether a priori or from measurements), sufficient knowledge is available to translate these demands into one criterion. In practice, the disturbance conditions are not known and may vary within a wide range. It might be possible to calculate the optimal controller for all relevant circumstances and to put the results in the form of tables or functions. If the disturbances change, a different set of controller parameters has be selected (automatically or manually) according to these tables or functions (gain scheduling). However, the experiments which were carried out at the MARIN in Wageningen (Van Amerongen and Van der Klugt, 1982) and with a 30 ft-long radiographically-controlled scale model at the Haringvliet (Van Amerongen and Van der Klugt, 1983) indicate that, in practice, this method is insufficient.
A practical application requires a controller to give a good performance under all conditions rather than an excellent performance under most conditions and a bad performance under some conditions. Due to the limitations of the steering machine a strong controller may disrupt the system's performance as soon as the disturbances become large. As a precaution, weak controllers should be used. However, the roll-reduction potential of a weak controller is low. In addition, as soon as the disturbances become "very" large even a weak controller may cause a bad performance of the system.

Apparently, it is not possible in practice to translate the above requirements into one quadratic criterion as required by the theory. In Section 5.4 a method will be introduced to solve this problem.

5.3 The Automatic Gain Controller

Section 5.2.2 describes some of the problems which may be introduced by the limitation of the rudder speed. Therefore, measures should be taken to prevent a controller from generating signals which cannot be followed by the steering machine. This section proposes a solution to this problem.

Assume that the steering machine is just able to follow the output of a certain roll controller. If the roll motions decrease or shift to lower frequencies, this will not cause any problems. In that case, the steering machine has some reserve and the controller may be adjusted to take advantage of that reserve.
However, the control performance deteriorates instantly if the roll motions or the roll rate increase. Commonly applied adaptation mechanisms respond slower than the largest time constants of the process to be controlled. They are too slow to prevent such a rapid deterioration. A robust solution of this problem is described below.

The problem can be defined as follows:

- Under all circumstances the following must hold:

$$\left|\dot{\delta}_g\right| \leq \dot{\delta}_{max} \tag{5.3}$$

where

$\dot{\delta}_g$ = the rate of change of the set point of the rudder
$\dot{\delta}_{max}$ = the maximum rudder speed

The solution is based on two principal ideas:

1. The realization of a velocity limitation which attenuates the control signal instantaneously by a certain factor such that the steering machine is just able to follow the control signal.

2. The realization of a memory function to maintain the attenuation for some time.

A phase lag cannot be prevented by the momentary attenuation of the control signal. Maintaining this attenuation over a longer time period will prevent a further phase lag in the near future, even if in the meantime the cause of the problem has disappeared. Without a memory, each time the control signal increases too much the phase lag will appear and the problem will remain.
A block diagram of the *Automatic Gain Controller* (**AGC**) is given in Fig. 5.5.

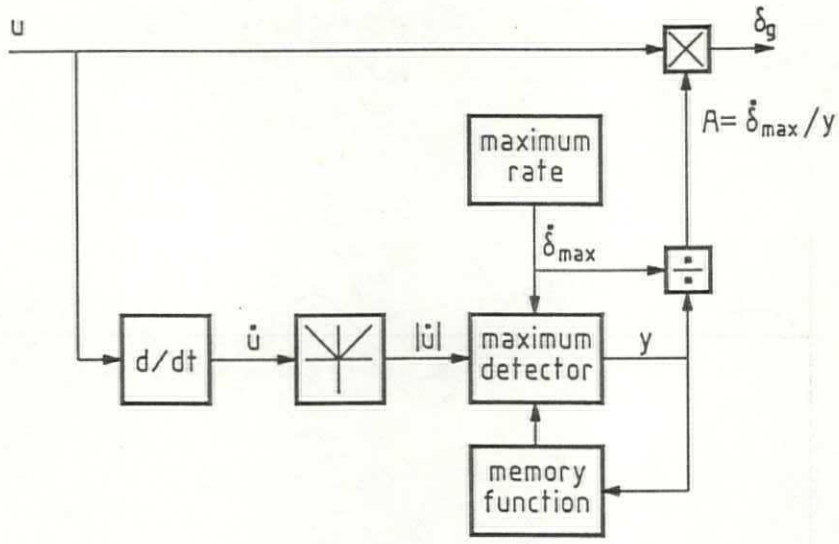

Fig. 5.5 The AGC.

In Fig. 5.5 the following holds:

u = the controller output
δ_g = the set point of the rudder
$\dot{\delta}_{max}$ = the maximum rudder rate
y = the maximum of three input signals:
1 the maximum rudder rate
2 the absolute value of the derivative of u
3 the output of a memory function
A = the gain needed to adjust the controller output u ($0 < A \leq 1$)
= $\dot{\delta}_{max}$ / y

A simulation result is shown in Fig. 5.6. In this simulation the controller output u is supposed to be a sinusoidal signal with increasing amplitude. The figure shows a comparison between the resulting actual rudder angle δ_w when the AGC is applied (solid line) and when it is not (dashed line). The set point rudder is shown in this figure as well (dotted line).

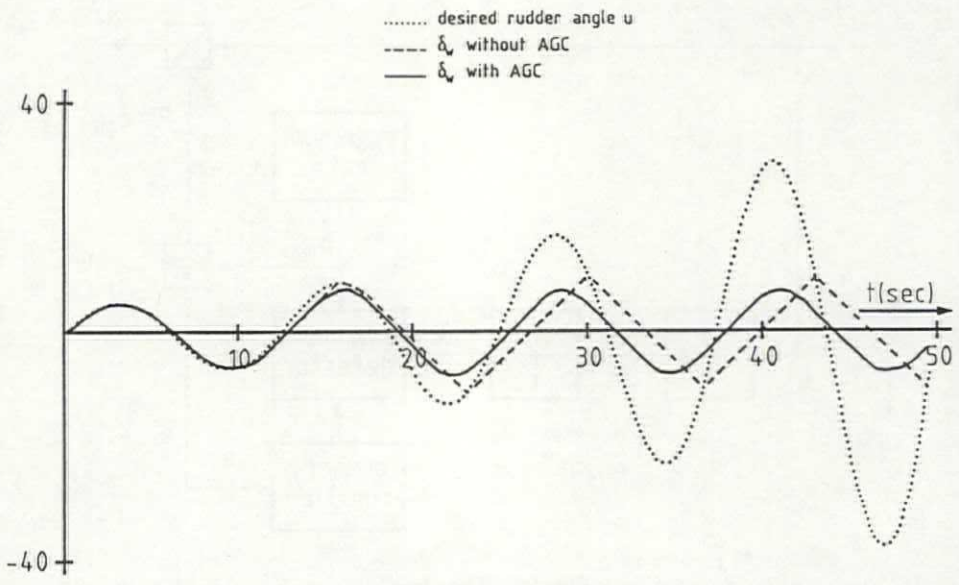

Fig. 5.6 Influence of the AGC with increasing controller output

In Fig. 5.7 the result of a similar simulation is shown, where the controller output u is decreasing.

Application of the AGC results in a smoother response of the rudder while the phase lag and the low-frequency components introduced are minimal.
The forgetting of old values depends on the system characteristics. It is a compromise between reducing the phase lag and reducing the influence of single large peaks in the controller output.
Application of the AGC is not an alternative to the adaptation mechanism which is proposed in Section 5.4. The AGC reduces all of the controller gains with the same ratio. In general, this does not guarantee that the system has the best possible performance. However, it is a useful addition to the adaptation mechanism of Section 5.4, as it allows a slow adaptation while preventing the system's performance

from deteriorating during the adaptation.

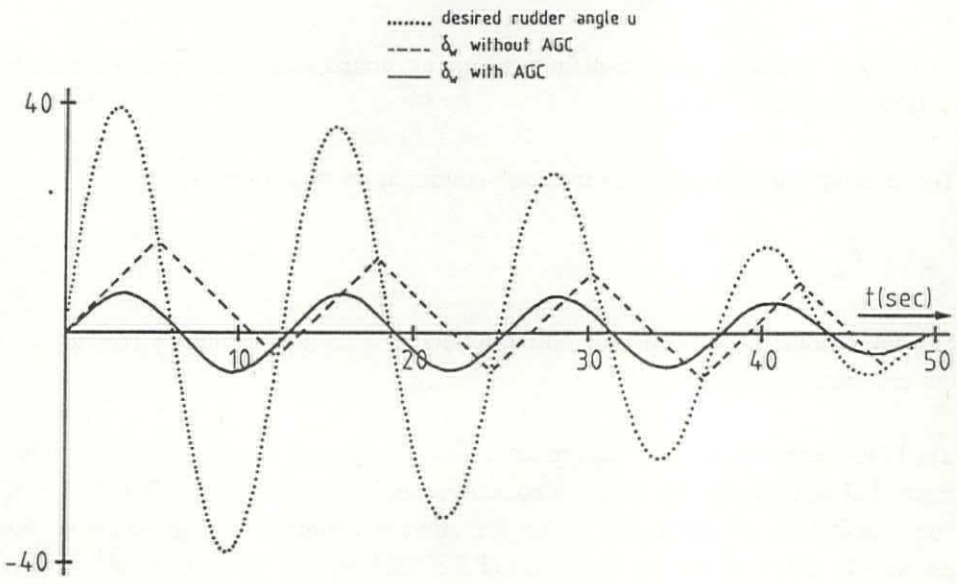

Fig. 5.7 Influence of the AGC with decreasing controller output

5.4 Criterion adjustment

5.4.1 Introduction

In Section 5.3 the AGC was introduced to cope with the consequences of having a steering machine which cannot follow the controller output. The effect of the AGC on the controller can be expressed as a simultaneous reduction in all of the feedback gains at the same ratio. This is not necessarily the optimal solution. A potentially better solution is to get at the root of the problem, i.e. having a steering machine which is too slow or having a control action which is too strong. In this section we tackle the latter problem; it is then assumed that the maximum rudder speed cannot be increased.

The application of the LQG method requires the following quadratic criterion to be defined:

$$J = \lim_{T\to\infty} \frac{1}{T} \int_0^T (\underline{y}^T Q \underline{y} + \underline{u}^T R \underline{u}) dt \qquad (5.4)$$

where Q is a (semi-) positive-definite weighting matrix and R is a positive-definite weighting matrix.

The steering machine poses a secondary condition on this criterion:

$$\dot{\delta}_g \leq \dot{\delta}_{max} \qquad (5.5)$$

Moreover, some of the demands posed in Section 5.2.3 add secondary conditions to the criterion.

The LQG method cannot be used to solve a boundary problem. A commonly applied method of solving such a problem is considered in Section 5.4.2. It deals with the off-line calculation of controller gains for several conditions. This solution was extensively tested during the first years of the RRS project. In Section 5.4.3 a more suitable method is introduced: adaptive adjustment of the weighting factors of the criterion.

5.4.2 Non-linear optimization

A system containing models of a ship, a steering machine and the disturbances has been simulated, using the simulation package PSI (Van den Bosch, 1981). This package enables optimization of a system by means of a hill-climbing procedure. Its use is not merely restricted to linear systems or to quadratic criteria. This makes it possible to use more appropriate criteria based on the requirements which were posed in Section 5.2.3 (Van Amerongen and Van Nauta Lemke, 1982; Van Amerongen, Van der Klugt and Pieffers, 1984) and to take into account the non-linear steering machine dynamics. Several experiments in which the following criterion has been used have been carried out:

$$J = 2 \max|\varphi| + 5 \max|\psi| \qquad \text{for } 0 < t \leq T \qquad (5.6)$$

where $\max|\varphi|$ and $\max|\psi|$ are the maximum values of the roll and heading signals

during the observed interval T. This criterion is based on the idea that it is more important to reduce the maximum roll angle and heading angle than the variances of these signals. As a direct means of judging the roll-reduction performance a suitable criterion is

$$J = 100\left(1 - \frac{\sigma^2_{\varphi(\text{closed})}}{\sigma^2_{\varphi(\text{open})}}\right) \quad (\%) \tag{5.7}$$

where

$$\sigma^2_{\varphi} = \overline{(\varphi - \bar{\varphi})^2}$$

$\bar{\varphi}$ = the average roll angle

and where σ^2_{φ}(open) and σ^2_{φ}(closed) denote the variance of the roll angle of respectively the system without the roll controller and the system with the roll controller.

Because of the non-linear nature of the problem it is not possible to find one set of controller parameters for all situations. However, it is possible to determine a table of controller gains as a function of the amplitude and dominant frequency of the disturbances. This table can be used to make an adaptive controller based on gain scheduling. The problem which remains is to measure or estimate the appropriate signals for adjusting the controller settings.
Several successful experiments have been carried out with controllers based on this method (Van Amerongen, Van der Klugt and Pieffers, 1984; Van Amerongen, Van der Klugt and Van Nauta Lemke, 1985). However, there are two major drawbacks which prevent this method from being used in a practical autopilot design:

1. The method requires accurate models of the ship, the steering machine and the disturbances.
   In practice, it is difficult to obtain a model which describes sufficiently accurately the influence of the disturbances on the ship's motions. If a worst case approach is followed, this might result in controller settings which are too weak. The Automatic Gain Controller has been proved to be a robust aid if the controller settings are too strong. Nevertheless, the resulting control action can be far from optimal.
2. The method requires that different sets of controller parameters have to be calculated for all situations, in principle for every particular ship. Therefore, it is a rather time-consuming method.

5.4.3 Adaptation of the criterion

In Chapter 3 a method is posed to compute the controller gains by solving the corresponding Ricatti equations on-line. An "innovation process' is introduced whose inputs are the weighting factors of the underlying quadratic criterion and whose outputs are the desired controller gains. This method does not require the weighting factors to be constant. It is allowed to adjust them to changing conditions or to changing operational requirements. By automatically adjusting its weighting factors to changing conditions the criterion becomes adaptive.

It has been stated earlier that the word "optimal" in relation to the LQG method is more an indication of the method than a guarantee of optimal performance. This is even more true when an adaptive criterion is used.
Behind the quadratic criterion there is another criterion (described in Section 5.2.3.) which really defines the optimal performance. This is illustrated by Fig. 5.8.

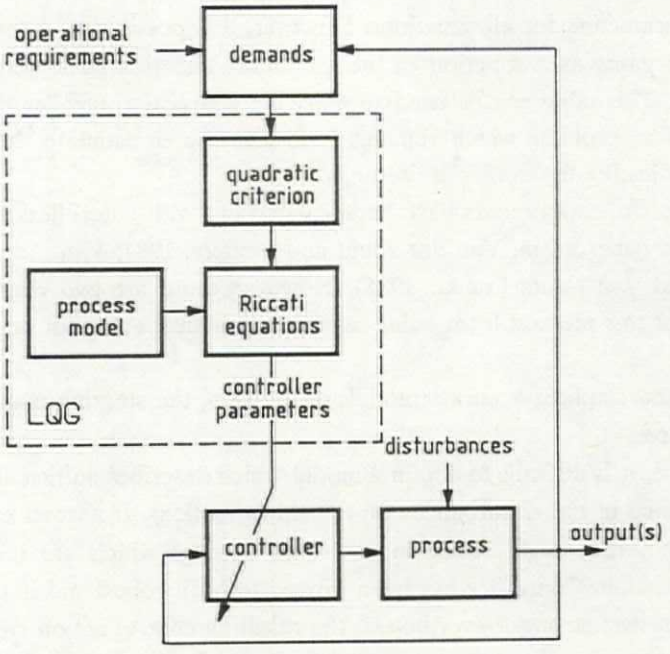

Fig. 5.8 LQG-controller design

The desired performance of a system is defined as a series of demands. Once these

demands are translated into the weighting factors of a (quadratic) criterion, the calculation of the corresponding optimal controller parameters is rather straightforward. In Section 6.4 this idea will be applied to the RRS problem.

The translation of the desired system's performance into the weighting factors of a quadratic criterion will be carried out by some sort of adaptation mechanism. For instance, Van Amerongen, Van der Klugt and Van Nauta Lemke (1986) describe a suitable mechanism for various types of non-linear elements, such as a dead band, a limiter and a rate limiter (the last one is the most relevant for rudder roll stabilization).
In return, such an adaptation mechanism will depend on the process as well as the desired system's performance and, in general, will bear a close resemblance to the way in which a control engineer would tune a controller. This indicates that it might be beneficial to include the insights obtained with artificial intelligence, expert systems or the theory of fuzzy sets in this adaptation mechanism (see for instance Van Nauta Lemke and De-zhao, 1985).

5.5 Filter adaptation

5.5.1 Introduction

The optimal filter problem, posed in Chapter 4, closely resembles the optimal control problem, posed in Chapter 3. This is indicated by Table 5.1.

The control problem	The filter problem
model of the process criterion performance demands	model of the process criterion disturbances

Table 5.1 Comparison of the optimal filter problem and the optimal control problem

Both problems require a model of the process to be known and a criterion to be defined. The criterion of the control problem is based on the demands posed on the system's performance, while the criterion of the filter problem is based on the disturbances influencing the system's performance and the measurements.
In Section 5.3 it was indicated that application of optimal control methods does not

necessarily lead to "the optimal controller" because the weighting matrices Q and R are not always known exactly. A solution to this problem is introduced by making the criterion adaptive.
A similar problem can be recognized in the application of optimal filter methods. In practice, the matrices Q and R, representing respectively the covariance matrices of system noise and measurement noise, are not known exactly. In such a case it is common practice to define a "worst case" situation and design the filter accordingly. A disadvantage of this approach is that in many situations a better filter could have been used. A better solution to this problem is posed in Section 5.2.2. It is based on a combination of on-line estimation of the covariance matrices R and Q and on-line calculation of the corresponding filter gains. This results in a filter with adaptive properties.
Some demands concerning a desired controller performance have to be realized by introducing a proper filter action. These demands may be subject to change. It will be shown that such demands can be included in the proposed adaptation mechanism.

Finally, in Section 5.5.3 and Section 5.5.4 the adaptation mechanism is used to improve the filtering of respectively the ship's speed and the yaw motions.

5.5.2 The adaptation mechanism

Let a process be given by the upper part of the block diagram of Fig. 5.9.
The problem of designing a suitable filter can be divided into two subproblems:

1. Designing the proper filter *structure* which describes all available knowledge concerning the structure and parameters of the process (the lower part in Fig. 5.9).
2. Collecting the proper knowledge concerning the noise statistics.

If these problems are solved for one fixed value of the noise statistics the result will be a filter with fixed gains. If the solution is based on on-line measurements the result will be a filter with adaptive properties.

In the following it will be assumed that the proces has only one disturbance input and one output. Therefore, the vectors $\underline{w}$ and $\underline{y}$ reduce to respectively w and y. In addition, it will be assumed that the process and its model are identical and that the covariance matrices Q and R are not known.

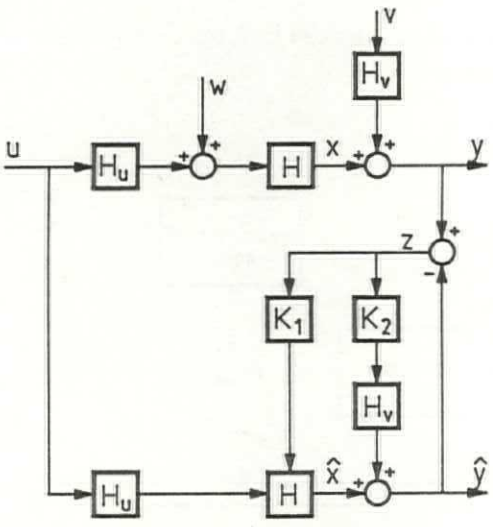

Fig. 5.9 Process and matching filter

The difference between the measurement y and the filter output $\hat{y}$ is denoted by z and can be described by the following transfer function:

$$z = \frac{H}{1 + (K_1 H) + (K_2 H_v)} w + \frac{H_v}{1 + (K_1 H) + (K_2 H_v)} v \qquad (5.8)$$

To be able to apply the theory, assumptions have to be made concerning the matrices Q and R. Based on these assumptions the "optimal filter" can be calculated, which results in a filter with fixed filter gains K_1 and K_2. Therefore, the transfer functions on the right-hand side of Eq. (5.8) and thus the statistics of the error signal z can be calculated in advance.

The error vector z and thus the statistics of z can be calculated on-line as well. The results of both calculations are the same if the original assumptions concerning the matrices Q and R were correct. Thus, the original assumptions concerning the disturbances w and v can be verified. This leads to the following adaptation mechanism:

1. Make an assumption concerning the a priori expected statistics of the error signal z. The result depends on the assumed statistics of w and v, which are the elements of the covariance matrices R and Q.

2. Compute on-line the statistics of the error signal z.

3 Under certain conditions rules can be found to adjust the covariance matrices R and/or Q accordingly.

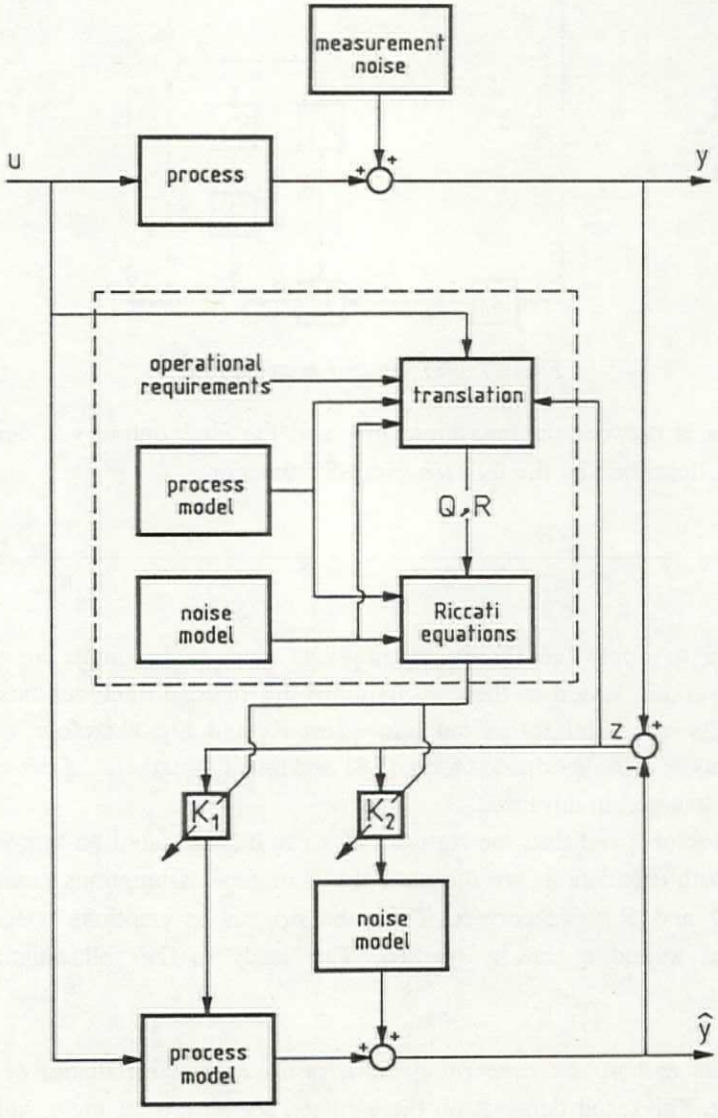

Fig. 5.10 Structure of an adaptive filter

Applying this mechanism in combination with the on-line calculation of the Riccati equations given in Chapter 4 will result in a filter which adapts to changing disturbance conditions. Because the matrices Q and R will be closer to reality with the adaptation than without it, it can be seen that an adaptive filter will be closer to the optimal filter.

Fig. 5.10 illustrates the general block diagram of the adaptation mechanism introduced. It is similar in shape to the block diagram of Fig. 5.8 describing the adaptation mechanism of the controller.

The block "translation" requires the available knowledge of the process as an input. This knowledge is comprised of a priori knowledge concerning the structure and parameters of the process and its disturbances as well as a posteriori knowledge obtained from on-line measurements.
The input "operational requirements" introduces a way to adjust the filter function to operational requirements. For instance, if the filter is used to obtain a smooth controller action, the definition of system noise or measurement noise can be subject to change. The input "operational requirements" allows the design of an optimal filter to be combined with the design of an optimal controller.

An interesting feature of this adaptation mechanism concerns its close resemblance to the adaptation mechanism which was introduced to adjust a controller to changing conditions (Section 5.4). In both cases the matrices R and/or Q are adjusted if the conditions change. The duality between designing an optimal filter and designing an optimal controller is well known in the literature. Apparently, this duality holds with respect to the adaptation mechanism too.

5.5.3 The ship's speed

A problem which cannot be solved adequately by the current optimal filter techniques is the estimation of a "constant" which is subject to change. A typical example is the problem given in Section 4.5, which deals with removing the undesired components from the measured ship's speed. It is shown that a compromise has to be found between a good reduction in the undesired components and a small phase lag if the ship's speed suddenly changes.
In this section it will be shown that the filter performance can be improved by the approach presented in Section 5.2.2.

Let the ship's speed change slowly and let the variance of the measurements be known. In that case, the theory can be used to design a suitable filter (see Section 4.5). The resulting first-order low-pass filter is described by:

$$H_f = \frac{1}{s\tau_f + 1} \quad , \quad \tau_f = \sqrt{E[v_p.v_p]/E[w.w]} \qquad (5.9)$$

where $E[v_p.v_p]$ equals the variance of the disturbances and E[w.w] that of the low-frequency speed changes.
In practice, the disturbances as well as the speed changes are not known exactly and therefore, a worst-case solution will commonly be used as a compromise between the above-mentioned conflicting demands. The method which is posed in Section 5.5.2 offers a better solution.

As indicated in Section 5.5.2 the first step concerns the definition of the proper filter *structure* where the variances of system noise E[w.w] and measurement noise E[v.v] are assumed to be known. This first step is identical to the standard solution which can be found by using the theory given in Chapter 4. A block diagram of the resulting filter structure is given in Fig. 4.14.

With respect to the filter design the following assumptions are made:

- The system noise can be described by integrated white noise with variance E[w.w].
- The variance of the measurement noise equals $E[v_p.v_p]$.
- The difference between the measured process output and the filter output is denoted as e_z.

The resulting filter based on these assumptions is described by Eq. (5.9) and will be referred to as the Constant (first-order low-pass) filter or the C-filter ("Constant" refers to the time constant which is actually a constant). The corresponding time constant will be referred to as τ_o.

The assumptions concerning the statistics of measurement noise and system noise imply a certain expectation of the variance $E[e_z.e_z]$ of the error signal e_z.

- Let the variance of e_z, resulting from these assumed noise statistics, be given by $E[e_z.e_z] = \sigma_z^2$. This is known a priori.

It can be found from measuring e_z whether the assumptions concerning the noise statistics are correct. If the measurements indicate that the assumptions are not

correct, they should be reconsidered.
In the following, the *actual* variances of the system noise and the measurement noise are denoted respectively as E[w.w] and $E[v_p.v_p]$. The *assumed* variances are denoted respectively as Q and R.

A possible measure p_1 to verify the assumptions is based on the standard deviation σ_z:

$$p_1 = c\sigma_z \qquad (5.10)$$

where c denotes a positive constant. Henceforth, the original assumptions are considered to be correct if $|e_z|$ is smaller than or equal to p_1. If $|e_z|$ is larger than p_1 the assumptions should be adjusted which results in a filter with another time constant τ_f.
Nevertheless, the original assumptions could have been correct. In that case the assumptions are adjusted unnecessarily, resulting in a worse filter performance. The possibility p_c that these assumptions were correct is given by

$$p_c = 100(1 - e^{-c}) \quad (\%) \qquad (5.11)$$

The selection of c influences the possibility that the filter will be adjusted correctly. The selection of a large c implies a large possibility that the assumptions were indeed wrong but it increases the possibility that the assumptions are modified too late. The selection of a small c implies that the assumptions are modified early but it increases the possibility that the assumptions are modified unnecessarily.

A possible adaptation mechanism is introduced by the following rule:

If $|e_z| \leq p_1$
then *no adaptation* $(\tau_f = \tau_0)$
else Q is changed into $Q(|e_z|/p_1)^{2n}$ $(\tau_f = \tau_0(p_1/|e_z|)^n)$

In practice, it is necessary to pose additionally a high limit Q_{max} on the assumed variance Q to prevent stability problems. This is similar to posing a low limit $t_{\varphi(min)}$ on the time constant τ_f.

The parameter "n" denotes a positive constant ($n \geq 0$) which influences the adaptation speed. If $n = 0$ the adaptation speed is zero and the filter is not adaptive. The adaptation speed is large if n is large. In the following, four filters are compared, all of which are characterized by the parameter "n":

- n = 0 the C-filter
- n = 1 the Linear (first-order low-pass) filter or the *L-filter*.
- n = 2 the Quadratic (first-order low-pass) filter or the *Q-filter*.
- n = ∞ the Switched (first-order low-pass) filter or the *S-filter*. The time constant τ_f of this filter will be "switched" between τ_0 and $\tau_{f(min)}$.

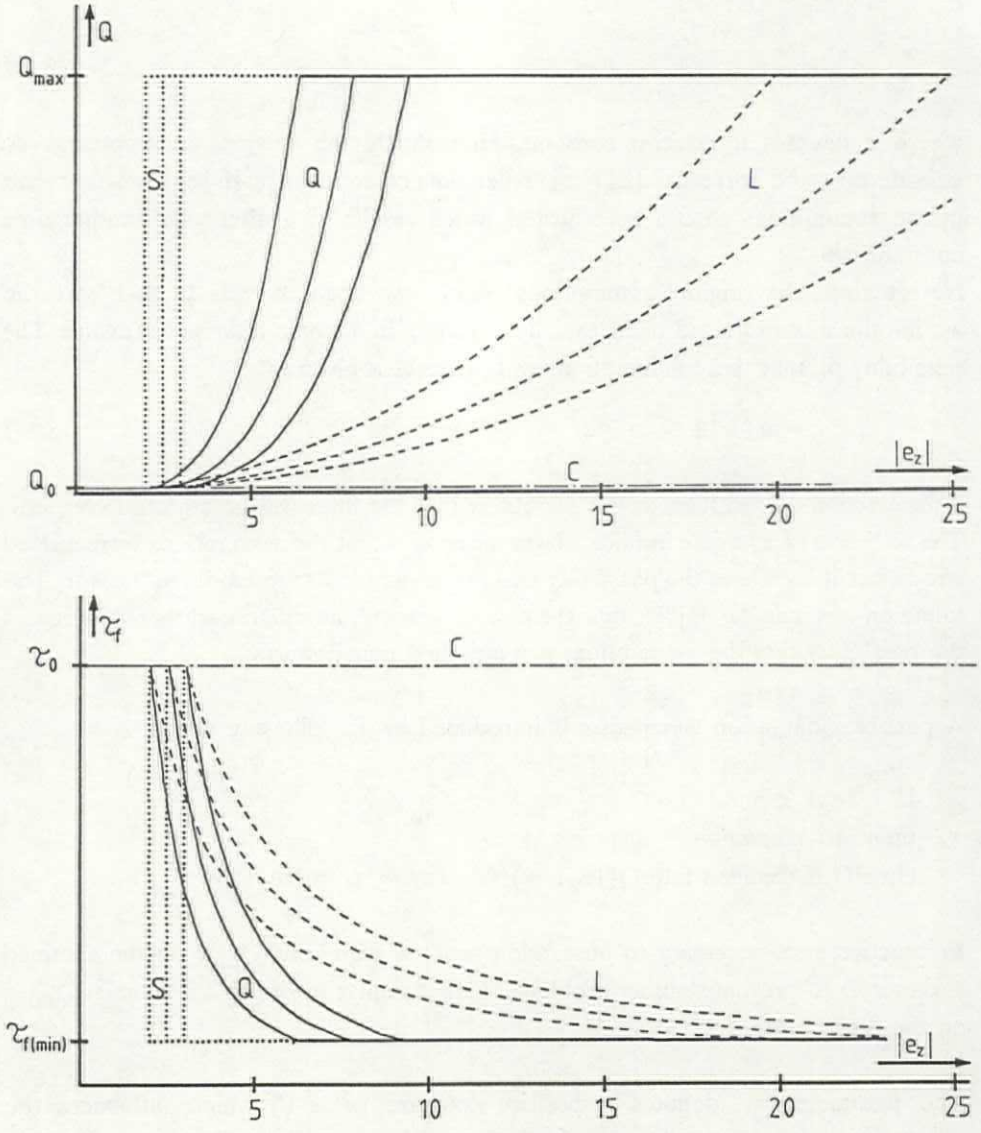

Fig. 5.11 Q and τ_f as a function of n, c and e_z

A comparison with respect to the *adaptation mechanism* is given in Fig. 5.11. The upper part shows the adjustment of Q as a function of the error signal e_z, while the lower part shows the corresponding time constant. The solid lines denote the results of the Q-filter, the dotted lines denote those of the S-filter and the dashed lines those of the L-filter. The comparison is given for three different values of parameter c (from left to right: 2, 2.5 and 3).
Fig. 5.11 indicates that Q and τ_f are rapidly adjusted if n is large. By selecting a larger value for the parameter c this effect becomes less pronounced. In that case, the adaptation mechanism starts at a higher value of e_z.

A comparison with respect to the *performance* is carried out under the following conditions:

- A simulation run takes 500 sec.

- $U = u + v$.

  where v denotes white noise with zero mean and variance 1,
  u denotes the actual ship's speed and
  U denotes the measured ship's speed.

- The parameter c is selected to be 1, 2, 3 or 4.

- $E[w.w] = 10^{-4}$ and thus $\tau_o = 100$.

- $Q_{max} = 100Q$.

Filter	$10^3\sigma_z^2$			
	c=1	c=2	c=3	c=4
C-filter	1.4	1.4	1.4	1.4
L-filter	8.3	2.4	1.5	1.4
Q-filter	29.4	5.8	1.7	1.4
S-filter	29.9	36.7	20.1	6.9

Table 5.2 The variance as a function of the parameter c

In Table 5.2 the variance σ_z^2 of the error e_z (= U - $\hat{u}$) is given for the filters mentioned above as measured during the simulations. The area indicated by the dotted lines indicates an acceptable performance.

If the statistics of the measurement noise and the system noise are known the C-filter is the optimal filter. Therefore, it is not surprising that, according to Table 5.2, the C-filter gives the best performance. The performance of the other filters is worse because the adaptation mechanism adjusts the filter unnecessarily.

The main advantage of the non-linear filters introduced is shown in the following comparison of the *performance*, in which the filters are tested with a step function. Two measures are used to compare the filters:

- $t_{5\%}$ is the time which passes before the error e_z becomes smaller than 5% .
- σ_z^2 is the variance of the error e_z.

Table 5.3 gives $t_{5\%}$ as a function of parameter c. Again, the area within the dotted lines indicates an acceptable performance.

Filter	$t_{5\%}$			
	c=1	c=2	c=3	c=4
C-filter	289	289	289	289
L-filter	128	188	245	270
Q-filter	58	159	203	245
S-filter	37	58	148	182

Table 5.3 $t_{5\%}$ as a function of the parameter c

Table 5.3 demonstrates the advantage of applying an adaptive filter; the error between filter output and actual speed is reduced more rapidly. Furthermore, this table indicates that $t_{5\%}$ increases if c becomes large.

Table 5.4 gives σ_z^2 as a function of the parameter c. As can be expected from Table 5.3 the C-filter yields the worst performance.

Filter	σ_z^2			
	c=1	c=2	c=3	c=4
C-filter	10.0	10.0	10.0	10.0
L-filter	1.7	3.4	4.9	6.2
Q-filter	1.1	1.6	2.7	4.2
S-filter	1.0	1.1	1.3	1.7

Table 5.4 The variance as a function of the parameter c

The desired filter can be found by comparing Table 5.2 with Table 5.3 and Table 5.4. Based on Table 5.2 the C-filter (where c = 1, 2, 3 or 4), the L-filter (c = 4) or the Q-filter (c = 4) should be selected. The performance of the other filters is acceptable if σ_z^2 is smaller than 2.
Based on Table 5.3 and Table 5.4 the S-filter (c = 1) should be selected. The performance of the other filters is acceptable if $t_{5\%}$ is smaller than 210 sec. and if σ_z^2 is smaller than 3.
The best compromise between these conflicting choices is the Q-filter with c = 3.

In Fig. 5.12 a qualitative impression of the performance of the non-linear filters is given. In this figure the following holds:

- c = 3 .
- $\tau_{f(min)}$ = 10 sec.
- $\tau_{f(max)}$ = 100 sec. = τ_0 = time constant of the C-filter.
- The input of the filter is a step function changing from 0 to 10.
- The dotted lines denote the measurements while the solid lines denote the outputs of the filters.

Fig. 5.12 demonstrates that an adaptive filter (in the figure indicated by L,Q or S) yields a better performance than the corresponding filter with a fixed time constant (indicated by C). This is confirmed by the results of the full-scale trials which are discussed in Section 7.4. At first glance the S-filter seems to have the best performance. This agrees with the results of Table 5.3 and Table 5.4. However, the other filters have a better performance than the S-filter as soon as the steady state has been reached.

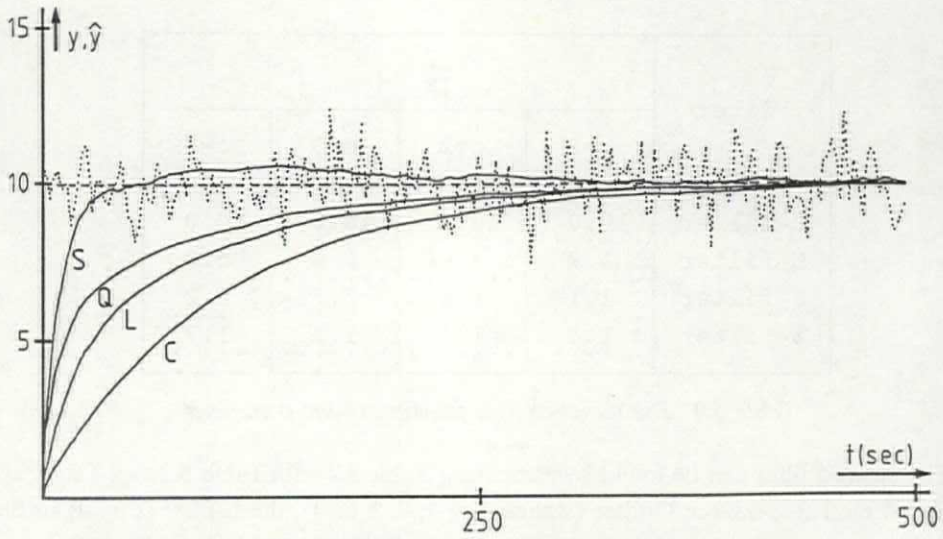

Fig. 5.12 Simulation results with c = 3

5.5.4 The yaw motions

The yaw controller, introduced in Section 3.4.2. requires noise-free estimates of the states of the process. In theory, these estimates can be found by the method introduced in Sections 4.2 and 4.3. However, this method requires knowledge of the statistics of the system noise and the measurement noise. In practice, this knowledge is generally not available.
In such a case, it is common practice to base the filter design on a *worst case* approach. However, in this case the worst case approach will result in a filter which does not have the desired properties most of the time. The basic idea which is introduced in Section 5.5.2, the adaptation of the filter gains, offers a better solution.

Let the process be given by the block diagram of Fig. 4.10. It is assumed that the measurement noise can be described by a first-order high-pass shaping filter. Furthermore, it is assumed that the system noise equals white noise with zero mean. (Therefore, $E[w_2.w_2]$ is assumed to be zero.)

In Fig. 4.11 the filter structure is given along with the block diagram of the process. This process and the matching filter are described by Eqs. (4.75) to (4.81). Simulations were carried out with this process to compare the process output ψ and filter output $\hat{\psi}$ in the following three cases:

a the optimal filter
b an "optimal" filter based on wrong assumptions
c an adaptive filter which is based on the same wrong assumptions as under "b".

The calculation of the optimal filter was carried out on-line by means of the method introduced in Chapter 4 (solving the Ricatti equations on-line by means of an "innovation process"). The variances of the system noise and the measurement noise of the process were selected as follows:

$$E[w_1 . w_1] = 1$$
$$E[w_2 . w_2] = 0$$
$$E[w_3 . w_3] = 0.1$$
$$E[v . v] = 0$$

This choice yields course deviations up to 12 degrees and "measurement errors" up to 0.3 degrees.

During simulations **b** and **c** the following assumptions were made with respect to the filter design:

$$E^*[w_1 . w_1] = 0.01$$
$$E^*[w_2\ w_2] = 0$$
$$E^*[w_3 . w_3] = 1$$

This choice implies that course deviations up to 4 degrees and "measurement errors" up to 3 degrees are expected.

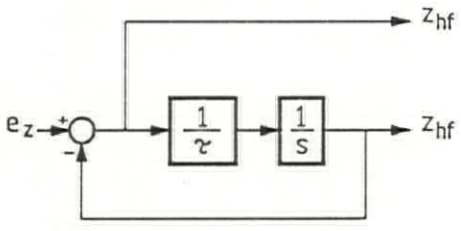

Fig. 5.13 Separation of the high- and the low-frequency components of the error signal z.

During simulation c the statistical parameter $E^*[w_3.w_3]$ was adjusted by means of a mechanism which is related to the mechanism proposed by Van Amerongen (1982):

$$E^*[w_3.w_3] = E_c = \frac{E[z_{hf}.z_{hf}]}{E[z_{lf}.z_{lf}]} \qquad (5.12)$$

The signals z_{hf} and z_{lf} are generated on-line by means of the filter given in Fig. 5.13.

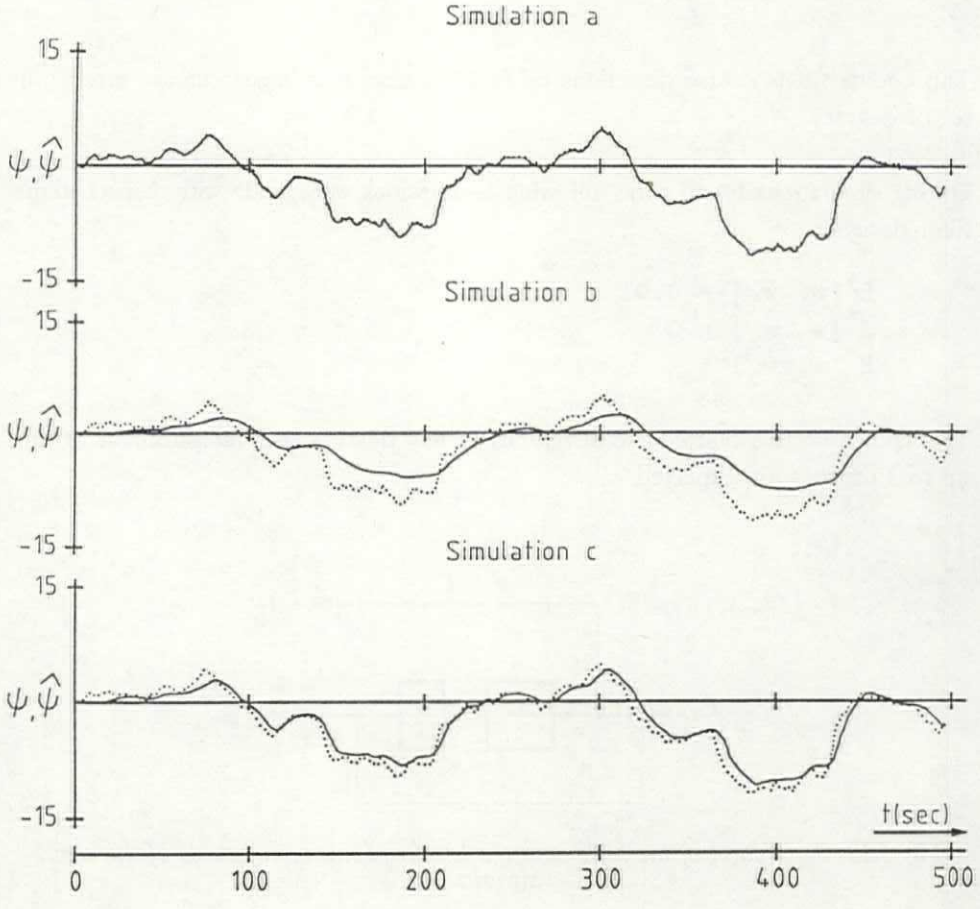

Fig. 5.14 Simulation results

The combination of the on-line calculation of the optimal filter and the adjustment of the assumptions concerning the measurement-noise-to-system-noise ratio results in an adaptation mechanism which is able to improve the filter performance if the original assumptions are wrong. This is demonstrated in Fig. 5.14, which gives a qualitative impression of the simulations mentioned above. The dotted lines represent the desired state variable while the solid lines represent the estimated state variable.

Simulation **a** shows that a good estimation is obtained if the design of the optimal filter is based on the proper assumptions. However, if the assumptions are wrong, the filter performance will be far from optimal, as is indicated by simulation **b**. Finally, simulation **c** demonstrates that, if the original assumptions are adjusted as indicated in Eq. (5.12) ($E^*[w_3.w_3]$ is selected to be E_c), the filter performance will be closer to the optimal performance.

A quantitative impression of these simulations is given in Table 5.5. In this table the parameter e_ψ represents the difference between the desired process output (process output minus measurement noise) and the estimated process output ($e_\psi = \psi - \hat{\psi}$).

Simulation	$E[e_\psi.e_\psi]$	E_c
a	0.01	0.7
b	4.74	0.02
c_1	0.93	0.08
c_2	0.37	0.16

Table 5.5 Simulation results

The best result is obtained if the noise statistics are known a priori (simulation a). In that case, $E^*[w_3.w_3]$ is selected to be $E[w_3.w_3]$. It should be noted that Eq. (5.12) does not yield the proper value of $E[w_3.w_3]$. This indicates that a correction factor should be introduced in Eq. (5.12) ($E^*[w_3.w_3] = E_c/7$).

If the noise statistics are not known, the best result is obtained with the adaptive filter (simulation c_2) where $E^*[w_3.w_3]$ is selected to be $E_c/7$. In addition, the variable E_c of simulation c_2 is closer to that of simulation a.

Apparently, the ratio introduced above (5.12) can be regarded as an approximation of the ratio between the variances of the measurement noise and the system noise. Therefore, further improvement may be obtained by improving the estimation of these variances.

Several authors have investigated the design of adaptive filters to solve the problem of changing noise statistics. As mentioned earlier, Van Amerongen (1982) introduced a filter which can be regarded as a simplified version of the optimal filter. He introduced an adaptation method which, although designed from a different point of view, bears a close resemblance to the method which is discussed above. Fung and Grimble (1981) suggest combining an optimal filter describing the available knowledge of the ship with a self-tuning filter to estimate the undesirable components. Given the filter structure which is required for a process disturbed by colored measurement noise (Section 4.3.1), the self-tuning filter can be regarded as an adaptive shaping filter. Therefore, this solution also resembles the method which is described above.

It was already pointed out in Section 5.5.2 that some demands with respect to a proper controller design have to be realized by means of an appropriate filter. A good example is the design of the course controller. Only low-frequency rudder motions are allowed and this can be accomplished by means of the filter design given above. This indicates that it might be advantageous to adjust some of the filter parameters by means of the translation mechanism which is given in Section 5.4 and which adjusts the criterion parameters of a controller as well. In this particular case, the filter time constant τ_f may be selected as:

$$\tau_f = a\tau_r \qquad (5.13)$$

where "a" is adjusted by means of the following rules:

- If the rudder motions contain too many high-frequency components, "a" should decrease.
- If the rudder motions contain only a few high-frequency components, "a" may increase.

6 REALIZATION

6.1 Introduction

The theoretical basis for the filter and controller algorithms of the RRS autopilot has been given in the foregoing chapters. This chapter describes the next step: the implementation of the algorithms in practice and the design of a laboratory realization of an RRS autopilot.

Section 6.2 introduces a first version of an RRS autopilot, developed at the Control Laboratory. In addition, it introduces some programs which are specially designed to simplify the verification of the autopilot algorithms and to carry out experiments. The autopilot algorithms basically comprise several adaptive filters (described in Section 6.3), a course controller and a roll controller (Section 6.4). The latter is adjusted to changing conditions according to the method which is introduced in Chapter 5. Finally, Section 6.5 poses several demands which must be met for a successful application of RRS.

6.2 The implementation

6.2.1 The hardware

The laboratory realization of the RRS autopilot is based on the following requirements:

1 It should be able to carry out two different tasks simultaneously: the autopilot function and data logging.
2 The experiments on board a ship should not interfere with the ship operation.
3 During full-scale trials it should be easy to switch from the RRS-autopilot back to the ship's system.
4 It should have sufficient inputs available for the signals to be measured and sufficient outputs for the control function and for monitoring purposes.
5 The RRS autopilot should be easy for the crew to operate.

Fig. 6.1 gives a block diagram of the components of the resulting RRS-autopilot.

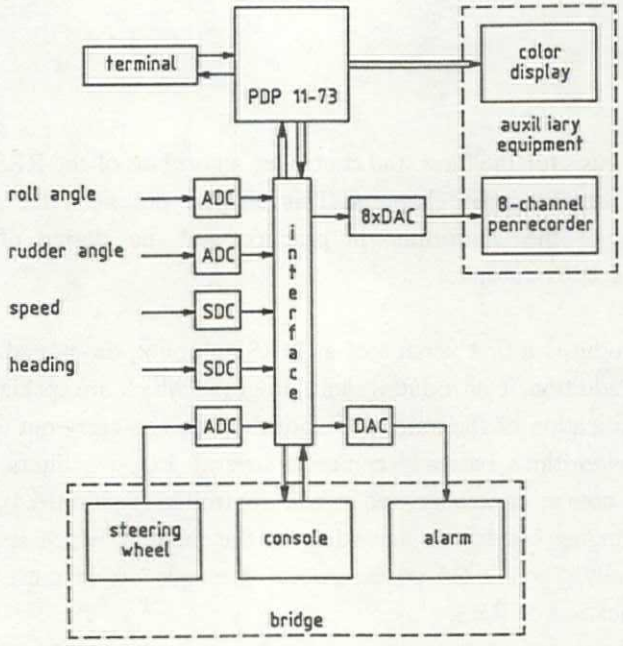

Fig. 6.1 Laboratory realization of the RRS-autopilot

The following elements can be recognized in Fig. 6.1:

- **PDP 11-73 minicomputer**

This computer has two floppy-disk drives and one hard disk. A multi-user and a multi-tasking environment enables the autopilot function to be combined with data logging. During the experiments, the data is stored on a hard disk. After the experiments have been carried out, a backup of the measurement data can be made on a floppy disk.

- **Interface**

The following inputs and outputs of the interface are used:
- 10 *digital-to-analog* converters (DAC) (the required rudder angle, the alarm and the 8 outputs to the pen recorder)
- 3 *analog-to-digital* converters (ADC) (the roll angle, the rudder angle and the

output of the steering wheel)
- 2 *synchro-to-digital* converters (SDC) (the heading and the ship's speed)
- 1 serial in/output (information to and from the operator's console)

- **Operator's Console**

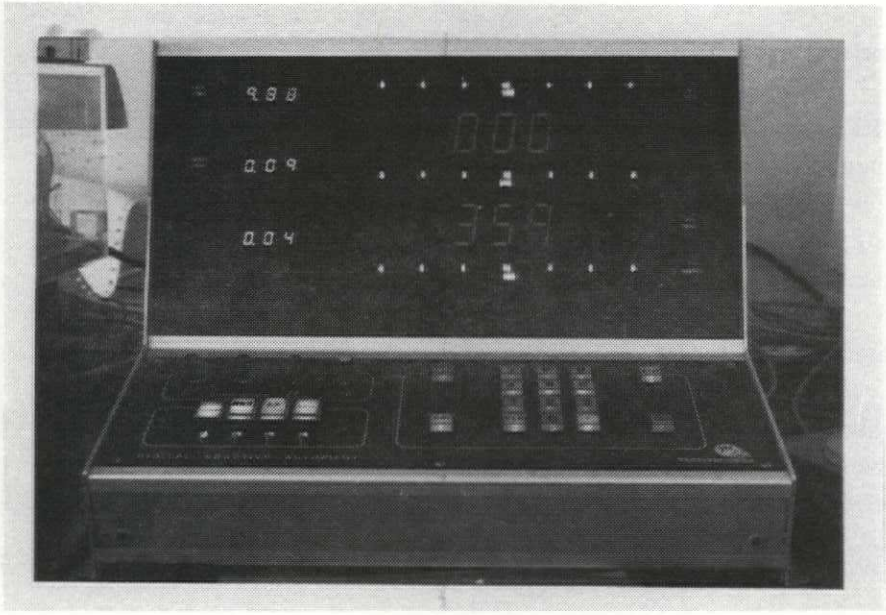

Fig. 6.2 The operator's console

The autopilot modes can be selected on the operator's console. In addition, several displays are available for data monitoring. The console is connected with the computer by a serial line. This enables the console to be installed on the bridge of a ship, while the computer and the other equipment are installed in a cabin.

- **Steering wheel**

In order not to interfere with the ship's hardware, an extra steering wheel is available to realize RRS in combination with manual control of the course.

- **Alarm**

If the autopilot fails, a watchdog timer will signal this at the bridge by means of an audible alarm.

These five items together comprise "the RRS autopilot". The available ship's sensors are used as the inputs of the autopilot. The output of the autopilot is connected to the ship's system. By means of a mere switch it is possible to choose between the rudder set point generated by the RRS autopilot and that of the ship's system.

In addition, some auxiliary equipment is available for data monitoring:

- Color display + TARDIS graphical unit

The RRS-autopilot is implemented within the measurement program RSXMET (Bernard and Ruigrok, 1985). This program makes it possible to show measurement data on a color screen. In addition, it is possible to monitor at random a selection of the autopilot variables on the color screen by a debugging program which is specially designed for this task.

- 8-channel pen recorder

The above-mentioned debugging program enables a selection of the autopilot variables to be monitored at random on an 8-channel pen recorder. This enables a better resolution and in many cases a more appropriate time scaling than monitoring the data on a color display.

6.2.2 The software

The interactive measurement program RSXMET, developed at the Control Laboratory, is specially designed to simplify measurements. It has the following features (Bernard and Ruigrok, 1985):

- It measures signals and scales them to a proper range. The desired signals and scales are obtained from the user in an interactive manner.
- It allows the definition of real time tasks, for instance a controller task. The definition of these tasks as well as the sampling ratio and the priority of the tasks are obtained from the user, again in an interactive manner.
- It stores the measurement signals as well as the signals generated by the user tasks on a hard disk.
- It plots the measurement signals as well as the signals generated by the user tasks on a color display.
- It contains several tasks which deal with the processing of the stored data.

Table 6.1 gives an overview of the tasks provided by the RSXMET program.

	task	programs
real-time	Measurement	(interactive RSXMET tasks)
	Control	(user defined tasks)
	Plotting	(interactive RSXMET tasks)
	Data storage	(interactive RSXMET tasks)
non-real-time	Operating	(interactive RSXMET tasks)
	Operating	(user defined tasks)
off-line	Data handling	(interactive RSXMET tasks)
	Data handling	(user defined tasks)

Table 6.1 The program RSXMET

The autopilot functions are realized within the framework offered by RSXMET. This results in the structure given in Table 6.2.

	task	programs
real-time	Measurement	(interactive RSXMET tasks)
	Control	CONSOL
		RRSASA
	Plotting	(interactive RSXMET tasks)
	Data storage	(interactive RSXMET tasks)
non-real-time	Operating	(interactive RSXMET tasks)
	Operating	ACCESS
		RRSNIT
		SAVRUN
		GETRUN
off-line	not relevant	

Table 6.2 The RRS-autopilot

The program *CONSOL* is the driver of the operator's console. It transmits the data received to the autopilot program RRSASA.
The program *RRSASA* contains the control and filter algorithms and the computation of the performance criteria. In addition, it handles the transmission of

data to the operator's console, to the pen recorder and the debugging program ACCESS. These functions are carried out in the following order:

Collection of measurements
|
Verification and adjustment to the desired representation
|
Primary controller calculations → *Desired rudder angle*
|
Scaling
|
Transmission of the desired rudder angle
|
Secondary controller calculations
|
Collection of operating knowledge
|
Validation and scaling
|
Calculation of operating aspects → *Display information*
|
Scaling
|
Transmission of the display information
|
End

The separation into primary and secondary controller calculations reduces the time delay in the control loop.

The program *ACCESS* is specially designed as a debugging tool for the autopilot. During the experiments it enables every relevant variable of the programs RRSASA and CONSOL to be monitored or changed.
The program *SAVRUN* is designed to write the current settings as an initialization file to the disk. The program *GETRUN* has to be used to initialize the autopilot with this initialization file. The program *RRSNIT* clears the autopilot variables.

6.3 The filter design

In Chapter 2 the disturbances which influence the motions of a ship are discussed. For rudder roll stabilization two motions are important: the roll motion and the yaw motion. The ship's speed is important as well because it has a large influence on these motions. In this section it is assumed that only the roll angle, the heading error and the ship's speed can be measured; the measurements are perturbated by noise. Filters are designed which remove the measurement noise to obtain a good estimate of the desired signal. The filter design is based on the theory given in Chapter 4. Each signal requires a filter with different characteristics:

The roll angle: It is not possible to reduce low-frequency roll motions. This would result in low-frequency rudder motions which cause (large) heading deviations. Therefore, low-frequency components have to be removed from the roll signal.

The heading error: Van Amerongen (1982) demonstrates that high-frequency components should be removed from the yaw signal. High-frequency yaw motions result in rudder motions which cause unnecessary drag while the course-keeping performance does not improve. Duetz (1985) demonstrates that if the disturbances are known and included in the controller design the optimal controller does not generate high-frequency rudder motions.

The ship's speed: The speed signal is comprised of the desired low-frequency components and of undesired high-frequency components.

It is assumed that the three sensors add white measurement noise with a zero mean to the measured signals. This noise has to be removed as well.

The theory for dealing with these filter problems, given in Chapter 4 and Section 5.5, is based on analog systems. The application of a computer makes it necessary to translate the analog solution to a time-discrete solution. This can be achieved in two ways:

1 *z-transformation* of the required model(s) and application of the appropriate time-discrete versions of the formulas which are given in Chapter 4.

A major disadvantage of the exact solution is the seeming lack of correlation between the physical process parameters and the time-discrete model parameters. For instance, the natural roll frequency of a ship can be clearly recognized as a

model parameter in an analog model of the ship, and it influences several parameters after z-transformation of this model.

2 replacing the analog integration by *numerical integration*, e.g. Euler, Runge Kutta 2 etc.

The main advantage of this solution is that the resulting time-discrete model bears a close resemblance to the physical model. A disadvantage of this method is that the integration time has to be small in comparison to the dominant time constants of the process. As a result, this method can be more time consuming than the application of the exact solution. Another disadvantage is that it may be difficult to apply some modern time-discrete algorithms.

In this thesis the second method is preferred, as it provides a greater understanding of the relation between the process parameters and the filter design. It is assumed that the sampling ratio is sufficiently high to allow the application of the following transformation:

$$\frac{1}{s} \rightarrow \frac{T}{z - 1} \qquad (6.1)$$

6.3.1 The roll motions

Fig. 4.8 shows a block diagram of the process describing the roll motions. It is assumed that the process parameters are known and that the measurements are disturbed by white noise with a non-zero mean. In addition, it is assumed that the process is disturbed by white system noise with a zero mean. Any constant component in the measured roll angle which, in practice, may be introduced by the system noise is considered to be caused by the measurement noise.

It is essential to remove the low-frequency components from the measured roll angle. If the roll rate is not available it should be reconstructed, because the controller design requires all states of the process to be available.

The sway velocity caused by the rudder should be reconstructed as well. In practice, the estimate and the actual value of this signal may differ due to differences between the model parameters and the process parameters. However, any errors in the control action caused by these differences are assumed to be caused by the system noise.

Section 4.4 describes a suitable filter designed in the analog domain. By applying the transformation (6.1) this analog filter converts into the time-discrete filter depicted in Fig. 6.3.

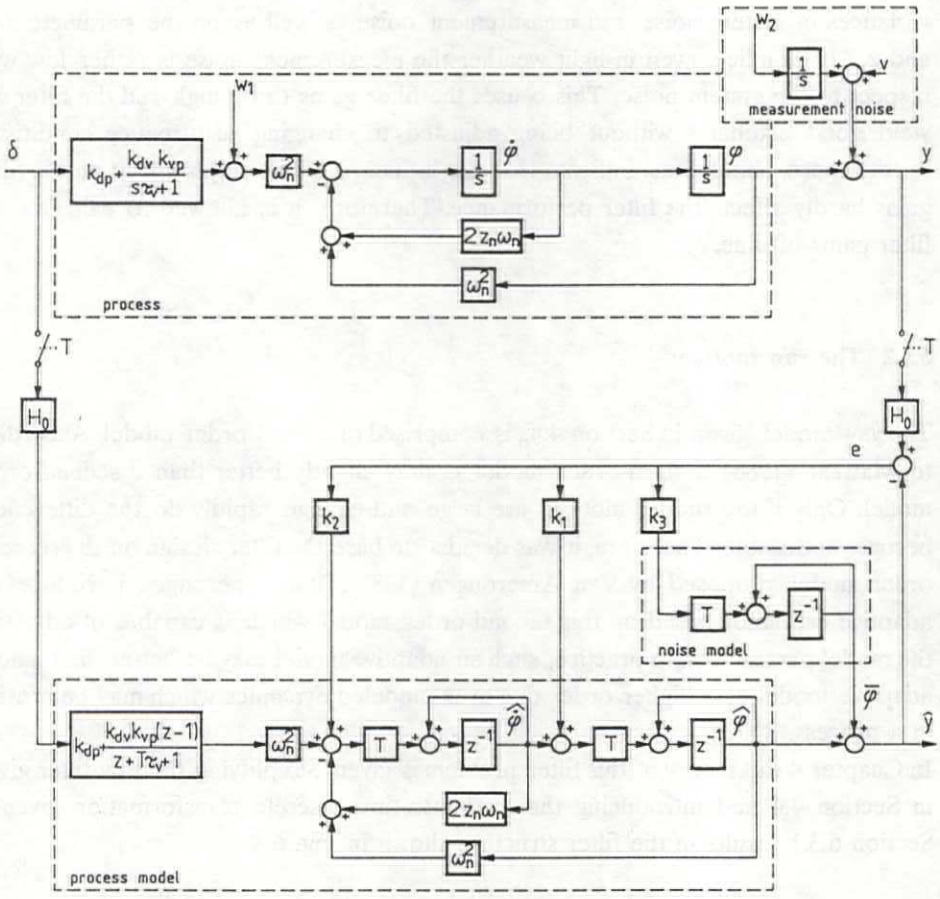

Fig. 6.3 Time-discrete filtering of the roll motions

The filter equations are given by:

$$(\hat{\underline{x}}(k) - \hat{\underline{x}}(k-1))/T = A\hat{\underline{x}}(k-1) + B\underline{u}(k-1) + Ke(k-1) \qquad (6.2)$$

$$\hat{\underline{y}}(k) = C\hat{\underline{x}}(k) \qquad (6.3)$$

$$\underline{e}(k) = \underline{y}(k) - \hat{\underline{y}}(k) \qquad (6.4)$$

The calculation of the filter gains K is given in Appendix E. They depend on the variances of system noise and measurement noise as well as on the parameters ω_n and z_n. In practice, even in light weather the measurement noise is rather low with respect to the system noise. This causes the filter gains to be high and the filter will yield good estimates without being adjusted to changing disturbance conditions. Furthermore, simulations indicate that the influence of the ship's speed on the filter gains hardly affects the filter performance. Therefore, it is allowed to calculate the filter gains off-line.

6.3.2 The yaw motions

The yaw model, given in Section 4.4., is comprised of a third-order model. According to Mattaar (1986) a third-order model is only slightly better than a second-order model. Only if the rudder motions are large and change rapidly do the differences become noticeable. Therefore, it was decided to base the filter design on the second-order model, proposed by Van Amerongen (1982). Van Amerongen introduces an adaptive estimator based on this second-order model which is capable of adjusting the model parameters. In practice, such an adaptive model may be better than a non-adaptive model of a higher order due to unmodeled dynamics which may be present in a process.
In Chapter 4 the theory of this filter problem is given. Simplifying the yaw filter given in Section 4.4 and introducing the analog-to-time-discrete transformation given in Section 6.3.1 results in the filter structure shown in Fig. 6.4.

The model parameters $k_{\delta r}$ and τ_r are obtained by means of on-line parameter estimation according to Van Amerongen (1982). The filter gains K are calculated on-line by means of on-line simulation of the innovation process described by the following time-discrete state-space equations:

$$L\underline{x}_m(k) = (A_m(k-1)-L)\underline{x}_m(k-1) + B_m(k-1)\underline{u}_m(k-1) \qquad (6.5)$$

$$\underline{y}_m(k) = C_m(k-1)\underline{x}_m(k) + D_m(k-1)\underline{u}_m(k) \qquad (6.6)$$

where

$$\underline{x}_m^T = (p_1, p_2, \ldots\ldots, p_{10})$$

$$\underline{u}_m^T = (E[w_1.w_1],\ E[w_2.w_2],\ E[w_3.w_3])$$

$$\underline{y}_m^T = (k_1, k_2, k_3, k_4)$$

$$L = \begin{bmatrix} 5/T & 0 & 0 & 0 \\ 0 & 5/T & 0 & 0 \\ 0 & 0 & 1/T & 0 \\ 0 & 0 & 0 & 1/T \end{bmatrix} \qquad (T = \text{sample time})$$

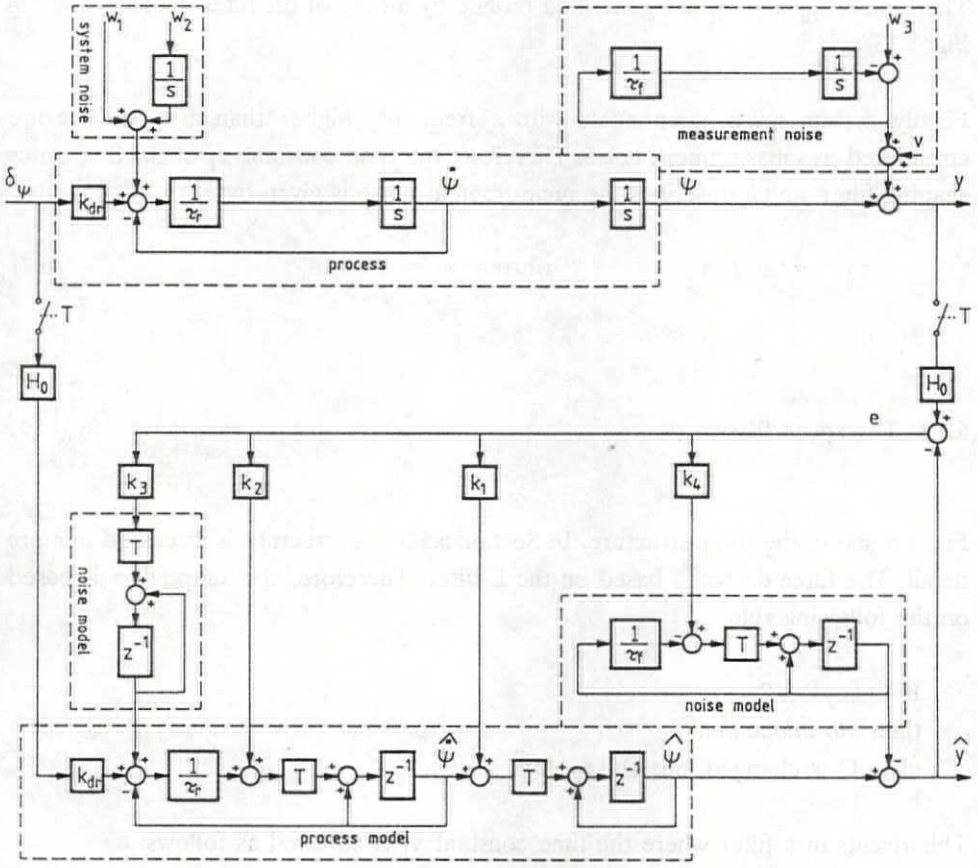

Fig. 6.4 Filtering the yaw motions

The matrices A_m, B_m, C_m and D_m can be found in Appendix F. Note that in Appendix F the extension "(k-1)" is not added because the original derivation is carried out in the analog domain. The statistical parameters $E[w_i.w_i]$ and $E[v.v]$ are selected as follows:

$$E[v.v] = 0.01$$

$$E[w_1.w_1] = 0.1$$

$$E[w_2.w_2] = 0.001E[w_1.w_1]$$

$$E[w_3.w_3] = \frac{E[z_{hf}.z_{hf}]}{E[z_{1f}.z_{1f}]}$$

The signals z_{hf} and z_{lf} are generated on-line by means of the filter which is given in Fig. 5.13.

Finally, system noise components with a frequency higher than a/τ_r rad/sec are considered as measurement noise. Therefore, the time constant τ_f of the first-order shaping filter which describes the measurement noise is given by:

$$\tau_f = a / \tau_r \qquad \text{where } a = 5 \qquad (6.7)$$

6.3.3 The speed filter

Fig. 6.5 shows the filter structure. In Section 5.5.3 this structure is discussed in more detail. The filter design is based on the L-filter. Therefore, the adaptation is based on the following rule:

If $|e_z| \leq 2$
then *no adaptation*
else Q is changed into $Q(|e_z|/2)^2$

This results in a filter where the time constant τ_f is adjusted as follows:

If $|e_z| \leq 2$
then $\tau_f = \tau_0$ (no adaptation)
else $\tau_f = \tau_0(2/|e_z|)$

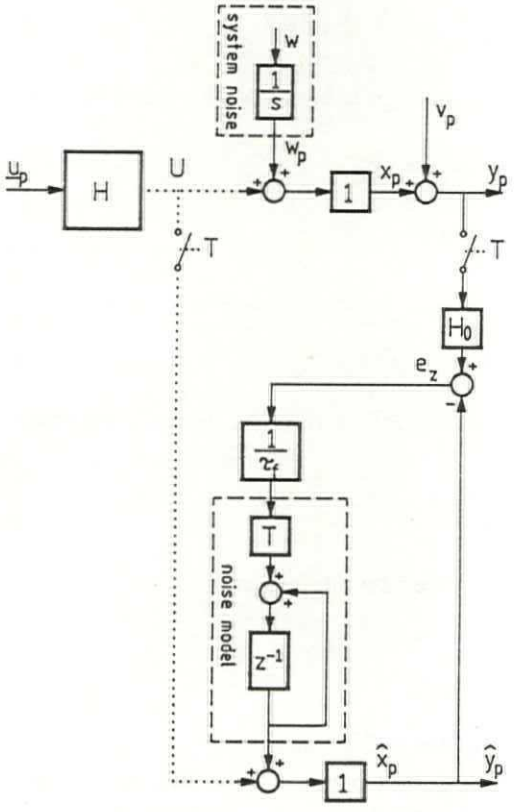

Fig. 6.5 Structure of the adaptive speed filter

In Section 5.5.3 it is indicated that the time constant may be adjusted unnecessarily. The possibility p_c that this will happen can be calculated by Eqs. (5.10) and (5.11):

$$p_c = 100(1 - e^{-2/\sigma_z}) \quad (\%) \tag{6.8}$$

where σ_z denotes the variance of the undesired fluctuations on the measurements.

6.4 The controller

Chapter 3 makes it plausible to separate the problem of designing a controller for this process with one input (the rudder) and two outputs (the heading error and the roll angle) into two subproblems: the design of a roll controller and the design of a course controller. Decoupling is obtained in the frequency domain by applying the filters of Section 6.3.

In principle, the controller design is based on the following criterion:

$$J = q_\varphi J_\varphi + J_\varphi + J_\delta \tag{6.9}$$

where

$$J_\varphi = E[\varphi.\varphi] \tag{6.10}$$

describes the influence of the roll motions on the criterion while

$$J_\psi = E[\psi.\psi]/\lambda \tag{6.11}$$

describes the influence of the yaw motions and

$$J_\delta = E[\delta.\delta] \tag{6.12}$$

describes the influence of the rudder motions.
λ and q_φ are weighting parameters. They will be discussed respectively in Section 6.4.1 and in Section 6.4.2.

Decoupling of the system in the frequency domain allows criterion (6.9) to be separated into two subcriteria:

1 The roll controller is designed with the following quadratic criterion:

$$J_\varphi = q_\varphi E[\varphi.\varphi] + E[\delta_\varphi.\delta_\varphi] \tag{6.13}$$

where δ_φ denotes the rudder motions caused by the roll-control action.

2 The course controller is designed with the criterion proposed by Van Amerongen (1982):

$$J_\psi = E[\psi.\psi]/\lambda + E[\delta_\psi.\delta_\psi] \qquad (6.14)$$

where δ_ψ denotes the rudder motions caused by the course-control action.

6.4.1 The course controller

Fig. 6.6 shows a block diagram of the process. It is comprised of a second-order heading model and the offset.

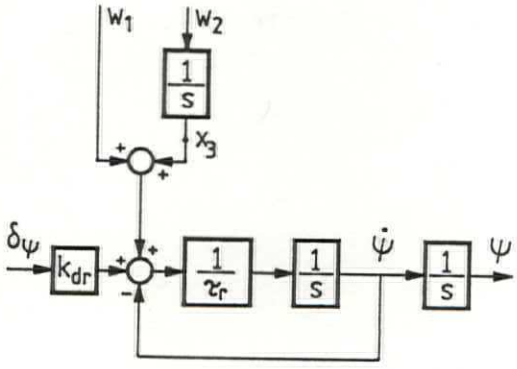

Fig. 6.6 The process

It is assumed that all the state variables are available. This assumption is allowed because, in practice, these states are estimated by means of the filter given in Section 6.3.2.

The process can be described by the following state-space equations:

$$\dot{\underline{x}} = A\underline{x} + B\underline{u} + D\underline{w} \qquad (6.15)$$

$$\underline{y} = C\underline{x} \qquad (6.16)$$

where

$$A = \begin{bmatrix} 0 & 1 & 0 \\ 0 & -1/\tau_r & 1/\tau_r \\ 0 & 0 & 0 \end{bmatrix} \qquad B = \begin{bmatrix} 0 \\ k_{dr}/\tau_r \\ 0 \end{bmatrix}$$

$$C = \begin{bmatrix} 1 & 0 & 0 \\ 0 & 1 & 0 \\ 0 & 0 & 1 \end{bmatrix} \qquad D = \begin{bmatrix} 0 & 0 \\ 1/\tau_r & 0 \\ 0 & 1 \end{bmatrix}$$

$$\underline{x}^T = (\psi,\ \dot{\psi},\ x_3) \qquad \underline{w}^T = (w_1,\ w_2) \qquad \underline{u} = \delta_\psi$$

The state variable x_3 represents the offset component.

The optimal control action with respect to criterion (6.14) can be found to be (see Appendix G):

$$\delta_\psi = -K\underline{x} \tag{6.17}$$

where

$$K = (k_1, k_2, k_3) \tag{6.18}$$

and

$$k_1 = \sqrt{1/\lambda} \tag{6.19}$$

$$k_2 = \frac{1}{k_{dr}}\left(\sqrt{1 + 2\tau_r k_{dr}\sqrt{1/\lambda}} - 1\right) \tag{6.20}$$

$$k_3 = \frac{1}{k_{dr}} \tag{6.21}$$

The weighting parameter λ depends on the required control action. Van Amerongen (1982) proposes the following values for λ:

$$1 \leq \lambda \leq 10$$

A strong controller is obtained by selecting λ to be small. A weak controller is obtained by selecting λ to be large.

6.4.2 The roll controller

Section 3.4.1 gives the roll controller which is optimal with respect to criterion (6.13). It is based on a third-order roll model described by:

$$\dot{\underline{x}} = A\underline{x} + B\underline{u} + D\underline{w} \qquad (6.22)$$

$$\underline{y} = C\underline{x} \qquad (6.23)$$

where

$$A = \begin{bmatrix} 0 & 1 & 0 \\ -\omega_n^2 & -2z_n\omega_n & \omega_n^2 k_{vp} \\ 0 & 0 & -1/\tau_v \end{bmatrix} \qquad B = \begin{bmatrix} 0 \\ \omega_n^2 k_{dp} \\ k_{dv}/\tau_v \end{bmatrix}$$

$$C = \begin{bmatrix} 1 & 0 & 0 \\ 0 & 1 & 0 \\ 0 & 0 & 1 \end{bmatrix} \qquad D = \begin{bmatrix} 0 \\ \omega_n^2 \\ 0 \end{bmatrix}$$

$\underline{x}^T = (\varphi,\ \dot{\varphi},\ v_\delta)$

$\underline{u} = \delta_\varphi$

$\underline{w}^T = w$ = white noise with zero mean

v_δ = the sway velocity caused by the rudder

Fig. 3.5 shows a block diagram of this process.

The optimal control action with respect to criterion (6.13) can be found to be (see Appendix C):

$$\delta_\varphi = -K\underline{x} \qquad (6.24)$$

where K can be found by applying the technique which is introduced in Chapter 3. This results in the definition of the following "innovation process":

$$L\underline{x}_m(k) = (A_m - L)\underline{x}_m(k-1) + B_m\underline{u}_m(k-1) \qquad (6.25)$$

$$\underline{y}_m(k) = C_m\underline{x}_m(k) \qquad (6.26)$$

where

$$\underline{x}_m^T = (p_1, p_2, \ldots, p_6)$$

= the elements of the upper triangle of matrix P

$$\underline{y}_m^T = (k_1, k_2, k_3) \quad = \text{the elements of the matrix K}$$

$$\underline{u}_m^T = (q_\varphi, 0, 0)$$

$$L = \begin{bmatrix} T^{-1} & 0 & 0 \\ 0 & T^{-1} & 0 \\ 0 & 0 & T^{-1} \end{bmatrix} \quad (T = \text{the sample time})$$

The matrices A_m, B_m and C_m are given in Appendix C.
As indicated in Section 5.2.3., the desired control action is determined by several demands. These demands may change due to operational requirements or to changing weather conditions.
It is not possible to select one single weighting factor q_φ in such a way that all these demands will be met under all circumstances. Section 5.4 poses a solution to this problem: the criterion should be adjusted on-line to the changing conditions.

Eq. (6.27) introduces a suitable mechanism to adjust q_φ:

$$q_\varphi(t) = q(0) + \alpha \int \Delta_q dt \qquad (6.27)$$

where

$$\Delta_q = \frac{a_1\Delta_{q1} + a_2\Delta_{q2} + \ldots\ldots + a_n\Delta_{qn}}{a_1 + a_2 + \ldots\ldots\ldots\ldots + a_n} \qquad (6.28)$$

The parameter Δ_q denotes the rate of change of the weighting parameter q_φ ($-1 \leq \Delta_q \leq 1$) while α determines the adaptation speed. The parameters a_i denote the relative importance of the particular demand. The selection of a_i is not very critical.
The requirements posed in Section 5.2.3. have to be translated into a rate of change Δ_{qi}. In the following, these requirements are subsequently translated.

The technical requirements

1 The rudder motions should be as small as possible.

This requirement is incorporated in the criterion by adding the following component:

$$\Delta_{q1} = -1$$

This implies that the rudder activity tends to decrease when there are no other requirements which cause more rudder activity.

2 The required rudder speed should remain lower than the limitations posed by the steering machine.

The parameter Δ_{q2} denotes the influence of the rudder speed on the criterion. Fig. 6.7 shows Δ_{q2} as a function of the required rudder speed. In Fig. 6.7 the maximum rudder speed is denoted by $\dot{\delta}_{max}$.

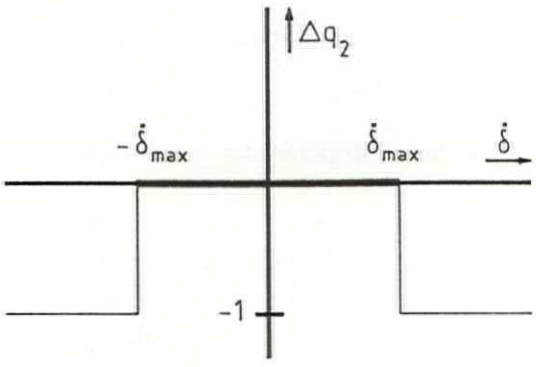

Fig. 6.7 The maximum rudder speed

3 The controller parameters should remain below a certain level to avoid stability problems.

There are two reasons for this requirement:
- Inaccuracies in the models on which the controller is based as well as dynamics which are neglected do not allow the controller gains to be very large.

- The bandwidth of the overall system is limited due to the fixed sampling rate of the discrete controller.

This requirement is similar to "the criterion parameter q_φ should remain below a certain level $q_{\varphi(max)}$". A simple realization of this requirement is introduced by limiting the weighting parameter q_φ to the allowed value. A more elegant method can be introduced by selecting Δ_{q3} as a function of q_φ according to Fig. 6.8.

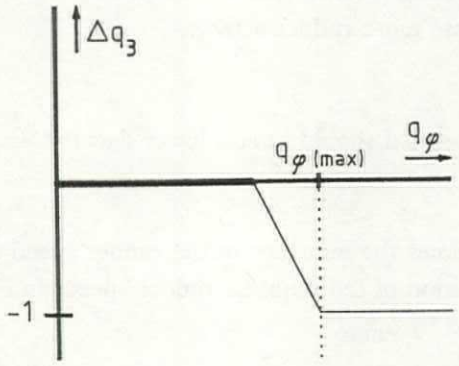

Fig. 6.8 Limitation of the weighting parameter q_φ.

In Fig. 6.8 q_{max} denotes the maximum allowed value of the weighting parameter q_φ.

4 The adjustment of the controller parameters should not react rapidly to incidental signals.

This requirement can be met by making sure that the rate of change of the weighting parameter q_φ remains small. This can be realized by selecting α in Eq. (6.27) to be small. In practice, the choice of α is not very critical.

5 The controller output should be a smooth signal.

This requirement is included in the combination of requirements 2 and 4.

6 The rudder angle should remain below a certain limit.

A possible translation of this demand is given in Fig. 6.9.

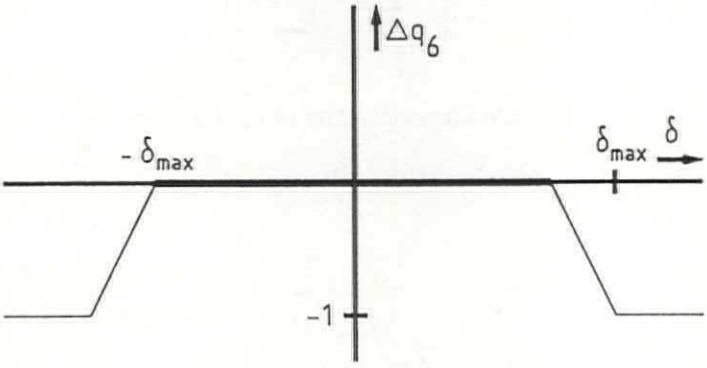

Fig. 6.9 The maximum rudder angle

In Fig. 6.9 δ_{max} denotes the maximum rudder angle. It may depend on the ship's speed.

The operational requirements

An important difference between the technical requirements and the operational requirements is that the technical requirements can only reduce the weighting parameter q_φ (thus leading to a weaker control) while some operational demands may increase it.

7 The variance of the roll angle should not exceed a certain value (σ_g^2).

Instead of the roll angle itself, the variance of the roll angle is a more commonly used measure to describe the roll performance of a ship. An approximation of the variance can be obtained by means of on-line calculation according to the block diagram of Fig. 6.10. The time constant of the low-pass filter should be large in comparison to the natural roll period of the ship.

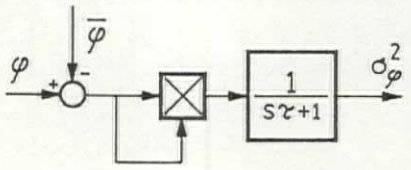

Fig. 6.10 On-line calculation of the roll variance

Fig. 6.11 shows Δ_{q7} as a function of the roll variance.

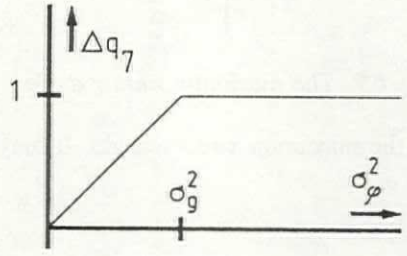

Fig. 6.11 Δ_{q7} as a function of the roll angle.

8 The heading error should not exceed a certain value (Ψ_{max}).

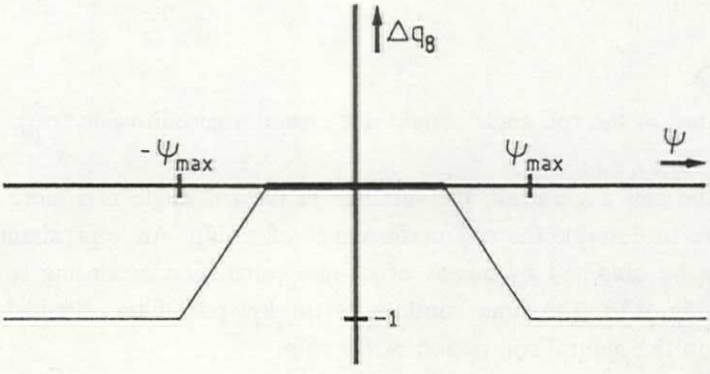

Fig. 6.12 The allowable heading error

If the heading error becomes too large, the roll control action should be reduced to allow a stronger course control action. Similar to the roll motions, the variance of the heading deviations could be used to describe the allowed heading deviations. Likewise, it can be approximated by means of on-line calculation with the structure shown in Fig. 6.10. However, this approach cannot be used in practice because it takes too long to calculate the required variance and thus to adjust the roll control action. Therefore, the heading error itself rather than the variance of the heading deviations is used to adjust the criterion. This is illustrated by Fig. 6.12.

9 The drag introduced by the rudder should be as low as possible.

This requirement is included in requirement 1.

Requirement 7 is in conflict with requirements 8 and 9. In practice, only the ship's operator can decide which requirement is more important. Therefore, an RRS autopilot should provide the means to select between much roll reduction and little roll reduction. The operator's choice can be incorporated in the list of requirements by adding the following requirement:

10 The weighting parameter q_φ should remain below a certain level $q_{\varphi o}$.

This requirement is similar to requirement 3. It should be noted that under all circumstances the following should hold:

$$q_{\varphi o} \leq q_{\varphi(max)}$$

Van Amerongen (1982) proposes a similar solution to select between economic course keeping (λ large) and accurate course keeping (λ small) in the course control loop.

The weighting parameter q_φ, and therefore the criterion, will be continuously adjusted to changing conditions. The optimal controller is obtained only if the controller parameters will be continuously calculated as well. This can be carried out by the method which is proposed in Chapter 3. The weighting parameter q_φ is used as the input of the "innovation process" (6.25). The outputs of this process approach the desired controller parameters.
If the conditions change slowly compared to the convergence speed of the "innovation process", the resulting controller will be optimal with respect to the

demands which are stated in Section 5.2.3.

This method has several useful properties, some of which are:

- It is relatively easy to add new constraints or demands to the criterion function.
- It is flexible. It is not necessary to calculate new gain scheduling tables for other ships or for different speeds of a ship.

6.5 RRS and ship design

6.5.1 Essential properties of the ship

The following requirements have to be met for a successful application of rudder roll stablilization:

1 The rudder should be able to generate a sufficiently large roll moment.

RRS is not possible if the rudder has no influence on the roll motions. At zero speed RRS is not possible, while at increasing ship's speed the potential roll reduction will increase. In addition, the ship should react to the roll moment well before it reacts to the yaw moment of the rudder. In that case, it is possible to obtain the required separation in the frequency domain.
In the design stage of a ship measures can be taken to meet these requirements as well as possible because they determine the potential roll reduction. If an existing ship has to be equipped with an RRS system, these requirements determine whether or not RRS is possible. The roll-reduction ability can be determined by a forced roll experiment. If the rudder is able to generate roll motions while causing only small yaw motions, it will also be able to reduce them.

2 The potential rudder speed should be sufficiently high.

The deteriorating effects of a limited rudder speed will be prevented by the solutions mentioned in Chapter 5. Nevertheless, only a minor reduction in the roll motions is possible if the rudder speed is too low. It appears that there is a relation between the maximum rudder speed, the maximum rudder angle and the natural roll frequency of a ship. Selecting the maximum rudder speed above a certain value will not result in

more roll reduction. In Section 6.5.2 the requirements which have to be posed on a ship's steering machine are discussed in more detail.

3 The aftship should be rigid.

The aftship has to be able to withstand the large forces due to the fast and large rudder motions. The same applies for the ship's rudder and the steering machine.

6.5.2 Essential properties of the steering machine

The ship's steering machine is the actuator which makes the actual rudder angle δ_w equal to the rudder angle δ_g set by the ship's autopilot.
In the ideal case the actuator can be disregarded. In practice, this cannot be realized. Therefore, the steering machine may have a deteriorating effect on the performance of the autopilot. For instance, the steering machine may limit the output of the autopilot and it may introduce phase lag due to, for example, the inertia and the limited speed of the rudder. Nevertheless, it is possible to formulate the requirements to minimize the influence of the steering machine. Two different modes of operation are distinguished:

- During *"large" changes in the set-point rudder* the performance of a steering machine is dominated by the limitations of the rudder angle and the rudder speed.

- During *"small" changes in the set-point rudder* the limitations of the steering machine have hardly any influence. In this situation requirements have to be posed with respect to the phase lag which is introduced by the time constants due to the inertia of the steering machine.

a Large changes in the set-point rudder

Let the maximum signal which can be followed without distortion be given by:

$$\delta = \delta_{max} \sin(\omega t) \qquad (6.29)$$

where δ_{max} denotes the maximum rudder angle.

In that case, the required rudder speed is described by:

$$\dot{\delta} = \delta_{max}\omega\cos(\omega t) \tag{6.30}$$

The maximum frequency which can be followed without distortion of the signal is then

$$\omega_{max} = \dot{\delta}_{max}/\delta_{max} \tag{6.31}$$

In general, the largest roll motions will occur around the natural frequency of a ship. From (6.31) it follows that

$$\dot{\delta}_{max} \geq \delta_{max}\omega_n \tag{6.32}$$

where ω_n denotes the natural frequency in rad/sec.

In practice, the maximum rudder angle can be determined by the ship's operator. For instance, at high speed it is general practice to allow less rudder than at low speed. In addition, the maximum roll moment may not be obtained by the maximum rudder angle. This is illustrated by means of Fig. 6.13.

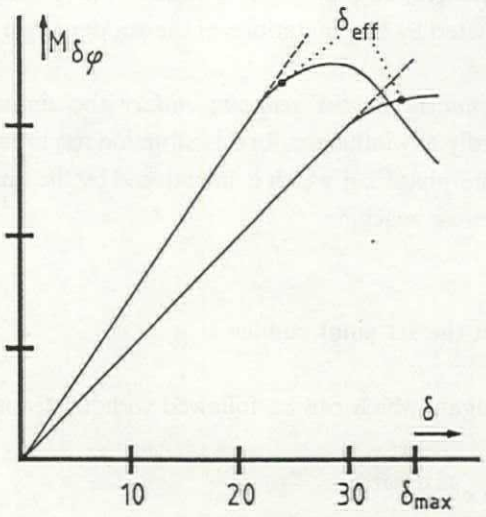

Fig. 6.13 The roll moment as a function of the rudder angle.

Fig. 6.13 shows a potential roll moment as a function of the rudder angle. It depends linearly on the rudder angle up to a certain point. If the rudder angle gets larger, the linear approximation fails and, depending on the rudder construction, the roll moment may even get smaller. In Fig. 6.13 this point is denoted by δ_{eff}, which stands for the "effective rudder angle". The maximum rudder angle is indicated by the dashed line. For RRS it is advantageous for the gain k_δ and δ_{eff} to be large. There is no point in generating a set-point rudder which is larger than the effective rudder angle. This reduces the requirements posed on the steering machine:

$$\dot{\delta}_{max} \geq \delta_{eff}\omega_n = \frac{2\pi}{T_n}\delta_{eff} \qquad (6.33)$$

where δ_{eff} is the effective rudder angle or (if smaller) the maximum rudder angle which is allowed by other requirements. T_n denotes the natural roll period.

For a ship to be equipped with RRS Eq. (6.33) gives an important relation between the design of a ship and the steering machine. If the effective rudder angle is given, it is sufficient to select a maximum rudder speed which satisfies Eq. (6.33). If the maximum rudder speed is selected higher, the potential roll reduction will only slightly increase. On the other hand, if Eq. (6.33) is not met, a substantial improvement in the potential roll reduction can be obtained by increasing the maximum rudder speed.

In order to express these requirements as specifications for a steering machine manufacturer two input signals will be considered: a step function and a sinusoidal function. In that case, the following measures can be used to specify the requirements of the steering machine:

- The allowable value of $t_{10\%}$
  If no overshoot is present $t_{10\%}$ is a suitable measure for determining the maximum rudder speed. $t_{10\%}$ is defined as the time which passes before the output of a process comes (and stays) within 10% of the desired value.
- The allowable time constant of the steering machine τ_δ
  This is a suitable measure for determining the time delay between the required and the actual rudder angle.
- The allowable phase lag
- The allowable dynamic rudder error e_{max}

These requirements can be derived from Eq. (6.33) and the simplified block diagram

of a steering machine, given in Fig. 2.8. The step function poses requirements on the steering machine concerning the rudder speed. The sinusoidal function poses requirements concerning, for example, the phase lag and the error between the set point of the rudder and the actual rudder. In addition, overshoot is not allowed in practice.

The allowable value of $t_{10\%}$

Let the set-point rudder change from 0 to δ_{eff} according to a step function (see Fig. 6.14). In that case, $t_{10\%}$ is described by (6.34):

$$t_{10\%} \approx 0.90\delta_{eff}/\dot{\delta}_{max} \leq 0.9/\omega_n \qquad (6.34)$$

The requirements concerning $t_{10\%}$ and the rudder speed are illustrated by Fig. 6.14.

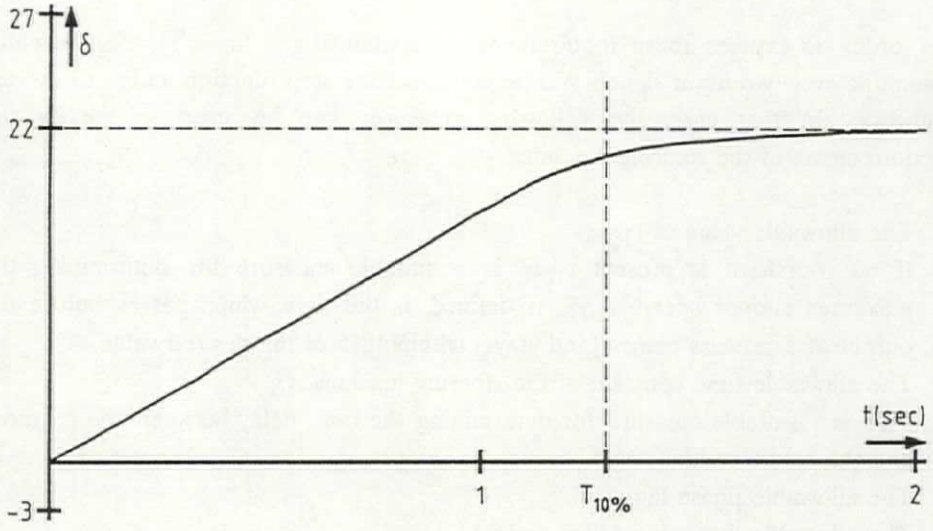

Fig. 6.14 The demands concerning rudder speed and $t_{10\%}$

In Fig. 6.14 the dotted line represents a step input of 22 degrees while the solid line represents a possible response of the steering machine. Within $t_{10\%}$ sec. the remaining error is 2.2 degrees.

The allowable time constant of the steering machine τ_δ

If the steering machine does not reach saturation it can be described by the following transfer function:

$$H_{\text{steering machine}} = \frac{1}{s\tau_\delta + 1} \tag{6.35}$$

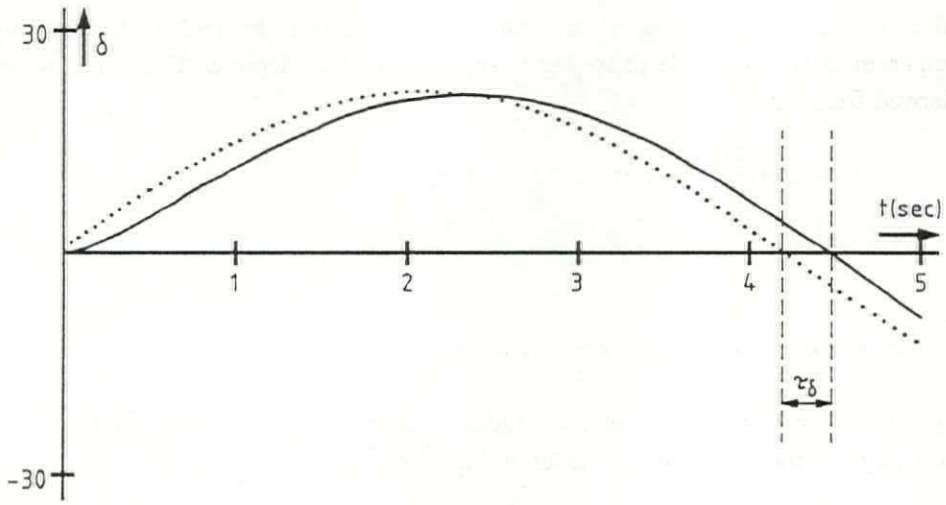

Fig. 6.15 The allowable delay time

As a rule of thumb in control engineering, a pole may be disregarded if the distance of the pole to the imaginary axis in the s-plane is at least 5 times larger than that of the dominating poles of the process. Therefore, in this case (6.36) must hold:

$$\frac{1}{\tau_\delta} \geq 5\omega_n \qquad (6.36)$$

or τ_δ has to satisfy (6.37) where

$$\tau_\delta \leq \frac{0.2}{\omega_n} = \frac{0.1T_n}{\pi} \qquad (6.37)$$

The time constant τ_δ represents the largest time delay which may occur between the required and the actual rudder angle. This is illustrated by Fig. 6.15. In this figure the dotted line represents the input signal, while the solid line represents a possible response of the steering machine. The maximum error between both signals is $0.2\delta_{max}$ degrees, while the maximum phase lag is about 11 degrees. The time between the corresponding zero crossings of the input signal and the response of the steering machine is τ_δ sec.

The allowable phase lag

The allowable phase lag is determined by requirement (6.36). Under this requirement the allowable phase lag is approximately 11 degrees. This can also be derived from Fig. 6.15:

$$\varphi \leq 360\frac{\tau_\delta}{T_n} = 36/\pi \approx 11 \text{ degrees}$$

The allowable dynamic rudder error e_{max}

e_δ is the error between the set-point rudder and the actual rudder angle. It can be derived from the block diagram given in Fig. 2.8:

$$e_\delta = \delta_g - \delta_w = \dot{\delta}_w/\tau_\delta \qquad (6.38)$$

The maximum error e_{max} is reached if the maximum rudder speed is required.

Therefore, e_{max} should satisfy (6.39):

$$e_{max} \leq \dot{\delta}_{max} \tau_{\delta} \tag{6.39}$$

With (6.33) and (6.37) this reduces to

$$e_{max} \leq 0.2 \delta_{eff} \tag{6.40}$$

Example 1:

Let the following parameters be given:

- The effective rudder angle δ_{eff} = 22 degrees.
- The natural frequency of the ship ω_n = 0.75 rad/sec.

These parameters result in the following requirements being posed on the ship's steering machine:

$\dot{\delta}_{max} \geq 16.5$ deg/sec. (from Eq. 6.33)
$T_{10\%} \leq 1.2$ sec. (from Eq. 6.34)
$\tau_{\delta} \leq 0.27$ sec. (from Eq. 6.37)
$e_{max} \leq 4.4$ degrees (from Eq. 6.40)
$\varphi \leq 11$ degrees
Overshoot is not allowed.

b Small changes in the set-point rudder

For small rudder motions the first-order approximation, given by Eq. (6.35), does not hold. A better description is obtained by replacing $1/\tau_{\delta}$ by the following transfer function (see Fig. 2.7):

$$1/\tau_{\delta} \rightarrow H_{\delta} = \frac{K}{s\tau + 1} \tag{6.41}$$

Therefore, Eq. (6.35) changes to:

$$H_{\text{steering machine}} = \frac{\omega_0^2}{s^2 + 2z_0\omega_0 s + \omega_0^2} \qquad (6.42)$$

where

$\omega_0^2 = K/\tau \quad , \; 2z_0\omega_0 = 1/\tau$

ω_0 = the natural frequency of the steering machine

Similar to the requirements concerning large rudder motions, the requirements concerning the parameters of the model of the steering machine can be translated into specifications for a steering machine manufacturer. The following specifications will be considered:

- The allowed natural frequency
- The allowed overshoot
- The allowed settling time
  The settling time T_s is defined to be the time within which the output signal remains within 2% of the desired value.
- The allowed phase lag at -3dB
- The allowed bandwidth
  The bandwidth B is defined as the -3dB point in the Bode diagram of a process.

Again, two input signals are considered: a sinusoidal input signal and a step function as input signal. By using a step function, requirements can be posed concerning overshoot and settling time. For a sinusoidal input signal, requirements can be posed concerning the bandwidth of the steering machine.

The allowed natural frequency of the steering machine

The two poles introduced by the steering machine can be disregarded if ω_0 is at least 10 times larger then ω_n belonging to the dominant poles of the ship:

$$\omega_0 \geq 10\omega_n \qquad (6.43)$$

The allowed overshoot

The steering machine may not show any overshoot. Therefore, in Eq. (6.42) the parameter z_0 is given by:

$$z_0 \geq 1 \tag{6.44}$$

Henceforth, it will be assumed that $z_0 = 1$.

The allowed settling time

T_s is given by:

$$T_s = 4/z_0\omega_0 \tag{6.45}$$

By using Eqs. (6.43) and (6.44) it follows that:

$$T_s \leq 0.4/\omega_n \tag{6.46}$$

Consequently, a relation is obtained between the natural roll frequency of a ship and the required settling time of the steering machine.

The bandwidth

As is shown in Appendix H it is possible to find a relation between ω_0 and the bandwidth B of the steering machine:

$$B = 0.64\omega_0 \tag{6.47}$$

Applying Eq. (6.43) yields:

$$B \geq 6.4\omega_n \tag{6.48}$$

Apparently a relation exists between the natural roll frequency of a ship and the bandwidth of the steering machine.

The phase lag at -3dB

The phase lag at the -3dB point is given by:

$$\varphi = -2\arctan(B/\omega_0) \qquad (6.49)$$

With (6.48) this reduces to:

$$\varphi \leq -65 \text{ degrees}$$

Example 2:

Let the natural roll frequency of the ship be equal to 0.75. In that case the steering machine should meet the following demands with respect to small rudder motions:

$\omega_0 \geq 7.5$ rad/sec. (from Eq. 6.43)
$T_s \leq 0.3$ sec. (from Eq. 6.46)
$B \geq 4.8$ rad. (from Eq. 6.48)
$\varphi \leq 65$ degrees
Overshoot is not allowed.

Concluding remarks

In this chapter the laboratory realization of an RRS autopilot is described. Furthermore, the control and filter algorithms are transformed from the analog domain to the time-discrete domain to enable their implementation in the RRS autopilot. Finally, some properties of a ship and its steering machine which are essential to enable a successful application of an RRS autopilot are given.
It should be investigated in practice whether the assumptions made during the design of the control and filter algorithms are valid by comparing the results with the simulation results. These experiments are described in the following chapter.

7 RESULTS

7.1 Introduction

As mentioned in Chapter 1, the cooperation between the University, the Royal Netherlands Navy and the company Van Rietschoten & Houwens made it possible to carry out a series of experiments during the development of an RRS system. The following diagram summarizes the experiments which were performed:

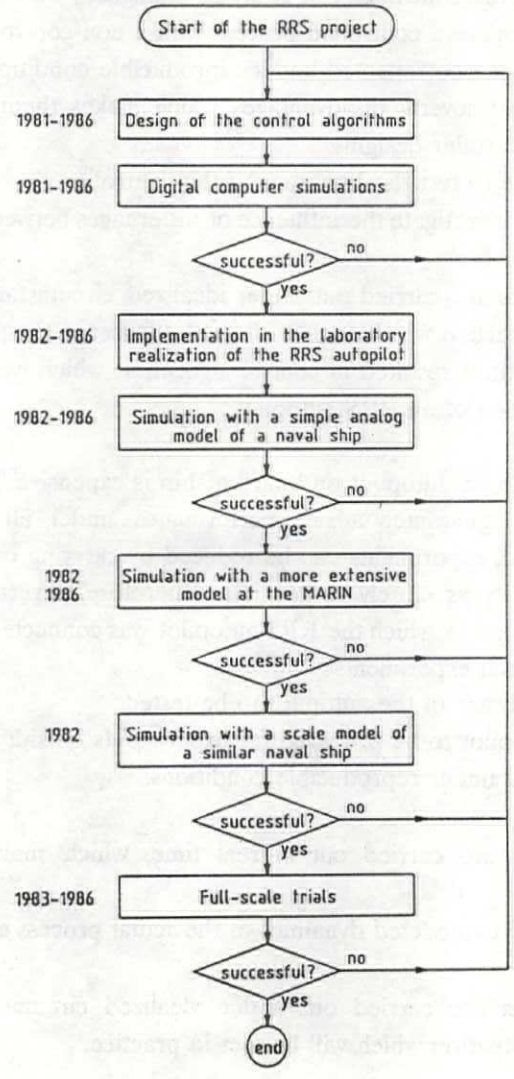

With respect to this flow diagram it should be noted that, if a certain series of experiments could not be arranged, the next series of experiments in the loop was arranged. For instance, the scale model experiments were carried out only once and the experiments at the MARIN were carried out only twice. The full-scale trials were carried out several times.

The *digital simulations* were carried out with the simulation package PSI (Van den Bosch, 1985a). They are suitable as the first step in a controller design because
- they do not have to be carried out in real time, so that many experiments can be carried out within a relatively short amount of time,
- the models and the controller can easily be changed,
- it is easy to compare a controlled process with a non-controlled process,
- the simulations can be repeated under reproducible conditions.

However, they have several disadvantages which makes them not suitable for the final steps in a controller design:
- It is not possible to test the hardware of the controller.
- It is difficult to investigate the influence of differences between the model and the actual process.
- The experiments are carried out under idealized circumstances while situations may occur in practice which cannot always be foreseen.

The digital simulations resulted in control algorithms which were implemented in a laboratory realization of an RRS autopilot.

Experimenting with an autopilot on board a ship is expensive. In addition, measures must be taken to guarantee a safe performance under all circumstances. The required number of experiments can be reduced by carrying out experiments which approach the reality as closely as possible. Therefore, several *analog experiments* have been performed in which the RRS autopilot was connected to an analog model of a naval ship. Such experiments
- enable the hardware of the autopilot to be tested,
- enable the autopilot to be prepared for experiments outside the Laboratory and
- can be repeated under reproducible conditions.

However,
- the simulations are carried out in real time, which makes them fairly time consuming,
- the influence of unmodeled dynamics of the actual process cannot be investigated and
- the experiments are carried out under idealized circumstances and may not include every situation which will be met in practice.

The Maritime Research Institute Netherlands in Wageningen has developed a mathematical model of a similar naval ship, based on a fundamental hydrodynamic approach. This *MARIN model* describes the motions of the ship in all degrees of freedom, including most of the effects of the coupling of the motions. Therefore, experimenting with the MARIN model can be considered to be closer to reality than the experiments with the analog model at the Control Laboratory. In Chapter 2 a model of a ship has been derived which has served as a basis for the controller and the filter design (the *control model*). If the results of the experiments at the MARIN agree with those of the analog and digital simulations at the Control Laboratory one can be confident that this model is sufficiently accurate.
Therefore, the Royal Netherlands Navy enabled experiments where the RRS autopilot was coupled with the MARIN maneuvering simulator. These experiments

- enable the influence of some dynamics which are not included in the control model to be investigated,
- enable the influence of modifying the ship design to be investigated and
- can be repeated under reproducible conditions.

However, these experiments

- are rather time consuming because they are carried out in real time,
- are expensive and
- do not include every situation which will be met in practice.

The number of full-scale experiments can be further reduced by carrying out scale-model experiments first. The Royal Netherlands Navy enabled experiments with a remote-controlled 8-meter long scale model of a naval ship. The experiments were carried out at the Haringvliet, a sea arm in the south west of the Netherlands.
The main advantages of such experiments are the following:

- They enable the RRS autopilot to be tested under more or less realistic conditions.
- It is possible to carry out many experiments within a relatively short amount of time because the model is scaled not only in size but in time as well.

However,

- they are expensive and require extensive preparations,
- the conditions may be far from ideal,
- they cannot be repeated under reproducible conditions and
- the results may be biased due to scaling effects.

The final step in any controller design is constituted by a test in practice. The above-mentioned experiments gave confidence that no severe problems would be met on board a full-size ship. Therefore, the Royal Netherlands Navy enabled trials to be

carried out on board a naval ship where the RRS autopilot was used instead of the ship's autopilot. The naval ship was equipped with an ordinary steering machine.
The main advantage of these trials is that they are carried out under realistic conditions. However,

- they are expensive and require a lot of preparation,
- their success depends on the presence of suitable weather conditions,
- they are rather time consuming,
- they cannot be repeated under reproducible conditions and
- it is not possible to investigate modifications of the ship design.

Section 7.2 describes the digital and analog simulation experiments. The resulting controller algorithms were implemented in a laboratory realization of an RRS autopilot. In addition, it describes the results of experiments with the RRS autopilot coupled to the MARIN maneuvering simulator.
Section 7.3 describes the experiments with a remote-controlled scale model of a naval ship. Finally, Section 7.4 gives an overview of the results obtained during several full-scale trials.

7.2 Experiments with mathematical models

7.2.1 Digital simulations

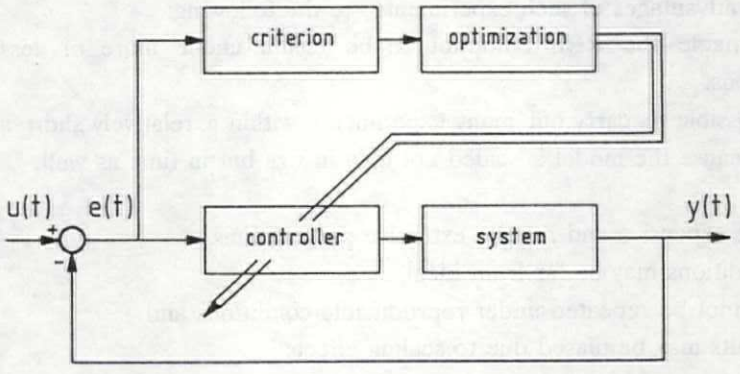

Fig. 7.1 Designing a controller using simulation and optimization.

The simulation package PSI enables an approach similar to the one used in Section

2.5 to identify model parameters to be used to design a controller (Van den Bosch, 1981). This is illustrated in Fig. 7.1. Simulation techniques are used to simulate the controller and the process and to calculate the error signal e. A criterion is defined, for instance one based on this error signal, which can be optimized with respect to the parameters of the controller.

Fig. 7.2 shows a typical example of a PSI simulation. Two equivalent ship models are responding to the same disturbances. The solid lines illustrate the performance of the ship with an RRS controller, while the dotted lines show the performance of the ship with only a course controller. In this particular run a reasonable roll reduction was obtained.

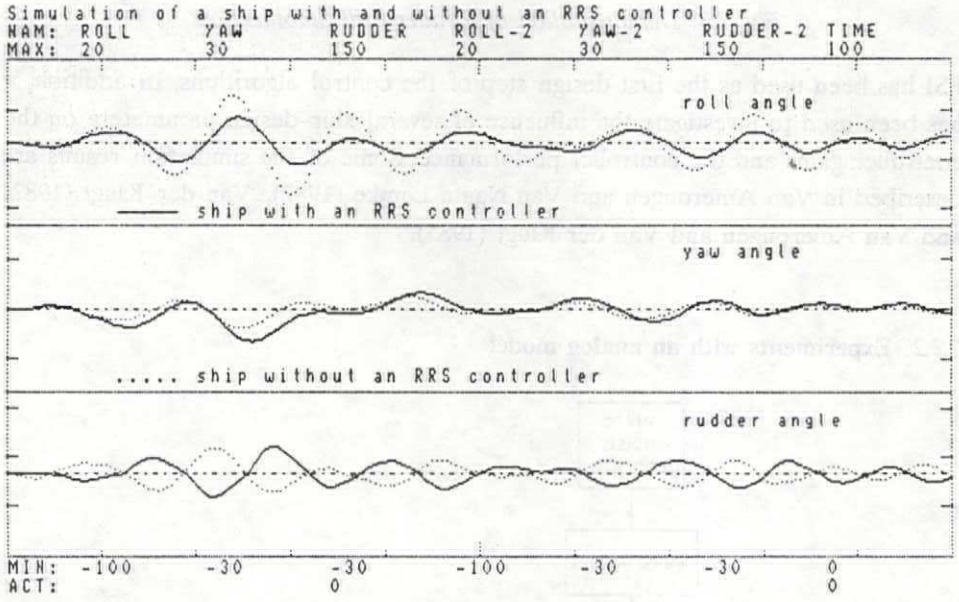

Fig. 7.2 Example of a PSI simulation

For demonstration purposes, PSI enables real-time simulation and the design of a dedicated display. Mattaar (1986) designed the display shown in Fig. 7.3.
The display on the left is based on the picture on the right taken during full-scale trials. It shows the view from the bridge of a ship through the window. In the display a beacon is placed on the horizon as a reference for the course-keeping performance. The ship's speed, the heading error and the rudder angle are shown as well.

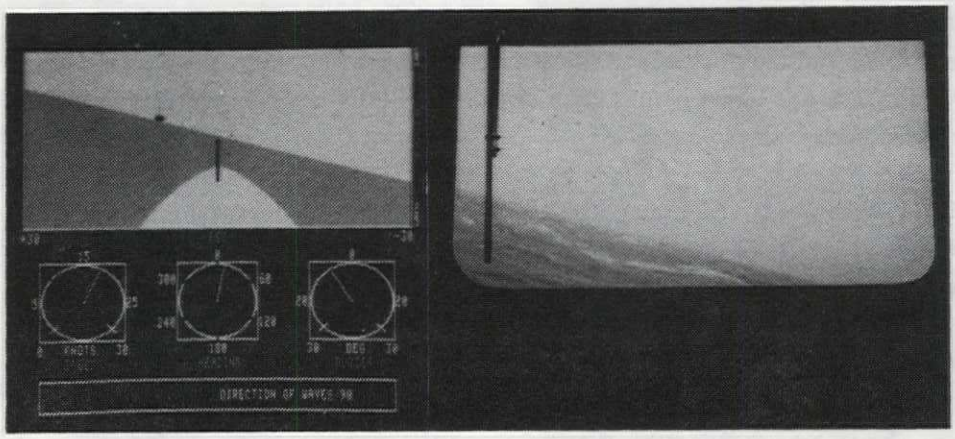

Fig. 7.3 Demonstration of Rudder Roll Stabilization

PSI has been used as the first design step of the control algorithms. In addition, it has been used to investigate the influence of several ship-design parameters on the controller gains and the controller performance. Some of the simulation results are described in Van Amerongen and Van Nauta Lemke (1982), Van der Klugt (1982) and Van Amerongen and Van der Klugt (1985).

7.2.2 Experiments with an analog model

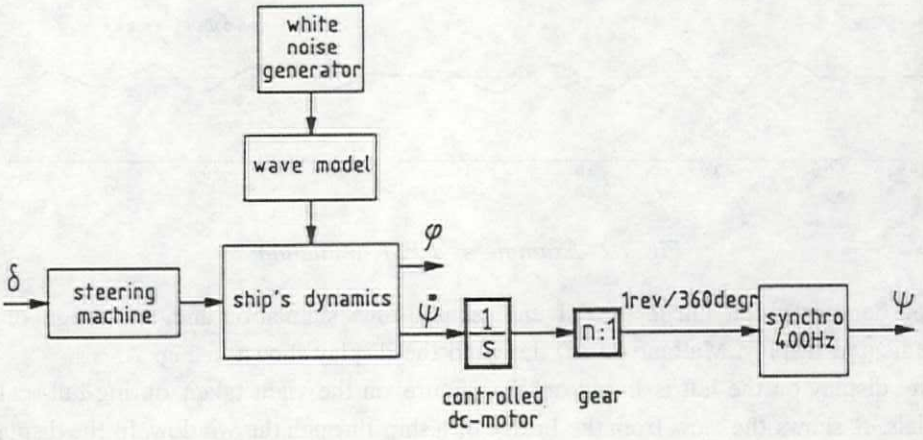

Fig. 7.4 The structure of the analog model

Schonebaum (1982) has designed a simple analog model of a ship. This model, modified by Albeda (1986), is comprised of a linear model of a ship, a model of the

steering machine and a simple shaping filter to generate the wave disturbances. The structure of the analog model is given in Fig. 7.4.
Several parameters of the analog model can be adjusted manually:

- the maximum rudder speed (5 to 25 deg/sec.)
- the maximum rudder angle (10 to 30 deg.)
- the speed of the ship (12 or 18 knots)

The following signals have been measured:

- the heading of the ship (synchro signal, $0 \leq \psi < 360$ deg.)
- the roll angle (analog signal, $-30 \leq \varphi \leq 30$ deg.)
- the rudder angle (analog signal, $-40 \leq \delta \leq 40$ deg.)

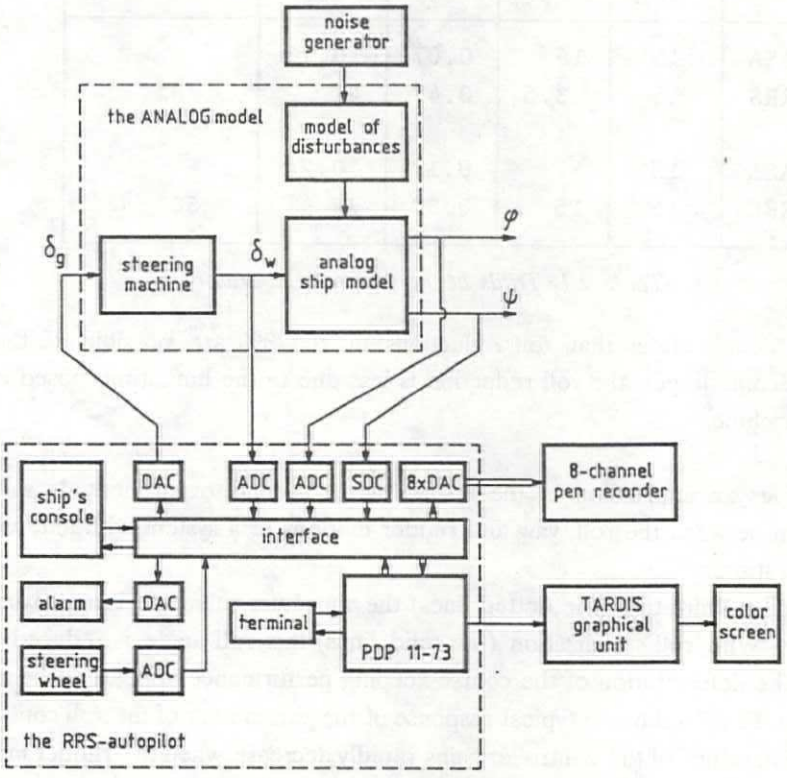

Fig. 7.5 Testing with the analog model

The RRS autopilot was coupled to the analog model of the ship, resulting in the configuration of Fig. 7.5. For monitoring purposes a color screen is available as well as an 8-channel pen recorder.

During the development of the RRS autopilot many experiments were carried out with the analog model. Table 7.1 gives the results of two typical experiments testing the RRS autopilot. These experiments give a comparison between the performance of the autopilot during course keeping only (referred to as ASA) and the performance of the autopilot if roll reduction is required (referred to as RRS).
During the first experiment the maximum roll angle was approximately 11 degrees. The maximum rudder speed was 15 deg/sec. while the maximum rudder angle was 22 degrees. During the second experiment the roll motions were increased.

Mode	$\dot{\delta}_{max}$	σ_φ^2	σ_ψ^2	σ_δ^2	Reduction
ASA	15	16	0.07	0.13	
RRS	15	3.5	0.47	41	78%
ASA	15	47	0.17	0.24	
RRS	15	15	0.30	74	68%

Table 7.1 Trials at the Control Laboratory

Table 7.1 demonstrates that roll reductions up to 78% are possible. If the roll motions become larger, the roll reduction is less due to the limitations posed by the steering machine.

Fig. 7.6 gives an impression of the results of the second experiment. It shows a comparison between the roll, yaw and rudder motions of a system with and without roll stabilization.
Without roll stabilization (the dotted lines) the maximum roll angle is approximately 22 degrees. With roll stabilization (the solid lines) this roll angle is reduced to 14 degrees. The deterioration of the course-keeping performance appears to be small. In addition, Fig. 7.6 shows a typical response of the parameters of the roll controller. The absolute values of the controller gains rapidly decrease when the rudder motions become too large, while they gradually increase when the rudder motions are low.

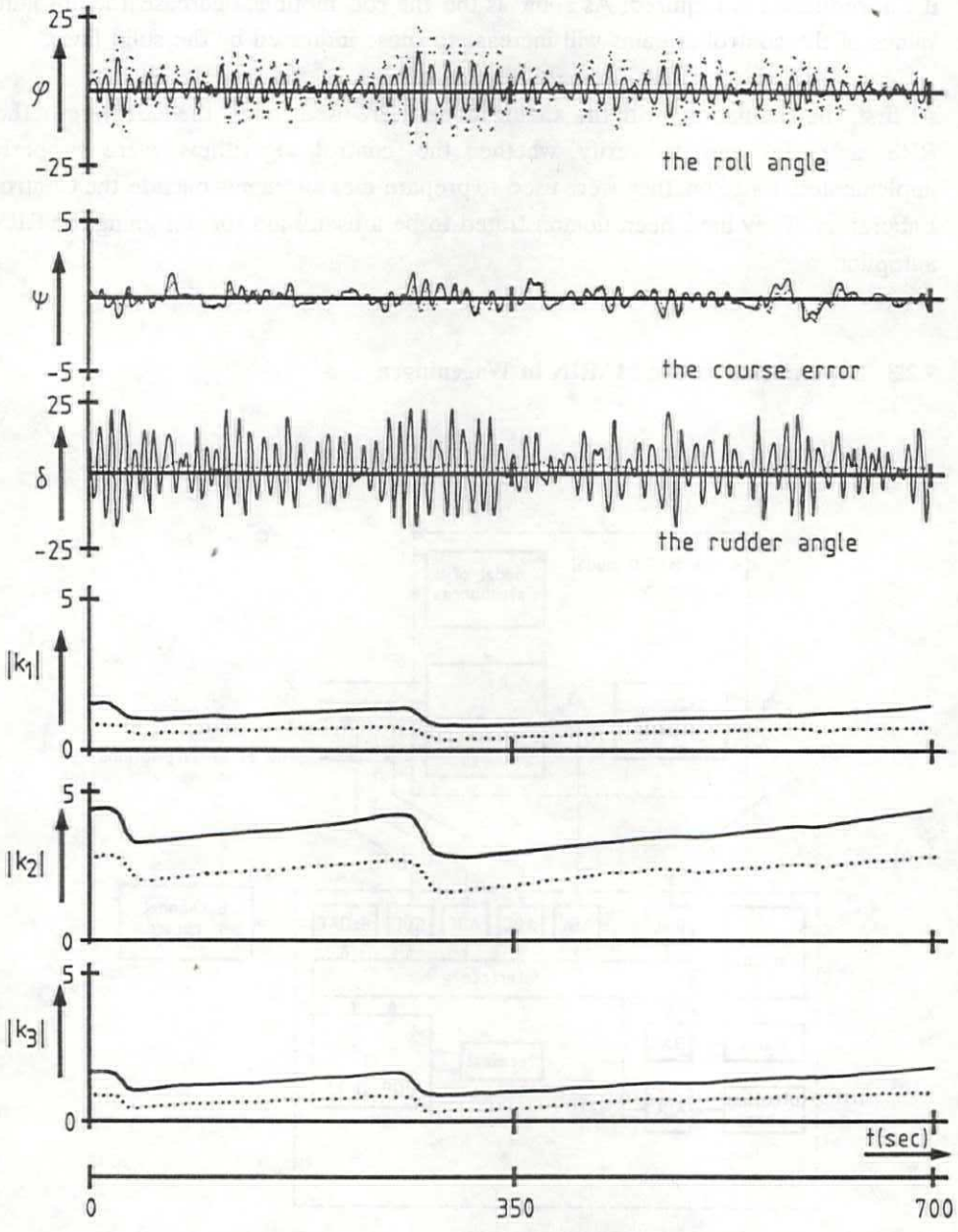

Fig. 7.6 A qualitative impression of roll, yaw and rudder motions

If no roll reduction is required the controller gains are also calculated (the dotted lines) although the resulting roll control action is not added to the set point of the

rudder. This guarantees that the proper control action will be obtained immediately if roll reduction is required. As soon as the the roll motions decrease the absolute values of the controller gains will increase to those indicated by the solid lines.

At first, the simulations with the analog model were used to test the hardware of the RRS autopilot and to verify whether the control algorithms were properly implemented. Later on, they were used to prepare measurements outside the Control Laboratory. They have been demonstrated to be a useful aid for designing the RRS autopilot.

7.2.3 Experiments at the MARIN in Wageningen

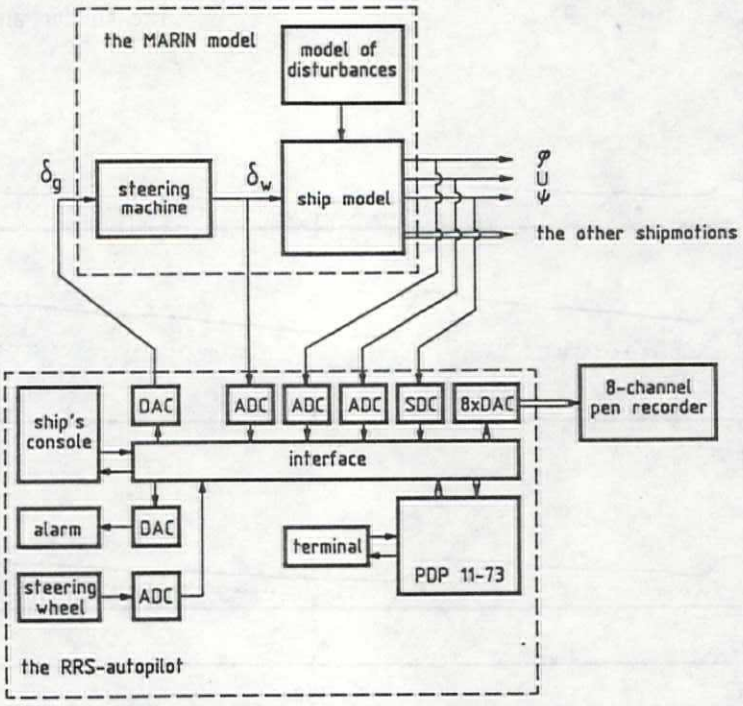

Fig. 7.7 Set-up of the simulation equipment during the MARIN trials.

The digital model as well as the analog model describe only the roll and the yaw motions. The potential influence of the other ship motions is not included.

The Royal Netherlands Navy made it possible to carry out two series of experiments where the laboratory realization of the RRS autopilot was coupled with the computer of the MARIN maneuvering simulator. The latter comprised an extensive model based on a hydrodynamic approach. This model describes the ship motions in all degrees of freedom, including most of the effects of the coupling of the motions. Fig. 7.7 shows the set-up of the simulation equipment during the second series of experiments. In Section 6.2 the RRS autopilot is discussed in more detail.

The first series of tests was carried out in September 1982 (Van Amerongen and Van der Klugt, 1982). No knowledge of the model implemented at the MARIN-computer was used for the controller design, except that it was known to be a model of a naval ship similar to the one used at the Control Laboratory.
The RRS autopilot used the roll angle, the roll rate, the rate of turn and the heading error as inputs. In addition, during these particular experiments the roll acceleration was used. The controller parameters were calculated in advance for all the required conditions. Therefore, different sets of controller parameters were available for different sea states, angles of incidence of the waves, ship's speeds, maximum rudder speeds etc. It had to be demonstrated that the controller settings, which were computed in advance, were also able to control the more complex MARIN mathematical model.

The following parameters were varied:

- Three different angles of incidence of the waves could be selected: 60, 90 or 120 degrees.
- Three combinations of maximum rudder angle and maximum rudder speed could be selected: 10/6, 20/15 and 30/20 (degrees / deg/sec.).
- In each situation the controller gains were selected as optimally computed before (nominal), 30 percent higher (+ nominal) and 30 percent lower (− nominal) in order to investigate the sensitivity to variations in the controller gains.

The experiments indicate that the rudder speed in particular is an important parameter which determines the maximum achievable roll reduction. Rudder speeds which are common at present (3 to 7 deg/s) are generally too low. A rudder speed of 15 deg/s appears to yield a considerable improvement.
Due to the limitations which are posed by the steering machine the system appears to be rather sensitive to variations made in the controller parameters. Settings which are too low are preferable to those which are too high.
Some of the results are summarized in Fig. 7.8.

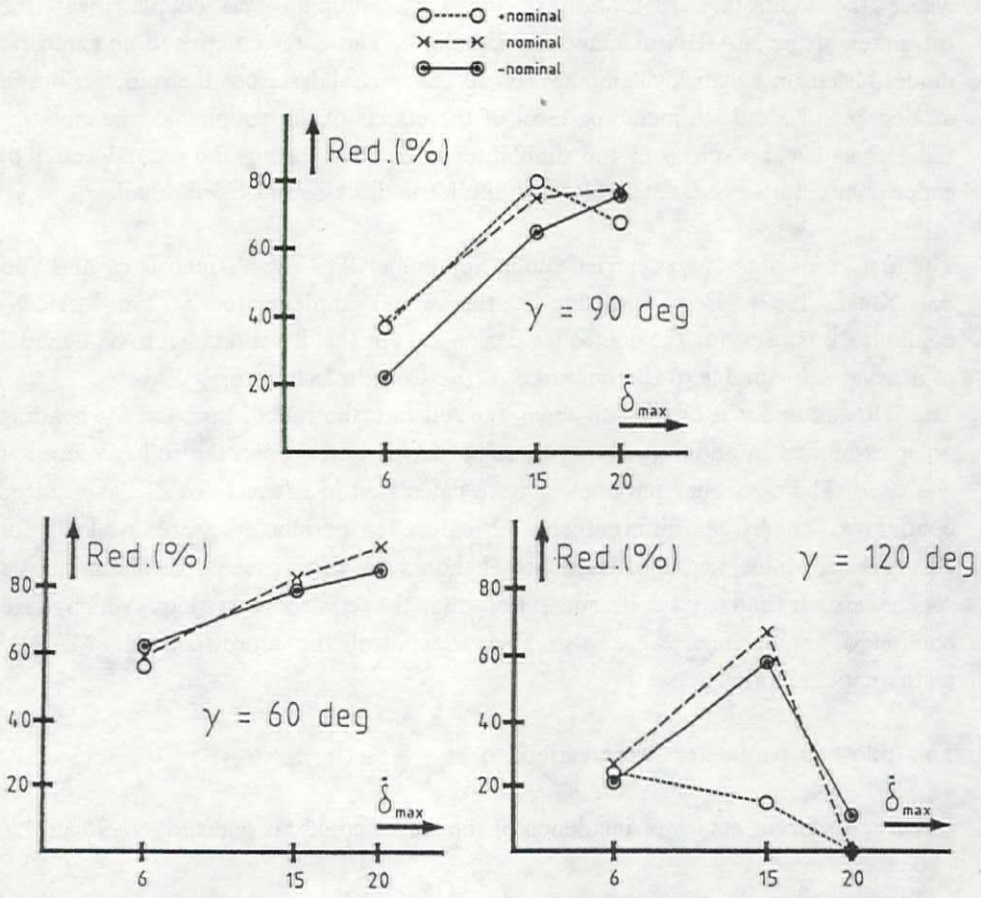

Fig. 7.8 Comparison of the controller performance for different conditions

A more detailed discussion of these and other results can be found in Van Amerongen and Van der Klugt (1982). All runs were successful except for those with a rudder speed of 20 deg/s and an angle of incidence of the waves of 120 degrees. During the latter the controller gains were apparently too high, causing the steering machine to saturate. This was caused by the differences between the simulated wave spectrum used at the Control Laboratory and that used during the MARIN experiments. The other experiments at the MARIN showed a good resemblence with those at the Control Laboratory.

With these results one can be confident that the mathematical models which are used at the Control Laboratory and at the MARIN are sufficiently reliable for use in developing an RRS autopilot.

The parameters of these models can easily be changed. Therefore, several experiments which were carried out at the Control Laboratory to investigate the influence of the model parameters on the ship's performance were repeated at the MARIN. The results of these experiments indicate that the rudder-induced roll moment and the maximum rudder speed, in particular, are important design parameters. A good roll reduction potential requires that the rudder-induced roll moment be large and that the maximum rudder speed be high.

The results of the MARIN trials as well as the results obtained during the full-scale trials (to be discussed in Section 7.4) convinced the Royal Netherlands Navy that roll stabilization by means of the rudder is an attractive alternative to fin stabilizers. Therefore, they decided to equip the ships which were at that time in the design phase with an RRS system. In addition, they used the results of the MARIN trials to change their ship design to improve the roll reduction potential of an RRS system. For instance, these ships will be equipped with a fast rudder.

The second series of tests with a MARIN model was carried out in August 1986 (Van Amerongen and Van der Klugt, 1987a). They were carried out with a new Laboratory realization of an RRS autopilot comprising the control algorithms given in Section 6. The aim of these experiments was to test the new RRS autopilot and to test the new adaptive mechanism.

Fig. 7.9 gives an impression of the lay-out of the equipment. In this figure the RRS autopilot, comprising the PDP 11/73 mini-computer, two monitors, an interface and a console, can be recognized.

It was not expected that the new autopilot would give a better performance than the old autopilot during the 1982 experiments because the latter comprised a roll controller based on gain scheduling which was optimally tuned for every other experiment. Furthermore, all the required state variables were measured.
The new autopilot comprises a roll controller which is adaptively tuned during an experiment. Contrary to the experiments with the old autopilot, the roll rate, the roll acceleration and the rate of turn were not measured. These signals were estimated by means of the methods which are introduced in Chapter 4 and Chapter 5. Therefore, it was expected that at best the new autopilot would give results similar to those of the old autopilot.

Fig. 7.9 Impression of the lay-out of the equipment

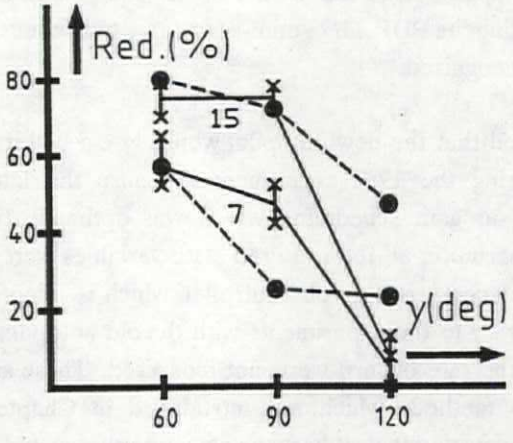

Fig. 7.10 Comparison of the performances of the old and the new controller algorithms.

Several experiments which were performed in 1982 were repeated. In Fig. 7.10 the results of these experiments are compared with the 1982 experiments for two

maximum rudder speeds: 7 deg/sec and 15 deg/sec. The solid lines indicate the performance of the new controller algorithms and the dashed lines the performance of the old algorithms under the same conditions.
Only if the waves are of a high frequency (γ = 120 deg) does the performance of the adaptive controller appear to be insufficient. However, in those conditions the roll motions remain below 4 degrees and the adaptation mechanism is at the point of switching itself off. If the rudder speed is low (7 deg/sec) while the ship encounters beam seas (γ = 90 deg) the adaptive controller gives a significantly better performance than the controller based on gain scheduling. From this comparison it can be concluded that for the conditions where roll stabilization is required the adaptive controller has a satisfactory performance.
Several additional experiments were carried out where the RRS autopilot controlled the mathematical model of another ship. In the following this ship will be referred to as ship 2 and the above ship as ship 1. Some of the results of the experiments with ship 2 are summarized in Fig. 7.11.

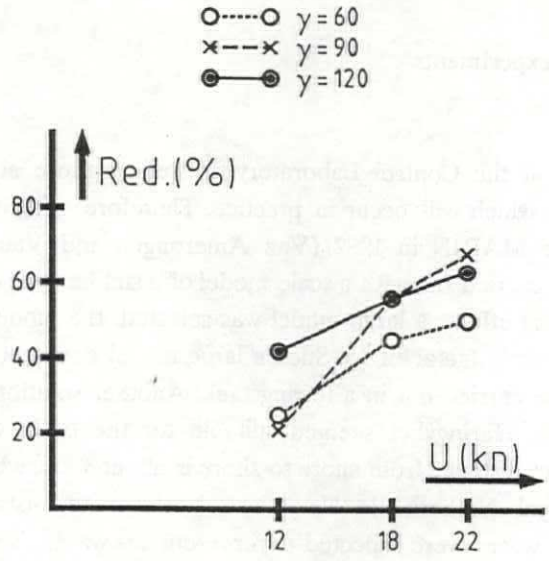

Fig. 7.11 The roll reduction as a function of the ship's speed

Fig. 7.11 gives the roll reduction of ship 2 as a function of the ship's speed for three angles of wave incidence: 60, 90 and 120 degrees. During all of the experiments roll reduction (up to 60%) appeared to be possible. However, ship 2 appears to be less suited to be equipped with a rudder roll stabilization system than ship 1.

Furthermore, several experiments have been carried out to test specific parts of the new autopilot algorithms. From these additional experiments the following conclusions can be drawn:

- The control model, proposed in Chapter 2, enables a better separation between high- and low-frequency rudder motions than the model proposed by Van Amerongen and Van Cappelle (1981).
- Increasing the maximum rudder speed of ship 2 from 15 deg/sec to 22 deg/sec will give 5 to 10% more roll reduction.
- With respect to the roll performance no relevant differences were noted between manual course keeping and automatic course keeping.

It was demonstrated that the experiments at the MARIN are a useful means to test the RRS autopilot. The results agreed quite well with those obtained with the analog and the digital models. Nevertheless, they led to some (small) modifications of the control algorithms. A more detailed discussion of the results of these experiments can be found in Van Amerongen and Van der Klugt (1987a).

7.3 Scale model experiments

The experiments at the Control Laboratory as well as those at the MARIN may conceal problems which will occur in practice. Therefore, after the first successful simulations at the MARIN in 1982 (Van Amerongen and Van der Klugt, 1982) experiments were carried out with a scale model of a similar type of ship. In order to diminish the scaling effects a large model was selected: the model had a length of 8 m., resulting in a scale factor of 15. Such a large model does not allow the planned type of trials to be carried out in a towing tank. Another solution had to be found. A location at the Haringvliet seemed suitable for the trials. Sufficient space is available there, the distance from shore to shore is about 3 km, while a measurement post of the Royal Netherlands Navy was available to install the equipment. Furthermore, the waves were expected to represent sea waves, which are scaled with respect to the model.
The experiments were carried out in close cooperation with the Royal Netherlands Navy, the MARIN and the Department of Maritime Technology of the Delft University of Technology.

Fig. 7.12 shows the set-up of the measurement equipment.

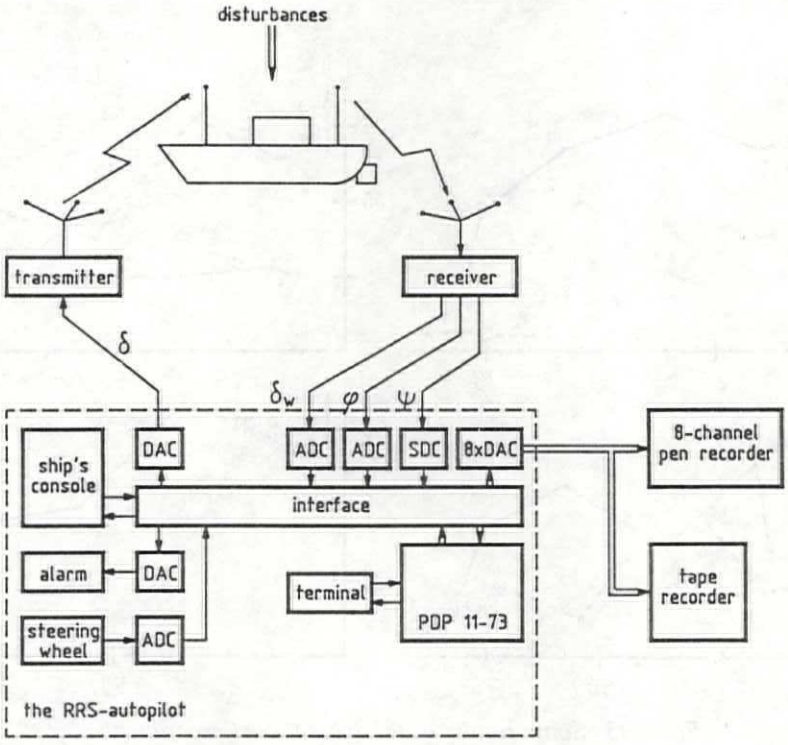

Fig. 7.12 Set-up of the measurement equipment

The model was propelled by a diesel engine and equipped with gyros and a speed log in order to measure the yaw, the yaw rate, the roll, the roll rate and the ship's speed. Radio communication channels were used to send these data to the shore, where the computer with the autopilot was installed. The desired rudder angle as well as the signals used to control the diesel engine were transmitted from the shore to the ship.

During the experiments several problems occurred which at first prevented successful trials:

- Rapidly changing weather conditions. Long periods without wind, periods with too much wind or with wind coming from an unfavorable direction made it difficult, sometimes even impossible, to carry out meaningful trials.
- Neither the scale model nor the wave spectrum represented accurately scaled replicas of respectively the naval ship and the sea wave spectrum.

Nevertheless, roll reduction could be demonstrated. This is indicated in Fig. 7.13

where the variances of the roll angle, the rudder angle and the course error as well as the roll reduction are shown as a function of time.

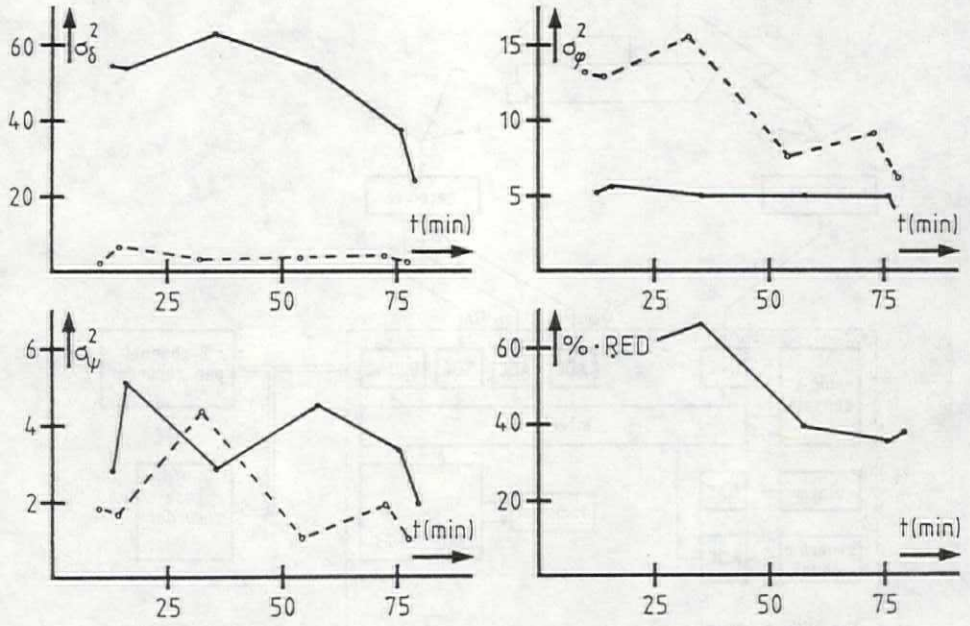

Fig. 7.13 Some results of the scale-model experiments.

In Fig. 7.13 the dashed lines connect the results which are obtained without a roll controller and the solid lines those obtained with a roll controller. This figure indicates that the maximum roll reduction was approximately 60%.
Furthermore, it shows that the roll variance changes in about one hour from 15 to 7. This demonstrates how rapidly the conditions may change. In this particular case, the wind force reduced while at the same time the wind direction changed.

Although the main purpose of carrying out the scale-model experiments (validation of the simulation results which were obtained at the Control Laboratory and at the MARIN) was not achieved, the experiments led to some important additions to the RRS autopilot, in particular the following:

- the AGC introduced in Section 5.3 and
- a high-pass filter which appeared to be necessary to remove low-frequency components on the measured roll signal.

The latter was the first step to obtain a proper separation of roll motions and yaw motions in the frequency domain. In addition, the experiments were a valuable learning experience which contributed for an important part to the success of the first full-scale experiments (see Section 7.4).
A more detailed discussion of these experiments can be found in Van Amerongen and Van der Klugt (1983).

Finally, Fig. 7.14 and Fig. 7.15 give an impression of these experiments.

Fig. 7.14 The scale-model

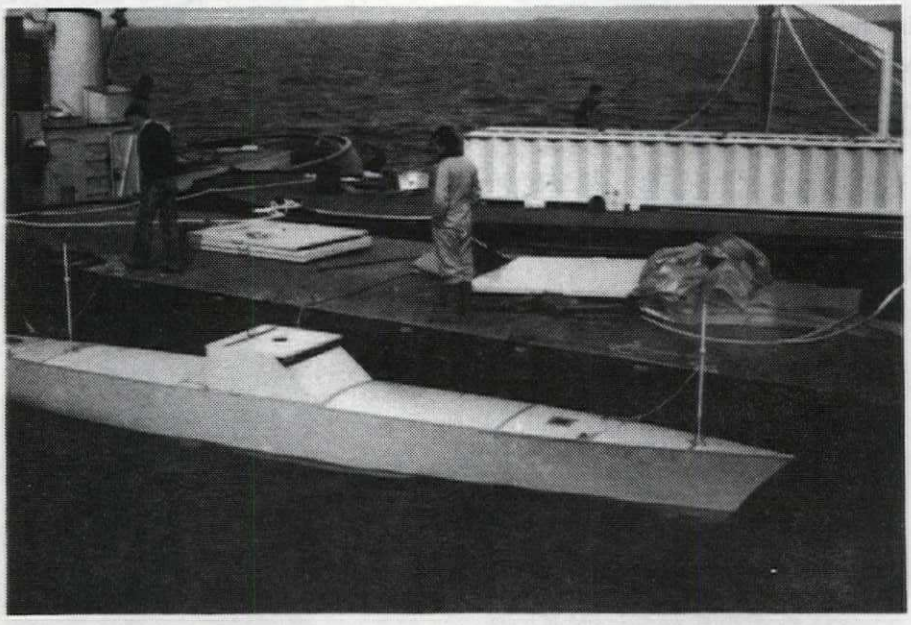

Fig. 7.15 The auxiliary equipment

7.4 Full-scale trials

The first full-scale trials were carried out in March 1983 on board a naval ship similar to the ship whose dynamics were simulated in the simulation experiments (Fig. 7.16).

The aim of these trials was

- to validate the simulation results,
- to test the AGC-mechanism (discussed in Section 5.4) and
- to compare RRS with the present fin-stabilizer system.

Fig. 7.16 Full-scale trials on board a naval ship

Fig. 7.17 shows the set-up of the equipment which was used during the experiments. Fig. 7.17 is basically similar to Fig. 7.7, which describes the set-up of the equipment used during the MARIN trials.

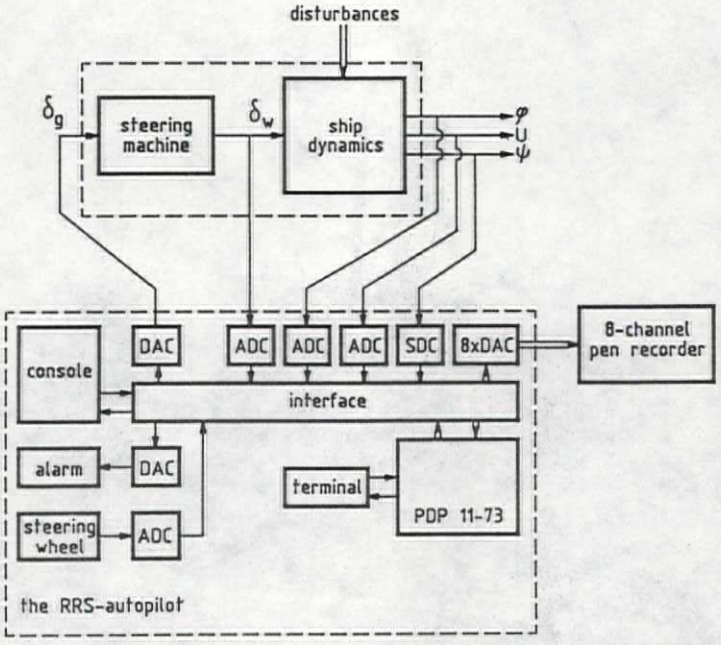

Fig. 7.17 Set-up of the measurement equipment

During these trials the following sensor information was available:

- the roll angle
- the heading
- the rudder angle
- the ship's speed

The roll rate, the roll acceleration and the rate of turn were estimated by means of filter structures similar to those introduced in Chapter 4.

The experiments were carried out on the North Sea and the circumstances appeared to be almost ideal for this kind of trial: wind forces up to Beaufort 10 (Van Amerongen, Van der Klugt and Pieffers, 1984). Fig. 7.18 gives a typical example of such an experiment. This figure shows a comparison of the ship's system and the RRS-autopilot with roll reduction (RRS) and without roll reduction (ASA). In this figure the roll reduction (64%) is clearly visible.

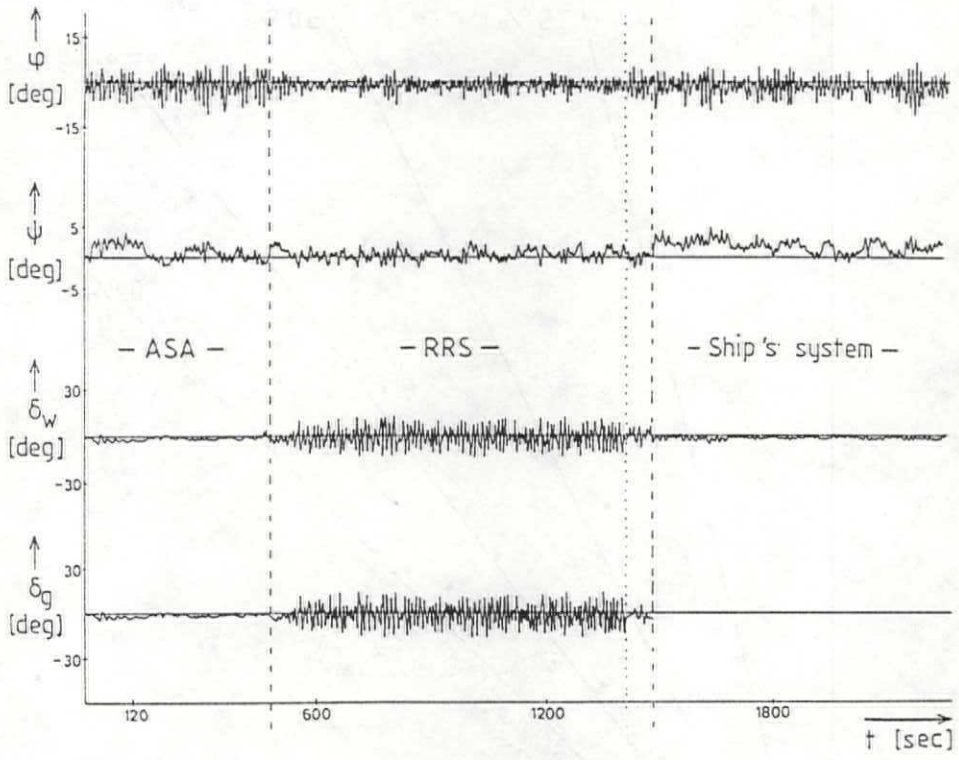

Fig. 7.18 A comparison between the RRS autopilot and the ship's autopilot

The RRS-autopilot performed well; the roll motions were reduced, sometimes as much as 60%. This is illustrated in Fig. 7.19, which gives a comparison between the roll motions of the ship with and without roll stabilization.

The figure demonstrates that roll reduction was obtained during almost all the runs except for a few which are indicated. The runs which are indicated by the number 1 were carried out during the first day and were of an experimental nature. During another series on the fourth day, indicated by the number 4, the combination of high speeds of the ship and following seas resulted in a low encounter frequency of the waves. Under these conditions rudder roll reduction is very difficult to obtain.

In addition, this figure demonstrates that significant reductions were measured for large roll motions as well. In judging these results it should be taken into account that the rudder of this ship has only a limited roll-reduction capability because of a relatively small maximum rudder speed of 7 deg/s.

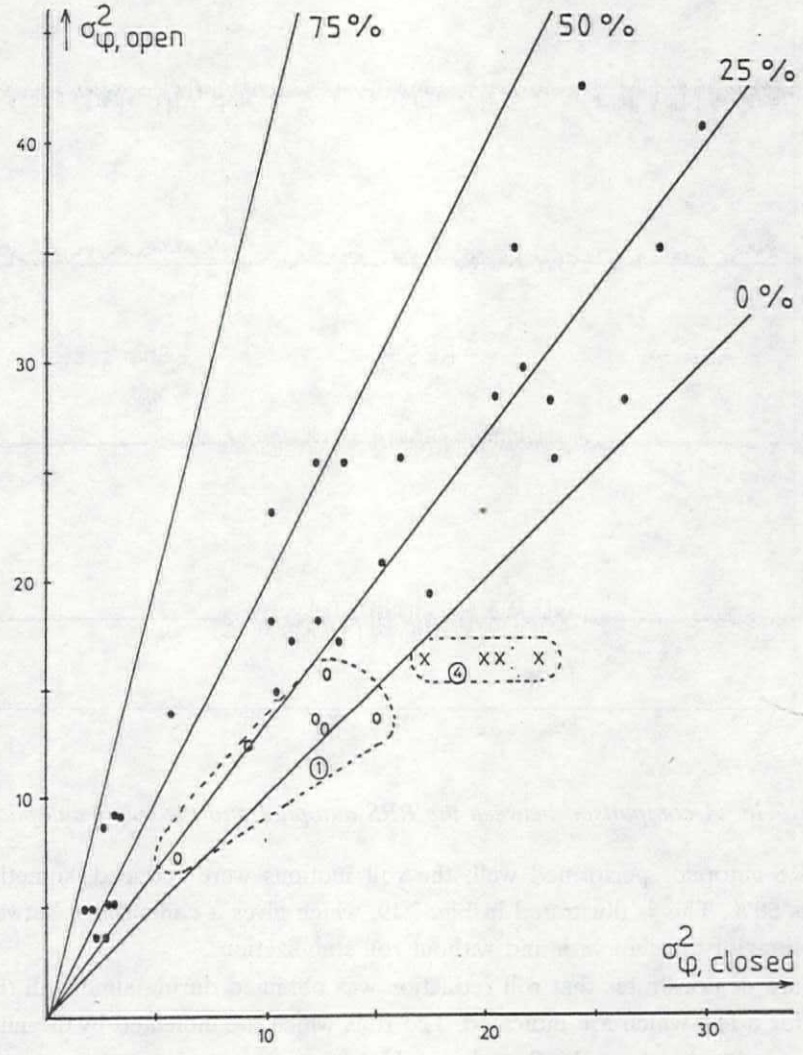

Fig. 7.19 Overview of the results of the first full-scale trials

Fig. 7.20 gives a comparison of the results of the MARIN experiments of 1982 (the solid lines) and these full-scale trials (denoted by "X").
It was not possible to determine a precise direction of the waves. Also, the frequency spectrum at sea was less sharp than during the simulations. Bearing these restrictions in mind the full-scale trials and the simulation experiments may be compared.

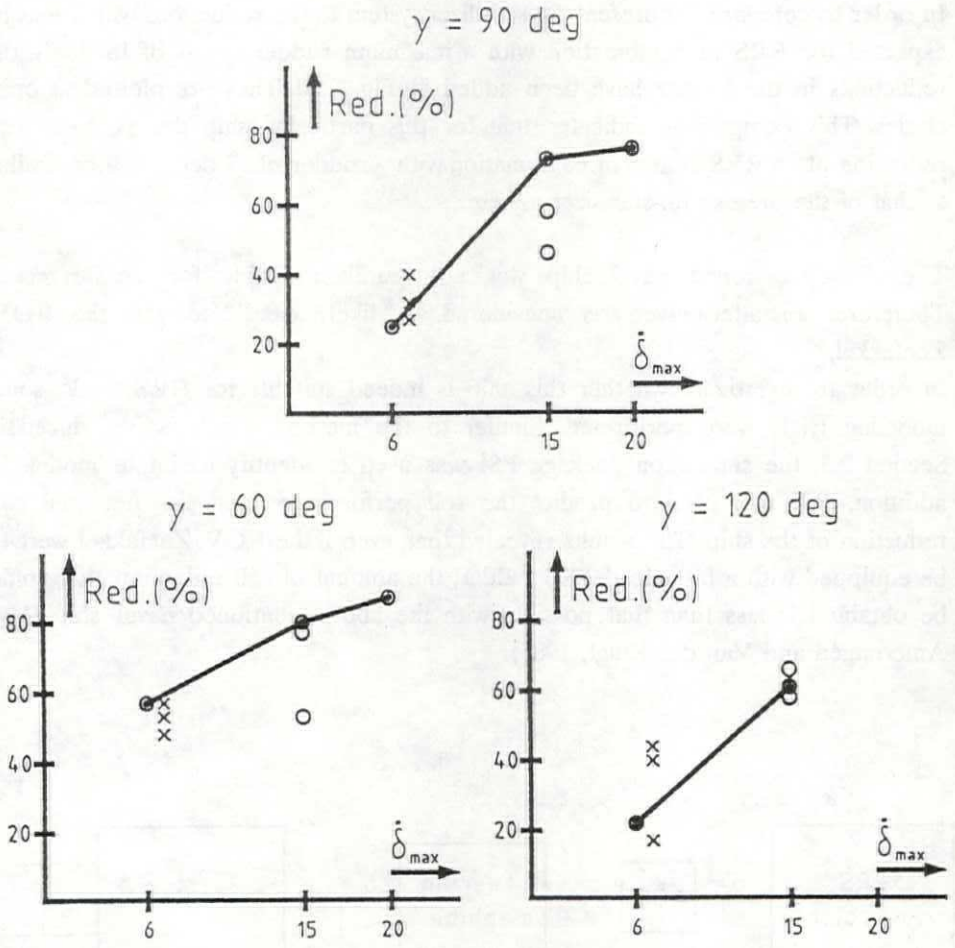

Fig. 7.20 A comparison between the results of the MARIN and the full-scale trials.

It can be observed that the roll reductions obtained during the full-scale trials are close to those obtained during the simulation experiments. In turn, this indicates that the simulation experiments at the MARIN and at the Control Laboratory are a good means of predicting the roll performance of a ship. Therefore, they may be used to anticipate the influence of changes in the ship's design. This result was used to answer two different questions:

1 What difference can be expected between the performance of a fin-stabilizer system and that of an RRS system in combination with a fast (15 deg/s.) rudder?
2 Is the ROV. Zeefakkel, the training vessel of the Royal Netherlands Naval College, suitable for carrying out RRS trials ?

In order to compare the present fin-stabilizer system to the reductions which may be expected for RRS in combination with a maximum rudder speed of 15 deg/s, the reductions in the former have been added in Fig. 7.20. They are plotted as open circles. This comparison indicates that for this particular ship the potential roll reduction of an RRS system in combination with a rudder of 15 deg/s. will be similar to that of the present fin-stabilizer system.

The above-mentioned naval ship was not readily available for measurements. Therefore, an alternative was considered. A likely candidate was the ROV. Zeefakkel.
In order to investigate whether this ship is indeed suitable for RRS trials, some modeling trials were performed. Similar to the method which is introduced in Section 2.5, the simulation package PSI was used to identify a simple model. In addition, PSI was used to predict the roll performance and the potential roll reduction of the ship. The results revealed that, even if the ROV. Zeefakkel were to be equipped with a fast (15 deg/s.) rudder, the amount of roll reduction that could be obtained is less than that possible with the above-mentioned naval ship (Van Amerongen and Van der Klugt, 1985).

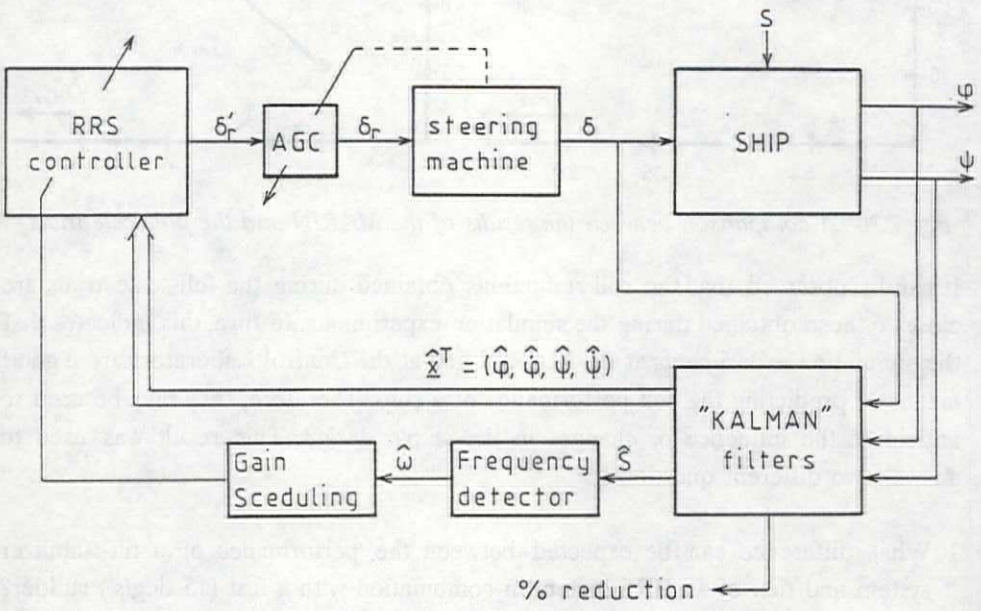

Fig. 7.21 The controller structure.

The next series of full-scale trials was planned for February and March 1984. However, due to a lack of wind the planned experiments could not be carried out and they had to be postponed until October 1984.
The controller algorithms were extended with an adaptation mechanism which was based on gain scheduling. The basic structure of the system is given in Fig. 7.21.
The simulation package PSI was used to calculate the controller parameters as a function of the *dominant frequency*, i.e. the peak in the frequency spectrum of the roll motions. This dominant frequency depends on, for instance, the frequency spectrum of the waves, the ship's speed and the natural roll frequency of the ship.

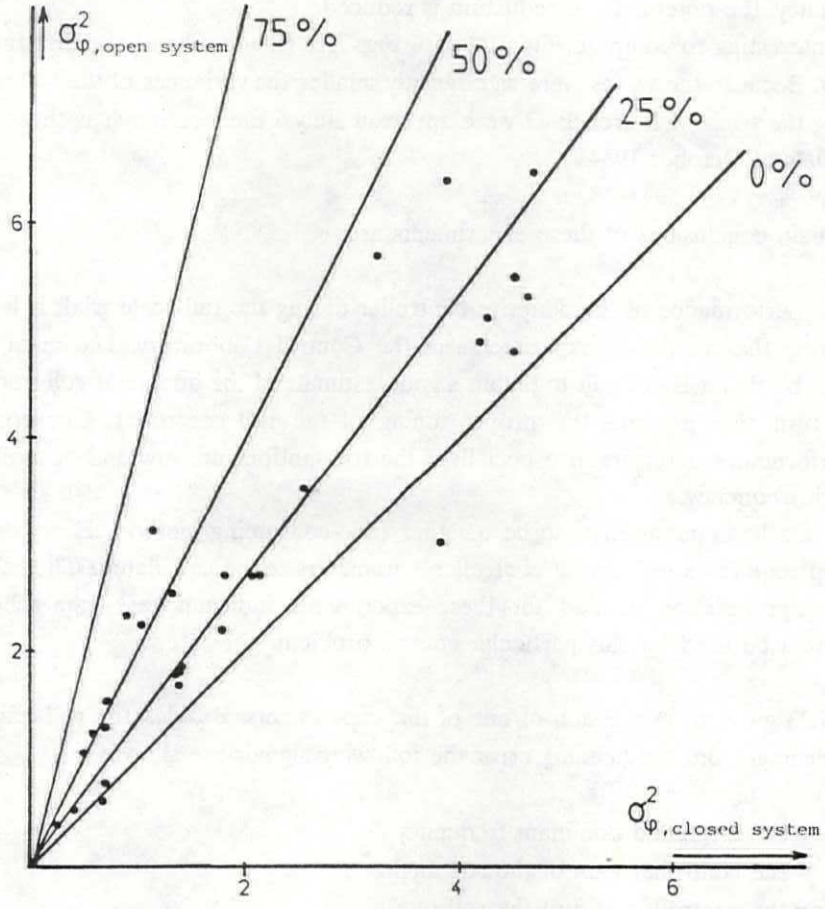

Fig. 7.22 Overview of the results of the full-scale trials

In addition, the automatic gain controller, introduced in Section 5.3, was used to

prevent the controller gains from becoming too large. The combination of the AGC and the on-line estimation of the dominant frequency represents an adaptation mechanism which automatically adjusts the roll controller to changing conditions.

The weather conditions appeared to be less favorable for RRS experiments than those during the first series of full-scale trials. Nevertheless, it was possible to test the new controller algorithms.
Fig. 7.22 gives an overview of some relevant results of these experiments.
During most of the experiments roll reduction could be demonstrated. A substantial roll reduction (more than 60%) is obtained if the peak of the wave spectrum approaches the natural roll frequency of the ship. If the disturbances are of a higher frequency, the potential roll reduction is reduced.
It is interesting to compare Fig. 7.22 with Fig. 7.19 (the results of the first full-scale trials). Because the waves were significantly smaller the variances of the roll motions during the trials of March 1983 were approximately 6 times as much as those during the trials of October 1984.

The main conclusions of these experiments are:

- The performance of the adaptive controller during the full-scale trials is less than during the simulation experiments at the Control Laboratory. The main reason may be that it is difficult to obtain a good estimate of the dominant roll frequency. In turn, this prevents the proper tuning of the roll controller. The controller performance deteriorates especially if the roll motions are low and of a relatively high frequency.
- Gain scheduling appears to be a rather time-consuming method. Every different ship requires a new set of controller parameters to be calculated. The relatively long preparation needed for these experiments indicates that gain scheduling cannot be used for this particular control problem.

Fig. 7.23 gives an impression of one of the experiments. Besides the roll angle, the rudder angle and the heading error the following signals are shown:

ω = the estimated dominant frequency
K_p = the controller gain of the roll angle
K_d = the controller gain of the roll rate
A = the automatic gain controller

During this particular experiment a considerable roll reduction was obtained (60%).

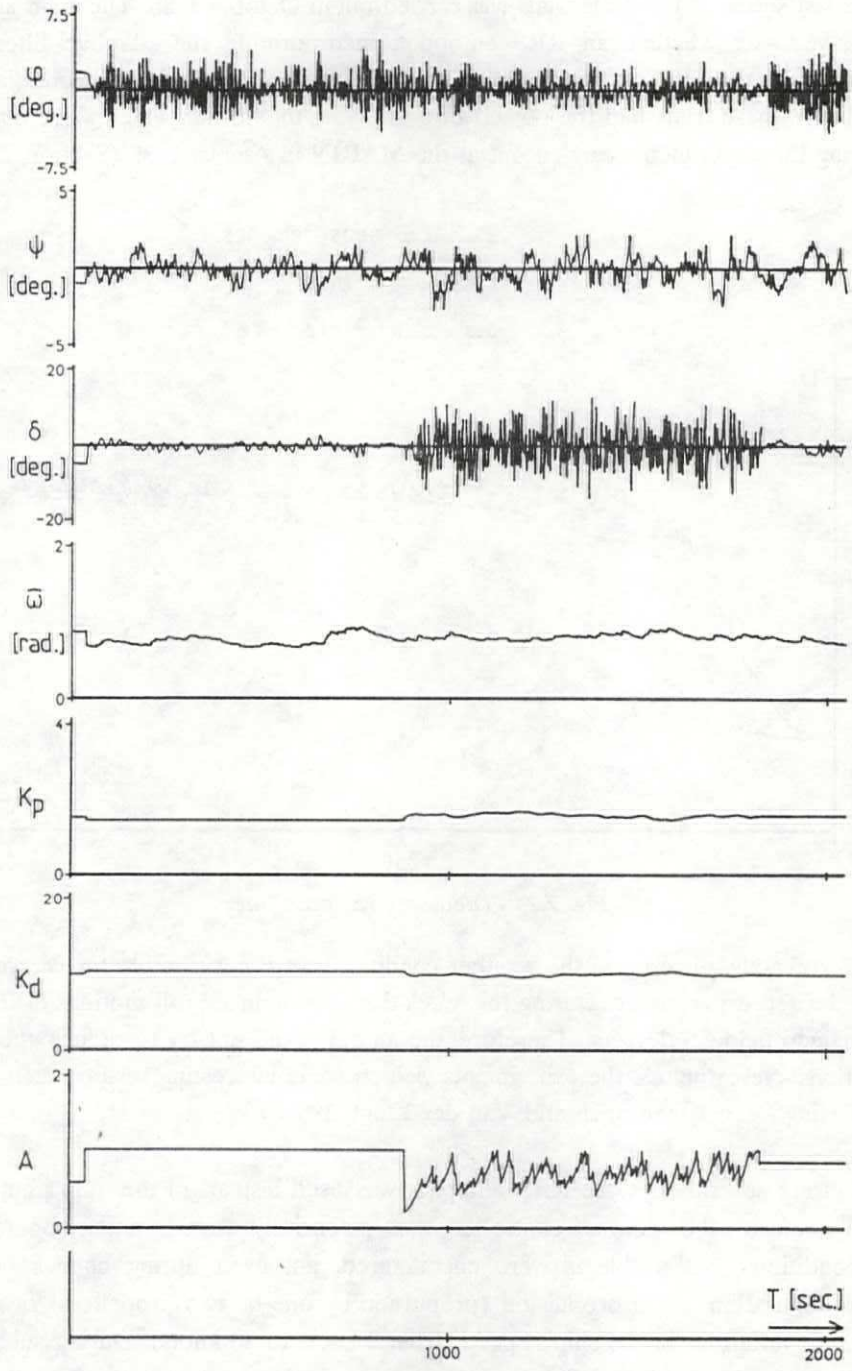

Fig. 7.23 An impression of one of the experiments

The last series of full-scale trials was carried out in October 1986. The main aim was to investigate whether an RRS autopilot, incorporating the adaptive filters and controllers given in Sections 5 and 6, behaves satisfactorily under all conditions. In addition, these trials had the objective of verifying the results which were obtained during the experiments carried out at the MARIN in August 1986 (Section 7.2.3).

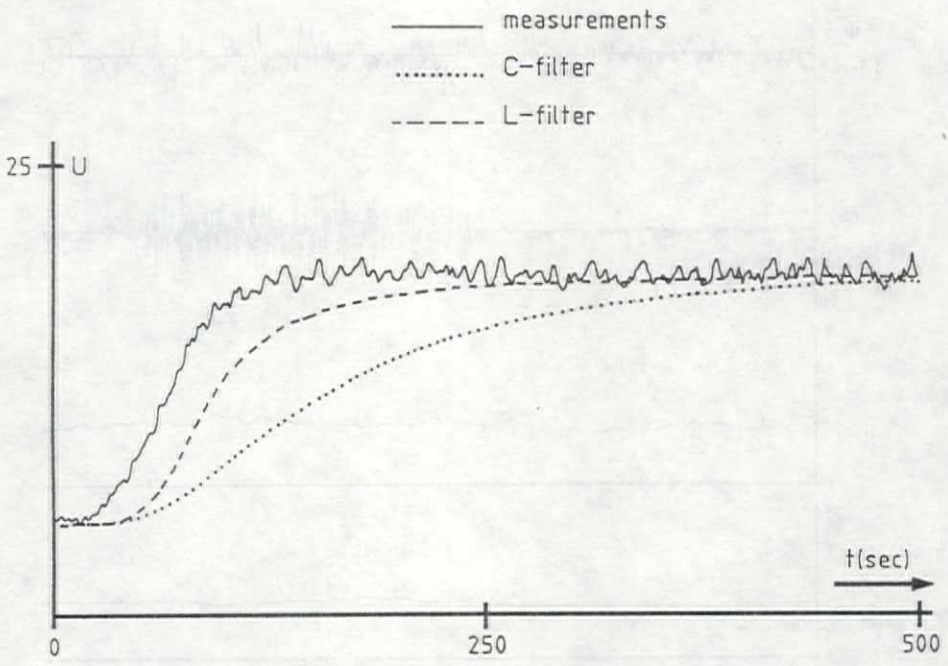

Fig. 7.24 The adaptive speed filter

Unfortunately, once again the weather conditions were not suitable for carrying out the desired experiments. During this week the wave-induced roll motions of the ship remained below 3 degrees. Therefore, the autopilot did not try to reduce these roll motions. Nevertheless, the experiments yielded some interesting results, such as the following (Van Amerongen and Van der Klugt, 1987b):

- During several days the RRS autopilot was used instead of the ship's autopilot. Therefore, the course controller was extensively tested under operational conditions. No problems were encountered, not even during changes in the configuration of the propulsion (propulsion by one or two propellers) or during large variations in the ship's speed (from 2 knots to 20 knots). During such large changes in propulsion it is common practice to change to manual control of the heading. The ship's officers appeared to be satisfied with the autopilot

- The adaptive speed filter could be tested as well. A typical response is shown in Fig. 7.24.

In this figure the upper signal represents the measured ship's speed. The adaptive filter, denoted as L-filter (see Section 5.6), is compared with a first-order low-pass filter, denoted as C-filter, with similar noise suppressing properties. The ship's propulsion is changed such that the ship's speed changes from 5 to 20 knots.
Fig. 7.24 demonstrates that the C-filter gives a considerable phase shift if the ship's propulsion changes. The adaptive filter is better able to follow the large change in the ship's speed.

Concluding remarks

The full-scale trials have contributed for an important part to the design of the RRS autopilot:

- They enabled the simulation results to be validated.
- During simulation experiments an adaptation mechanism based on gain scheduling gave good results. However, the full-scale trails demonstrated that in practice this method is not applicable.
- Some additions to the RRS autopilot which are important for a practical application were based on simply observing the autopilot performance and on discussions with the ship's officers.

Several attempts to carry out meaningful trials failed due to unfavorable weather conditions. A possible solution to this problem is to install the measurement equipment for a longer period on board a ship. In that case, the measurement crew may board the ship as soon as the weather forecasts are favorable for conducting the experiments.

8 REVIEW, CONCLUSIONS AND SUGGESTIONS

8.1 Review

This thesis reports the results of the cooperation between a university (more specifically, the Control Laboratory of the Faculty of Electrical Engineering of the Delft University of Technology), a government department (the Royal Netherlands Navy) and an industrial firm (the company Van Rietschoten & Houwens, Rotterdam).
A cooperation between different parties, each with its own wishes and resources, can only be successful if all parties involved benefit from the cooperation. This cooperation has led to the development of an advanced autopilot for ships. This autopilot provides a good course keeping and a course changing performance and is capable of reducing the roll motions by means of the rudder. The main contributions and benefits of the three parties are the following:

- The university has the necessary theoretical knowledge concerning modern filter and control techniques. In addition, many studies are interesting topics for work at a master's degree level.
  The university gained the opportunity to develop and test in practice modern control and filter techniques. They obtained additional knowledge concerning adaptive controllers and filters and their applicability. The results have been reported in many publications. In addition, many students had the opportunity to carry out challenging application-oriented undergraduate research.
- The Royal Netherlands Navy made it possible to carry out full-scale trials on board her ships as well as simulation experiments at the MARIN.
  Based on the results of the project the Royal Netherlands Navy was able to choose between roll reduction by means of fin stabilizers and roll reduction by means of the rudder. In addition, the Royal Netherlands Navy obtained knowledge of how to modify the design of a ship to increase its rudder-roll-reduction potential.
- The company Van Rietschoten & Houwens provided financial support and the ability to convert the ideas into a product.
  The firm gained the know-how necessary to build an advanced ship's autopilot. In addition, they obtained more generally applicable innovative knowledge concerning ship control systems and modern control techniques.

The cooperation between an industrial partner, a university and the Royal Netherlands Navy enabled the following series of experiments to be carried out:

1 *Full-scale modeling trials.*
At the start of the project full-scale modeling experiments on board a naval ship were carried out. These resulted in a simple mathematical model of the rudder-to-roll transfer and the rudder-to-yaw transfer.
2 *Digital simulations.*
With this model simulation experiments were carried out at the university. The results of these experiments indicated that roll reduction by means of the rudder may be a promising alternative to fin stabilizers. In addition, it was found that the limitations which are posed by the steering machine are of crucial importance with respect to the potential roll reduction.
3 *Simulations with an analog model.*
An initial version of the RRS autopilot was developed and tested by means of experiments with an analog model of the same naval ship. The roll controller settings were calculated off-line by means of the simulation package PSI. This resulted in a table of controller settings dependent on the frequency spectrum of the waves, the ship's speed and the limitations posed by the steering machine.
4 *Simulations at the MARIN.*
The Maritime Research Institute Netherlands in Wageningen has developed an extended mathematical model of a similar naval ship, based on a fundamental hydrodynamic approach. The Royal Netherlands Navy made it possible to carry out experiments where the prototype of the RRS autopilot was used to control this MARIN model. The results of these experiments confirmed the results which were obtained at the university.
5 *Scale model experiments.*
The MARIN in Wageningen also possessed an 8 meter long scale model of a similar naval ship. In cooperation with the Faculty of Maritime Technology of the Delft University of Technology this scale model was equipped with a diesel engine and radio equipment to enable remote control of the model. Subsequently, the Royal Netherlands Navy made it possible to carry out experiments at the Haringvliet, a sea arm in the South-West of the Netherlands. The main benefit of these trials was that several realistic situations were encountered which were not foreseen during the simultations. One of these was the constant roll angle, as a result of the wind force. It also became clear that even with a fast steering machine, saturation cannot be completely prevented. The steering problems related to these situations had to be solved by modifications of or extensions to the controller algorithms. This led, for instance, to the Automatic Gain Control (AGC)

mechanism which diminishes the deteriorating influence of the limitations which are posed by the steering machine of the ship.

6 *Full-scale trials.*
This first series of experiments was finished after carrying out full-scale trials, again on board a similar naval ship. This ship was equipped with a relatively slow rudder (7 deg/sec.). During weather conditions with wind forces up to Beaufort 10, the results obtained agreed with the simulation results obtained at the university and at the MARIN. In favorable conditions a roll reduction up to 60% appeared to be possible.

The results of these experiments convinced the Royal Netherlands Navy that RRS is an attractive alternative to fin stabilizers. Therefore, they decided to equip their new ships with an RRS system.

The roll controller settings depend on, for instance, the disturbances and the operational requirements. A ship's operator is not able to change these settings if either the disturbances or the operational requirements change. Therefore, a practical RRS system requires the controller to be adjusted automatically.
The first approach to solving this problem was based on a "natural" extension of the method used during the first series of experiments. The controller settings were determined off-line (by means of the simulation package PSI) as a function of the peak in the frequency spectrum of the disturbances. The AGC as well as a mechanism to estimate this peak in the frequency spectrum were added to the control algorithms. Although reasonable results were obtained during the simulation experiments with the analog model at the university as well as during the full-scale trials, this approach appeared to be unsatisfactory. It is rather time consuming and a different ship requires a different set of functions.

In this thesis a better method has been described. It is based on the LQG approach with additional automatic adjustment of the criterion parameters to changing operational conditions and requirements. The resulting controller algorithms were implemented in a second version of the RRS autopilot. Experiments similar to those mentioned above were carried out:

- To start with, the RRS autopilot was extensively tested during experiments at the university with an *analog model* of a naval ship.
- The Royal Netherlands Navy enabled several experiments to be carried out at the MARIN in Wageningen where the RRS autopilot was connected with the MARIN simulation computer. The results of these experiments agreed with the results of

the experiments at the university. Therefore, it has been concluded that the RRS autopilot is ready to be applied in practice.

- In October 1986 full-scale trials were carried out for an additional verification of this conclusion. For several days the prototype of the RRS autopilot was used instead of the ship's autopilot. Unfortunately, due to light weather the roll motions of the ship were too low to justify the need for roll reduction. Therefore, the roll controller was switched off automatically by the RRS autopilot. Only the forced roll mode and the course keeping properties could be tested.

During the design of the RRS autopilot several problems were encountered and subsequently solved:

The limitations which are posed by the ship's steering machine make the process to be controlled essentially non-linear. Therefore, in principle it is not allowed to use linear design techniques.

It is shown that the main problems are caused by the limited rudder speed; the limited rudder angle has less influence. The AGC mechanism can effectively remove the deteriorating influence of the limited rudder speed from the control loop. Therefore, linear techniques can be used to design the roll controller.

It is not possible to define one (quadratic) criterion which leads to a controller which is optimal under all conditions. The criterion depends on such factors as operational conditions and requirements.

An adaptation mechanism has been developed which is comprised of the automatic adjustment of the criterion parameters to changing operational conditions and requirements as well as the on-line calculation of the optimal controller settings. The method requires a model of the process to be known.
Basically, the criterion is adjusted by means of a set of rules which define the increment or decrement of a criterion parameter. This mechanism has some features which make it useful for application in practice:

- The rules consist of simple IF - THEN - ELSE statements.
- It is relatively simple to add new rules, including heuristic rules.
- It is possible to diminish the influence of a number of non-linear elements in the control loop by means of an appropriate rule.
- It is possible to define a non-linear control action by means of the appropriate rule(s).

- The adaptation mechanism can be applied to all controller designs based on a criterion.

An iterative method is proposed for the on-line calculation of the controller parameters. Means have been introduced to influence the rate of convergence of the method. Besides, the method introduced has an important practical advantage: it requires only a limited amount of computer time. This is guaranteed by taking advantage of the fact that the criterion parameters as well as the parameters of the model of the process change relatively slowly.

In a rudder-roll stabilization system only one input (the rudder) is available to control two outputs (yaw and roll). Decoupling of the yaw and the roll has to be obtained by restricting low-frequency rudder motions to control the yaw while high-frequency rudder motions are restricted to the roll reduction. With respect to the rudder-to-roll transfer, suppression of (large) low-frequency rudder motions is also necessary due to the non-minimum phase character of this transfer.

A new mathematical model of a ship is proposed which describes the rudder-to-roll transfer and the rudder-to-yaw transfer. This model has several advantages over the previous model (proposed by Van Amerongen and Van Cappelle, 1981):

- It gives a better fit during modeling experiments.
- The structure of the model more closely resembles the structure which will be found by means of a fundamental hydrodynamic approach.
- The structure of the model allows a better separation of the low-frequency and the high-frequency rudder motions.

This new mathematical model is used as the basis for two filters. The first filter suppresses the high-frequency components in the measured yaw motions. This results in a course-control action which comprises mainly low-frequency rudder motions. The second filter suppresses the low-frequency components in the measured roll motions. This results in a roll-control action which comprises mainly high-frequency rudder motions.

The parameters of the new mathematical model depend on the measured ship's speed, which may contain a substantial amount of undesired components.

In order to have a model which is sufficiently accurate, these components have to be removed from the measurements. A low-pass filter may be used to provide sufficient damping of the undesired components. However, such a filter causes an undesirably large phase lag during transients of the ship's speed. An adaptive filter is proposed, which provides a good damping of the undesired components without such a large phase lag.

The design of the controller algorithms will accumulate into a practical realization of an RRS autopilot. This poses restrictions on the potential adjustments to be carried out by an operator and emphasizes the need for robust algorithms.

Basically, the laboratory version of the RRS autopilot offers the following adjustments, to be carried out by an operator:

- the desired course,
- the allowed maximum rudder angle,
- the allowed maximum rate of turn,
- the choice between *manual* course control and *automatic* course control,
- the choice between *economic* steering and *accurate* steering,
- the choice between roll stabilization *ON*, roll stabilization *OFF* and Forced roll.

The autopilot adjusts itself to changing weather conditions. In addition, means are introduced to prohibit unrealistic settings or combinations of settings, such as:

- During manual course control the helmsman cannot generate high-frequency rudder motions.
- The roll control function is switched off automatically if the roll motions become low.

During experiments at the university as well as during experiments at the MARIN in Wageningen attempts were made to disrupt the performance of the adaptation mechanism by abruptly switching from a low to a high sea state or by abruptly changing the ship's speed. These experiments demonstrated the robustness of the controller.

8.2 Conclusions

In the course of the RRS project many experiments were carried out. From the results of these experiments several conclusions can be drawn, such as:

The potential roll reduction of an RRS system depends on the ship design.

This thesis poses several demands on the ship design to enable a substantial roll reduction. The most important design parameters are the influence of the rudder on the roll motions and the maximum rudder speed.
If the rudder has a large influence on the roll motions, it has a large roll-reduction potential as well. The rudder induced roll moment depends, for instance, on the ship's speed; the roll-reduction potential is small if the ship's speed is small and increases as the ship's speed increases.
It is shown that the required maximum rudder speed depends, for instance, on the natural roll frequency of the ship and the maximum effective rudder angle. Currently, sea-going ships have maximum rudder speeds between 2.5 and 7 deg/sec. Roll reduction by means of the rudder requires maximum rudder speeds from 15 to 25 deg/sec.

The potential roll reduction of an RRS system is comparable to the potential roll reduction of fin stabilizers.

Several advantages of an RRS system, such as the lower investment and the potential fuel savings, make roll stabilization by means of the rudder an attractive alternative to fin stabilizers. Compared with fin stabilizers, it may be relatively easy to equip an existing ship with an RRS system.

The method introduced to calculate the controller on line is sufficiently robust.

Several experiments have been carried out where the conditions and requirements were varied over a large range. However, the sensitivity of the control performance to these variations appeared to be low.

Besides the conclusions concerning the application and performance of an RRS system, several other conclusions could be drawn from the results of the experiments:

- The Interactive Simulation Package PSI, developed at the Control Laboratory of

the Faculty of Electrical Engineering of the Delft University of Technology, has been extensively used for identification as well as simulation purposes. It has proved to be a flexible and reliable aid for developing control systems.

- Although simulation experiments are a flexible means of designing and testing controllers, they do not make experiments in practice superfluous. Many ideas used in the controller design and the filter design are the result of observations made during full-scale trials on board the ship and during the scale-model experiments.

8.3 Suggestions

The RRS principle is ready to be applied in practice. The company van Rietschoten & Houwens is currently developing the RRS autopilot for a series of new ships of the Royal Netherlands Navy. Nevertheless, it may be possible to improve the performance of the underlying control algorithms.

- On-line estimation of the disturbances.
  With respect to the roll-controller design the roll moment which is caused by the disturbances is assumed to be white noise. In practice, the disturbing roll moment resembles colored noise. Some experiments indicate that the roll reduction increases if the coloring of the disturbances is taken into account in the control algorithms. However, the shape of the spectrum is not sufficiently known; in addition it changes with, for instance, a changing ship's speed, the angle of wave incidence and the sea state. By means of on-line identification of the disturbances the coloring of the system noise can be taken into account. This indicates that control techniques which are comprised of an identification mechanism (for instance self-tuning control) may provide a better performance. This is especially true if the frequency shape of the disturbances becomes pronounced.

- It may be advantageous to include the roll rate, the rate of turn and the sway velocity which is caused by the rudder in the criterion which is used to design the roll controller.
  The method posed to adjust the parameters of the roll criterion has been applied to adjust only one criterion parameter. Extension to include more parameters should be investigated. The method shows a close resemblence to knowledge-base and fuzzy-control techniques. These may offer a better adjustment mechanism.

- It may be advantageous to investigate the properties of the iterative method to calculate the controller gains and the filter gains.
  This method comprises the "L-matrix" which can be used to increase the convergence speed of the method or to obtain filtering properties. Some experimental results indicate that the elements of the L-matrix can be selected independently. In that case, it may be possible to increase a low convergence speed caused by large time constants of the process, while decreasing the computer time required for small time constants of the process.

- Adjust the weighting parameter of the yaw criterion similar to that of the roll criterion.
  The course controller designed has been based on a philosophy which resembles the approach proposed by Van Amerongen (1982). However, it would be worthwhile to investigate whether the method described in this thesis may improve the performance of the course controller. In addition, it may be advantageous to include information concerning the roll motions in the yaw criterion.

In this thesis, no attention has been paid to verifying the potential advantages of an RRS system over a fin-stabilizer system. The probability that an RRS system causes less drag, thus enabling a higher maximum speed of the ship or a lower fuel consumption, should be investigated. Moreover, the probability that an RRS system causes less underwater noise (important for naval ships) should be investigated.

APPENDICES

Appendix A

Calculation of a controller for a second-order process with a second-order shaping noise-filter

Let a process, described by the following state-space equations, be given:

$$\dot{\underline{x}}_p = A_p\underline{x}_p + B_p\underline{u}_p + D_p\underline{w}_p \qquad (A.1)$$

$$\underline{y}_p = C_p\underline{x}_p \qquad (A.2)$$

where

$$A_p = \begin{bmatrix} 0 & 1 \\ 0 & -1/\tau_r \end{bmatrix} \quad B_p = \begin{bmatrix} 0 \\ n_\delta/\tau_r \end{bmatrix} \quad C_p = \begin{bmatrix} 1 & 0 \\ 0 & 1 \end{bmatrix} \quad D_p = k_w/\tau_r$$

$$\underline{x}_p^T = (x_{p1},\ x_{p2}) \quad \underline{u}_p = \delta \quad \underline{y}_p^T = (y_{p1},\ y_{p2}) \quad \underline{w}_p = w_p$$

Let $\underline{w}_p$ be colored noise, described by the following second-order shaping filter:

$$\dot{\underline{x}}_f = A_f\underline{x}_f + D_f\underline{w}_f \qquad (A.3)$$

$$\underline{y}_f = C_f\underline{x}_f = \underline{w}_p \qquad (A.4)$$

where

$$A_f = \begin{bmatrix} 0 & 1 \\ -w_n^2 & -2z_nw_n \end{bmatrix} \quad C_f = \begin{bmatrix} 1 & 0 \\ 0 & 1 \end{bmatrix} \quad D_f = \begin{bmatrix} 0 \\ 1 \end{bmatrix}$$

$$\underline{x}_f^T = (x_{f1},\ x_{f2}) \qquad \underline{y}_f^T = (w_p,\ y_{f2})$$

$\underline{w}_f$ = w = white noise with zero mean

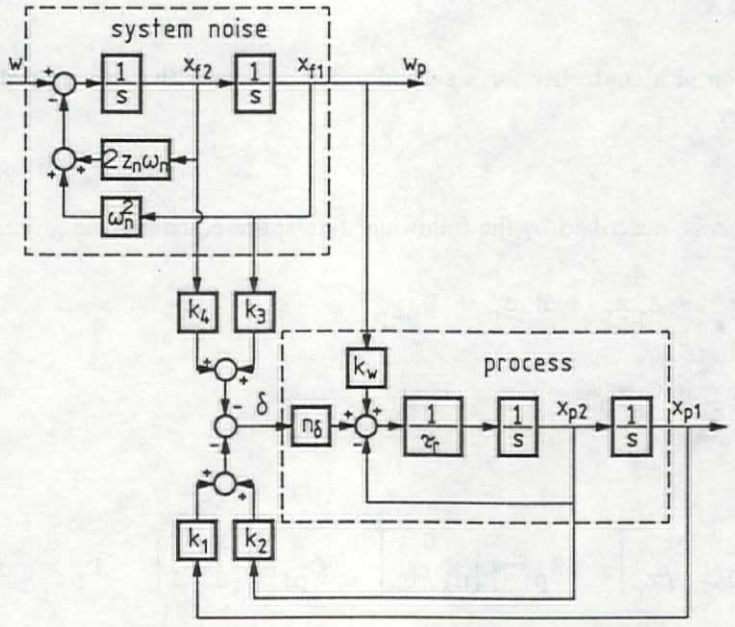

Fig. A.1 A block diagram of the process

Combining Eqs. (A.1), (A.2), (A.3) and (A.4) in one fourth-order model results in the process described by the following state-space equations:

$$\dot{\underline{x}} = A\underline{x} + B\underline{u} + D\underline{w} \qquad (A.5)$$

$$\underline{y} = C\underline{x} \qquad (A.6)$$

where

$$A = \begin{bmatrix} 0 & 1 & 0 & 0 \\ 0 & -1/\tau_r & k_w/\tau_r & 0 \\ 0 & 0 & 0 & 1 \\ 0 & 0 & -\omega_n^2 & -2z_n\omega_n \end{bmatrix} \quad B = \begin{bmatrix} 0 \\ n_\delta/\tau_r \\ 0 \\ 0 \end{bmatrix}$$

$$C = \begin{bmatrix} 1 & 0 & 0 & 0 \\ 0 & 1 & 0 & 0 \\ 0 & 0 & 1 & 0 \\ 0 & 0 & 0 & 1 \end{bmatrix} \qquad D = \begin{bmatrix} 0 \\ 0 \\ 0 \\ 1 \end{bmatrix}$$

$$\underline{x}^T = (x_{p1},\ x_{p2},\ x_{f1},\ x_{f2})$$

$$\underline{y}^T = (y_{p1},\ y_{p2},\ w_p,\ y_{f2})$$

$$\underline{u} = \delta$$

$$\underline{w} = w = \text{white noise with zero mean}$$

A block diagram of the process is given in Fig. A.1.

The optimal controller, with respect to criterion

$$J = \sum_{i=1}^{2} q_i E[y_i . y_i]/r + E[\delta . \delta] \qquad (A.7)$$

can be found to be:

$$\delta = -K^T \underline{x} \qquad (A.8)$$

The matrix K is found by simulation of the following "innovation process" (see Section 3.2):

$$\dot{P} = A^T P + PA + C^T Q C - PBK \qquad (A.9)$$

$$K = R^{-1} B^T P \qquad (A.10)$$

where

$$P = \begin{bmatrix} p_5 & p_6 & p_1 & p_2 \\ p_6 & p_7 & p_3 & p_4 \\ p_1 & p_3 & p_8 & p_9 \\ p_2 & p_4 & p_9 & p_{10} \end{bmatrix} \qquad Q = \begin{bmatrix} q_1/r & 0 & 0 & 0 \\ 0 & q_2/r & 0 & 0 \\ 0 & 0 & 0 & 0 \\ 0 & 0 & 0 & 0 \end{bmatrix}$$

This yields

$$K = (k_1\ k_2\ k_3\ k_4) = B^T P =$$

$$= (0\ \ n_\delta/\tau_r\ \ 0\ \ 0)\begin{bmatrix} p_5 & p_6 & p_1 & p_2 \\ p_6 & p_7 & p_3 & p_4 \\ p_1 & p_3 & p_8 & p_9 \\ p_2 & p_4 & p_9 & p_{10} \end{bmatrix}$$

or

$$k_1 = n_\delta p_6/\tau_r \qquad (A.11)$$

$$k_2 = n_\delta p_7/\tau_r \qquad (A.12)$$

$$k_3 = n_\delta p_3/\tau_r \qquad (A.13)$$

$$k_4 = n_\delta p_4/\tau_r \qquad (A.14)$$

$$C^T Q C = \begin{bmatrix} q_1/r & 0 & 0 & 0 \\ 0 & q_2/r & 0 & 0 \\ 0 & 0 & 0 & 0 \\ 0 & 0 & 0 & 0 \end{bmatrix}$$

$$PBK = \begin{bmatrix} p_5 & p_6 & p_1 & p_2 \\ p_6 & p_7 & p_3 & p_4 \\ p_1 & p_3 & p_8 & p_9 \\ p_2 & p_4 & p_9 & p_{10} \end{bmatrix}\begin{bmatrix} 0 \\ n_\delta/\tau_r \\ 0 \\ 0 \end{bmatrix}(k_1\ k_2\ k_3\ k_4) =$$

$$= \begin{bmatrix} n_\delta k_1 p_6/\tau_r & n_\delta k_2 p_6/\tau_r & n_\delta k_3 p_6/\tau_r & n_\delta k_4 p_6/\tau_r \\ n_\delta k_1 p_7/\tau_r & n_\delta k_2 p_7/\tau_r & n_\delta k_3 p_7/\tau_r & n_\delta k_4 p_7/\tau_r \\ n_\delta k_1 p_3/\tau_r & n_\delta k_2 p_3/\tau_r & n_\delta k_3 p_3/\tau_r & n_\delta k_4 p_3/\tau_r \\ n_\delta k_1 p_4/\tau_r & n_\delta k_2 p_4/\tau_r & n_\delta k_3 p_4/\tau_r & n_\delta k_4 p_4/\tau_r \end{bmatrix}$$

$$PA = \begin{bmatrix} p_5 & p_6 & p_1 & p_2 \\ p_6 & p_7 & p_3 & p_4 \\ p_1 & p_3 & p_8 & p_9 \\ p_2 & p_4 & p_9 & p_{10} \end{bmatrix}\begin{bmatrix} 0 & 1 & 0 & 0 \\ 0 & -1/\tau_r & k_w/\tau_r & 0 \\ 0 & 0 & 0 & 1 \\ 0 & 0 & -\omega_n^2 & -2z_n\omega_n \end{bmatrix} =$$

$$= \begin{bmatrix} 0 & p_5-p_6/\tau_r & k_w p_6/\tau_r-\omega_n^2 p_2 & p_1-2z_n\omega_n p_2 \\ 0 & p_6-p_7/\tau_r & k_w p_7/\tau_r-\omega_n^2 p_4 & p_3-2z_n\omega_n p_4 \\ 0 & p_1-p_3/\tau_r & k_w p_3/\tau_r-\omega_n^2 p_9 & p_8-2z_n\omega_n p_9 \\ 0 & p_2-p_4/\tau_r & k_w p_4/\tau_r-\omega_n^2 p_{10} & p_9-2z_n\omega_n p_{10} \end{bmatrix} = (A^T P)^T$$

and for the elements of P this yields:

$$\dot{p}_1 = -\omega_n^2 p_2 + (k_w - n_\delta k_3) p_6/\tau_r \qquad (A.15)$$

$$\dot{p}_2 = p_1 - 2z_n\omega_n p_2 - n_\delta k_4 p_6/\tau_r \qquad (A.15)$$

$$\dot{p}_3 = p_1 - p_3/\tau_r - \omega_n^2 p_4 + (k_w - n_\delta k_3) p_7/\tau_r \qquad (A.16)$$

$$\dot{p}_4 = p_3 + p_2 - (2z_n\omega_n - 1/\tau_r) p_4 - n_\delta k_4 p_7/\tau_r \qquad (A.17)$$

$$\dot{p}_5 = -n_\delta k_1 p_6/\tau_r + q_1/r \qquad (A.18)$$

$$\dot{p}_6 = p_5 - (1+n_\delta k_2) p_6/\tau_r \qquad (A.19)$$

$$\dot{p}_7 = 2p_6 - (2+n_\delta k_2) p_7/\tau_r + q_2/r \qquad (A.20)$$

$$\dot{p}_8 = (2k_w - n_\delta k_3) p_3/\tau_r - 2\omega_n^2 p_9 \qquad (A.21)$$

$$\dot{p}_9 = -n_\delta k_4 p_3/\tau_r + k_w p_4/\tau_r + p_8 - 2z_n\omega_n p_9 - \omega_n^2 p_{10} \qquad (A.22)$$

$$\dot{p}_{10} = -n_\delta k_4 p_4/\tau_r + 2p_9 - 4z_n\omega_n p_{10} \qquad (A.23)$$

Eqs. (A.21), (A.22) and (A.23) are not required to calculate the control gains k_1 to k_4. The innovation process, described by Eqs. (A.9) to (A.10), can be reformulated into the innovation process described by the following state-space equations:

$$L\dot{\underline{x}}_m = A_m \underline{x}_m + B_m \underline{u}_m \qquad (A.24)$$

$$\underline{y}_m = C_m \underline{x}_m \qquad (A.25)$$

where

$\underline{x}_m^T = (p_1, p_2, \ldots, p_7)$

= the elements of the upper two rows of P.

$\underline{y}_m^T = (k_1, k_2, k_3, k_4)$ = the elements of K.

$\underline{u}_m^T = (q_1/r, q_2/r)$

$$B_m^T = \left[\begin{array}{cccc:ccc} 0 & 0 & 0 & 0 & 1 & 0 & 0 \\ 0 & 0 & 0 & 0 & 0 & 0 & 1 \end{array}\right]$$

$$C_m = \left[\begin{array}{cccc:ccc} 0 & 0 & 0 & 0 & 0 & n_\delta/\tau_r & 0 \\ 0 & 0 & 0 & 0 & 0 & 0 & n_\delta/\tau_r \\ 0 & 0 & n_\delta/\tau_r & 0 & 0 & 0 & 0 \\ 0 & 0 & 0 & n_\delta/\tau_r & 0 & 0 & 0 \end{array}\right]$$

Finally, A_m =

$$\left[\begin{array}{cccccc:c} 0 & -\omega_n^2 & 0 & 0 & 0 & (k_w - n_\delta k_3)/\tau_r & 0 \\ 1 & -2z_n\omega_n & 0 & 0 & 0 & -n_\delta k_4/\tau_r & 0 \\ 1 & 0 & -1/\tau_r & 0 & 0 & 0 & (k_w - n_\delta k_3)/\tau_r \\ 0 & 1 & 0 & -2z_n\omega_n - 1/\tau_r & 0 & 0 & -n_\delta k_4/\tau_r \\ 0 & 0 & 0 & 0 & 0 & -n_\delta k_1/\tau_r & 0 \\ 0 & 0 & 0 & 0 & 1 & -(1+n_\delta k_2)/\tau_r & 0 \\ 0 & 0 & 0 & 0 & 0 & 2 & -(2+n_\delta k_2)/\tau_r \end{array}\right]$$

The steady-state outputs of the innovation process are the desired parameters of the optimal controller.

Note that the matrices B_m, C_m and A_m reduce to the submatrices which are indicated by the dotted lines if the system noise is white noise.

Appendix B

Calculation of the controller for a fifth-order process

Let a process, described by the following state-space equations, be given:

$$\dot{\underline{x}} = A\underline{x} + B\underline{u} + D\underline{w} \tag{B.1}$$

$$\underline{y} = C\underline{x} \tag{B.2}$$

where

$$A = \begin{bmatrix} 0 & 1 & 0 & 0 & 0 \\ -\omega_n^2 & -2z_n\omega_n & \omega_n^2 k_{vp} & 0 & 0 \\ 0 & 0 & -1/\tau_v & 0 & 0 \\ 0 & 0 & k_{vr}/\tau_r & -1/\tau_r & 0 \\ 0 & 0 & 0 & 1 & 0 \end{bmatrix} \quad B = \begin{bmatrix} 0 \\ \omega_n^2 k_{dp} \\ k_{dv}/\tau_v \\ k_{dr}/\tau_r \\ 0 \end{bmatrix}$$

$$D = \begin{bmatrix} 0 & 0 \\ \omega_n^2 & 0 \\ 0 & 0 \\ 0 & 1/\tau_r \\ 0 & 0 \end{bmatrix} \quad C = \begin{bmatrix} c_1 & 0 & 0 & 0 & 0 \\ 0 & c_2 & 0 & 0 & 0 \\ 0 & 0 & c_3 & 0 & 0 \\ 0 & 0 & 0 & c_4 & 0 \\ 0 & 0 & 0 & 0 & c_5 \end{bmatrix}$$

$$\underline{x}^T = (\varphi,\ \dot{\varphi},\ v',\ \dot{\psi},\ \psi)$$

$$\underline{u} = \delta$$

$$\underline{w}^T = (w_\varphi,\ w_\psi) \quad = \text{white noise with zero mean}$$

$$\underline{y}^T = (y_1,\ y_2,\ y_3,\ y_4,\ y_5)$$

A block diagram of the process is given in Fig. B.1.

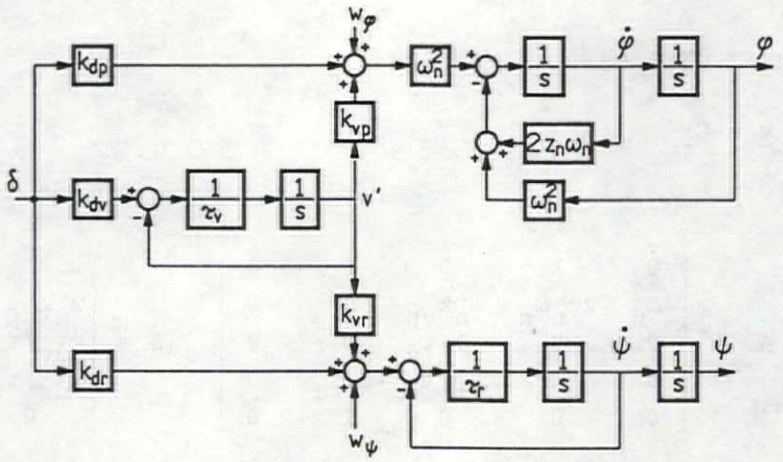

Fig. B.1 A block diagram of the process

The optimal controller with respect to criterion

$$J = \sum_{i=1}^{5} q_i E[y_i . y_i] + E[\delta . \delta] \qquad (B.3)$$

is described by

$$\delta = -K^T \underline{x} \qquad (B.4)$$

The matrix K is found by simulation of the following "innovation process" (see Section 3.2):

$$\dot{P} = A^T P + PA + C^T QC - PBK \qquad (B.5)$$

$$K = B^T P \qquad (B.6)$$

where

$$P = \begin{bmatrix} p_5 & p_6 & p_7 & p_1 & p_2 \\ p_6 & p_8 & p_9 & p_3 & p_4 \\ p_7 & p_9 & p_{10} & p_{11} & p_{12} \\ p_1 & p_3 & p_{11} & p_{13} & p_{14} \\ p_2 & p_4 & p_{12} & p_{14} & p_{15} \end{bmatrix} \qquad Q = \begin{bmatrix} q_1/r & 0 & 0 & 0 & 0 \\ 0 & q_2/r & 0 & 0 & 0 \\ 0 & 0 & q_3/r & 0 & 0 \\ 0 & 0 & 0 & q_4/r & 0 \\ 0 & 0 & 0 & 0 & q_5/r \end{bmatrix}$$

The steady-state outputs of this process are the desired controller parameters. Solving Eq. (B.5) yields

$$K = (k_1 \; k_2 \; k_3 \; k_4 \; k_5) = B^T P =$$

$$= (0 \quad \omega_n^2 k_{dp} \; k_{dv}/\tau_v \; k_{dr}/\tau_r \quad 0) \begin{bmatrix} p_5 & p_6 & p_7 & p_1 & p_2 \\ p_6 & p_8 & p_9 & p_3 & p_4 \\ p_7 & p_9 & p_{10} & p_{11} & p_{12} \\ p_1 & p_3 & p_{11} & p_{13} & p_{14} \\ p_2 & p_4 & p_{12} & p_{14} & p_{15} \end{bmatrix}$$

or

$$k_1 = \omega_n^2 k_{dp} p_6 + k_{dv} p_7/\tau_v + k_{dr} p_1/\tau_r \qquad (B.7)$$

$$k_2 = \omega_n^2 k_{dp} p_8 + k_{dv} p_9/\tau_v + k_{dr} p_3/\tau_r \qquad (B.8)$$

$$k_3 = \omega_n^2 k_{dp} p_9 + k_{dv} p_{10}/\tau_v + k_{dr} p_{11}/\tau_r \qquad (B.9)$$

$$k_4 = \omega_n^2 k_{dp} p_3 + k_{dv} p_{11}/\tau_v + k_{dr} p_{13}/\tau_r \qquad (B.10)$$

$$k_5 = \omega_n^2 k_{dp} p_4 + k_{dv} p_{12}/\tau_v + k_{dr} p_{14}/\tau_r \qquad (B.11)$$

$$C^T Q C = \begin{bmatrix} c_1^2 q_1/r & 0 & 0 & 0 & 0 \\ 0 & c_2^2 q_2/r & 0 & 0 & 0 \\ 0 & 0 & c_3^2 q_3/r & 0 & 0 \\ 0 & 0 & 0 & c_4^2 q_4/r & 0 \\ 0 & 0 & 0 & 0 & c_5 q_5^2/r \end{bmatrix}$$

$$PBK = \begin{bmatrix} p_5 & p_6 & p_7 & p_1 & p_2 \\ p_6 & p_8 & p_9 & p_3 & p_4 \\ p_7 & p_9 & p_{10} & p_{11} & p_{12} \\ p_1 & p_3 & p_{11} & p_{13} & p_{14} \\ p_2 & p_4 & p_{12} & p_{14} & p_{15} \end{bmatrix} \begin{bmatrix} 0 \\ \omega_n^2 k_{dp} \\ k_{dv}/\tau_v \\ k_{dr}/\tau_r \\ 0 \end{bmatrix} (k_1 \; k_2 \; k_3 \; k_4 \; k_5) =$$

$$\begin{bmatrix} \omega_n^2 k_{dp} k_1 p_6 + k_1 k_{dv} p_7/\tau_v + k_1 k_{dr} p_1/\tau_r & \omega_n^2 k_{dp} k_2 p_6 + k_2 k_{dv} p_7/\tau_v + k_2 k_{dr} p_1/\tau_r \\ \omega_n^2 k_{dp} k_1 p_8 + k_1 k_{dv} p_9/\tau_v + k_1 k_{dr} p_3/\tau_r & \omega_n^2 k_{dp} k_2 p_8 + k_2 k_{dv} p_9/\tau_v + k_2 k_{dr} p_3/\tau_r \\ \omega_n^2 k_{dp} k_1 p_9 + k_1 k_{dv} p_{10}/\tau_v + k_1 k_{dr} p_{11}/\tau_r & \omega_n^2 k_{dp} k_2 p_9 + k_2 k_{dv} p_{10}/\tau_v + k_2 k_{dr} p_{11}/\tau_r \\ \omega_n^2 k_{dp} k_1 p_3 + k_1 k_{dv} p_{11}/\tau_v + k_1 k_{dr} p_{13}/\tau_r & \omega_n^2 k_{dp} k_2 p_3 + k_2 k_{dv} p_{11}/\tau_v + k_2 k_{dr} p_{13}/\tau_r \\ \omega_n^2 k_{dp} k_1 p_4 + k_1 k_{dv} p_{12}/\tau_v + k_1 k_{dr} p_{14}/\tau_r & \omega_n^2 k_{dp} k_2 p_4 + k_2 k_{dv} p_{12}/\tau_v + k_2 k_{dr} p_{14}/\tau_r \end{bmatrix}$$

$$= \begin{bmatrix} \omega_n^2 k_{dp} k_3 p_6 + k_3 k_{dv} p_7/\tau_v + k_3 k_{dr} p_1/\tau_r & \omega_n^2 k_{dp} k_4 p_6 + k_4 k_{dv} p_7/\tau_v + k_4 k_{dr} p_1/\tau_r & \omega_n^2 k_{dp} k_5 p_6 + k_5 k_{dv} p_7/\tau_v + k_5 k_{dr} p_1/\tau_r \\ \omega_n^2 k_{dp} k_3 p_8 + k_3 k_{dv} p_9/\tau_v + k_3 k_{dr} p_3/\tau_r & \omega_n^2 k_{dp} k_4 p_8 + k_4 k_{dv} p_9/\tau_v + k_4 k_{dr} p_3/\tau_r & \omega_n^2 k_{dp} k_5 p_8 + k_5 k_{dv} p_9/\tau_v + k_5 k_{dr} p_3/\tau_r \\ \omega_n^2 k_{dp} k_3 p_9 + k_3 k_{dv} p_{10}/\tau_v + k_3 k_{dr} p_{11}/\tau_r & \omega_n^2 k_{dp} k_4 p_9 + k_4 k_{dv} p_{10}/\tau_v + k_4 k_{dr} p_{11}/\tau_r & \omega_n^2 k_{dp} k_5 p_9 + k_5 k_{dv} p_{10}/\tau_v + k_5 k_{dr} p_{11}/\tau_r \\ \omega_n^2 k_{dp} k_3 p_3 + k_3 k_{dv} p_{11}/\tau_v + k_3 k_{dr} p_{13}/\tau_r & \omega_n^2 k_{dp} k_4 p_3 + k_4 k_{dv} p_{11}/\tau_v + k_4 k_{dr} p_{13}/\tau_r & \omega_n^2 k_{dp} k_5 p_3 + k_5 k_{dv} p_{11}/\tau_v + k_5 k_{dr} p_{13}/\tau_r \\ \omega_n^2 k_{dp} k_3 p_4 + k_3 k_{dv} p_{12}/\tau_v + k_3 k_{dr} p_{14}/\tau_r & \omega_n^2 k_{dp} k_4 p_4 + k_4 k_{dv} p_{12}/\tau_v + k_4 k_{dr} p_{14}/\tau_r & \omega_n^2 k_{dp} k_5 p_4 + k_5 k_{dv} p_{12}/\tau_v + k_5 k_{dr} p_{14}/\tau_r \end{bmatrix}$$

$$PA = (A^T P)^T = \begin{bmatrix} p_5 & p_6 & p_7 & p_1 & p_2 \\ p_6 & p_8 & p_9 & p_3 & p_4 \\ p_7 & p_9 & p_{10} & p_{11} & p_{12} \\ p_1 & p_3 & p_{11} & p_{13} & p_{14} \\ p_2 & p_4 & p_{12} & p_{14} & p_{15} \end{bmatrix} \begin{bmatrix} 0 & 1 & 0 & 0 & 0 \\ -\omega_n^2 & -2z_n\omega_n & \omega_n^2 2k_{vp} & 0 & 0 \\ 0 & 0 & -1/\tau_v & 0 & 0 \\ 0 & 0 & k_{vr}/\tau_r & -1/\tau_r & 0 \\ 0 & 0 & 0 & 1 & 0 \end{bmatrix}$$

$$= \begin{bmatrix} -\omega_n^2 p_6 & p_5 - 2z_n\omega_n p_6 & \omega_n^2 k_{vp} p_6 - p_7/\tau_v + k_{vr} p_1/\tau_r & p_2 - p_1/\tau_r & 0 \\ -\omega_n^2 p_8 & p_6 - 2z_n\omega_n p_8 & \omega_n^2 k_{vp} p_8 - p_9/\tau_v + k_{vr} p_3/\tau_r & p_4 - p_3/\tau_r & 0 \\ -\omega_n^2 p_9 & p_7 - 2z_n\omega_n p_9 & \omega_n^2 k_{vp} p_9 - p_{10}/\tau_v + k_{vr} p_{11}/\tau_r & p_{12} - p_{11}/\tau_r & 0 \\ -\omega_n^2 p_3 & p_1 - 2z_n\omega_n p_3 & \omega_n^2 k_{vp} p_3 - p_{11}/\tau_v + k_{vr} p_{13}/\tau_r & p_{14} - p_{13}/\tau_r & 0 \\ -\omega_n^2 p_4 & p_2 - 2z_n\omega_n p_4 & \omega_n^2 k_{vp} p_4 - p_{12}/\tau_v + k_{vr} p_{14}/\tau_r & p_{15} - p_{14}/\tau_r & 0 \end{bmatrix}$$

This yields for the elements of P:

$$\dot{p}_1 = -(1+k_4 k_{dr}) p_1/\tau_r + p_2 - \omega_n^2 p_3 - \omega_n^2 k_{dp} k_4 p_6 - k_4 k_{dv} p_7/\tau_v \qquad (B.12)$$

$$\dot{p}_2 = -k_5 k_{dr} p_1/\tau_r - \omega_n^2 p_4 - \omega_n^2 k_{dp} k_5 p_6 - k_5 k_{dv} p_7/\tau_v \quad (B.13)$$

$$\dot{p}_3 = p_1 - (2z_n\omega_n + (1+k_4 k_{dr})/\tau_r) p_3 + p_4 - \omega_n^2 k_{dp} k_4 p_8 - k_4 k_{dv} p_9/\tau_v \quad (B.14)$$

$$\dot{p}_4 = p_2 - k_5 k_{dr} p_3/\tau_r - 2z_n\omega_n p_4 - \omega_n^2 k_{dp} k_5 p_8 - k_5 k_{dv} p_9/\tau_v \quad (B.15)$$

$$\dot{p}_5 = -k_1 k_{dr} p_1/\tau_r - \omega_n^2 (2+k_{dp} k_1) p_6 - k_1 k_{dv} p_7/\tau_v + c_1^2 q_1/r \quad (B.16)$$

$$\dot{p}_6 = -k_2 k_{dr} p_1/\tau_r + p_5 - (2z_n\omega_n + \omega_n^2 k_{dp} k_2) p_6 - k_2 k_{dv} p_7/\tau_v - \omega_n^2 p_8 \quad (B.17)$$

$$\dot{p}_7 = (k_{vr} - k_3 k_{dr}) p_1/\tau_r + \omega_n^2 (k_{vp} - k_{dp} k_3) p_6 - (1+k_3 k_{dv}) p_7/\tau_v - \omega_n^2 p_9 \quad (B.18)$$

$$\dot{p}_8 = -k_2 k_{dr} p_3/\tau_r + 2p_6 - (4z_n\omega_n + \omega_n^2 k_{dp} k_2) p_8 - k_2 k_{dv} p_9/\tau_v + c_2^2 q_2/r \quad (B.19)$$

$$\dot{p}_9 = (k_{vr} - k_3 k_{dr}) p_3/\tau_r + p_7 + \omega_n^2 (k_{vp} - k_{dp} k_3) p_8 - (2z_n\omega_n + (1+k_3 k_{dv})/\tau_v) p_9 \quad (B.20)$$

$$\dot{p}_{10} = \omega_n^2 (2k_{vp} - k_{dp} k_3) p_9 - (2+k_3 k_{dv}) p_{10}/\tau_v + (2k_{vr} - k_3 k_{dr}) p_{11}/\tau_r + c_3^2 q_3/r \quad (B.21)$$

$$\dot{p}_{11} = \omega_n^2 k_{vp} p_3 - \omega_n k_{dp}^2 k_4 p_9 - k_4 k_{dv} p_{10}/\tau_v - (1/\tau_v + 1/\tau_r + k_4 k_{dr}/\tau_r) p_{11} + p_{12} + k_{vr} p_{13}/\tau_r \quad (B.22)$$

$$\dot{p}_{12} = \omega_n^2 k_{vp} p_4 - \omega_n k_{dp}^2 k_5 p_9 - k_5 k_{dv} p_{10}/\tau_v - k_5 k_{dr} p_{11}/\tau_r - p_{12}/\tau_v + k_{vr} p_{14}/\tau_r \quad (B.23)$$

$$\dot{p}_{13} = -\omega_n^2 k_{dp} k_4 p_3 - k_4 k_{dv} p_{11}/\tau_v - (2+k_4 k_{dr}) p_{13}/\tau_r + 2p_{14} + c_4^2 q_4/r \quad (B.24)$$

$$\dot{p}_{14} = -\omega_n^2 k_{dp} k_5 p_3 - k_5 k_{dv} p_{11}/\tau_v - k_5 k_{dr} p_{13}/\tau_r - p_{14}/\tau_r + p_{15} \quad (B.25)$$

$$\dot{p}_{15} = -\omega_n^2 k_{dp} k_5 p_4 - k_5 k_{dv} p_{12}/\tau_v - k_5 k_{dr} p_{14}/\tau_r + c_5^2 q_5/r \quad (B.26)$$

It is possible to reformulate this result into the process described by the following state-space equations:

$$\dot{\underline{x}}_m = A_m \underline{x}_m + B_m \underline{u}_m \quad (B.27)$$

$$\underline{y}_m = C_m \underline{x}_m \quad (B.28)$$

where

$$\underline{x}_m^T = (p_1, p_2, \ldots, p_{15})$$

$$\underline{y}_m^T = (k_1, k_2, \ldots, k_5)$$

$$\underline{u}_m^T = (q_1/r, q_2/r, \ldots, q_5/r)$$

$$B_m^T = \begin{bmatrix} 0 & 0 & 0 & 0 & c_1^2 & 0 & 0 & 0 & 0 & 0 & 0 & 0 & 0 & 0 & 0 \\ 0 & 0 & 0 & 0 & 0 & 0 & 0 & c_2^2 & 0 & 0 & 0 & 0 & 0 & 0 & 0 \\ 0 & 0 & 0 & 0 & 0 & 0 & 0 & 0 & 0 & c_3^2 & 0 & 0 & 0 & 0 & 0 \\ 0 & 0 & 0 & 0 & 0 & 0 & 0 & 0 & 0 & 0 & 0 & 0 & c_4^2 & 0 & 0 \\ 0 & 0 & 0 & 0 & 0 & 0 & 0 & 0 & 0 & 0 & 0 & 0 & 0 & 0 & c_5^2 \end{bmatrix}$$

$$C_m^T = \begin{bmatrix} K_{dr}/T_r & 0 & 0 & 0 & 0 \\ 0 & 0 & 0 & 0 & 0 \\ 0 & K_{dr}/T_r & 0 & w_n^2 K_{dp} & 0 \\ 0 & 0 & 0 & 0 & w_n^2 K_{dp} \\ 0 & 0 & 0 & 0 & 0 \\ w_n^2 K_{dp} & 0 & 0 & 0 & 0 \\ K_{dv}/T_v & 0 & 0 & 0 & 0 \\ 0 & w_n^2 K_{dp} & 0 & 0 & 0 \\ 0 & K_{dv}/T_v & w_n^2 K_{dp} & 0 & 0 \\ 0 & 0 & K_{dv}/T_v & 0 & 0 \\ 0 & 0 & K_{dr}/T_r & K_{dv}/T_v & o \\ 0 & 0 & 0 & 0 & K_{dv}/T_v \\ 0 & 0 & 0 & K_{dr}/T_r & 0 \\ 0 & 0 & 0 & 0 & K_{dr}/T_r \\ 0 & 0 & 0 & 0 & 0 \end{bmatrix}$$

And finally A_m equals:

$$
\begin{bmatrix}
-(1+k_4k_{dr})/\tau_r & 1 & -\omega_n^2 & 0 & 0 & -\omega_n^2k_{dp}k_4 & -k_4k_{dv}/\tau_v & 0 \\
-k_5k_{dr}/\tau_r & 0 & -2z_n\omega_n-(1+k_4k_{dr})/\tau_r & -\omega_n^2 & 0 & -\omega_n^2k_{dp}k_5 & -k_5k_{dv}/\tau_v & 0 \\
1 & 0 & -k_5k_{dr}/\tau_r & 1 & 0 & 0 & 0 & -\omega_n^2k_{dp}k_4 \\
0 & 0 & 0 & -2z_n\omega_n & 0 & 0 & 0 & -\omega_n^2k_{dp}k_5 \\
-k_1k_{dr}/\tau_r & 0 & 0 & 0 & 0 & -\omega_n^2(2+k_{dp}k_1) & -k_1k_{dv}/\tau_v & 0 \\
-k_2k_{dr}/\tau_r & 0 & 0 & 0 & 1 & -(2z_n\omega_n+\omega_n^2k_{dp}k_2) & -k_2k_{dv}/\tau_v & -\omega_n^2 \\
(k_{vr}-k_3k_{dr})/\tau_r & 0 & 0 & 0 & 0 & \omega_n^2(k_{vp}-k_{dp}k_3) & -(1+k_3k_{dv})/\tau_v & 0 \\
0 & 0 & -k_2k_{dr}/\tau_r & 0 & 0 & 2 & 0 & -(4z_n\omega_n+\omega_n^2k_{dp}k_2) \\
0 & 0 & (k_{vr}-k_3k_{dr})\tau_r & 0 & 0 & 0 & 1 & \omega_n^2(k_{vp}-k_{dp}k_3) \\
0 & 0 & 0 & 0 & 0 & 0 & 0 & 0 \\
0 & 0 & \omega_n^2k_{vp} & 0 & 0 & 0 & 0 & 0 \\
0 & 0 & 0 & \omega_n^2k_{vp} & 0 & 0 & 0 & 0 \\
0 & 0 & -\omega_n^2k_{dp}k_4 & 0 & 0 & 0 & 0 & 0 \\
0 & 0 & -\omega_n^2k_{dp}k_5 & 0 & 0 & 0 & 0 & 0 \\
0 & 0 & 0 & -\omega_n^2k_{dp}k_5 & 0 & 0 & 0 & 0
\end{bmatrix}
$$

$$
\begin{bmatrix}
0 & 0 & 0 & 0 & 0 & 0 & 0 \\
0 & 0 & 0 & 0 & 0 & 0 & 0 \\
-k_4k_{dv}/\tau_v & 0 & 0 & 0 & 0 & 0 & 0 \\
-k_5k_{dv}/\tau_v & 0 & 0 & 0 & 0 & 0 & 0 \\
0 & 0 & 0 & 0 & 0 & 0 & 0 \\
0 & 0 & 0 & 0 & 0 & 0 & 0 \\
-\omega_n^2 & 0 & 0 & 0 & 0 & 0 & 0 \\
-k_2k_{dv}/\tau_v & 0 & 0 & 0 & 0 & 0 & 0 \\
-2z_n\omega_n-(1+k_3k_{dv})/\tau_v & 0 & 0 & 0 & 0 & 0 & 0 \\
\omega_n^2(2k_{vp}-k_{dp}k_3) & -(2+k_3k_{dv})/\tau_v & (2k_{vr}-k_{dr}k_3)/\tau_r & 0 & 0 & 0 & 0 \\
-\omega_n^2k_{dp}k_4 & -k_4k_{dv}/\tau_v & -1/\tau_v-(1+k_{dr}k_4)/\tau_r & 1 & k_{vr}/\tau_r & 0 & 0 \\
-\omega_n^2k_{dp}k_5 & -k_5k_{dv}/\tau_v & -k_{dr}k_5/\tau_r & -1/\tau_v & 0 & k_{vr}/\tau_r & 0 \\
0 & 0 & -k_{dv}k_4/\tau_v & 0 & -(2+k_{dr}k_4)/\tau_r & 2 & 0 \\
0 & 0 & -k_{dv}k_5/\tau_v & 0 & -k_{dr}k_5/\tau_r & -1/\tau_r & 1 \\
0 & 0 & 0 & -k_{dv}k_5/\tau_v & 0 & -k_{dr}k_5/\tau_r & 0
\end{bmatrix}
$$

Note : The upper dotted area in matrix A_m denotes the A_m matrix of the rudder-to-roll submodel, given in Appendix C, while the lower dotted area denotes the A_m matrix of the rudder-to-rate-of-turn submodel, given in Appendix D. Similar areas can be recognized in the matrices B_m and C_m.

Appendix C

Calculation of the third-order roll controller

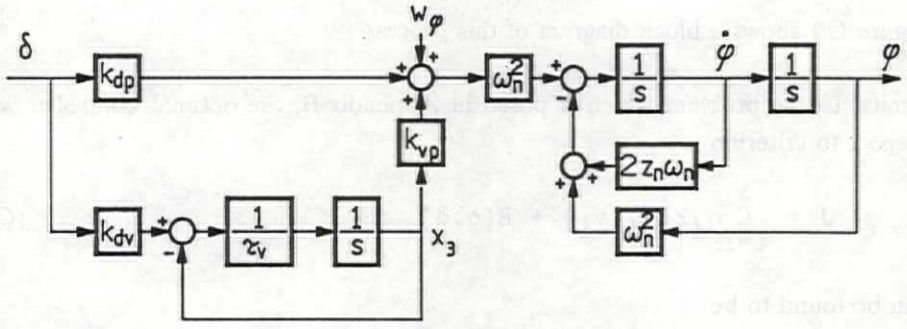

Fig. C.1 Block diagram of the process

Let a process, described by the following state-space equations, be given:

$$\dot{\underline{x}} = A\underline{x} + B\underline{u} + D\underline{w} \qquad (C.1)$$

$$\underline{y} = C\underline{x} \qquad (C.2)$$

where

$$A = \begin{bmatrix} 0 & 1 & 0 \\ -\omega_n^2 & -2z_n\omega_n & \omega_n^2 k_{vp} \\ 0 & 0 & -1/\tau_v \end{bmatrix} \qquad B = \begin{bmatrix} 0 \\ \omega_n^2 k_{dp} \\ k_{dv}/\tau_v \end{bmatrix}$$

$$C = \begin{bmatrix} c_1 & 0 & 0 \\ 0 & c_2 & 0 \\ 0 & 0 & c_3 \end{bmatrix} \qquad D = \begin{bmatrix} 0 \\ \omega_n^2 \\ 0 \end{bmatrix}$$

$$\underline{x}^T = (\varphi,\ \dot{\varphi},\ x_3)$$

$$\underline{u} = \delta$$

$$\underline{w} = w_{\varphi} = \text{white noise with zero mean}$$

$$\underline{y}^T = (y_1, y_2, y_3)$$

Figure C.1 shows a block diagram of this process.

Similar to the problem which is posed in Appendix B, the optimal controller with respect to criterion

$$J = \sum_{i=1}^{3} q_i E[y_i . y_i] + E[\delta . \delta] \qquad (C.3)$$

can be found to be

$$\delta = -K^T \underline{x} \qquad (C.4)$$

The matrix K is found by simulation of the following "innovation process" (see Section 3.2):

$$\dot{P} = A^T P + PA + C^T Q C - PBK \qquad (C.5)$$

$$K = B^T P \qquad (C.6)$$

where

$$P = \begin{bmatrix} p_5 & p_6 & p_7 \\ p_6 & p_8 & p_9 \\ p_7 & p_9 & p_{10} \end{bmatrix} \qquad Q = \begin{bmatrix} q_1/r & 0 & 0 \\ 0 & q_2/r & 0 \\ 0 & 0 & q_3/r \end{bmatrix}$$

The outputs of this process (the elements of the matrix K) are the desired controller parameters. Solving Eq. (C.6) yields:

$$K = (k_1 \; k_2 \; k_3) = B^T P = (0 \; \omega_n^2 k_{dp} \; k_{dv}/\tau_v) \begin{bmatrix} p_5 & p_6 & p_7 \\ p_6 & p_8 & p_9 \\ p_7 & p_9 & p_{10} \end{bmatrix}$$

and therefore

$$k_1 = \omega_n^2 k_{dp} p_6 + k_{dv} p_7/\tau_v \qquad (C.7)$$

$$k_2 = \omega_n^2 k_{dp} p_8 + k_{dv} p_9/\tau_v \qquad (C.8)$$

$$k_3 = \omega_n^2 k_{dp} p_9 + k_{dv} p_{10}/\tau_v \qquad (C.9)$$

Solving Eq. (C.5) yields:

$$C^T Q C = \begin{bmatrix} c_1^2 q_1/r & 0 & 0 \\ 0 & c_2^2 q_2/r & 0 \\ 0 & 0 & c_3^2 q_3/r \end{bmatrix}$$

$$PBK = \begin{bmatrix} p_5 & p_6 & p_7 \\ p_6 & p_8 & p_9 \\ p_7 & p_9 & p_{10} \end{bmatrix} \begin{bmatrix} 0 \\ \omega_n^2 k_{dp} \\ k_{dv}/\tau_v \end{bmatrix} (k_1 \; k_2 \; k_3) =$$

$$= \begin{bmatrix} \omega_n^2 k_{dp} k_1 p_6 + k_1 k_{dv} p_7/\tau_v & \omega_n^2 k_{dp} k_2 p_6 + k_2 k_{dv} p_7/\tau_v & \omega_n^2 k_{dp} k_3 p_6 + k_3 k_{dv} p_7/\tau_v \\ \omega_n^2 k_{dp} k_1 p_8 + k_1 k_{dv} p_9/\tau_v & \omega_n^2 k_{dp} k_2 p_8 + k_2 k_{dv} p_9/\tau_v & \omega_n^2 k_{dp} k_3 p_8 + k_3 k_{dv} p_9/\tau_v \\ \omega_n^2 k_{dp} k_1 p_9 + k_1 k_{dv} p_{10}/\tau_v & \omega_n^2 k_{dp} k_2 p_9 + k_2 k_{dv} p_{10}/\tau_v & \omega_n^2 k_{dp} k_3 p_9 + k_3 k_{dv} p_{10}/\tau_v \end{bmatrix}$$

$$PA = (A^T P)^T = \begin{bmatrix} p_5 & p_6 & p_7 \\ p_6 & p_8 & p_9 \\ p_7 & p_9 & p_{10} \end{bmatrix} \begin{bmatrix} 0 & 1 & 0 \\ -\omega_n^2 & -2z_n\omega_n & \omega_n^2 k_{vp} \\ 0 & 0 & -1/\tau_v \end{bmatrix} =$$

$$= \begin{bmatrix} -\omega_n^2 p_6 & p_5 - 2z_n\omega_n p_6 & \omega_n^2 k_{vp} p_6 - p_7/\tau_v \\ -\omega_n^2 p_8 & p_6 - 2z_n\omega_n p_8 & \omega_n^2 k_{vp} p_8 - p_9/\tau_v \\ -\omega_n^2 p_9 & p_7 - 2z_n\omega_n p_9 & \omega_n^2 k_{vp} p_9 - p_{10}/\tau_v \end{bmatrix}$$

This yields for the elements of P:

$$\dot{p}_5 = -\omega_n^2(2 + k_{dp} k_1) p_6 - k_1 k_{dv} p_7/\tau_v + c_1^2 q_1/r \qquad (C.10)$$

$$\dot{p}_6 = p_5 - (2z_n\omega_n+\omega_n^2k_{dp}k_2)p_6 - k_2k_{dv}p_7/\tau_v - \omega_n^2p_8 \qquad (C.11)$$

$$\dot{p}_7 = \omega_n^2(k_{vp}-k_{dp}k_3)p_6 - (1+k_3k_{dv})p_7/\tau_v - \omega_n^2p_9 \qquad (C.12)$$

$$\dot{p}_8 = 2p_6 - (4z_n\omega_n+\omega_n^2k_{dp}k_2)p_8 - k_2k_{dv}p_9/t_v + c_2^2q_2/r \qquad (C.13)$$

$$\dot{p}_9 = p_7 + \omega_n^2(k_{vp}-k_{dp}k_3)p_8 - (2z_n\omega_n+(1+k_3k_{dv})/\tau_v)p_9 \qquad (C.14)$$

$$\dot{p}_{10} = \omega_n^2(2k_{vp}-k_{dp}k_3)p_9 - (2+k_3k_{dv})p_{10}/\tau_v + c_3^2q_3/r \qquad (C.15)$$

It is possible to reformulate this result as a process with the following state-space equations:

$$L\dot{\underline{x}}_m = A_m\underline{x}_m + B_m\underline{u}_m \qquad (C.16)$$

$$\underline{y}_m = C_m\underline{x}_m \qquad (C.17)$$

where

$$\underline{x}_m^T = (p_5, p_6, \cdots, p_{10})$$

= the elements of P.

$$\underline{y}_m^T = (k_1, k_2, k_3) \quad = \text{the elements of K.}$$

$$\underline{u}_m^T = (q_1/r, q_2/r, q_3/r)$$

$$B_m^T = \begin{bmatrix} c_1^2 & 0 & 0 & 0 & 0 & 0 \\ 0 & 0 & 0 & c_2^2 & 0 & 0 \\ 0 & 0 & 0 & 0 & 0 & c_3^2 \end{bmatrix}$$

$$C_m = \begin{bmatrix} 0 & \omega_n^2 k_{dp} & k_{dv}/\tau_v & 0 & 0 & 0 \\ 0 & 0 & 0 & \omega_n^2 k_{dp} & k_{dv}/\tau_v & 0 \\ 0 & 0 & 0 & 0 & \omega_n^2 k_{dp} & k_{dv}/\tau_v \end{bmatrix}$$

$$A_m = \begin{bmatrix} 0 & -\omega_n^2(2+k_{dp}k_1) & -k_{dv}k_1/\tau_v & 0 & 0 & 0 \\ 1 & -2z_n\omega_n-\omega_n^2 k_{dp}k_2 & -k_{dv}k_2/\tau_v & -\omega_n^2 & 0 & 0 \\ 0 & \omega_n^2(k_{vp}-k_{dp}k_3) & -(1+k_{dv}k_3)/\tau_v & 0 & -\omega_n^2 & 0 \\ 0 & 2 & 0 & -4z_n\omega_n-\omega_n^2 k_{dp}k_2 & -k_{dv}k_2/\tau_v & 0 \\ 0 & 0 & 1 & \omega_n^2(k_{vp}-k_{dp}k_3) & -2z_n\omega_n-(1+k_{dv}k_3)/\tau_v & 0 \\ 0 & 0 & 0 & 0 & \omega_n^2(2k_{vp}-k_{dp}k_3) & -(2+k_{dv}k_3)/\tau_v \end{bmatrix}$$

As is indicated in Appendix B, the matrices A_m, B_m and C_m form subsets of the corresponding matrices of the fifth-order model.

Appendix D

Calculation of the third-order yaw controller

Let a process, described by the following state-space equations, be given:

$$\dot{\underline{x}} = A\underline{x} + B\underline{u} + D\underline{w} \qquad (D.1)$$

$$\underline{y} = C\underline{x} \qquad (D.2)$$

where

$$A = \begin{bmatrix} -1/\tau_v & 0 & 0 \\ k_{vr}/\tau_r & -1/\tau_r & 0 \\ 0 & 1 & 0 \end{bmatrix} \quad B = \begin{bmatrix} k_{dv}/\tau_v \\ k_{dr}/\tau_r \\ 0 \end{bmatrix}$$

$$C = \begin{bmatrix} c_3 & 0 & 0 \\ 0 & c_4 & 0 \\ 0 & 0 & c_5 \end{bmatrix} \qquad D = \begin{bmatrix} 0 \\ 1/\tau_r \\ 0 \end{bmatrix}$$

$$\underline{x}^T = (x_3,\ \dot{\psi}_4,\ \psi_5)$$

$$\underline{u} = \delta$$

$$\underline{w} = w_\psi = \text{white noise with zero mean}$$

$$\underline{y}^T = (y_3,\ y_4,\ y_5)$$

Figure D.1 shows a block diagram of this process.

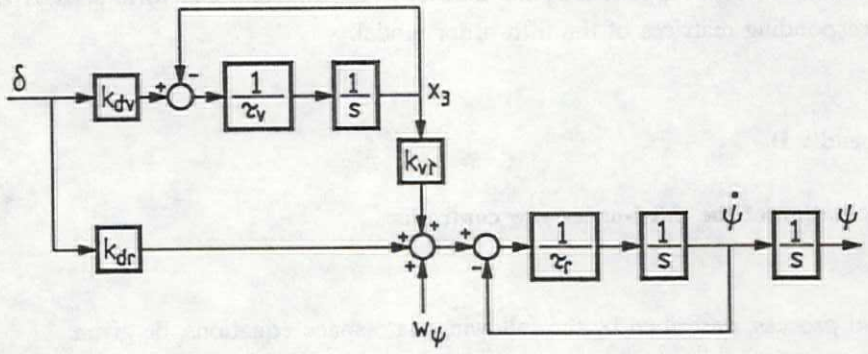

Fig. D.1 Block diagram of the process

Analogous to the problems posed in Appendix B and Appendix C, the optimal controller with respect to criterion

$$J = \sum_{i=3}^{5} q_i E[y_i \cdot y_i] + E[\delta \cdot \delta] \qquad (D.3)$$

can be found to be

$$\delta = -K^T \underline{x} \qquad (D.4)$$

The matrix K is found by simulation of the following "innovation process" (see Section 3.2):

$$\dot{P} = A^T P + PA + C^T Q C - PBK \qquad (D.5)$$

$$K = B^T P \qquad (D.6)$$

where

$$P = \begin{bmatrix} p_{10} & p_{11} & p_{12} \\ p_{11} & p_{13} & p_{14} \\ p_{12} & p_{14} & p_{15} \end{bmatrix} \qquad Q = \begin{bmatrix} q_3/r & 0 & 0 \\ 0 & q_4/r & 0 \\ 0 & 0 & q_5/r \end{bmatrix}$$

The outputs of this process (the elements of the matrix K) are the desired controller parameters. Solving Eq. (D.6) yields:

$$K = (k_3 \; k_4 \; k_5) = B^T P =$$

$$= (k_{dv}/\tau_v \; k_{dr}/\tau_r \; 0) \begin{bmatrix} p_{10} & p_{11} & p_{12} \\ p_{11} & p_{13} & p_{14} \\ p_{12} & p_{14} & p_{15} \end{bmatrix}$$

and therefore

$$k_3 = k_{dv} p_{10}/\tau_v + k_{dr} p_{11}/\tau_r \qquad (D.7)$$

$$k_4 = k_{dv} p_{11}/\tau_v + k_{dr} p_{13}/\tau_r \qquad (D.8)$$

$$k_5 = k_{dv} p_{12}/\tau_v + k_{dr} p_{14}/\tau_r \qquad (D.9)$$

Solving Eq. (D.5) yields:

$$C^T Q C = \begin{bmatrix} c_3^2 q_3/r & 0 & 0 \\ 0 & c_4^2 q_4/r & 0 \\ 0 & 0 & c_5^2 q_5/r \end{bmatrix}$$

$$PBK = \begin{bmatrix} p_{10} & p_{11} & p_{12} \\ p_{11} & p_{13} & p_{14} \\ p_{12} & p_{14} & p_{15} \end{bmatrix} \begin{bmatrix} k_{dv}/\tau_v \\ k_{dr}/\tau_r \\ 0 \end{bmatrix} (k_3 \; k_4 \; k_5) =$$

$$= \begin{bmatrix} k_3k_{dv}p_{10}/\tau_v+k_3k_{dr}p_{11}/\tau_r & k_4k_{dv}p_{10}/\tau_v+k_4k_{dr}p_{11}/\tau_r & k_5k_{dv}p_{10}/\tau_v+k_5k_{dr}p_{11}/\tau_r \\ k_3k_{dv}p_{11}/\tau_v+k_3k_{dr}p_{13}/\tau_r & k_4k_{dv}p_{11}/\tau_v+k_4k_{dr}p_{13}/\tau_r & k_5k_{dv}p_{11}/\tau_v+k_5k_{dr}p_{13}/\tau_r \\ k_3k_{dv}p_{12}/\tau_v+k_3k_{dr}p_{14}/\tau_r & k_4k_{dv}p_{12}/\tau_v+k_4k_{dr}p_{14}/\tau_r & k_5k_{dv}p_{12}/\tau_v+k_5k_{dr}p_{14}/\tau_r \end{bmatrix}$$

$$PA = (A^TP)^T = \begin{bmatrix} p_{10} & p_{11} & p_{12} \\ p_{11} & p_{13} & p_{14} \\ p_{12} & p_{14} & p_{15} \end{bmatrix} \begin{bmatrix} -1/\tau_v & 0 & 0 \\ k_{vr}/\tau_r & -1/\tau_r & 0 \\ 0 & 1 & 0 \end{bmatrix} =$$

$$= \begin{bmatrix} -p_{10}/\tau_v+k_{vr}p_{11}/\tau_r & p_{12}-p_{11}/\tau_r & 0 \\ -p_{11}/\tau_v+k_{vr}p_{13}/\tau_r & p_{14}-p_{13}/\tau_r & 0 \\ -p_{12}/\tau_v+k_{vr}p_{14}/\tau_r & p_{15}-p_{14}/\tau_r & 0 \end{bmatrix}$$

and for the elements of matrix P this yields:

$$\dot{p}_{10} = -(2+k_3k_{dv})p_{10}/\tau_v + (2k_{vr}-k_3k_{dr})p_{11}/\tau_r + c_3^2q_3/r \qquad (D.10)$$

$$\dot{p}_{11} = -k_4k_{dv}p_{10}/\tau_v - (1/\tau_v+1/\tau_r+k_4k_{dr}/\tau_r)p_{11} + p_{12} + k_{vr}p_{13}/\tau_r \qquad (D.11)$$

$$\dot{p}_{12} = -k_5k_{dv}p_{10}/\tau_v - k_5k_{dr}p_{11}/\tau_r - p_{12}/\tau_v + k_{vr}p_{14}/\tau_r \qquad (D.12)$$

$$\dot{p}_{13} = -k_4k_{dv}p_{11}/\tau_v - (2+k_4k_{dr})p_{13}/\tau_r + 2p_{14} + c_4^2q_4/r \qquad (D.13)$$

$$\dot{p}_{14} = -k_5k_{dv}p_{11}/\tau_v - k_5k_{dr}p_{13}/\tau_r - p_{14}/\tau_r + p_{15} \qquad (D.14)$$

$$\dot{p}_{15} = -k_5k_{dv}p_{12}/\tau_v - k_5k_{dr}p_{14}/\tau_r + c_5^2q_5/r \qquad (D.15)$$

It is possible to reformulate this result as a process with the following state space equations:

$$L\dot{\underline{x}}_m = A_m\underline{x}_m + B_m\underline{u}_m \qquad (D.16)$$

$$\underline{y}_m = C_m\underline{x}_m \qquad (D.17)$$

where

$$\underline{x}_m^T = (p_{10}, p_{11}, \cdots, p_{15})$$
$$= \text{the elements of P.}$$

$$\underline{y}_m^T = (k_3, k_4, k_5) \quad = \text{the elements of K.}$$

$$\underline{u}_m^T = (q_3/r, q_4/r, q_5/r)$$

$$B_m^T = \begin{bmatrix} c_3^2 & 0 & 0 & 0 & 0 & 0 \\ 0 & 0 & 0 & c_4^2 & 0 & 0 \\ 0 & 0 & 0 & 0 & 0 & c_5^2 \end{bmatrix}$$

$$C_m = \begin{bmatrix} k_{dv}/\tau_v & k_{dr}/\tau_r & 0 & 0 & 0 & 0 \\ 0 & k_{dv}/\tau_v & 0 & k_{dr}/\tau_r & 0 & 0 \\ 0 & 0 & k_{dv}/\tau_v & 0 & k_{dr}/\tau_r & 0 \end{bmatrix}$$

$$A_m = \begin{bmatrix} -(2+k_{dv}k_3)/\tau_v & (2k_{vr}-k_{dr}k_3)/\tau_r & 0 & 0 & 0 & 0 \\ -k_{dv}k_4/\tau_v & -1/\tau_v-(1+k_{dr}k_4)/\tau_r & 1 & k_{vr}/\tau_r & 0 & 0 \\ -k_{dv}k_5/\tau_v & -k_{dr}k_5/\tau_r & -1/\tau_v & 0 & k_{vr}/\tau_r & 0 \\ 0 & -k_{dv}k_4/\tau_v & 0 & -(2+k_{dr}k_4)/\tau_r & 2 & 0 \\ 0 & -k_{dv}k_5/\tau_v & 0 & -k_{dr}k_5/\tau_r & -1/\tau_r & 1 \\ 0 & 0 & -k_{dv}k_5/\tau_v & 0 & -k_{dr}k_5/\tau_r & 0 \end{bmatrix}$$

As is indicated in Appendix B the matrices A_m, B_m and C_m form subsets of the corresponding matrices of the fifth-order model.

Appendix E

Calculation of the roll-filter gains

Let a process described by the following state-space equations be given:

$$\dot{\underline{x}} = A\underline{x} + B\underline{u} + D\underline{w} \qquad (E.1)$$

$$\underline{y} = C\underline{x} + \underline{v} \qquad (E.2)$$

where

$$A = \begin{bmatrix} 0 & 1 & 0 \\ -\omega_n^2 & -2z_n\omega_n & 0 \\ 0 & 0 & 0 \end{bmatrix} \qquad B = \begin{bmatrix} 0 \\ \omega_n^2 \\ 0 \end{bmatrix} \qquad D = \begin{bmatrix} 0 & 0 \\ \omega_n^2 & 0 \\ 0 & 1 \end{bmatrix}$$

$$C = (1 \quad 0 \quad 1)$$

$$\underline{x}^T = (\varphi, \dot{\varphi}, x_v) \qquad \underline{w}^T = (w_1, w_2)$$

$$\underline{u} = u \qquad \underline{v} = v$$

The "optimal" filter for this process is described by the following state-space equations:

$$\dot{\hat{\underline{x}}} = A\hat{\underline{x}} + B\underline{u} + K\underline{z} \qquad (E.3)$$

$$\hat{\underline{y}} = C\hat{\underline{x}} \qquad (E.4)$$

$$\underline{z} = \underline{y} - \hat{\underline{y}} \qquad (E.5)$$

Fig. E.1 gives the block diagram of the process in combination with the optimal filter structure.

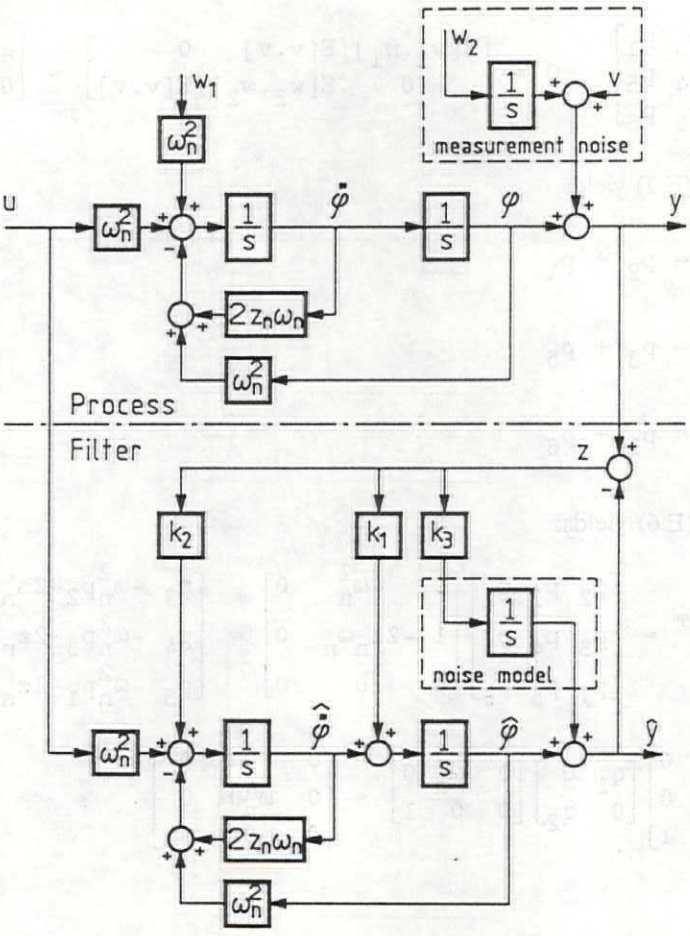

Fig. E.1 Block diagram of process and corresponding filter

K can be found by solving the following equations:

$$\dot{P} = AP + PA^T + DQD^T - KCP \qquad (E.6)$$

$$K = PC^T \qquad (E.7)$$

where

$$P = \begin{bmatrix} p_2 & p_3 & p_1 \\ p_3 & p_4 & p_5 \\ p_1 & p_5 & p_6 \end{bmatrix} \qquad Q = \begin{bmatrix} E[w_1.w_1]/E[v.v] & 0 \\ 0 & E[w_2.w_2]/E[v.v] \end{bmatrix} = \begin{bmatrix} q_1 & 0 \\ 0 & q_2 \end{bmatrix}$$

Solving Eq. (E.7) yields:

$$k_1 = p_2 + p_1 \tag{E.8}$$

$$k_2 = p_3 + p_5 \tag{E.9}$$

$$k_3 = p_1 + p_6 \tag{E.10}$$

Solving Eq. (E.6) yields:

$$PA^T = (AP)^T = \begin{bmatrix} p_2 & p_3 & p_1 \\ p_3 & p_4 & p_5 \\ p_1 & p_5 & p_6 \end{bmatrix} \begin{bmatrix} 0 & -\omega_n^2 & 0 \\ 1 & -2z_n\omega_n & 0 \\ 0 & 0 & 0 \end{bmatrix} = \begin{bmatrix} p_3 & -\omega_n^2 p_2 - 2z_n\omega_n p_3 & 0 \\ p_4 & -\omega_n^2 p_3 - 2z_n\omega_n p_4 & 0 \\ p_5 & -\omega_n^2 p_1 - 2z_n\omega_n p_5 & 0 \end{bmatrix}$$

$$DQD^T = \begin{bmatrix} 0 & 0 \\ \omega_n^2 & 0 \\ 0 & 1 \end{bmatrix} \begin{bmatrix} q_1 & 0 \\ 0 & q_2 \end{bmatrix} \begin{bmatrix} 0 & \omega_n^2 & 0 \\ 0 & 0 & 1 \end{bmatrix} = \begin{bmatrix} 0 & 0 & 0 \\ 0 & \omega_n^4 q_1 & 0 \\ 0 & 0 & q_2 \end{bmatrix}$$

and finally

$$KCP = \begin{bmatrix} k_1 \\ k_2 \\ k_3 \end{bmatrix} (1\ 0\ 1) \begin{bmatrix} p_2 & p_3 & p_1 \\ p_3 & p_4 & p_5 \\ p_1 & p_5 & p_6 \end{bmatrix} = \begin{bmatrix} k_1p_2+k_1p_1 & k_1p_3+k_1p_5 & k_1p_1+k_1p_6 \\ k_2p_2+k_2p_1 & k_2p_3+k_2p_5 & k_2p_1+k_2p_6 \\ k_3p_2+k_3p_1 & k_3p_3+k_3p_5 & k_3p_1+k_3p_6 \end{bmatrix}$$

Therefore

$$\dot{p}_1 = p_5 - k_1p_1 - k_1p_6 \tag{E.11}$$

$$\dot{p}_2 = 2p_3 - k_1p_2 - k_1p_1 \tag{E.12}$$

$$\dot{p}_3 = p_4 - \omega_n^2 p_2 - 2z_n\omega_n p_3 - k_1 p_3 - k_1 p_5 \qquad (E.13)$$

$$\dot{p}_4 = -2\omega_n^2 p_3 - 4z_n\omega_n p_4 - k_2 p_3 - k_2 p_5 + \omega_n^4 q_1 \qquad (E.14)$$

$$\dot{p}_5 = -\omega_n^2 p_1 - 2z_n\omega_n p_5 - k_2 p_1 - k_2 p_6 \qquad (E.15)$$

$$\dot{p}_6 = -k_3 p_1 - k_3 p_6 + q_2 \qquad (E.16)$$

The solution of Eqs. (E.6) and (E.7) can be found to be the steady state of an innovation process described by the following state-space equations:

$$L\dot{\underline{x}}_m = A_m \underline{x}_m + B_m \underline{u}_m \qquad (E.17)$$

$$\underline{y}_m = C_m \underline{x}_m \qquad (E.18)$$

where

$$A_m = \begin{bmatrix} -k_1 & 0 & 0 & 0 & 1 & -k_1 \\ -k_1 & -k_1 & 2 & 0 & 0 & 0 \\ 0 & -\omega_n^2 & -2z_n\omega_n - k_1 & 1 & -k_1 & 0 \\ 0 & 0 & -2\omega_n^2 - k_2 & -4z_n\omega_n & -k_2 & 0 \\ -\omega_n^2 - k_2 & 0 & 0 & 0 & -2z_n\omega_n & -k_2 \\ -k_3 & 0 & 0 & 0 & 0 & -k_3 \end{bmatrix}$$

$$B_m^T = \begin{bmatrix} 0 & 0 & 0 & \omega_n^2 & 0 & 0 \\ 0 & 0 & 0 & 0 & 0 & 1 \end{bmatrix} \qquad C_m = \begin{bmatrix} 1 & 1 & 0 & 0 & 0 & 0 \\ 0 & 0 & 1 & 0 & 1 & 0 \\ 1 & 0 & 0 & 0 & 0 & 1 \end{bmatrix}$$

$$\underline{x}_m^T = (p_1, p_2, \ldots\ldots, p_6)$$

$$\underline{u}_m^T = (q_1, q_2)$$

$$\underline{y}_m^T = (k_1, k_2, k_3)$$

When only the model of the process is considered (i.e. v_p is white noise with zero mean) A_m, B_m and C_m reduce to the matrices indicated by the dotted lines.

Appendix F

Calculation of the yaw-filter gains

Let a process described by the following state-space equations be given:

$$\dot{\underline{x}} = A\underline{x} + B\underline{u} + D\underline{w} \qquad (F.1)$$

$$\underline{y} = C\underline{x} + F\underline{v} \qquad (F.2)$$

where

$$A = \begin{bmatrix} 0 & 1 & 0 & 0 \\ 0 & -1/\tau_r & 1/\tau_r & 0 \\ 0 & 0 & 0 & 0 \\ 0 & 0 & 0 & -1/\tau_f \end{bmatrix} \qquad B = \begin{bmatrix} 0 \\ 1/\tau_r \\ 0 \\ 0 \end{bmatrix}$$

$$D = \begin{bmatrix} 0 & 0 & 0 \\ 1/\tau_r & 0 & 0 \\ 0 & 1 & 0 \\ 0 & 0 & 1/\tau_f \end{bmatrix} \qquad C = (1\ 0\ 0\ -1) \qquad F = (1\ \ 1)$$

$$\underline{x}^T = (\psi \quad \dot{\psi} \quad x_3 \ x_4) \qquad \underline{w}^T = (w_1\ w_2\ w_3)$$

$$\underline{u} = u \qquad \underline{v}^T = (w_3\ v)$$

w_1, w_2, w_3 and v denote uncorrelated white noise with zero mean.

The "optimal" filter for this process is described by the following state-space equations:

$$\dot{\hat{\underline{x}}} = A\hat{\underline{x}} + B\underline{u} + K\underline{z} \qquad (F.3)$$

$$\hat{\underline{y}} = C\hat{\underline{x}} \tag{F.4}$$

$$\underline{z} = \underline{y} - \hat{\underline{y}} \tag{F.5}$$

Fig. F.1 gives the block diagram of the process in combination with the optimal filter.

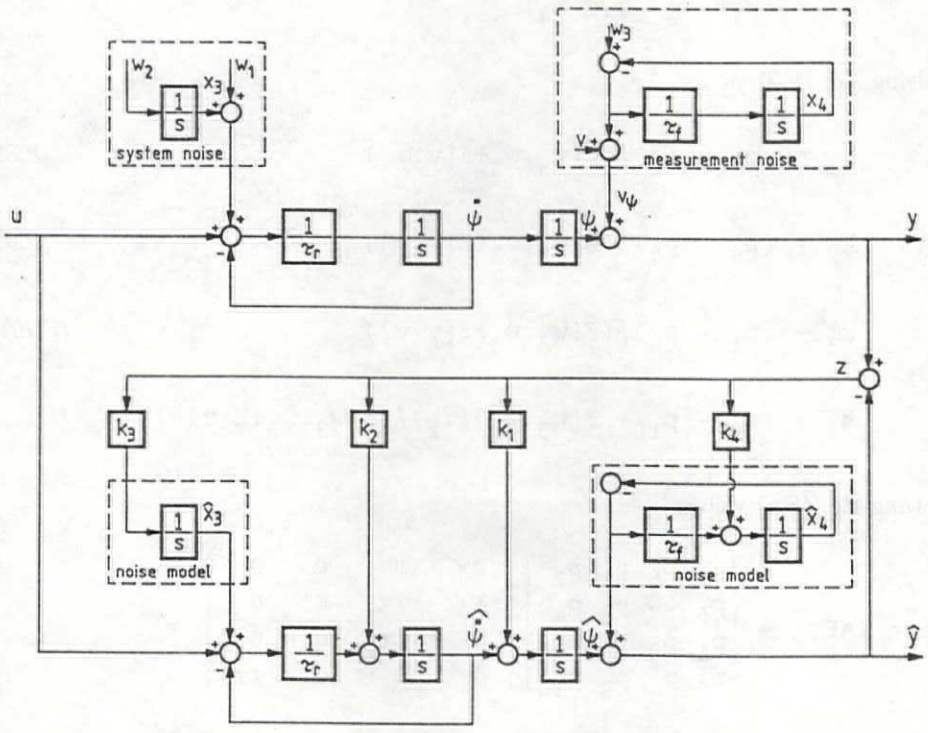

Fig. F.1 The process in combination with the optimal filter

K can be found by solving the following equations:

$$\dot{P} = AP + PA^T + DQD^T - K(PC^T + DSF^T)^T \tag{F.6}$$

$$K = (PC^T + DSF^T)(FRF^T)^{-1} \tag{F.7}$$

where

$$P = \begin{bmatrix} p_5 & p_6 & p_1 & p_2 \\ p_6 & p_7 & p_3 & p_4 \\ p_1 & p_3 & p_8 & p_9 \\ p_2 & p_4 & p_9 & p_{10} \end{bmatrix} \quad Q = \begin{bmatrix} E[w_1.w_1] & 0 & 0 \\ 0 & E[w_2.w_2] & 0 \\ 0 & 0 & E[w_3.w_3] \end{bmatrix}$$

$$R = \begin{bmatrix} E[w_3.w_3] & 0 \\ 0 & E[v.v] \end{bmatrix} \quad S = \begin{bmatrix} 0 & 0 \\ 0 & 0 \\ E[w_3.w_3] & 0 \end{bmatrix}$$

$$K^T = (k_1 \quad k_2 \quad k_3 \quad k_4)$$

Solving Eq. (F.7) yields:

$$k_1 = (p_5 - p_2)/(E[w_3.w_3+E[v.v]) \qquad (F.8)$$

$$k_2 = (p_6 - p_4)/(E[w_3.w_3+E[v.v]) \qquad (F.9)$$

$$k_3 = (p_1 - p_9)/(E[w_3.w_3+E[v.v]) \qquad (F.10)$$

$$k_4 = (p_2 - p_{10}+ E[w_3.w_3]/\tau_f)/(E[w_3.w_3+E[v.v]) \qquad (F.11)$$

Solving Eq. (F.6) yields:

$$PA^T = (AP)^T = \begin{bmatrix} p_5 & p_6 & p_1 & p_2 \\ p_6 & p_7 & p_3 & p_4 \\ p_1 & p_3 & p_8 & p_9 \\ p_2 & p_4 & p_9 & p_{10} \end{bmatrix} \begin{bmatrix} 0 & 0 & 0 & 0 \\ 1 & -1/\tau_r & 0 & 0 \\ 0 & 1/\tau_r & 0 & 0 \\ 0 & 0 & 0 & -1/\tau_f \end{bmatrix} =$$

$$= \begin{bmatrix} p_6 & p_1/\tau_r - p_6/\tau_r & 0 & -p_2/\tau_f \\ p_7 & p_3/\tau_r - p_7/\tau_r & 0 & -p_4/\tau_f \\ p_3 & p_8/\tau_r - p_3/\tau_r & 0 & -p_9/\tau_f \\ p_4 & p_9/\tau_r - p_4/\tau_r & 0 & -p_{10}/\tau_f \end{bmatrix}$$

$$DQD^T = \begin{bmatrix} 0 & 0 & 0 \\ 1/\tau_r & 0 & 0 \\ 0 & 1 & 0 \\ 0 & 0 & 1/\tau_f \end{bmatrix} \begin{bmatrix} E[w_1.w_1] & 0 & 0 \\ 0 & E[w_2.w_2] & 0 \\ 0 & 0 & E[w_3.w_3] \end{bmatrix} \begin{bmatrix} 0 & 1/\tau_r & 0 & 0 \\ 0 & 0 & 1 & 0 \\ 0 & 0 & 0 & 1/\tau_f \end{bmatrix}$$

$$= \begin{bmatrix} 0 & 0 & 0 & 0 \\ 0 & E[w_1.w_1]/\tau_r^2 & 0 & 0 \\ 0 & 0 & E[w_2.w_2] & 0 \\ 0 & 0 & 0 & E[w_3.w_3]/\tau_f^2 \end{bmatrix}$$

$$KCP = \begin{bmatrix} k_1 \\ k_2 \\ k_3 \\ k_4 \end{bmatrix} (1\ 0\ 0\ -1) \begin{bmatrix} p_5 & p_6 & p_1 & p_2 \\ p_6 & p_7 & p_3 & p_4 \\ p_1 & p_3 & p_8 & p_9 \\ p_2 & p_4 & p_9 & p_{10} \end{bmatrix} =$$

$$= \begin{bmatrix} p_5k_1-p_2k_1 & p_6k_1-p_4k_1 & p_1k_1-p_9k_1 & p_2k_1-p_{10}k_1 \\ p_5k_2-p_2k_2 & p_6k_2-p_4k_2 & p_1k_2-p_9k_2 & p_2k_2-p_{10}k_2 \\ p_5k_3-p_2k_3 & p_6k_3-p_4k_3 & p_1k_3-p_9k_3 & p_2k_3-p_{10}k_3 \\ p_5k_4-p_2k_4 & p_6k_4-p_4k_4 & p_1k_4-p_9k_4 & p_2k_4-p_{10}k_4 \end{bmatrix}$$

and finally

$$KFS^TD^T = \begin{bmatrix} k_1 \\ k_2 \\ k_3 \\ k_4 \end{bmatrix} (1\ 1) \begin{bmatrix} 0 & 0 & E[w_3.w_3] \\ 0 & 0 & 0 \end{bmatrix} \begin{bmatrix} 0 & 1/\tau_r & 0 & 0 \\ 0 & 0 & 1 & 0 \\ 0 & 0 & 0 & 1/\tau_f \end{bmatrix} =$$

$$= \begin{bmatrix} 0 & 0 & 0 & k_1E[w_3.w_3]/\tau_f \\ 0 & 0 & 0 & k_2E[w_3.w_3]/\tau_f \\ 0 & 0 & 0 & k_3E[w_3.w_3]/\tau_f \\ 0 & 0 & 0 & k_4E[w_3.w_3]/\tau_f \end{bmatrix}$$

Therefore, the elements of the covariance matrix P are described by:

$$\dot{p}_1 = - k_1p_1 + p_3 + k_1p_9$$

$$\dot{p}_2 = -p_2/\tau_f - k_1 p_2 + p_4 + k_1 p_{10} - k_1 E[w_3.w_3]/\tau_f$$

$$\dot{p}_3 = -k_2 p_1 - p_3/\tau_r + p_8/\tau_r + k_2 p_9$$

$$\dot{p}_4 = -k_2 p_2 - p_4/\tau_f - p_4/\tau_r + p_9/\tau_r + k_2 p_{10} - k_2 E[w_3.w_3]/\tau_f$$

$$\dot{p}_5 = k_1 p_2 - k_1 p_5 + 2p_6$$

$$\dot{p}_6 = p_1/\tau_r + k_1 p_4 - k_1 p_6 - p_6/\tau_r + p_7$$

$$\dot{p}_7 = 2p_3/\tau_r + k_2 p_4 - k_2 p_6 - 2p_7/\tau_r + E[w_1.w_1]/\tau_r^2$$

$$\dot{p}_8 = -k_3 p_1 + k_3 p_9 + E[w_2.w_2]$$

$$\dot{p}_9 = -k_3 p_2 - p_9/\tau_f + k_3 p_{10} - k_3 E[w_3.w_3]/\tau_f$$

$$\dot{p}_{10} = -k_4 p_2 - 2p_{10}/\tau_f + k_4 p_{10} + E[w_3.w_3/\tau_f^2 - k_4 E[w_3.w_3]/\tau_f$$

It is possible to reformulate this result as an "innovation" process described by the following state-space equations:

$$L\dot{\underline{x}}_m = A_m \underline{x}_m + B_m \underline{u}_m \qquad (F.12)$$

$$\underline{y}_m = C_m \underline{x}_m + D_m \underline{u}_m \qquad (F.13)$$

where

$$A_m = \begin{bmatrix} -k_1 & 0 & 1 & 0 & 0 & 0 & 0 & 0 & +k_1 & 0 \\ 0 & -1/\tau_f-k_1 & 0 & 1 & 0 & 0 & 0 & 0 & 0 & +k_1 \\ -k_2 & 0 & -1/\tau_r & 0 & 0 & 0 & 0 & 1/\tau_r & +k_2 & 0 \\ 0 & -k_2 & 0 & -1/\tau_f-1/\tau_r & 0 & 0 & 0 & 0 & 1/\tau_r & +k_2 \\ 0 & +k_1 & 0 & 0 & -k_1 & 2 & 0 & 0 & 0 & 0 \\ 1/\tau_r & 0 & 0 & +k_1 & 0 & -1/\tau_r-k_1 & 1 & 0 & 0 & 0 \\ 0 & 0 & 2/\tau_r & +k_2 & 0 & -k_2 & -2/\tau_r & 0 & 0 & 0 \\ -k_3 & 0 & 0 & 0 & 0 & 0 & 0 & 0 & +k_3 & 0 \\ 0 & -k_3 & 0 & 0 & 0 & 0 & 0 & 0 & -1/\tau_f & +k_3 \\ 0 & -k_4 & 0 & 0 & 0 & 0 & 0 & 0 & 0 & k_4-2/\tau_f \end{bmatrix}$$

$$B_m^T = \begin{bmatrix} 0 & 0 & 0 & 0 & 0 & 0 & 1/\tau_r^2 & 0 & 0 & 0 \\ 0 & 0 & 0 & 0 & 0 & 0 & 0 & 1 & 0 & 0 \\ 0 & -k_1/\tau_f & 0 & -k_2/\tau_f & 0 & 0 & 0 & 0 & -k_3/\tau_f & (1/\tau_f-k_4)/\tau_f \end{bmatrix}$$

$$C_m = \begin{bmatrix} 0 & c & 0 & 0 & c & 0 & 0 & 0 & 0 & 0 \\ 0 & 0 & 0 & c & 0 & c & 0 & 0 & 0 & 0 \\ c & 0 & 0 & 0 & 0 & 0 & 0 & 0 & c & 0 \\ 0 & c & 0 & 0 & 0 & 0 & 0 & 0 & 0 & c \end{bmatrix}$$

$$c^{-1} = E[w_3.w_3] + E[v.v]$$

$$D_m^T = \begin{bmatrix} 0 & 0 & 0 & 0 \\ 0 & 0 & 0 & 0 \\ 0 & 0 & 0 & c^{-1} \end{bmatrix}$$

$$\underline{x}_m^T = (p_1, p_2, \ldots\ldots, p_{10})$$

$$\underline{u}_m^T = (E[w_1.w_1], E[w_2.w_2], E[w_3.w_3])$$

$$\underline{y}_m^T = (k_1, k_2, k_3, k_4)$$

When only the model of the process is considered (i.e. w_p and v_p denote white noise with zero mean) A_m, B_m, C_m and F_m reduce to the matrices indicated by the dotted lines.

Appendix G

Calculation of the yaw controller

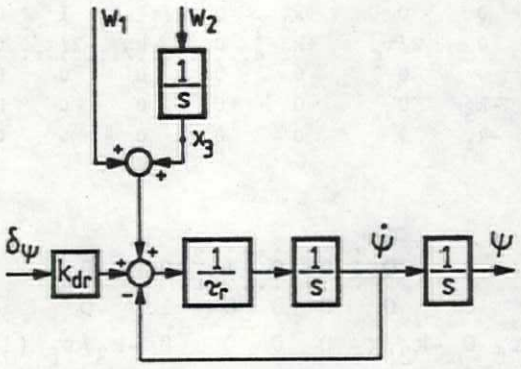

Fig. G.1 Block diagram of the process

Let a process, described by the following state-space equations, be given:

$$\dot{\underline{x}} = A\underline{x} + B\underline{u} + D\underline{w} \qquad (G.1)$$

$$\underline{y} = C\underline{x} \qquad (G.2)$$

where

$$A = \begin{bmatrix} 0 & 1 & 0 \\ 0 & -1/\tau_r & 1/\tau_r \\ 0 & 0 & 0 \end{bmatrix} \qquad B = \begin{bmatrix} 0 \\ k_{dr}/\tau_r \\ 0 \end{bmatrix}$$

$$C = \begin{bmatrix} 1 & 0 & 0 \\ 0 & 1 & 0 \\ 0 & 0 & 1 \end{bmatrix} \qquad D = \begin{bmatrix} 0 \\ 1/\tau_r \\ 0 \end{bmatrix}$$

$$\underline{x}^T = (\psi, \dot{\psi}, x_3)$$

$$\underline{u} = \delta$$

$$\underline{w}^T = (w_1, w_2) \quad = \text{white noise with zero mean}$$

Fig. G.1 shows a block diagram of this process.

Similar to the problems posed in Appendix A and Appendix B the optimal controller with respect to criterion

$$J = E[\delta.\delta] + E[\psi.\psi]/\lambda \qquad (G.3)$$

can be found by solving

$$0 = A^T P + PA + C^T QC - PBK \qquad (G.4)$$

$$K = B^T P \qquad (G.5)$$

where

$$P = \begin{bmatrix} p_1 & p_2 & p_4 \\ p_2 & p_3 & p_5 \\ p_4 & p_5 & p_6 \end{bmatrix} \qquad Q = \begin{bmatrix} 1/\lambda & 0 & 0 \\ 0 & 0 & 0 \\ 0 & 0 & 0 \end{bmatrix}$$

Solving Eq. (G.5) yields:

$$K = (k_1 \; k_2 \; k_3) = B^T P = (0 \; k_{dr}/\tau_r \; 0) \begin{bmatrix} p_1 & p_2 & p_4 \\ p_2 & p_3 & p_5 \\ p_4 & p_5 & p_6 \end{bmatrix}$$

Therefore,

$$k_1 = k_{dr} p_2/\tau_r \qquad (G.6)$$

$$k_2 = k_{dr} p_3/\tau_r \qquad (G.7)$$

$$k_3 = k_{dr} p_5/\tau_r \qquad (G.8)$$

Solving Eq. (G.4) yields:

$$C^T QC = \begin{bmatrix} 1/\lambda & 0 & 0 \\ 0 & 0 & 0 \\ 0 & 0 & 0 \end{bmatrix}$$

$$PBK = \begin{bmatrix} p_1 & p_2 & p_4 \\ p_2 & p_3 & p_5 \\ p_4 & p_5 & p_6 \end{bmatrix} \begin{bmatrix} 0 \\ k_{dr}/\tau_r \\ 0 \end{bmatrix} (k_1 \; k_2 \; k_3) =$$

$$= \begin{bmatrix} k_1 k_{dr} p_2/\tau_r & k_2 k_{dr} p_2/\tau_r & k_3 k_{dr} p_2/\tau_r \\ k_1 k_{dr} p_3/\tau_r & k_2 k_{dr} p_3/\tau_r & k_3 k_{dr} p_3/\tau_r \\ k_1 k_{dr} p_5/\tau_r & k_2 k_{dr} p_5/\tau_r & k_3 k_{dr} p_5/\tau_r \end{bmatrix}$$

$$PA = (A^T P)^T = \begin{bmatrix} p_1 & p_2 & p_4 \\ p_2 & p_3 & p_5 \\ p_4 & p_5 & p_6 \end{bmatrix} \begin{bmatrix} 0 & 1 & 0 \\ 0 & -1/\tau_r & 1/\tau_r \\ 0 & 0 & 0 \end{bmatrix} =$$

$$= \begin{bmatrix} 0 & p_1 - p_2/\tau_r & p_2/\tau_r \\ 0 & p_2 - p_3/\tau_r & p_3/\tau_r \\ 0 & p_4 - p_5/\tau_r & p_5/\tau_r \end{bmatrix}$$

and for the elements of matrix P this yields:

$$0 = -k_1 k_{dr} p_2/\tau_r + 1/\lambda \qquad (G.9)$$

$$0 = p_1 - (1+k_2 k_{dr}/\tau_r) p_2 \qquad (G.10)$$

$$0 = 2p_2 - (2+k_2 k_{dr}) p_3/\tau_r \qquad (G.11)$$

$$0 = (1-k_3 k_{dr}) p_2/\tau_r \qquad (G.12)$$

$$0 = (1-k_3 k_{dr})/\tau_r p_3 + p_4 - p_5/\tau_r \qquad (G.13)$$

$$0 = (1-k_3 k_{dr}) p_5/\tau_r \qquad (G.14)$$

From (G.6) and (G.9) it follows that

$$k_1 = \sqrt{1/\lambda} \qquad (G.15)$$

Adding (G.7) and (G.11) gives

$$k_2 = \frac{1}{k_{dr}} \left(\sqrt{1 + 2\tau_r k_{dr} \sqrt{1/\lambda}} - 1 \right) \qquad (G.16)$$

Finally, from (G.12), (G.13) and (G.14) it follows that

$$k_3 = \frac{1}{k_{dr}} \qquad (G.17)$$

Appendix H

Calculation of the bandwidth of the steering machine

Let the transferfunction of the steering machine H_{sm} be given by:

$$H_{sm} = \frac{\omega_0^2}{s^2 + 2\omega_0 s + \omega_0^2}$$

In order to determine the bandwidth of the steering machine the frequency has to be determined where

$$20 \log |H_{sm}| = -3 \text{ dB}$$

This gives

$$\left| \frac{\omega_0^2}{-B^2 + 2j\omega_0 B + \omega_0^2} \right| = \frac{1}{\sqrt{2}} = A^{-1}$$

or

$$(\omega_0^2 - B^2)^2 + 4\omega_0^2 B^2 = \omega_0^4 A^2$$

and therefore

$$B^4 + 2\omega_0^2 B^2 + \omega_0^4 (1 - A^2) = 0$$

Introduction of $x = B^2$ gives:

$$x^2 + 2\omega_0 x + \omega_0^4 (1 - A^2) = 0$$

and therefore

$$x = \frac{-2\omega_0^2 + \sqrt{4\omega_0^4 - 4\omega_0^4(1 - A^2)}}{2} = \omega_0^2(A - 1)$$

The resulting bandwidth is given by:

$$B = \omega_0\sqrt{A - 1} = \omega_0\sqrt{\sqrt{2} - 1} = 0.64\omega_0$$

REFERENCES

Albeda, J.P.A., *Een zelf-instellende regelaar t.b.v. de "Rudder Roll Stabilization" van schepen*, Masters thesis (in Dutch), Control Laboratory, Fac. of El. Eng., Delft University of Technology, 1986.

Amerongen, J. van, and J.C.L. van Cappelle, *Mathematical modeling for rudder roll stabilization*, 6th Ship Control Systems Symposium, Ottawa, Canada, 1981.

Amerongen, J. van, "**Adaptive steering of ships - a model-reference approach to improved manoeuvring and economical course keeping**", Ph. D. thesis, Delft University of Technology, p. XII, 195, April 1982.

Amerongen, J. van, and H.R. van Nauta Lemke, *Rudder Roll Stabilization*, Proceedings of the 4th ISSOA International Symposium on Ship Operation Automation, Genua, Italy, pp. 43-50, September 20-22, 1982.

Amerongen, J. van and P.G.M. van der Klugt, *Rudder Roll Stabilization - Measurements at the NSMB*, Internal report no. R82.051, Control Laboratory, Fac. of El. Eng., Delft University of Technology, 1982.

Amerongen, J. van and P.G.M. van der Klugt, *RRS measurements with a scale model at the Haringvliet*, Internal report no. R83.031, Control Laboratory, Fac. of El. Eng., Delft University of Technology, 1983.

Amerongen, J. van, P.G.M. van der Klugt and H.R. van Nauta Lemke, *Roll stabilization of ships by means of the rudder*, Proceedings Third Yale Workshop on Applications of Adaptive Systems Theory, New Haven, Conn., USA, pp. 19-26, 1983.

Amerongen, J. van, *Adaptive steering of ships - a model-reference approach*, **Automatica**, Vol. 20, no. 1, pp. 3-14, 1984.

Amerongen, J. van, P.G.M. van der Klugt and J.B.M. Pieffers, *Model tests and full-scale trials with a rudder-rolll stabilization system*, Proceedings Seventh Ship Control Systems Symposium, Bath, U.K., 1984.

Amerongen, J. van and P.G.M. van der Klugt, *Modeling and simulation of roll motions of a ship*, Proceedings First Intercontinental Maritime Simulation Symposium and Mathematical Modeling Workshop, Munchen, W-Germany, June 1985.

Amerongen, J. van, P.G.M. van der Klugt and H.R. van Nauta Lemke, *Adaptive adjustment of the weighting factors in a criterion*, **Journal A**, vol. 27, no. 3 pp. 163-168, 1986.

Amerongen, J. van and P.G.M. van der Klugt, *Rudder Roll Stabilization - Measurements at the MARIN*, Internal report no. R87.004, Control Laboratory, Fac. of El. Eng., Delft University of Technology, 1987a.

Amerongen, J. van and P.G.M. van der Klugt, *Rudder Roll Stabilization - Full-scale trials*, Internal report no. R87.017, Control Laboratory, Fac. of El. Eng., Delft University of Technology, 1987b.

Baitis, A.E., *The development and evaluation of a Rudder Roll Stabilisation System for the WHEC Hamilton Class*, DTNSRDC Report, Bethesda, Md. USA, 1980.

Bernard, C.J. and J.L.J. Ruigrok, *Het ontwerpen van een meet- en regelsysteem gebaseerd op een microcomputer*, Masters thesis (in Dutch), Control Laboratory, Fac. of El. Eng., Delft University of Technology, 1985.

Bhattacharyya, R., **Dynamics of marine vehicles**, John Wiley & Sons, New York, 1978.

Bosch, P.P.J. van den, *PSI - Software Tool for Control System Design*, **Journal A**, vol. 22, no. 2, pp. 55-61, 1981.

Bosch, P.P.J. van den, *PSI Interactive Simulation Program*, **Advances in computer-aided control systems engineering** (M. Jamshidi and C.J. Herget eds.), Amsterdam, the Netherlands, pp. 362-364, 1985a.

Bosch, P.P.J. van den, *TRIP Transformation and Identification Program*, **Advances in computer-aided control systems engineering** (M. Jamshidi and C.J. Herget eds.), Amsterdam, the Netherlands, pp. 359-360, 1985b.

Burger, W. and A.G. Corbet, "**Ship Stabilizers. Their design and operation in correcting the rolling of ships. A handbook for merchant navy officers.**", Pergamon Press. Ltd., London, 1966.

Carley, J.B., *Feasibility study of steering and stabilising by rudder*, Proceedings 4th Ship Control Systems Symposium, The Hague, The Netherlands, 1975.

Cowley, W.E., and T.H. Lambert, *The use of the rudder as a roll stabiliser*, Proceedings 3rd Ship Control Systems Symposium, Bath, UK, 1972.

Cowley, W.E., and T.H. Lambert, *Sea trials on a roll stabiliser using the ship's rudder*, Proceedings 4th Ship Control Systems Symposium, The Hague, The Netherlands, 1975.

Dorf, R.C., **Modern Control Systems**, Addison-Wesley Publishing Company, Inc., 1980.

Duetz, H., *Het koersgedrag van de RRS automaat*, Masters thesis (in Dutch), Control Laboratory, Fac. of El. Eng., Delft University of Technology, 1985.

Fung, P.T.K. and M.J. Grimble, *Self-tuning control of ship positioning systems*, Proceedings IEEE Workshop on the Theory and Application of Adaptive Control, Oxford, GB., 1981.

Gerritsma, J., *Scheepshydrodynamica - Golven*, Report no. 473-K, Ship Hydrodynamicals Laboratory, Delft University of Technology, 1979.

Groen, P. and R. Dorrestein, *Zeegolven*, KNMI, Opstellen op oceanografisch en maritiem meteorologisch gebied, no. 11, Staatsdrukkerij, 's Gravenhage, 1976

Hoogenraad, *Rudder Roll Stabilization: toestandschatting met behulp van extended Kalman filtering*, Masters thesis (in Dutch), Control Laboratory, Fac. of El. Eng., Delft University of Technology, 1983.

Källström, C.G., *Control of yaw and roll by a Rudder/Fin Stabilisation System*, 6th Ship Control Systems Symposium, Ottawa, Canada, 1981.

Klugt, P.G.M. van der, *Rudder Roll Stabilization*, Masters thesis (in Dutch), Control Laboratory, Fac. of El. Eng., Delft University of Technology, 1982.

Koot, W.J.L., *Rudder Roll Stabilization - Ontwerp en realisatie van een adaptieve regelaar t.b.v. slingerstabilisatie van schepen*, Masters thesis (in Dutch), Control Laboratory, Fac. of El. Eng., Delft University of Technology, 1983.

Kwakernaak, H., and R. Sivan, **Linear Optimal Control Systems**, John Wiley & Sons, Inc. 1972.

Lloyd, A.E.J.M, *Roll stabilisation by rudder*, Proceedings 4th Ship Control Systems Symposium, The Hague, The Netherlands, 1975.

Mattaar, T.C., *Modelvorming en simulatie van het gier- en slingergedrag van een schip*, Masters thesis, Control laboratory, Fac. of El. Eng., Delft University of Technology, 1986.

Nauta Lemke, H.R. van and W. De-zhao, *Fuzzy PID Supervisor*, Proceedings 24th Conference on Decision and Control, pp. 602-608, Ft. Lauderdale, USA, 1985.

Nomoto, K., T. Taguchi, K. Honda and S. Hirano, *On the steering qualities of ships*, Int. Shipbuilding Progress, Vol.4, 1957.

Sage, A.P., **Optimum systems control**, Prentice-Hall, Inc., London, 1968.

Schelling, C.H., *The influence of disturbances on the steering of a ship*, Masters thesis, Control Laboratory, Fac. of El. Eng., Delft University of Technology, 1977.

Schonebaum, K.W., *Simulatieopstelling voor de gier en slingerbewegingen van een schip*, Internal report (in Dutch), Control Laboratory, Fac. of El. Eng., Delft University of Technology, 1982.

CURRICULUM VITAE

De auteur van dit proefschrift werd op 22 januari 1956 geboren te Noordwijkerhout, Zuid Holland. Na het behalen van het diploma Gymnasium Beta aan het Triniteits Lyceum te Haarlem studeerde hij van 1974 tot 1982 elektrotechniek aan de Technische Universiteit Delft.

In augustus 1982 trad hij in dienst bij de firma Van Rietschoten & Houwens BV Rotterdam. Door dit bedrijf werd hij tot 1987 gedetacheerd op de vakgroep Regeltechniek van de faculteit der Electrotechniek van de TU Delft ter ontwikkeling van de regelalgoritmen voor een RRS (Rudder Roll Stabilization) stuurautomaat.

Het door de auteur verrichte onderzoek heeft geleid tot een laboratorium realisatie van een RRS stuurautomaat alsmede tot diverse publikaties en, uiteindelijk, tot dit proefschrift.

STELLINGEN

behorende bij het proefschrift van

P.G.M. van der Klugt

Delft, 17 september 1987

1 Het gebruik van een eerste orde smoothing filter impliceert de onderstelling dat de systeemruis slechts een constante component bevat.

2 Het door Van Amerongen gebruikte filter om de hoogfrequente componenten van de gemeten gierbewegingen van een schip te onderdrukken is een Kalman filter waarvan de versterkings factoren niet op de volgens Kalman optimale wijze worden berekend.

J. van Amerongen, "Adaptive steering of ships - a model-reference approach to improved manoeuvring and economical course keeping", proefschrift, Technische Universiteit Delft, 1982.

3 Bij het ontwerpen van een systeem gebaseerd op een kwadratisch criterium dient tevens het werkelijke criterium te worden gegeven.

4 Het is niet aan te raden het ontwerp van een koersregelaar te baseren op één van de kriteria met vaste weegfactoren zoals die in de literatuur worden voorgesteld en in Grimble, Wilkie and Katebi worden samengevat.

M.J. Grimble, J. Wilkie and M.R. Katebi, "Ship Steering Control Systems Modelling and Control Design", Proceedings 7th Ship Control Systems Symposium, Bath, U.K., 1984.

5 Een apparaat dat ook onder gevaarlijke omstandigheden wordt gebruikt, zoals een stuurautomaat voor een schip, dient zodanig te zijn ontworpen dat de gebruiker dit zonder instructie op de juiste manier weet te bedienen.

6 De resultaten van het in dit proefschrift beschreven onderzoek maken RRS een concurrent voor stabilisatie vinnen.

7 De overheid kan innovatie bevorderen door het creëren van zodanige vraag dat het bedrijfsleven wordt gedwongen om onderzoek te verrichten in samenwerking met een universiteit.

8 Het aantal mensen dat een computer gebruikt om een ziekte te simuleren zal fors toenemen.

9 De gemiddelde amateur voetballer voetbalt beter dan de gemiddelde Prof.

10 Indien alle schepen worden uitgerust met slingerstabilisatie dienen de bewegingen die men uitvoert bij het zingen van het lied "Klap eens in je handjes" te worden aangepast.

11 Op de lange termijn is de werkgelegenheid meer gediend door het verplicht stellen van het volgen van geschikte cursussen onder werktijd dan door arbeidstijdverkorting.

12 Tegenover een leverancier van stabilisatievinnen die stelt "Gemiddeld 1 op de 5 dagen op zee zal een op vinnen gebaseerd slingerstabilisatie systeem een belangrijke winst opleveren" dient een leverancier van RRS systemen te stellen "In tegenstelling tot een RRS systeem zal een op vinnen gebaseerd slingerstabilisatie systeem gemiddeld 4 op de 5 dagen op zee onnodig verlies opleveren".